1-1-2011

Comparison of analysis techniques for the seismic evaluation of an 88-storey concrete building

Andrew Shaffu
Ryerson University

COMPARISON OF ANALYSIS TECHNIQUES FOR THE SEISMIC EVALUATION OF AN 88-STOREY REINFORCED CONCRETE BUILDING

by

Andrew Shaffu
B.Sc., American University in Dubai, 2007

A thesis
presented to Ryerson University
in partial fulfillment of the
requirements for the degree of
Master of Applied Science
in the Program of
Civil Engineering

Toronto, Ontario, Canada 2011

AUTHOR'S DECLARATION

I hereby declare that I am the sole author of this thesis.

I authorize Ryerson University to lend this thesis to other institutions or individuals for the purpose of scholarly research.

_____

Andrew Shaffu

I further authorize Ryerson University to reproduce this thesis by photocopying or by other means, in total or in part, at the request of other institutions or individuals for the purpose of scholarly research.

_____

Andrew Shaffu

BORROWER'S PAGE

NAME	ORGANIZATION	DATE	SIGNATURE

ABSTRACT

COMPARISON OF ANALYSIS TECHNIQUES FOR THE SEISMIC EVALUATION OF AN 88-STOREY REINFORCED CONCRETE BUILDING

Andrew Shaffu
Master of Applied Science in Civil Engineering
Department of Civil Engineering, Ryerson University
Toronto, Ontario, Canada 2011

This thesis presents the comparison of results for an 88-storey reinforced concrete building subjected to static and dynamic analyses. Similar to a building designed in a moderate seismic zone, the structure is designed and detailed according to the ACI 318M (2002) Code provisions and the seismic provisions of the UBC (1997).

The building is modeled according to structural drawings and element design specifications are used in describing members' deformation characteristics. Resistance to dynamic motion is provided through boxed core-wall assemblies acting as cantilever walls in one direction and linked with coupling beams at storey levels in the orthogonal direction.

The equivalent static, dynamic modal spectrum, linear time-history and nonlinear time-history analyses are employed and a comparison of maximum inter-storey drift response is provided. The results of the analyses show that the linear time-history analysis is the most appropriate method in capturing the behavior of this particular building under dynamic loading.

ACKNOWLEDGEMENTS

First and foremost, I would like to express profound gratitude to my graduate supervisor, Dr. Reza Kianoush, for his valuable assistance and continual guidance throughout the duration of my graduate education. Dedicating his vast experience towards developing successful means for carrying out this research, Dr. Kianoush is a devoted leader to this work, where his direction and constructive suggestions make this thesis a possibility.

I am genuinely indebted to my graduate co-supervisor, Mr. Amir Poshnejad, for his relentless support, motivation and incessant drive in the development and completion of this work. Throughout our association, Mr. Poshnejad closely held his belief in me through stressful times. For these and countless more reasons, I am exceptionally grateful.

I would also like to thank the loved ones who surround me. Their existence all the way through my graduate education not only helped me maintain sanity, but also gave rise to lifelong friendships I now treasure.

DEDICATION

Reflecting on the struggle I endured reaching this point of my life, without my loving family, I would have never risen when I had fallen.

This thesis is dedicated to them.

TABLE OF CONTENTS

LIST OF TABLES

LIST OF FIGURES

LIST OF SYMBOLS

A	coefficient dependent on the grade of concrete
A_c	area of core of section enclosed by center lines of perimeter hoop
A_e	area of effectively confined concrete core
A_i	total plan area of ineffectually confined core concrete at hoop level
A_{cc}	area bound by centerlines of perimeter hoop
A_{sx}, A_{sy}	total area of transverse bars in the x- and y-directions, respectively
B	coefficient dependent on the grade of concrete
b_c	core dimension to centerline of perimeter hoop in the x-direction
C	proportional damping matrix
C_a	seismic coefficient given in UBC (1997) Table 16-Q = 0.18
C_t	seismic coefficient given in UBC (1997) = 0.0488
C_v	seismic coefficient given in UBC (1997) Table 16-R = 0.25
DL	Dead Load
d_c	core dimension to centerline of perimeter hoop in the y-direction
E_c	Young's modulus of elasticity of concrete
E_s	Young's modulus of elasticity of steel
E_{sec}	secant modulus of confined concrete at peak stress
F_t	portion of base shear concentrated at the top of the structure, in addition to F_n
F_x	Design Seismic Force applied to Level x
F_i, F_n	Design Seismic Force applied to Level i or n, respectively
f	concrete stress
f_c	longitudinal compressive concrete stress
f_l	lateral pressure from transverse reinforcement
f_y	yield stress of reinforcing steel
f_{co}	unconfined concrete compressive stress
f_{ci}	unconfined concrete compressive stress at inflection point of descending branch
f_{lx}, f_{ly}	lateral confining stress on concrete in the x- and y-directions, respectively
f_{su}	ultimate stress of steel

f_{ys}	yield stress of steel
$f_i(t)$	time functions
f'_c	concrete compressive strength
f'_l	effective lateral confining pressure
f'_{cc}	confined concrete compressive strength
f'_{co}	unconfined concrete strength
f'_{cu}	confined concrete ultimate strength
f'_{lx}, f'_{ly}	effective lateral confining stress in the x- and y-directions, respectively
h_n	height (m) above the base to Level n
h_i, h_x	height (m) above the base to Level i or x, respectively
I	importance factor given in UBC (1997) Table 16-K = 1.0
K	stiffness matrix
K_L	stiffness matrix for linear elastic elements
k_e	confinement effectiveness coefficient
LL	Live Load
M	moment force
M	diagonal mass matrix
m_x, m_y, m_z	unit acceleration loads
M/V	mass per unit volume (density)
n	number of longitudinal bars
p_i	spatial load vectors
R	force reduction factor given in UBC (1997) Table 16-N = 5.5
r	vector of applied load
r_N	vector of forces from nonlinear degrees of freedom in link elements
SDL	Superimposed Dead Load
s	center to center spacing of hoop bars
s'	clear vertical spacing between hoop bars
T	structural period of vibration (s) of the building in the considered direction
$u, \dot{u}, \ddot{u}$	displacements, velocities and accelerations relative to the ground, respectively

$\ddot{u}_{gx}, \ddot{u}_{gy}, \ddot{u}_{gz}$	components of uniform ground acceleration
V	shear force
V	total design lateral force or shear at the base
W	total building weight including 25% live load = 1,653,580 kN
w_i, w_x	portion of building weight located at or assigned to Level i or x, respectively
w'_i	i^{th} clear distance between longitudinal bars
W/V	weight per unit volume (specific weight)
α	coefficient of thermal expansion
α_1	locates the pivot point for unloading to zero from positive force
α_2	locates the pivot point for unloading to zero from negative force
β_1	locates the pivot point for reverse loading from zero toward positive force
β_2	locates the pivot point for reverse loading from zero toward negative force
ε_c	strain of concrete
ε_u	ultimate concrete strain capacity
ε_{cc}	confined concrete strain
ε_{ci}	unconfined concrete compressive strain at inflection point of descending branch
ε_{co}	unconfined concrete peak compressive strain
ε_{cu}	confined concrete ultimate strain
ε_{sh}	strain hardening of steel
ε_{sp}	spalling strain
ε_{su}	ultimate strain of steel
ε_{ys}	yield strain of steel
ε'_c	concrete compressive strain at f'_c
η	determines amount of degradation of elastic slopes after plastic deformation
Ø	curvature
ρ_w	volumetric ratio of confined transverse reinforcement to concrete
ρ_x, ρ_y	transverse confining reinforcement in the x- and y-directions, respectively
ρ_{cc}	ratio of the area of longitudinal reinforcement to the area of core of the section
σ_c	stress of concrete
ν	Poisson's ratio

CHAPTER 1 - INTRODUCTION

1.1 Overview

The focus of Earthquake Engineering has gained considerable popularity over the past few decades. As a result of passed earthquake events causing significant amounts of damage to varying structures worldwide, frequent developments in the areas of special design and construction techniques for structures withstanding seismic activity incessantly expand in reputation. Continual updates in structural design and detailing requirements forming the seismic design provisions of building codes are periodically revised and modernized.

Despite ongoing developments in the seismic design of structures, the level of protection afforded to high-rise buildings designed according to modern codes of practice still faces substantial concern. Modern buildings designed and built according to recent codes may still experience structural damage, and even collapse, when subjected to seismic activity. Examples of such buildings built according to recent code provisions would be attributed to one of the worst natural disasters in terms of financial loss in U.S history: the 1994 Northridge earthquake. Such historical events reiterate the need for furthering research in earthquake engineering.

In the United States, rising concerns about code-designed buildings experiencing unexpected levels of damage induced the Structural Engineers Association of California (SEAOC) in 1992 to form the Vision 2000 committee in an effort to establish a developed design framework resulting in structures with predictable performances. The first recommendations of the Vision 2000 committee consisted of the formation of design procedures meeting specific performance-based criteria resulting from the seismic analysis and design of structures (SEAOC, 1995).

Among the essential classes of structural systems in tall buildings generally used to resist lateral loads in the form of earthquakes, reinforced concrete shear walls serve as exceptional lateral force resisting systems. Due to the high in-plane stiffness of such systems, lateral deflections and inter-storey drifts are easy to control, and achieving the required strength is relatively easy to provide through adequate reinforcement (Stonehouse et al., 1999). Through such characteristics,

the performance of shear walls under strong seismic occurrences over the past few decades have shown outstanding lateral load carrying behavior (Fintel, 1995).

Shear wall systems may be configured as parallel cantilevers in the form of separate walls with or without connected coupling beams or slabs, or they may incorporate an assembly of walls forming a core wall system around stairwells and elevator shafts. A shear wall system formed by connecting in-plane walls using beams or slabs is referred to as a coupled shear wall system. Such shear wall systems may also serve as permanent partitions between units and corridors in a building, making them ideal for apartment-type occupancy buildings.

1.2 Objective and Scope of the Thesis

This thesis investigates a high-rise building incorporating tall reinforced concrete shear wall systems as it is subjected to the types of strong earthquake ground motions which can be expected in moderate seismic zones. As there are limited comparisons of analysis techniques conducted on high-rise buildings designed for moderate seismic zones, this work focuses on the comparison of static and dynamic analyses.

The building presented throughout this thesis is an 88-storey reinforced concrete tower, detailed according to the ACI 318M (2002) Code and designed in accordance to the seismic provisions of the UBC (1997). The structure is modeled to resist dynamic motion through six boxed core wall assemblies acting as cantilever walls in one direction, and linked with coupling beams at storey levels in the orthogonal direction.

Throughout this study, modeling according to the design specification and structural detailing of the building is performed. Element design specifications are used to develop moment-curvature relationships to describe members' deformation characteristics for use in the nonlinear time-history analysis. The equivalent static, dynamic modal, linear and nonlinear time-history analyses are executed and the results of the analyses are compared on the basis of maximum inter-storey drift response.

1.3 Organization of the Thesis

This thesis is organized into six chapters as follows:

Chapter 1 provides introductory material and establishes the objective and scope of the thesis.

Chapter 2 introduces the seismic design of reinforced concrete shear walls, reviews relevant analysis programs, hysteretic models, concrete models and reinforcing steel used throughout analyses.

Chapter 3 presents the building and design specifications, the selection of lateral force resisting systems and their modeling in ETABS.

Chapter 4 includes the modeling of seismic reinforcement detail afforded to the shear wall systems and structural components according to the structural drawings of the building. Material properties and hysteretic characteristics are defined and the subsequent moment-curvature relationships are incorporated into the modeling of structural members into SAP2000.

Chapter 5 discusses the relevant analysis techniques and their seismic input parameters. The results are presented and compared in terms of maximum inter-storey drift response.

Chapter 6 provides a summary of the work presented throughout this thesis, concluding remarks and recommendations for future work.

CHAPTER 2 - LITERATURE REVIEW

2.1 Introduction to the Seismic Design of Reinforced Concrete Shear Walls

In the seismic design and construction of buildings, a seismic design philosophy has been developed over the years based on the anticipation of a strong earthquake causing some structural damage. The occurrences of earthquakes with great intensities are relatively sporadic, and it is usually deemed uneconomical and redundant to design and construct buildings for such relatively infrequent occurrences. Within the earthquake-resistant design of structures, the main objective lies in limiting damage to an acceptable level for the building. Structures designed in accordance to this seismic design philosophy should technically be able to resist minor seismic activity without damage to any of its structural and non-structural components; withstand moderate seismic activity with the possibility of some non-structural damage, but free of structural damage; and endure major seismic activity with structural and non-structural damage, but free of collapse or loss of life.

As the basis for seismic design lies in the concept of acceptable levels of damage afforded to buildings under one or more seismic events of specified intensities, the performance objective of the building is key to determining the acceptable level of damage for design. The performance of a building should ideally be specified as an acceptable probability of exceedance, which is the acceptable probability of the structure exceeding certain limit states throughout its likelihood of experiencing various earthquakes over its lifespan.

Another dependant of the acceptable seismic level of damage afforded to a structure lies in its operational requirements as a building. As an example, a hospital must essentially remain in service after the occurrence of seismic activity. Therefore, such a building must be designed for a higher performance level, opposed to other buildings without essential post-earthquake service requirements. The suggested performance objectives for varying building types are provided by the SEAOC Vision 2000 Committee (1995). Although numerous studies over past decades have extensively explored the response of reinforced concrete shear wall systems and their structural elements, the prevailing information focuses on the response of coupled shear wall systems as

well as the effects of detailing within specific lateral load carrying components (Paulay et al., 1992).

Seismic performance investigations afforded to shear wall systems designed according to standards in the United States have been initiated (Munshi et al., 1998). The study presents the detailed design of a 12-storey reinforced concrete frame and shear wall system with its analysis and design according to the Uniform Building Code (1994) standards. In one of the principal directions, the lateral force resisting system consisted of a reinforced concrete frame combined with a pair of shear walls coupled at storey levels. To determine the performance of the structure, an inelastic analysis using a pushover analysis and a dynamic time-history analysis was conducted. In order to vary the degree of coupling between shear walls, several wall and beam designs were used. The resulting investigation determined that when the coupling beam to shear wall strength ratio is high enough to ensure adequate shear wall system strength, and the walls are not subject to high ductility demands following the loss of coupling beam strength, performance of the coupled shear wall system is enhanced. The conclusions of this study suggest further research involving additional earthquake ground motion records.

A research framework for seismic level of protection evaluation is conducted in a study provided by Heidebrecht (1997). Within the presented work, a study on the seismic performance of two six-storey ductile moment-resisting reinforced concrete buildings is described. The buildings were designed based on the NBCC 1995 seismic provisions with a seismic hazard corresponding to Vancouver, and their performance evaluated on the basis of minimum transient inter-storey drift criteria as specified by the Vision 2000 Committee (1995). Both structures detailed identical design parameters except for the design drift limit. As specified by NBCC (1995), one of the structures was designed to limit inter-storey drift to 1%, while the other limits inter-storey drift to 2%. The buildings were exhausted over 15 ground motion time-histories which were scaled to the peak horizontal velocity. The time-history spectral shapes used were similar to those expected in Vancouver. Various excitation levels ranging from 0.5 to 3.0 times the design level seismic ground motions were used in the dynamic analysis for the determination of the performance for a full range of excitations expected over the lifespan of the structures. The nonlinear dynamic analysis results of this study found the structures exhibiting a performance

level equivalent to ‘operational’ throughout the design level seismic ground motion, and a performance level equivalent to ‘life-safe’ during excitations about 3.0 times the design level seismic ground motion.

Another study performed by Stonehouse et al. (1999) presents the seismic performance of shear wall buildings designed according to the NBCC (1995) seismic provisions. The study explores the results of an investigation into the performance of a 30-storey reinforced concrete building boasting a lateral load resisting central core wall assembly composed of three walls which are linked by coupling beams in one direction and act as simple cantilever walls in the orthogonal direction. Using a static pushover analysis and an inelastic dynamic analysis, the behavior of the orthogonal shear wall systems is determined. The structure is designed in accordance to the NBCC (1995) provisions and detailed according to the CAN3–A23.3–M94 (1994) code provisions. The structure is similar to an existing building designed and constructed in Vancouver. The building’s performance is evaluated according to the performance criteria recommended by the SEAOC Vision 2000 Committee (1995), where the performance evaluation is executed by studying response parameters such as inter-storey drift and element (wall and coupling beam) curvature. The results of both analyses confirm the structural system responding very effectively in the resistance of high levels of lateral loading, and indicate lateral drifts significantly below the limits defined by the NBCC (1995). Moreover, members designed to respond in a ductile manner achieve their goal by deforming in advance of other wall elements. The conclusions of the study suggest further research investigating the design, detailing, and performance of a system using a slab to couple the walls of a shear wall building with thirty storeys or more.

Although the studies investigated throughout this section are not exhaustive, they do provide an understanding of the basic behavior, performance levels, and seismic level of protection afforded to reinforced concrete shear wall structures.

2.1.1 Definition of Hazard

Seismic hazards, depending on the severity of seismic activity, may result in building damage through physical phenomena such as ground shaking or ground fault rupture. Such seismic hazards consequently affect the achieved performance level of a building. The damage potential attributed to seismic hazards is a function of the earthquake magnitude, the distance from the actual zone of fault rupture to the earthquake site, the direction of fault rupture propagation, the geological makeup of the region, and any unique geological conditions of an individual site (SEAOC, 1995).

Performance-based engineering aims to control the level of damage in a structure over the range of seismic events which may occur at a specific site. In order to assist in its practical application, the continuous range of seismic events for a given site is replaced by a series of discrete seismic events. This discrete series of seismic events represents the spectrum of seismic hazards for a desired building performance level. Such discrete earthquake events are termed earthquake design levels.

Earthquake design levels are typically expressed in terms of a recurrence interval or a probability of exceedance. The recurrence interval, or return period, of seismic activity is the average time span between earthquakes with similar or greater severities at a particular site. The probability of exceedance is a statistical interpretation of the likelihood that seismic events with similar or greater severities will occur at a particular site within a specified number of years. The Vision 2000 committee (1995) suggests levels of design earthquakes defined as shown in Table 2.1, and are recommended for its use in performance-based engineering.

Table 2.1: Design Earthquakes (SEAOC, 1995)

Earthquake Design Level	Recurrence Interval	Probability of Exceedance
Frequent	43 years	50% in 30 years
Occasional	72 years	50% in 50 years
Rare	475 years	10% in 50 years
Very Rare	970 years	10% in 100 years
Extremely Rare	2500 years	2% in 50 years

2.1.2 Recommended Performance Levels

A performance level is expressed as the maximum acceptable level of damage when subjected to a specific level of seismic activity. In defining the performance levels, damage to structural and non-structural components, damage to contents, and the availability of site utilities necessary for building function are all taken into consideration. The SEAOC Vision 2000 committee (1995) recommends specific performance levels for the seismic design of structures. The qualitative measures of performance levels recommended by the Vision 2000 committee (1995) are categorized as follows:

Fully Operational Performance Level

A building is deemed fully operational if it is essentially free of damage with repairs generally not required, remains safe to occupy immediately following a seismic occurrence, and the equipment and services necessary to its primary function remain available for use.

Operational Performance Level

A building is deemed operational if it endured moderate damage to its contents and non-structural components, light damage to its structural components, but remains safe to occupy immediately following a seismic occurrence. Moreover, negligible damage to the structure's vertical load resisting elements is expected. Light damage to the lateral load resisting elements is also expected, although the lateral load resisting system maintains nearly all its original strength and stiffness with minor cracking of its structural elements. With regard to the shear wall system, some cracking in the coupling beams is expected, as is minor cracking in the walls. Although some disruptions to its primary function are anticipated due to the damage of some contents, utilities, and non-structural components, repairs may be carried out at the owners and occupants' expediency.

Life-Safe Performance Level

A building is deemed life-safe if it endured moderate damage to its structural components, non-structural components, and contents, but retains a margin against collapse. The lateral stiffness and capacity for additional lateral load resistance of the structure are greatly reduced. With regard to the shear wall system, some crushing and cracking of concrete due to flexure is expected. Coupling beams suffer shear and flexural cracking, although the concrete remains in its original position. As for the vertical load carrying components, they retain substantial capacity to resist gravity loads. Although the structure might be repairable, it may be uneconomical to restore as the building is considered unavailable for post-earthquake occupancy.

Near Collapse Performance Level

A building is deemed near collapse if it endured extreme damage and its vertical and lateral load resisting capacities have substantially diminished. With regard to the shear wall system, severe flexural and shear cracking is expected, including the crushing of concrete and buckling of steel reinforcement. Damage includes coupling beams practically disintegrated, permanent damage to utilities, non-structural systems, as well as severe damage to building contents. The building remains unsafe for occupancy after such a seismic occurrence and repair of the structure may be uneconomical or impractical to carry out.

Collapse Performance Level

A building is deemed to have reached collapse if its primary structural system, or a portion of its structural system, collapses.

For the purpose of engineering applications, the Vision 2000 report (1995) provides suggestions on the quantitative measures of performance-based drift levels. Drift is defined as the ratio of inter-storey deflection to storey height. Table 2.2 presents the permissible drift levels for the various performance levels.

Table 2.2: Performance Levels and Permissible Drift Levels (SEAOC, 1995)

Damage Parameter	Performance Level				
	Fully Operational	Operational	Life-Safe	Near Collapse	Collapse
Transient Drift	< 0.2%	< 0.5%	< 1.5%	< 2.5%	> 2.5%
Permanent Drift	Negligible	Negligible	< 0.5%	< 2.5%	> 2.5%

2.1.3 Building Categories and Design Performance Objectives

For a given building, its design performance objective can be defined as the structure's desired performance level for each earthquake design level. The design performance objectives are selected based on economic considerations, the significance of events taking place within the building, the building's occupancy, and any cultural or historical importance the structure may have to its public. On this basis, buildings are classified into the following three categories (SEAOC, 1995):

Safety Critical Facilities

Buildings under this category contain hazardous materials in large quantities, the release of which would result in unacceptable hazards to the general public. Examples of hazardous materials include toxic materials, explosives and radioactive materials.

Essential / Hazardous Facilities

Essential facilities are those that must retain their operation and function following seismic activity, such as hospitals, police stations and fire departments.

Hazardous facilities contain hazardous materials in large quantities, but their release would be contained within the boundaries of the facility with negligible public impact. Examples of such facilities include oil refineries and microchip manufacturing facilities.

Basic Facilities

Any structures not classified as Safety Critical Facilities or Essential / Hazardous Facilities fall under this category.

The recommended performance objectives of these categories are summarized in Table 2.3.

Table 2.3: Recommended Performance Objectives (SEAOC, 1995)

Earthquake Design Level	Minimum Performance Level		
	Safety Critical Facilities	Essential / Hazardous Facilities	Basic Facilities
Frequent	Fully Operational	Fully Operational	Fully Operational
Occasional	Fully Operational	Fully Operational	Operational
Rare	Fully Operational	Operational	Life-Safe
Very Rare	Operational	Life-Safe	Near Collapse

2.1.4 Seismic Level of Protection

The damage potential of structures constructed with loading, design and detailing according to code requirements, and subjected to earthquake ground motions associated with a specific seismic hazard and location, is defined as the seismic level of protection. Seismic design in accordance to code provisions defines the level of seismic protection afforded to structures as being in part a function of the minimum lateral design forces. The lateral force used in the seismic design of structures is applied as a design load and is a function of the seismic hazard and lateral force resisting system. Buildings built with identical structural types and plan dimensions may not behave with the same performance under identical seismic activity. Several aspects of the structure, some of which are material properties, member proportioning and detailing, design philosophies and site-specific locations, have a profound effect on the response of a building subjected to seismic ground motions, and subsequently, the structure's level of performance. The level of performance of a building is related to the maximum degree of damage that may be endured by the structure. Damage to the structure is in turn associated with various code-based limitations, some of which are parameters like lateral deflection, inter-storey drift and member ductility. Such parameters allow for the evaluation of local damage to

structural components as well as overall building damage. These damage related performance expectations can be used to assess the seismic level of protection afforded to structures built with the intent of resisting seismic activity.

2.1.5 Evaluation Methods

With regard to the shear wall system, several analysis techniques are employed to determine the structural response of the building. Throughout this research, the structure is designed and detailed according to the UBC (1997) and the ACI 318M (2002) Codes. The seismic design forces for the building type and location are calculated, and a tall reinforced concrete shear wall structure is dimensioned and modeled. An elastic analysis is performed using equivalent static and dynamic modal spectrum analyses. The wall, column and beam elements are modeled and reinforcement is detailed according to specifications in the structural drawings. In order to effectively determine building response, the production of member moment-curvature relationships and the inclusion of necessary details for expected hysteretic response are afforded to the inelastic modeling of the shear wall system. The tower is subjected to a nonlinear dynamic time-history analysis to evaluate its inelastic performance.

Existing structures in regions defined as having moderate to high seismic hazard risks use tall reinforced concrete shear wall structures as their lateral load resisting systems. As the construction of these building types will continue in the future, there remains the need for a comprehensive comparison of analysis techniques afforded to such tall reinforced concrete shear wall structures.

2.2 Ductility Design

Ensuring a ductile response of the shear wall structure to strong seismic ground motions is essential. By effectively designing and detailing the shear wall structure and its components, a ductile behavioral response can be warranted. The specification of the force modification factor, R, reflects the ductility capacity of the shear wall structure. For the shear wall system in the coupled and uncoupled directions, a force modification factor is specified as 5.5 in accordance

with the UBC (1997). The use of this factor reduces the lateral design forces while maintaining the capability of the ductile system to absorb considerable amounts of energy through inelastic cyclic deformations. In order to ensure that structural elements preserve their load carrying capacities throughout extensive load reversals and deformations induced by an earthquake ground motion, carefully designing and detailing the shear wall system with adequate ductility is essential.

2.3 Capacity Design Approach

As a design tool, the capacity design approach is widely recognized in the field of earthquake engineering. Resulting from nonlinear response and energy absorption ability ($R > 1.5$), structures subjected to nonlinear analyses with reduced seismic design forces require use of the capacity design approach. As this approach is used in the seismic design of such structures, its application is appropriate for the design and detailing of the coupled and uncoupled shear wall systems.

The main energy dissipating elements in the lateral force resisting system are designed and detailed according to the capacity design approach to ensure stable response behavior under strong seismically induced inelastic lateral deformations. The remaining structural elements that do not particularly contribute to such a behavioral response are designed and detailed as non-ductile structural components. Through an effective design and detailing of the main energy dissipating structural components, inelastic lateral deformations are forced to occur in those elements. By utilizing the approach as such, a capacity designed structure is able to endure greater seismically generated ground motions than those specified by design levels.

2.3.1 Capacity Design of Shear Wall Systems

Ductile structural elements possess critical regions designed for inelastic deformations, which are termed potential plastic hinge regions. Applying the capacity design approach involves the selection of potential plastic hinge regions where a practical plastic mechanism for the structure can be applied. The choice of an appropriate plastic mechanism integrates the priority of

minimizing inelastic rotations in the plastic hinges. For the structural components afforded to the shear wall system in the coupled direction, the potential plastic hinge regions are located at the bases of the shear walls as well as the coupling beam ends. These potential plastic hinge regions are attributed to the shear walls as well as the coupling beams.

Following the selection of ductile elements, potential plastic hinge zones, and consequently an appropriate plastic mechanism, the plastic hinge regions in the coupling beams are detailed according to the ACI 318M (2002) Code. Detailing of the shear walls is initiated where the potential plastic hinge regions occur at the base of the structure. In order to prevent any abrupt failures due to shear, the shear capacity at the base of the shear walls is designed in excess of its corresponding flexural capacity. Above the base of the shear wall system, the shear walls are detailed such that the development of inelastic deformations occurs in the potential plastic hinge regions.

2.4 SAP2000 Analysis Program

The accurate modeling of structural elements and their essential characteristics relating to the inelastic response of the shear wall system is necessary to achieve meaningful results from the nonlinear analysis of the building undergoing seismically induced ground motions. For its appropriate modeling features and analysis capabilities, the Structural Analysis Program 2000 (SAP2000) is used for the objectives of this research.

Developed by Computers and Structures, Inc., SAP2000 is a three-dimensional nonlinear analysis program boasting an intuitive interface allowing for several types of structural analyses. Among its broad range of capabilities, SAP2000 provides options for applying incremental static loads, quasi-static cyclic loads (cyclic loads varying slowly with time), combinations of horizontal and vertical excitations, inelastic dynamic analyses, as well as general purpose hysteretic models. Utilizing multilinear moment-curvature relationships which include the uncracked, cracked and post-yielding stiffness member properties, the structural components response characteristics are modeled for analyzing the shear wall system through dynamic nonlinear time-history analyses.

Incorporated into the analysis are long-term static gravity loads and the influence of lateral drifts causing additional overturning moments, which are also known as P-Delta effects. These secondary effects of storey drifts laterally displacing static gravity loads causes lateral deflections on the moments in the structural members, resulting in an increase in the overturning moment on the building. Accordingly, SAP2000 performs the necessary calculations and then applies the overturning moment as an additional lateral load equal in magnitude to the shear resisting the additional P-Delta induced moment.

For the creation of complex concrete sections, SAP2000 integrates Section Designer into its software, as developed by Computers and Structures, Inc. Section Designer allows the creation of cross sections with arbitrary geometries and provides a powerful graphical interface for locating reinforcement. This integrated software calculates section properties, biaxial moment and interaction curves, as well as section moment-curvature relationships. For the purpose of creating an effective model used in dynamic analysis, Section Designer is utilized in this research for modeling the individual structural components of the building.

2.4.1 Hysteretic Models

In a dynamic analysis, hysteresis loops are described by a hysteresis model and its corresponding rules, which define the load reversal paths within the hysteresis loops. These hysteresis loops depend on material properties and reflect the force-deformation characteristics of structural members as they are subjected to cyclic loading. In order to appropriately select the hysteresis type, SAP2000 provides three hysteresis types for nonlinear analyses: Kinematic Hysteresis, Takeda Hysteresis and Pivot Hysteresis. The following describes the hysteretic models pre-programmed into SAP2000.

Multilinear Kinematic Model

The Multilinear Kinematic Model, based on the kinematic hardening behavior commonly observed in metals, presents a nonlinear force-deformation relationship under monotonic loading provided by a multilinear curve described by a set of user-defined points, as seen in Figure 2.1.

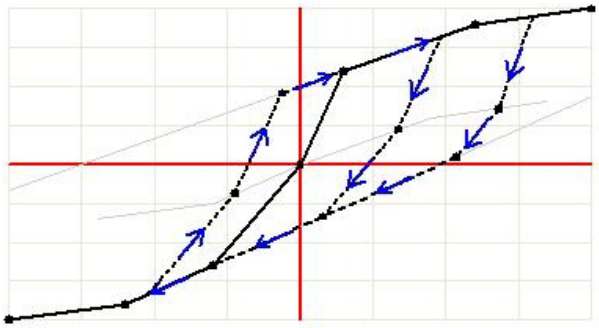

Figure 2.1: SAP2000 Multilinear Kinematic Plasticity Property Type for Uniaxial Deformation

In Figure 2.1, the first slope on either side of the origin is elastic and the remaining portions of the curve define plastic deformation. Upon reversals of deformation, the hysteresis path follows the two elastic segments of the curve from either side of the origin before initiating plastic deformation in the reverse direction. Once initiated, plastic deformation in one direction of loading "pulls" with it the curve for the reverse direction of loading.

To appropriately illustrate the behavior of load reversal paths under cyclic loading of increasing magnitude, Figure 2.2 defines the origin as point 0, the points on the positive axis as 1, 2, 3 from the origin, and the points on the negative axis as -1, -2, -3 from the origin.

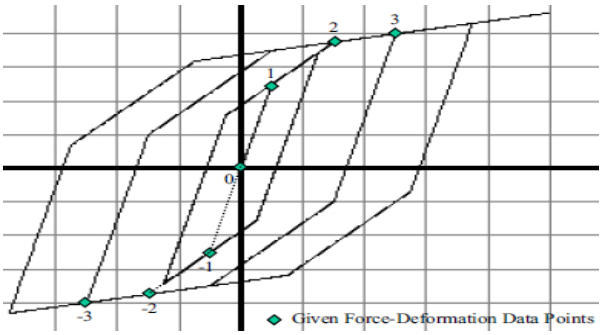

Figure 2.2: SAP2000 Behavior Under Cyclic Loading of Increasing Magnitude for the Multilinear Kinematic Plasticity Property Type for Uniaxial Deformation

In Figure 2.2, the loading is initially elastic and is described from point 0 to point 1 on the curve.

- As loading increases from point 1 to point 2, the onset of plastic deformation begins and is described by the movement of point 1 toward point 2 on the curve. In effect, points -1 and 0 are pulled by point 1, moving the same amount in the force and deformation directions. The movement of point 0 along with points -1 and 1 occurs to preserve the elastic slopes.

- Upon load reversal, unloading occurs along the shifted elastic line from point 1 to point -1 and then toward point -2, which will not move until it is forced by loading in the negative direction, or until loading in the positive direction forces movement in point 2, which consequently pulls point -2 by an identical amount.

- Upon the reversal of load once more, point 1 is advanced toward point 2, and together they are forced toward point 3, thereby pulling along with them points -1 and -2.

Throughout the rest of the analysis, the procedure described above is continued. Beyond points 3 and -3 the slopes are maintained even as these points carry on shifting with the furthering of the analysis.

Multilinear Takeda Model

The hysteresis model developed by Takeda et al. (1970) is based on the experimental behavioral observation on a number of medium-size reinforced concrete members subjected to lateral load reversals with light to medium amount of axial load. The Takeda model includes stiffness changes at flexural cracking and yielding by using a multilinear skeleton force-deformation relationship.

The Multilinear Takeda Model is identical to the Multilinear Kinematic Model in the specification of properties and portrays close similarities to cyclic load behavior. The distinguishable factor between the two models lies in the Multilinear Takeda Model using a degrading hysteretic loop, as seen in Figure 2.3.

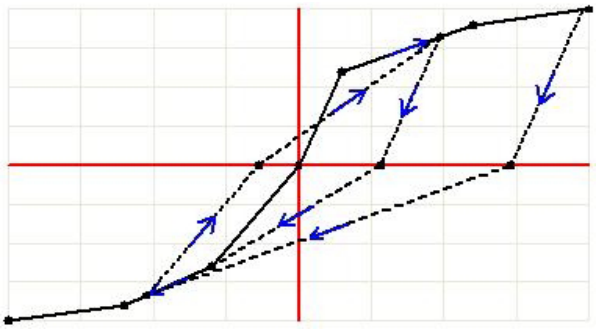

Figure 2.3: SAP2000 Multilinear Takeda Plasticity Property Type for Uniaxial Deformation

The behavior of the Multilinear Takeda Model differs from that of the Multilinear Kinematic Model particularly in the unloading path, as seen in Figure 2.3. When crossing the horizontal axis, the Multilinear Takeda Model curve follows a secant path to the backbone force-deformation relationship upon unloading for the reversed direction.

The full description of this model is provided by Takeda et al. (1970).

Multilinear Pivot Hysteretic Model

The Multilinear Pivot Hysteretic Model is identical to the Multilinear Takeda and Kinematic Models in the specification of properties and portrays close similarities to cyclic load behavior. The distinguishable factor between the Multilinear Pivot Hysteretic Model and the Multilinear Takeda Model lies in the requirement of specifying additional scalar parameters to control the degrading hysteretic loop in the Multilinear Pivot Hysteretic Model. The additional scalar parameters in this model are illustrated in Figure 2.4.

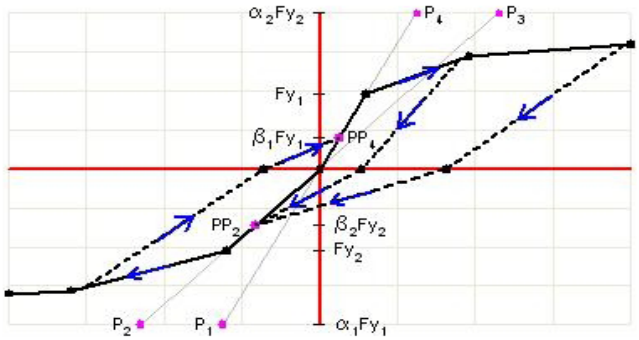

Figure 2.4: SAP2000 Multilinear Pivot Hysteretic Plasticity Property Type for Uniaxial Deformation

This hysteretic model is based on the unloading and reversed loading paths portraying the tendency to be directed to specific points in the force-deformation plane. These specific points are termed pivot points that are defined according the following:

- α_1 : locates the pivot point for unloading to zero from positive force
- α_2 : locates the pivot point for unloading to zero from negative force
- β_1 : locates the pivot point for reverse loading from zero toward positive force
- β_2 : locates the pivot point for reverse loading from zero toward negative force
- η : determines the amount of degradation of the elastic slopes after plastic deformation

The full description of this model is provided by Dowell et al. (1998).

2.4.2 Moment-Curvature Generation

The moment-curvature relationships of structural elements are critical to define their hysteresis response and ensure an accurate nonlinear structural analysis of the building. The development of moment-curvature relationships for the structural members is performed on Section Designer. The program uses the strain compatibility approach to analyze reinforced concrete sections under constant axial loads and their corresponding moment-curvature relationships are developed through section evaluations under various strain conditions. Section Designer evaluates a reinforced concrete section by representing the actual cross-section by a series of thin layers with the assumption of each layer in the cross-section under uniform stress and strain. The concrete forces are calculated by multiplying the layer stress by its area, and reinforcing steel forces are calculated by multiplying the bar area by the stress at the center of the bar. By summing the concrete and steel forces, the force resultants are then calculated. The contribution from moment is calculated by multiplying the resultant layer force from concrete and steel forces by the distance from the reference axis to the centerline of the layer.

As different material properties can be specified to the program, it is crucial to define the material properties for concrete and reinforcing steel. In order to effectively generate moment-curvature relationships using Section Designer, the unconfined concrete, confined concrete and reinforcing steel properties need to be appropriately defined.

2.4.3 Concrete Models

The capability of an element to withstand a change in its natural form without breaking or being caused irreversible damage is referred to as ductility. Among the cardinal requirements within the mechanical behavior of structural members subjected to seismic loading, the concept of ductility is of primary importance for a structural member's ability to deform. Within an element, ductility should be developed simultaneously with the element's capability to resist substantial inelastic deformations without experiencing a considerable reduction in strength. Furthermore, ductility should also be developed simultaneously with the element's ability to consume and dispel energy in a seismic occurrence through relatively stable time-history hysteresis loops

when subjected to dynamic loading. In order for the ductility of a reinforced concrete structural element to be secured, it is paramount to obtain a ductile behavior of the concrete and steel present in the element, as well as a suitable composite action of the materials under seismically induced conditions. To effectively address the level of ductility comprised within a structural element, it is first necessary to understand the stress-strain relationship of each material individually, then to describe a stress-strain relationship for the materials composite action. Once the stress-strain relationship defines the composite action of the materials, the level of ductility exhibited by a structural member is established through the implementation of the stress-strain behavior towards its moment-curvature relationship.

Within the seismic design of reinforced concrete members, regions exhibiting potential plastic hinges must be thoroughly detailed for ductility. The adequate ductility of reinforced concrete members is necessary to ensure that effective moment redistribution between members can occur, and most importantly, cyclic loading caused by seismic activity will not cause collapse to the members of the structure. In the design for ductility in plastic hinge regions of reinforced concrete members, the most important design consideration is for the provision of sufficient transverse reinforcement. The presence of transverse reinforcement is crucial in providing confinement to the compressed concrete, thereby preventing the buckling of longitudinal bars as well as preventing failure due to shear.

Research conducted on tests developed for reinforced concrete subjected to uniaxial compressive loading and confined by transverse reinforcement has shown that suitable arrangements of transverse reinforcement results in significantly increasing the strength and ductility of concrete (Mander et al., 1988). The strength enhancement exhibited by core confinement has a considerable influence on the ductility and flexural strength of reinforced concrete members. In general, reinforced concrete members subjected to higher axial loads exhibit the need for a greater amount of transverse reinforcement to achieve ductile performance. As the axial load becomes more pronounced, the neutral axis depth of the section gets larger and the flexural capacity of the reinforced concrete member becomes more dependent on the concrete compressive stress distribution. A well confined concrete core is essential for a reinforced concrete member to maintain its flexural strength at high curvatures. As the concrete cover is

unconfined, it will become ineffective in resisting loads after the compressive strength is eventually attained, and the confined concrete core will assume load-resisting responsibility thereafter. Providing the member with a reasonable amount of transverse core confinement allows for an increase in member strength, as well as an increase in the plastic rotational capacity of the section.

The main influencing factor in the seismic behavior of reinforced concrete sections is found in the lateral confinement of its transverse reinforcement. The presence of lateral reinforcement manipulates the behavior of concrete thereby boasting a favorable effect on its strength and ductility. As the presence of lateral reinforcement provides a positive influence on concrete, it is essential to examine the earthquake-resistant properties of unconfined and confined concrete separately to provide for a thorough understanding of the behavior of the structural element with respect to its ductility. The earthquake-resistant properties of a material are evaluated by its stress-strain diagram, which reflects the strength and deformation characteristics of the material. The following sections present the concrete models investigated and the resulting concrete models used to describe the stress-strain relationships afforded to modeled structural members in the building.

2.4.3.1 Unconfined (Plain) Concrete Model

In describing the stress-strain relationship of unconfined concrete, several constitutive models were investigated to appropriately select the determining unconfined concrete model to be used for structural members throughout the height of the building. Among the constitutive models of unconfined concrete investigated, two models are presented here for the purpose of this research.

2.4.3.1.1 Attard and Setunge Unconfined Concrete Model

As adopted from Bai et al. (2007), the first model presented in this work is developed for a concrete stress-strain envelope curve in compression and selected based on its applicability in use towards a broad range of in-situ concrete strengths ranging from 20 to 130 MPa. For the sake of convenience, compressive stresses and strains of concrete are taken as positive.

Under compression, the stress of concrete is related to the strain of concrete by:

$$\frac{\sigma_c}{f_{co}} = \frac{A\left(\frac{\varepsilon_c}{\varepsilon_{co}}\right) + B\left(\frac{\varepsilon_c}{\varepsilon_{co}}\right)^2}{1 + (A-2)\left(\frac{\varepsilon_c}{\varepsilon_{co}}\right) + (B+1)\left(\frac{\varepsilon_c}{\varepsilon_{co}}\right)^2}$$

Where:

σ_c = the stress of concrete

ε_c = the strain of concrete

f_{co} = the peak compressive stress of concrete

ε_{co} = the peak compressive strain of concrete

And A and B are coefficients dependent on the grade of concrete.

In describing the ascending branch of the stress-strain curve where $\varepsilon_c \leq \varepsilon_{co}$, the equations of the coefficients dependent on the grade of concrete are given by:

$$A = \frac{E_c\ \varepsilon_{co}}{f_{co}} \quad | \quad B = \frac{(A-1)^2}{0.55} - 1$$

For the descending branch of the stress-strain curve where $\varepsilon_c > \varepsilon_{co}$, the equations of the coefficients dependent on the grade of concrete are given by:

$$A = \frac{f_{ci}\ (\varepsilon_{ci} - \varepsilon_{co})^2}{\varepsilon_{co}\ \varepsilon_{ci}\ (f_{co} - f_{ci})} \quad | \quad B = 0$$

Where:

f_{ci} = the compressive stress at the inflection point on the descending branch

ε_{ci} = the compressive strain at the inflection point on the descending branch

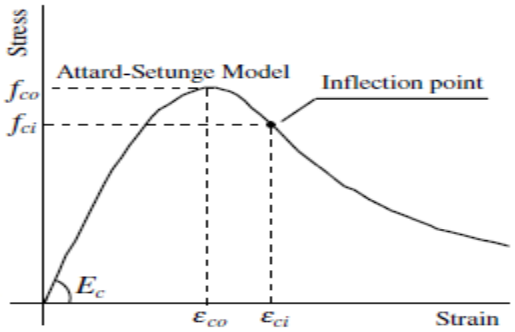

Figure 2.5: Parameters defining stress-strain curve of unconfined concrete (Bai et al., 2007)

The parameters found in the former equations are related to the peak compressive stress of concrete (f_{co}) through the following:

$$E_c = 4370\ (f_{co})^{0.52} \quad | \quad \varepsilon_{co} = \frac{4.11\ (f_{co})^{0.75}}{E_c}$$

$$\frac{f_{ci}}{f_{co}} = 1.41 - 0.17\ ln(f_{co}) \quad | \quad \frac{\varepsilon_{ci}}{\varepsilon_{co}} = 2.50 - 0.30\ ln(f_{co})$$

Where:

E_c = the initial Young's modulus of elasticity

2.4.3.1.2 Mander Unconfined Concrete Model

The second model presented in this work is also selected based on its applicability towards a broad range of concrete strengths, but is primarily chosen based on the limitations of SAP2000 with regard to the pre-programmed unconfined concrete models made available for analysis.

As developed by Mander and pre-programmed into SAP2000 for use in describing the stress-strain relationship of unconfined concrete, this concrete model describes the Mander unconfined stress-strain compression curve consisting of a curved portion and a linear portion.

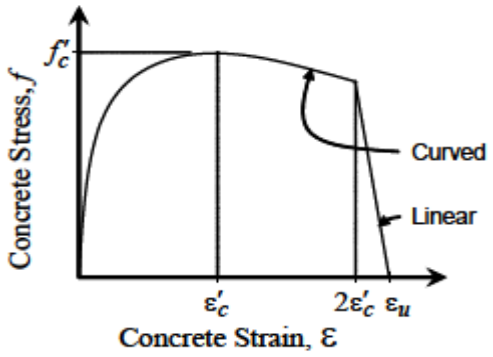

Figure 2.6: SAP2000 Mander Unconfined Concrete Stress-Strain Curve

For the unconfined concrete stress-strain curve where $\varepsilon_c \leq 2\varepsilon'_c$, the following equation describes the curved portion of the graph:

$$f = \frac{f'_c \, x \, r}{r - 1 + x^r}$$

Where:

f = the concrete stress

ε_c = the concrete strain

f'_c = the concrete compressive strength

ε'_c = the concrete compressive strain at f'_c

For the unconfined concrete stress-strain curve where $2\varepsilon'_c < \varepsilon_c \leq \varepsilon_u$, the following equation describes the linear portion of the graph:

$$f = \left(\frac{2 \, f'_c \, r}{r - 1 + 2^r}\right)\left(\frac{\varepsilon_u - \varepsilon_c}{\varepsilon_u - 2 \, \varepsilon'_c}\right)$$

Where:

ε_u = the ultimate concrete strain capacity

The variables x and r are described by the following equations:

$$x = \frac{\varepsilon_c}{\varepsilon'_c} \qquad | \qquad r = \frac{E_c}{E_c - \frac{f'_c}{\varepsilon'_c}}$$

Where:

E_c = the initial Young's modulus of elasticity

It should be noted that the post-cracking resistance in tension is neglected in developing the stress-strain curve for unconfined concrete in both the models previously described. For analysis purposes, members subjected to lateral loading require effective resistance in their compressive states, where concrete portrays relatively high compressive strength opposed to its significantly lower tensile strength. Moreover, the literature described assumes compressive stresses and strains of concrete to be positive for the sake of convenience.

2.4.3.2 Confined Concrete Model

The accurate development of stress-strain behavior for confined concrete is crucial in developing reliable moment-curvature relationships with respect to the available ductility from reinforced concrete members containing transverse reinforcement. As the appropriate stress-strain curves and moment-curvature relationships are established, an element by element behavioral response is acquired in order to appropriately model structural elements with reasonable plastic rotational capacities simulating those exhibited by the members of the actual structure.

2.4.3.2.1 Characteristics of Confinement

A concrete member is deemed confined with the presence of transverse reinforcement in the form of hoop ties or spirals which prevent lateral swelling of concrete in the member when subjected to axial compression. The following describes the general characteristics of confinement:

Advantages of Confinement

By confining structural elements, there are two main advantages with regard to their seismic behavior:

1. *Confinement increases the strength of concrete*. This is especially favorable for compensating possible losses caused by spalling, which is attributed to the failure of the concrete cover in a structural element.

2. *Confinement increases the ductility of concrete*. This effect of transverse reinforcement is imperative to the notion of confinement as confined structural elements experience a reduction in the slope of the descending branch of the stress-strain curve. This reduction in slope of the descending branch of the stress-strain curve allows for an increase in the maximum usable strain to values superseding the 0.3% accepted by the ACI 318M (2002) Code for flexural design.

Types of Confinement

Various experimental investigations confirm that circular spirals used for confinement are generally more effective in confining sections than square or rectangular hoops (Penelis et al., 1997). Confinement by circular spirals can lead to a comparable behavior caused by a moderate hydrostatic pressure, as shown in Figure 2.7.

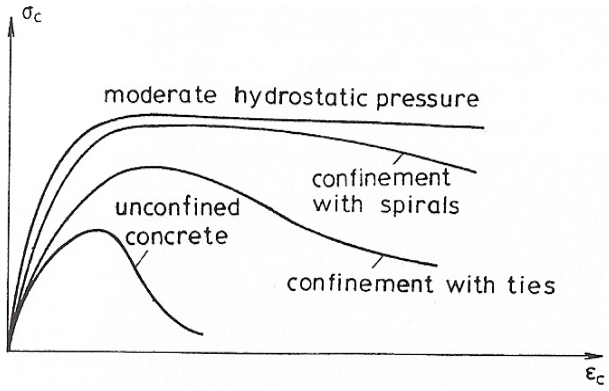

Figure 2.7: Stress-strain diagrams for concrete subjected to various types of confinement (Penelis et al., 1997)

Circular spirals are subjected to hoop tension due to their shape, thereby creating uninterrupted confining pressures along its circumference, as shown in Figure 2.8 (a). In comparison, substantial amounts of pressure can be produced by square or rectangular hoops at their corners, where an outward deflection of the hoop legs is caused by the lateral expansion of concrete thereby creating unconfined regions in the concrete. This concept is illustrated in Figure 2.8 (b).

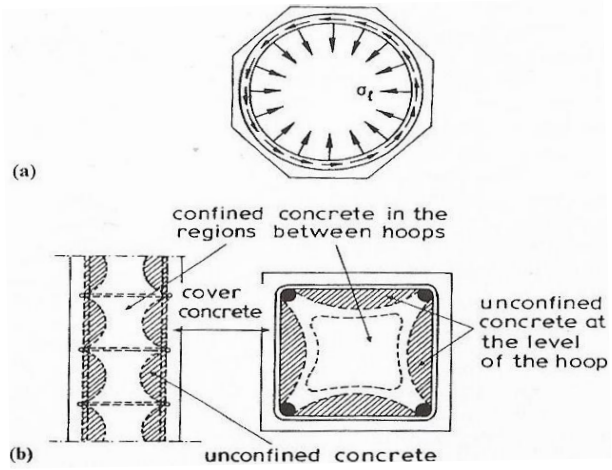

Figure 2.8: Common types of confinement: (a) with circular spiral; (b) with rectangular hoops (Penelis et al., 1997)

Parameters Affecting Confinement

The issues attributed to confinement are mainly affected by the parameters that follow:

1. *Ratio of transverse reinforcement*. This ratio is generally expressed in the form of a volumetric ratio, ρ_w, which is defined as the ratio of the volume of hoops to the volume of the confined concrete core of a structural element. By reasonably increasing the volumetric ratio of a confined concrete member, its strength and ductility thereby increase.

2. *Yield strength of transverse reinforcement*. By increasing the strength of the transverse reinforcement within a confined concrete member, there follows an increase in the confining pressure the stirrups can exert on the confined concrete.

3. *Compressive strength of concrete*. Placed under axial loading, lower strength concrete exhibits greater ductility, and consequently greater lateral expansions, than higher strength concrete. Due to a greater lateral bulge in members with lower strength concrete, confining such concrete anticipates increased efficiency opposed to higher strength concrete since the confining hoops experience higher stresses upon lateral expansion.

4. *Spacing of hoops*. The efficiency of confinement is increased with closer spacing of hoop-ties for a given volumetric ratio of hoops, which occurs due to regions of members remaining unconfined decreasing in size. Under compressive loading, closely spaced stirrups boast a favorable effect on the concrete by increasing its ductility capacity. An increase in ductility develops since after spalling of the concrete cover, closely spaced stirrups prevent the premature buckling of longitudinal reinforcement. The unconfined regions are illustrated in Figure 2.8 (b).

5. *Hoop pattern*. Confined concrete featuring a multiple hoop pattern exhibits smaller regions of effectively unconfined concrete, thereby increasing its strength and ductility capacities.

6. *Longitudinal reinforcement*. To a certain extent, closely spaced longitudinal bars contribute to the prevention of lateral expansion in the confined core, thereby increasing the confinement effects. In addition, the use of larger diameter bars increases the confinement ratio, which further contributes to the favorable effects of confinement.

2.4.3.2.2 Analytical Models for Confined Concrete

This section presents three analytical models from Sheikh and Yeh (1992) targeting theoretical stress-strain relationships for confined concrete.

Modified Kent and Park Model

The original model considers the ascending branch of the stress-strain curve for concrete to be unaffected by confinement, and describes the slope of the descending branch as a function of the amount of lateral steel and the ratio between core width and tie spacing. This earlier model for concrete confined by rectangular transverse reinforcement neglects the increase in concrete strength but takes into account the increase in ductility due to rectangular confining steel.

Later modified, the model allows for the enhancement of concrete strength and peak strain due to confinement. For the descending branch of the curve, the slope remains the same as that of the original model up to 20% of the maximum stress and follows a horizontal line thereafter on the curve.

Sheikh and Uzumeri Model

This model assumes the effectively confined concrete area being less than the core area, which is determined by the distribution of longitudinal steel, tie configuration and tie spacing.

As the model is based on specimens using strength of concrete in the order of 28 MPa, a more general equation modifying the model was later suggested to account for varying concrete strengths. The general equation creates the possibility to use a second-order parabolic equation representing the unconfined and confined concrete ascending branches of the stress-strain curves without affecting the initial tangent modulus of elasticity.

Fafitis and Shah Model

This model is based on the experimental results of tests conducted on small-diameter concrete cylinders and proposes equations representing stress-strain curves for confined and unconfined concrete. Within the set of proposed equations, the confinement parameters pose no effects on the initial tangent of the curve (initial modulus of elasticity). The proposed equations not only affect the peak-point stress and strain values, but also determine the shape of the descending branch of the stress-strain curve.

2.4.3.2.3 Mander Confined Concrete Model

In describing the stress-strain relationship of confined concrete, several constitutive models were investigated to appropriately select the determining confined concrete model to be used for structural members throughout the height of the building. Among the constitutive models of confined concrete investigated, as well as the limitations SAP2000 poses in regard to the pre-programmed confined concrete models made available for analysis, the Mander Confined Concrete Model is used for the purpose of this work. The research presented is adopted from Mander et al., (1988).

The Basic Equation for Monotonic Compression Loading

Presented is a unified stress-strain approach for confined concrete with rectangular shaped transverse reinforcement as proposed by Mander. Based on an equation suggested by Popovics (Mander et al., 1988), the proposed stress-strain model for confined and unconfined concrete under monotonic loading is illustrated in Figure 2.9.

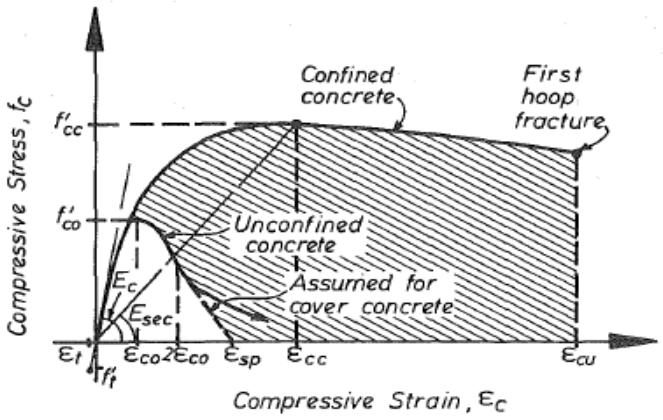

Figure 2.9: Mander Stress-Strain Model (Mander et al., 1988)

The longitudinal compressive concrete stress (f_c) for a slow, quasi-static strain rate and monotonic loading is given by:

$$f_c = \frac{f'_{cc}\, x\, r}{r - 1 + x^r}$$

Where:

f'_{cc} = compressive strength of confined concrete

The variable x is given by:

$$x = \frac{\varepsilon_c}{\varepsilon_{cc}}$$

Where:

ε_c = longitudinal compressive concrete strain

The strain at maximum concrete stress (f'_{cc}) is given by:

$$\varepsilon_{cc} = \varepsilon_{co}\left[1 + 5\left(\frac{f'_{cc}}{f'_{co}} - 1\right)\right]$$

Where:

f'_{co} = the unconfined concrete strength

ε_{co} = the unconfined concrete strain

The variable r is given by:

$$r = \frac{E_c}{E_c - E_{sec}}$$

The secant modulus of confined concrete at peak stress is given to be:

$$E_{sec} = \frac{f'_{cc}}{\varepsilon_{cc}}$$

The behavior of the concrete cover follows the trend of the falling branch of the stress-strain curve in the region where $\varepsilon_c > 2\,\varepsilon_{co}$ is assumed as a straight line reaching zero stress at the spalling strain (ε_{sp}).

Effective Lateral Confining Pressure and the Confinement Effectiveness Coefficient

The maximum pressure from the confining transverse reinforcement is effectively exerted on the section of the concrete core where, due to arching action, the confining stress has fully developed. As the arching action is assumed to act with an initial tangent slope of 45°, it assumes the form of second-degree parabolas where arching occurs between longitudinal bars horizontally, and between layers of transverse reinforcement bars vertically. Shown in Figure 2.10 is the effectively confined area of concrete where the arching action is assumed to occur between levels of rectangular hoop reinforcement.

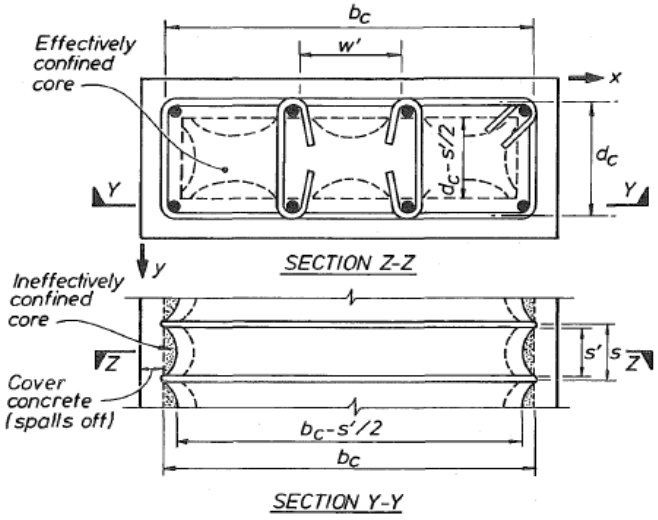

Figure 2.10: Effectively Confined Core for Rectangular Hoop Reinforcement (Mander et al., 1988)

In using the stress-strain relationship for determining the ductility and strength of reinforced concrete columns it is assumed that the area bound within the centerlines of the perimeter hoop (excluding the area of longitudinal steel), A_{cc}, is the concrete area considered to be confined. The effective lateral confining pressure is taken as:

$$f'_l = f_l \, k_e$$

Which allows for $A_{cc} > A_e$, where the lateral pressure from transverse reinforcement, f_l, is assumed to be uniformly distributed over the surface of the concrete cover.

The confinement effectiveness coefficient is given by:

$$k_e = \frac{A_e}{A_{cc}}$$

Where:

A_e = the area of effectively confined concrete core

The area of the concrete core bound by the center lines of the perimeter hoop is given by:

$$A_{cc} = A_c \, (1 - \rho_{cc})$$

Where:

ρ_{cc} = the ratio of area of longitudinal reinforcement to the area of core of section

A_c = the area of core of section enclosed by the center lines of the perimeter hoop

Confinement Effectiveness for Rectangular Concrete Sections Confined by Hoops

The effectively confined area of concrete can be found by subtracting the parabolic areas containing the ineffectively confined concrete at hoop level. The total plan area of ineffectually confined core concrete at hoop level, with n longitudinal bars and w'_i being the i^{th} clear distance between longitudinal bars, is given as:

$$A_i = \sum_{i=1}^{n} \frac{(w'_i)^2}{6}$$

Where $\frac{(w'_i)^2}{6}$ is the ineffectual area of unconfined concrete at hoop level for one parabola.

The area of effectively confined concrete core between hoop levels at midway is given as:

$$A_e = \left(b_c d_c - \sum_{i=1}^{n} \frac{(w'_i)^2}{6}\right)\left(1 - \frac{s'}{2b_c}\right)\left(1 - \frac{s'}{2d_c}\right)$$

Where:

$b_c \geq d_c$

b_c = core dimension to centerline of perimeter hoop in the x-direction

d_c = core dimension to centerline of perimeter hoop in the y-direction

s' = clear vertical spacing between hoop bars

The confinement effectiveness coefficient for rectangular hoops is given by:

$$k_e = \frac{\left(1 - \sum_{i=1}^{n} \frac{(w'_i)^2}{6 b_c d_c}\right)\left(1 - \frac{s'}{2b_c}\right)\left(1 - \frac{s'}{2d_c}\right)}{(1 - \rho_{cc})}$$

As rectangular reinforced concrete members may have varying quantities of transverse confining reinforcement in either the x-or y-directions, these quantities may be given as:

$$\rho_x = \frac{A_{sx}}{s\ d_c} \quad | \quad \rho_y = \frac{A_{sy}}{s\ b_c}$$

Where:

A_{sx} = the total area of transverse bars in the x-direction

A_{sy} = the total area of transverse bars in the y-direction

s = the center to center spacing of hoops

The lateral confining stress on the concrete is depicted by the total transverse bar force of the member divided by the vertical area of confined concrete in the section. The lateral confining stress on the concrete in the x- and y-directions, respectively, is given by:

$$f_{lx} = \frac{A_{sx}}{s\ d_c}\ f_{yh} = \rho_x\ f_{yh} \quad | \quad f_{ly} = \frac{A_{sy}}{s\ b_c}\ f_{yh} = \rho_y\ f_{yh}$$

The effective lateral confining stress in the x- and y-directions, respectively, is given by:

$$f'_{lx} = k_e\ \rho_x\ f_{yh} \quad | \quad f'_{ly} = k_e\ \rho_y\ f_{yh}$$

Compressive Strength of Confined Concrete

As the resulting data of the failure and ultimate strength surfaces provide excellent agreement with triaxial tests, a constitutive model incorporating a specified ultimate strength surface for multiaxial compressive stresses is used to determine the confined compressive strength (Mander et al., 1988).

Under triaxial compression with equal lateral confining stresses from transverse reinforcement, the confined concrete core exhibits confined compressive strength given as:

$$f'_{cc} = f'_{co}\left(-1.254 + 2.254\sqrt{1 + \frac{7.94f'_l}{f'_{co}}} - 2\frac{f'_l}{f'_{co}}\right)$$

Where:

f'_{co} = the unconfined concrete compressive strength

The multiaxial failure criterion general solution, given in terms of the two lateral confining stresses, is shown in Figure 2.11. By following the figure using the largest and smallest confining stress ratios, the compressive strength of the confined concrete can be found.

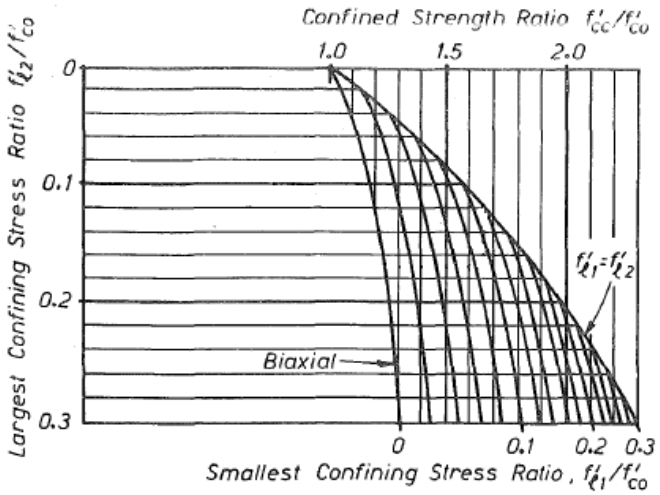

Figure 2.11: Confined Strength Determination from Lateral Confining Stresses for Rectangular Sections (Mander et al., 1988)

It is noted that the literature described in the Mander Confined Concrete Model assumes compressive stresses and strains of concrete to be positive for the sake of convenience.

2.4.3.3 Reinforcing Steel

This section presents the main requirements of reinforcing steel used in reinforced concrete for seismic performance.

2.4.3.3.1 Reinforcing Steel Main Requirements for Seismic Performance

Earthquake-resistant structures detailing concrete members reinforced with steel bars comprise the following main requirements for steel, as adopted from Penelis et al. (1997):

The Ultimate Strain of Steel

In ensuring that a reinforced concrete structural member has sufficient ductility, the ultimate strain of steel (ε_{su}) has to be suitably large. As the ultimate deformation of reinforcing steel is 12% or more (Penelis et al., 1997), the ultimate strain of steel tends to decrease as the steel yield strength increases.

The Actual Yield Stress of Steel

In regard to the actual yield stress (f_y) of the reinforcing steel, a significant increase in its specified value causes an increase in the resistance of structural members. Structural members with such an increase in their resistance result with higher shear forces, which significantly reduce the ductility of members, and consequently, exhibit an unfavorable effect on the seismic behavior of reinforced concrete members. Furthermore, a large increase in the yield stress of reinforcing steel beyond its specified value facilitates the development of higher moments in the member, and consequently may induce the undesirable formation of plastic hinges in the member.

Strain Hardening in Steel

Strain hardening in steel allows for the development of bending moments higher than those exhibited by the first yielding of reinforcing bars at sections exceeding the critical one. Through an increase in the development of bending moments, strain hardening generally creates a favorable effect in regard to the seismic behavior of plastic hinge zones thereby providing for a more dispersed arrangement of plastic hinges in larger parts of the member.

Composite Action of Steel and Concrete

The presence of reinforcing steel bars in earthquake-resistant structural elements must create an efficient and favorable composite action with its surrounding concrete, even in plastic hinge regions where the development of inelastic deformations result from earthquake-induced cyclic loading. The composite action of concrete and steel should be ensured through the bond of the two materials; the adequacy of bond conditions between the steel and concrete materials reflect the satisfactory seismic performance of reinforced concrete structural members.

CHAPTER 3 - BUILDING CONFIGURATION

3.1 Building Specifications

The preliminary structure presented throughout this work consists of a pre-modeled 88-storey high-rise building standing 300.4 m in height. The structure is pre-designed and provided by structural drawings for use within the purpose of this research. The designed full scale model is shown in Figure 3.1.

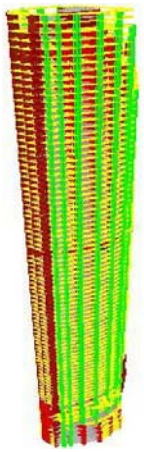

Figure 3.1: ETABS full scale preliminary model

The preliminary building model extends from the 76th floor down to the 3rd basement level with mechanical floors found between storey levels as shown in Table 3.1.

Table 3.1: Mechanical floors between storey levels

Storey Range	Mechanical Floor
L72 – L71	L71A
L41 – L40	L40A
L2 – L1	L1A
L1 – P4	P4A
P4 – P3	P3M

The model features varying storey heights at some of its floor levels throughout the elevation of the building. Table 3.2 shows the heights of these floor levels expressed through their respective storey ranges.

Table 3.2: Storey heights and respective storey ranges

Storey Range	Storey Height (m)
L76	3.0
L75	3.8
L74 – L3	3.3
L2 – L1A	3.0
L1 – P4A	4.8
P4 – P3M	4.5
P3 – P2	5.5
P1	4.5
B1 – B3	3.1

The designed structure details several structural elements comprising the general framework of its design. The plan view of a typical storey of the structure found on the 3rd floor is shown in Figure 3.2.

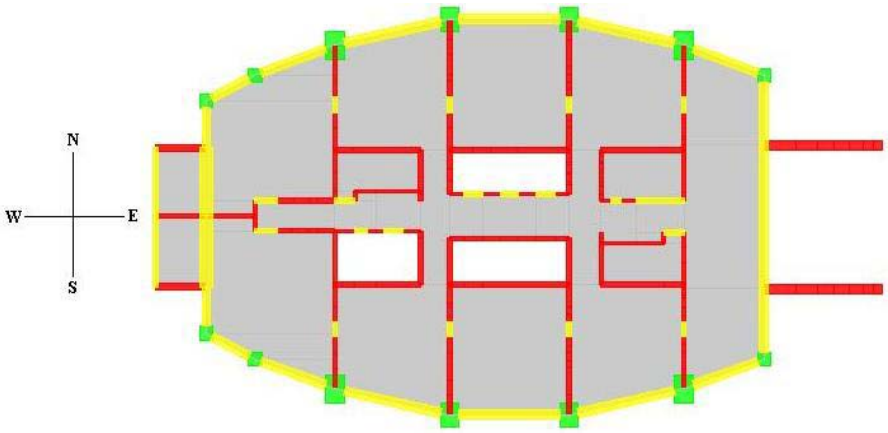

Figure 3.2: L3 - Typical Storey Plan View

As seen in Figure 3.2, each typical floor level details a total of six boxed core walls functioning as shear walls, which serve as the lateral force resisting systems of the structure under dynamic

loading. The structural elements found within the preliminary model are column members, coupling beam members, shear wall members, peripheral beam members, slab members and wall members. Examples of these structural elements are shown in Figure 3.3 for an alienated boxed core wall located centrally at the bottom of the floor plan in the 3rd storey level of the building.

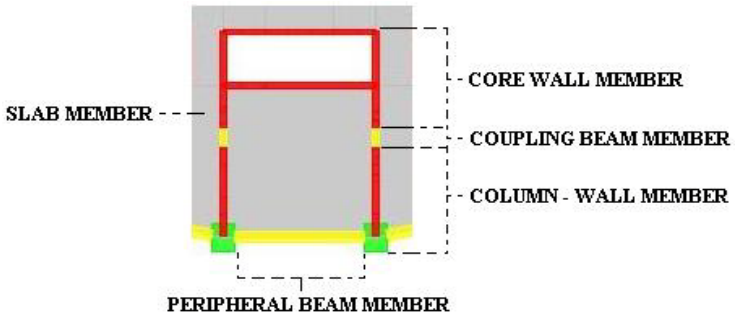

Figure 3.3: L3 - Plan view of central bottom core detailing structural elements

Within the material specifications of the structural elements, the column members, coupling beam members, shear wall members and wall members are all designed using high strength concrete with a specified compressive strength of 85 MPa. The peripheral beam members and slab members are designed using high strength concrete with a specified compressive strength of 40 MPa. The reinforcing steel yield strength is specified at 460 MPa with a reinforcing steel modulus of 200 000 MPa.

3.2 Design Specifications

In accordance to the design specifications, the following section provides an overview of the concepts considered in the design of the tower.

Usage

The following table presents the architects designated usage for each area:

Table 3.3: Architects Designated Usage per Area

Location	Usage
Basement	Car Park, Water storage, Plant
Podium Level 1	Retail, Pools, Loading docks, Supermarket, F&B, Landscaping
Podium Level 2	Retail, F&B, Ramps, Landscaping. Plant
Podium Level 3	Retail, F&B, Ramps, Landscaping. Lobbies
Podium Level 3M	Wet & Dry Gymnasium, Sauna, Spas
Podium Level 4	Ballroom, Function Rooms, Kitchen, BOH
Tower	Apartments, Plant Levels

Storey Heights

The following table presents the typical storey heights proposed for each location:

Table 3.4: Proposed Typical Storey Heights per Location

Location	Storey Height (mm)
Basement	3100
Podium Level 1	4500
Podium Level 2	5500
Podium Level 3	5500
Podium Level 3M	4500
Podium Level 4	4500
Tower	3300

Number of Floors

The number of stories above Podium Level P4 indicated by the design specifications totals eighty floors.

3.3 Design Criteria

Design Standards

Within the design specifications, the Uniform Building Code (1997) and the ACI 318M (2002) are used for seismic design and detailing.

Material Densities

The following material densities are indicated according to design specifications:

Table 3.5: Material Densities according to Design Specifications

Material	Density (kN/m^3)
Blockwork (core filled)	22.0
Blockwork (lightweight)	8.00
Clay Blocks	6.50
Concrete (reinforced)	24.5
Concrete (lightweight)	15.0
Steel	78.5
Grout	24.0

Design Superimposed Dead Loads

The following table presents the design superimposed dead loads according to design specifications:

Table 3.6: Superimposed Dead Loads according to Design Specifications

Location		Superimposed Dead Load (KPa)
Ceiling & Services	Retail Apartments Car Park Plant Rooms	0.8 (0.3 ceiling, 0.5 services) 0.3 (0.1 ceiling, 0.2 services) 0.3 (services) 0.3 (0.1 ceiling under, 0.2 services under)
Finishes	Retail Apartments Car Park Plant Rooms Roof-Trafficable Terraces	1.9 (80 mm total screed / tile thickness) 1.5 (60 mm total screed / tile thickness) 0.3 2.4 3.6
Internal Wall Partition	Tower Stud Partitions	2.3 1.0
Glazed Façade		0.5
Masonry Partitions		3.0

Design Live Loads

The following table presents the design live loads according to design specifications:

Table 3.7: Design Live Loads according to Design Specifications

Location	Live Load (KPa, unless shown otherwise)
Apartments	2.00
Apartment Balconies	4.00
Bathrooms	2.00
Common Areas / Corridors	4.00
Compactus Zones	10.0
General Filing	5.00
Plant Rooms	7.50
Non-Trafficable Roof	0.60
Trafficable Roof	5.00
Water Storage	10.0 kN/m^3
Lightweight Soil Loads	9.00 kN/m^3
Retail	5.00
Car Park	3.00
Roadways	15.0 slabs, 10.0 beams & vertical elements

Lateral Loading

1. *Wind Loading*. The wind loading for the high-rise tower is assessed by means of a series of aerolastic wind tunnel tests which measures the forces acting on the tower. The podium is considered rigidly connected to the tower with movement joints, and the vertical column elements are generally considered in a non-sway mode.

2. *Seismic Loading*. All seismic loads and accidental torsion effects are assessed in accordance with the Uniform Building Code (1997) using the assumed seismic Zone 2A. The design of the structure is carried out in accordance with the UBC (1997) using the following parameters:

Table 3.8: UBC (1997) Design Parameters for Seismic Loading according to Design Specifications

Factor	Value	Notes
Zone	2A	Municipality rating
Z	0.15	Table 16-I
Soil Profile Type	S_c	Very dense soil / soft rock
Ca	0.18	Table 16-Q, UBC (1997)
Cv	0.25	Table 16-R, UBC (1997)
Response Spectrum	UBC 97	Dynamic analysis, Figure 16-3, UBC (1997)
R	5.5	Dual System Shear Wall with OMRF, Table 16-N, UBC (1997)
Occupancy Category	4.0	Standard Occupancy, Table 16-K, UBC (1997)
Importance Factor	1.0	Table 16-J, UBC (1997)

Water Pressures

The basement raft slabs are designed to resist uplift forces due to the ground water pressure, while the basement walls are designed to resist inward loads due to external water pressure.

Thermal Effects

As a result of thermal effects, the movement of the structure is considered in the design of the tower, particularly with respect to the design of movement joints. The thermal effects account for a differential temperature range of 10 – 55 degrees Centigrade.

Load Combinations

The following table presents the ACI 318M (2002) load combinations according to design specifications:

Table 3.9: ACI 318M (2002) Load Combinations according to Design Specifications

Loading	ACI 318M (2002)	Dead Load (D)	Live Load (L)	Superimposed Dead Load (SD)	Wind Load (W) $+M_x$ peak / M_y mean	Temperature (T)
D + SD	Comb 1	1.0	-	1.0	-	-
	Comb 2	1.0	1.6	1.0	-	-
	Comb 3	1.4	-	1.4	-	-
	Comb 4	1.4	1.6	1.4	-	-
D + W	Comb 5	1.0	-	0.5	1.4	-
	Comb 6	1.0	-	0.5	-	-
	Comb 7	1.0	-	0.5	-	-
	Comb 8	1.4	-	1.4	1.4	-
	Comb 9	1.4	-	1.4	-	-
	Comb 10	1.4	-	1.4	-	-
	Comb 11	1.0	-	0.5	-	-
	Comb 12	1.0	-	0.5	-	-
	Comb 13	1.0	-	0.5	-	-
	Comb 14	1.4	-	1.4	-	-
	Comb 15	1.4	-	1.4	-	-
	Comb 16	1.4	-	1.4	-	-
D + SD + W	Comb 17	1.2	1.2	1.2	-	-
	Comb 18	1.2	1.2	1.2	1.2	-
	Comb 19	1.2	1.2	1.2	-	-
D + T	Comb 20	1.4	-	-	-	1.4
D + SD + T	Comb 21	1.2	1.2	1.2	-	1.2

The following table presents the UBC (1997) load combinations according to design specifications:

Table 3.10: UBC (1997) Load Combinations according to Design Specifications

					Response Spectrum		
	Lateral Load Combinations	Dead Load (D)	Live Load (L)	Superimposed Dead Load (SD)	U1 (x)	U2 (y)	U1 + U2
UBC (1997) SPECTRUM	Comb 1	0.9	-	0.5	1.0	-	-
	Comb 2	0.9	-	0.5	-	1.0	-
	Comb 3	0.9	-	0.5	-	-	1.0
	Comb 4	0.9	-	0.5	-1.0	-	-
	Comb 5	0.9	-	0.5	-	-1.0	-
	Comb 6	0.9	-	0.5	-	-	-1.0
	Comb 7	1.2	0.5	1.2	1.0	-	-
	Comb 8	1.2	0.5	1.2	-	1.0	-
	Comb 9	1.2	0.5	1.2	-	-	1.0
	Comb 10	1.2	0.5	1.2	-1.0	-	-
	Comb 11	1.2	0.5	1.2	-	-1.0	-
	Comb 12	1.2	0.5	1.2	-	-	-1.0

Deflection Limits

The following table presents the deflection limits indicated according to design specifications:

Table 3.11: Deflection Limits according to Design Specifications

	Design Criteria-Maximum, under Serviceability Load Case			
Vertical Structure	Dead	Live	Wind (1 in 10 year wind)	Wind (1 in 50 year wind)
Overall Building Sway	-	-	-	$H/500$
Inter-Storey Drift	-	-	$H/500$	-
Non-Trafficable Roof Beams (structural steel)	$L/300$	$L/240$	$L/240$	$L/240$
Differential settlement between adjacent columns	$\frac{\text{COL to COL Dist}}{1000}$	$\frac{\text{COL to COL Dist}}{1000}$	$L/500$	$L/500$

3.4 Selection of Lateral Force Resisting Systems

In order to effectively select the lateral force resisting systems, a frame consisting of several rows of wall, column and beam members typically found ranging the elevation of the structure are chosen as reinforced concrete shear wall systems.

The following sections present the selected framing systems in the coupled and uncoupled directions. Throughout the work presented in this research, the y-direction (spanning North to South) and the x-direction (spanning East to West) are referred to as the coupled and uncoupled directions respectively.

3.4.1 Shear Wall System in the Coupled Direction

In the coupled direction, the selected shear wall systems serving as lateral force resisting frames are shown in Figure 3.4 for Podium Level 4 of the building.

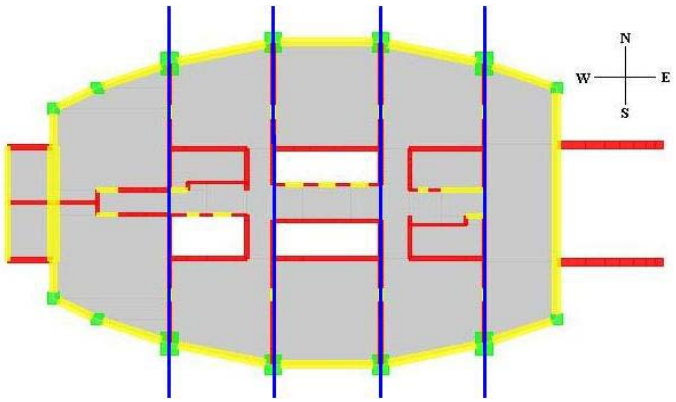

Figure 3.4: Shear wall systems in the coupled direction at Level P4

In order to appropriately illustrate the shear wall systems in the coupled direction, shown in Figure 3.5 is an elevation view spanning the 3rd to the 14th storey levels.

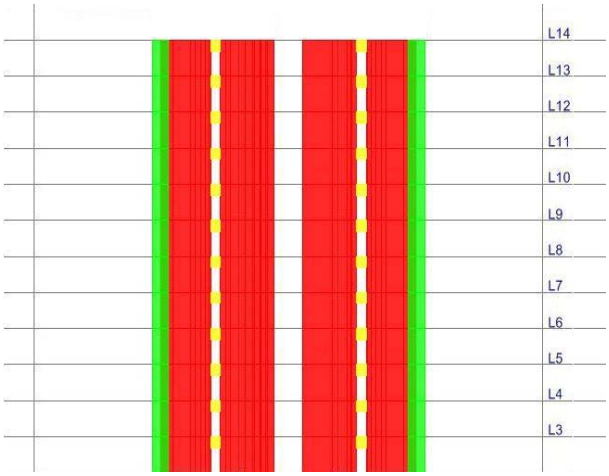

Figure 3.5: Coupled direction elevation view spanning L3 to L14

In this direction, the structure provides resistance to all local gravity loads and dynamic loads using the two sets of core walls coupled by connecting beams.

3.4.2 Shear Wall System in the Uncoupled Direction

In the uncoupled direction, the selected shear wall systems serving as lateral force resisting frames are shown in Figure 3.6 for Podium Level 4 of the building.

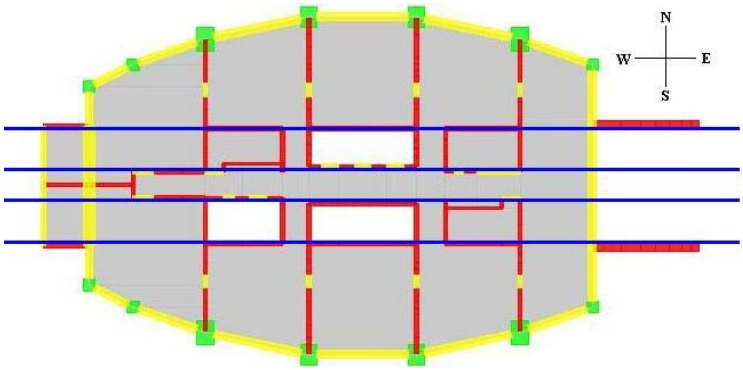

Figure 3.6: Shear wall systems in the uncoupled direction at Level P4

In order to appropriately illustrate the shear wall systems in the uncoupled direction, shown in Figure 3.7 is an elevation view spanning the 3rd to the 14th storey levels.

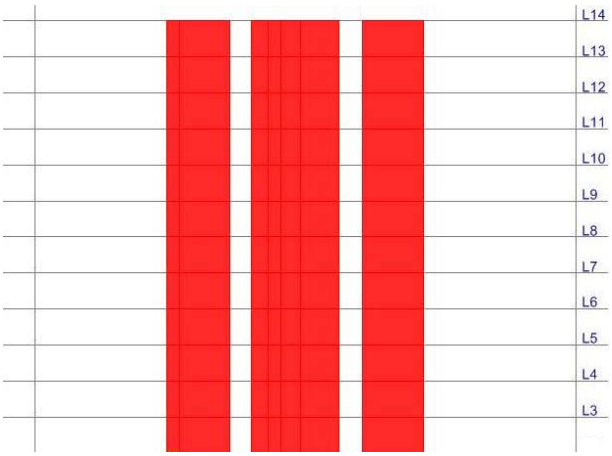

Figure 3.7: Uncoupled direction elevation view spanning L3 to L14

In this direction, the structure provides resistance to all local gravity loads and dynamic loads using the three core walls acting as cantilevers.

3.5 ETABS Modeling

In order to successfully analyze the building for lateral loading effects, the structure is appropriately modeled in ETABS according to the structural drawings of the building. While modeling the structure, a framing procedure used to create shear wall systems in the model is incorporated as discussed in the previous sections of this chapter.

Throughout the framing procedure, a frame consistent with the structural drawings is chosen as reinforced concrete shear wall systems over the entire height of the structure. Once selected, the ETABS modeling involves a process of using horizontal and vertical basic line elements to model walls, columns and beams. The ETABS model features identical floor plan configurations, member dimensions and material properties as those required by the structural drawings of the building.

3.5.1 Modeling in the Coupled Direction

To further illustrate the mechanics of modeling in ETABS, a sample elevation view in the coupled direction is shown in Figure 3.8.

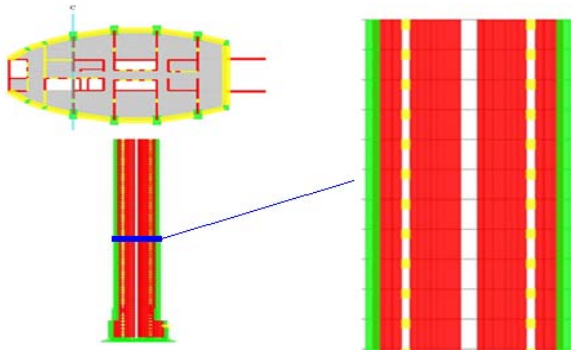

Figure 3.8: ETABS Model Coupled Direction Elevation View (C)

As seen in Figure 3.8, the modeled building incorporates uniform arrangements of columns, walls and coupling beams throughout the height of the structure in the coupled direction.

3.5.2 Modeling in the Uncoupled Direction

To further illustrate the mechanics of modeling in ETABS, a sample elevation view in the uncoupled direction is shown in Figure 3.9.

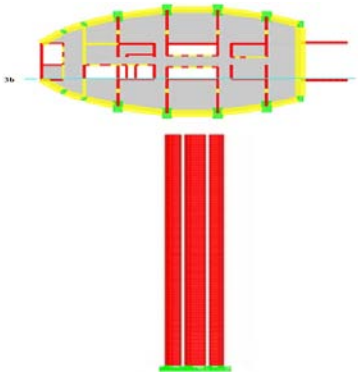

Figure 3.9: ETABS Model Uncoupled Direction Elevation View (3b)

As seen in Figure 3.9, the modeled building incorporates a uniform arrangement of walls throughout the height of the structure in the uncoupled direction.

By creating a replica of the building using the structural drawings, the ETABS model boasts matching material properties, dimensions and floor plan configurations to the original building at all storey levels of the structure.

CHAPTER 4 - SEISMIC DETAILING AND MODELING FOR ANALYSES

4.1 Shear Wall Structure Modeling

The primary modeling stages involve replicating the model provided by structural drawings for use in SAP2000. The model is initially analyzed in ETABS for static gravity loads using the load combination:

$$\sum (\text{DL} + \text{SDL} + 0.25\ \text{LL})$$

Where:

DL = Dead Load

SDL = Superimposed Dead Load

LL = Live Load

An assumption of 25% live load affecting the structure during a seismic event is made based on researched literature and found to be consistent with design practice. Following the analysis of the structure, ETABS provides the base reactions of the building and the axial loads found acting on structural members. The axial load acting on a member in any given storey level represents the cumulative static load applied to the member by the floors above. Targeted floors used to re-construct the building model on SAP2000 are exported and the cumulative floor weight of the structural members in every targeted storey is determined from the base reactions of the analysis results. ETABS also provides options for displaying the forces acting on elements in the model. Using the load combination previously described, the forces corresponding to the loads are displayed on the line elements when spanning loads tributary to that particular element. As such, results for the static gravity loads acting tributary to each individual element are acquired. These loads acting directly on and tributary to the individual elements are incorporated into the completed SAP2000 model to replicate the distribution of static gravity loads and members weights from the ETABS building model. Section 4.2 provides detail on the procedure used in distributing static gravity loads while modeling the structural members.

The building is modeled on SAP2000 using vertical frame elements linked by weightless rigid members in the horizontal direction, for which the rigid member is defined with an exceedingly large moment of inertia. By defining a sizeable moment of inertia, the rigid member maintains no bending stiffness and only transfers axial loads. Using this modeling technique, the vertical frame elements linked with the rigid members create a unified floor model per building storey, which consequently permits the individual structural members to move together under lateral loading. The weightless definition of the rigid member ensures that no additional mass is contributed to the structure.

The lateral force resisting system of the building is modeled with a total of six boxed core assemblies running over the height of the building, which function as the shear wall systems. As seen in Figure 3.3 for the coupled direction, the boxed cores are connected to adjacent column-wall members using coupling beams, which results in the formation of two sets of core walls. From an elevation perspective as presented in Figure 3.5, the coupled direction features each set of core walls as two shear walls connected by coupling beams at storey levels, totaling into four shear walls extending over the height of the building. As shown in Figure 3.7 for the uncoupled direction, the core walls form three separated shear walls from an elevation perspective, where the walls behave as cantilevers in resisting all static gravity loads and dynamic loads.

For effectively modeling the building in its entirety, the second podium, third and thirty-sixth storey levels are chosen and accurately modeled according to structural drawings. Within the specified reinforcing details, the second podium level details similar reinforcement in members found from the third basement level to the second floor level; the third floor level details similar reinforcement in members found from the third floor level to the thirty-fifth floor level; and the thirty-sixth floor level details similar reinforcement in members found from the thirty-sixth floor level to the seventy-sixth floor level. These storey levels are selected based on the changes in reinforcement at these floors presented by the structural drawings of the building. Moreover, the three storey levels selected present floor plan configurations which change in cross-section with respect to one another, but are found to be similar in floor plan configurations to other storeys throughout the height of the building. Table 4.1 presents the storey levels representative of other similar storeys in the structure.

Table 4.1: Storey levels representing similar storeys in the building

Representative Storey Level	Similar Storey Levels
P2	B3 – L2
L3	L3 – L35
L36	L36 – L76

The structural members throughout the height of the building remain unchanged in terms of material properties, member dimensions and floor plan locations. Most importantly, the structural members forming the shear wall system remain unaltered in material properties or floor plan location over the height of the building. Following the complete modeling of the representative storey levels, each of the three aforementioned storey levels are entirely replicated to build their corresponding similar floor levels, and consequently form the floors in the overall building.

4.2 Structural Elements Modeling

In the modeling of structural members, the same basic elements are used to model the wall, column and beam members. Each structural member is individually modeled using Section Designer and detailed according to the structural drawings of the pre-designed building. Placement of the members is performed using SAP2000, where the members are placed into the floor model at their respective center of masses in accordance to the framing plan of the pre-designed building. After placing the structural members in the floor plan, they are rotated with the axes of their local coordinate systems pointing in the same direction. The accurate placement of modeled members at their center of masses helps prevent accidental lateral eccentricities caused by the location of individual members with respect to the floor model. As such eccentricities would cause torsional problems in floor responses throughout the tower when excited with seismic ground motions, this methodology permits for an effective overall building model for use in a dynamic analysis.

The wall members comprising the shear wall systems are modeled in Section Designer as assembled units of walls forming boxed cores. To further illustrate the modeling of the wall members creating boxed core sections, Figure 4.1 presents the plan view of a central boxed core at the third storey level, located towards the bottom of the floor plan.

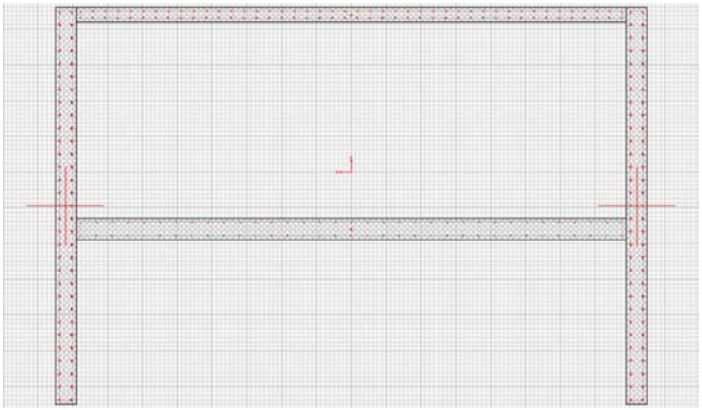

Figure 4.1: L3 - Section Designer Plan View of central bottom boxed core assembly

As seen in Figure 4.1, the boxed core section consists of four wall members designed as an assembled unit. This assembled unit is placed in SAP2000 at its center of mass into the floor plan. SAP2000 then represents the assembled boxed core as a single vertical line element. As described in the previous section, the vertical line element is then linked by weightless rigid members in the horizontal direction. This procedure is used in creating all six boxed cores in the floor plan, where the individual walls forming these boxed cores craft the shear wall systems in the coupled and uncoupled directions that extend over the height of the building.

The remaining structural components of the building include coupling beams, column members, peripheral beams and slabs. Aside from the slabs, the remaining structural components are modeled using the same methodology described for the boxed core wall assemblies. The coupling beam members are modeled in Section Designer and then placed into SAP2000 as horizontal line elements attached to rigid members that connect the boxed core assemblies on one side, and connect adjacent column-wall members on its other side. The column members are modeled in Section Designer and then placed into SAP2000 as basic vertical line elements at their center of masses. They are then framed to structural members in the floor plan using rigid

members. The peripheral beams, also modeled using Section Designer, are placed into SAP2000 as horizontal line elements that span each column member around the floor plan. All the structural components included in the SAP2000 model are placed at the exact nodal coordinates they are found in the ETABS model. The overall floor model designed in SAP2000 for the third storey level is similar to that shown in Figure 3.2.

In order to reduce analysis time, the slab member from the ETABS model is removed from the floor model of SAP2000. The base reactions and forces acting tributary to individual elements from the ETABS model, as discussed in Section 4.1, are applied to the SAP2000 model. For the horizontal line elements (coupling beams and peripheral beams), the loads are assigned as horizontally distributed loads acting on the rigid members framing the floor plan. The distribution of loads in the SAP2000 model are identical in magnitude and location to the corresponding ETABS model. For the vertical line elements, the loads are assigned in SAP2000 as point loads placed at the end nodes of the structural members at storey levels.

Following the equivalent distribution of loads, the SAP2000 and ETABS models are individually analyzed and the targeted floors are compared for matching floor weights and load distribution of structural elements. The resulting model in SAP2000 features similar floor weights and load distributions of structural elements to the ETABS model. A comparison of the floor weights and their corresponding difference between both models is shown in Table 4.2.

Table 4.2: Targeted storey levels weights and differences

	Floor Weight (kN)		
Floor Level	ETABS	SAP2000	Difference (%)
P2	26064.73	25284.58	3.09
L3	17253.62	16875.04	2.24
L36	17647.30	17434.47	1.22

Furthermore in the modeling of structural elements, moment-curvature relationships are necessary to model the response of the elements under cyclic loading. For the structural elements modeled in the tower, moment-curvature relationships are developed for every individual structural component using Section Designer, and are attributed to both ends of the individual member in SAP2000. The development of moment-curvature relationships requires the definition of concrete models using unconfined or confined concrete. As detailed by the structural drawings, the wall members containing the six boxed core assemblies are modeled using unconfined concrete definitions, while the column, beam and remaining wall members use confined concrete definitions. All the structural members requiring confinement are modeled based on the design drawings detailing a volumetric ratio of confined transverse reinforcement to concrete, ρ_w, of 0.6%. This volumetric confinement value is found consistent in the structural drawings throughout the entire height of the building. Table 4.3 summarizes the concrete grade and its corresponding volumetric confinement percentage used for detailing varying structural members.

Table 4.3: Concrete Grade and corresponding Volumetric Confinement

Structural Member	Concrete Grade (MPa)	Confinement, ρ_w (%)
Column	85	0.6
Wall	85	0.6
Shear Wall	85	unconfined
Coupling Beam	85	0.6
Peripheral Beam	40	0.6
Slab	40	unconfined

In describing the material properties of different concrete grades, isotropic (having equal physical properties along all axes), normal weight concrete materials are introduced to SAP2000 according to the design specifications of the building. In order to effectively determine the modulus of elasticity for each concrete grade, the ACI 318M (2002) Code specifies the equation for normal weight concrete:

Grade 85 Concrete: $E_c = 4700\sqrt{f'_c} = 4700\sqrt{85} \approx 43\,322\ MPa$

Grade 40 Concrete: $E_c = 4700\sqrt{f'_c} = 4700\sqrt{40} \approx 29\,725\ MPa$

The concrete properties introduced into SAP2000 detail the following characteristics for defined concrete grades:

Table 4.4: Concretes Properties

Concrete Grade (MPa)	M/V (Kg/m^3)	W/V (kN/m^3)	E_c (MPa)	ν (m/m)	α ($1/°C$)	f'_c (MPa)	ε_{co} (m/m)	f_{ys} (MPa)
85	2.45	24	43 332	0.2	$9.9\ e^{-6}$	85	$2.613\ e^{-3}$	460
40	2.45	24	29 725	0.2	$9.9\ e^{-6}$	40	$2.197\ e^{-3}$	460

Where:

M/V = mass per unit volume (density)

W/V = weight per unit volume (specific weight)

E_c = Young's modulus of elasticity of concrete

ν = Poisson's ratio

α = coefficient of thermal expansion

f'_c = specified concrete compressive strength

ε_{co} = unconfined concrete strain

f_{ys} = steel reinforcement yield stress

Following the modeling of structural members, the selection of concrete models, the generation and the application of moment-curvature relationships, hysteretic modeling is needed to describe the force-deformation characteristics of modeled members subjected to cyclic load reversals. The following sections describe the procedure used for hysteretic modeling as well as the selection of concrete models.

4.3 Hysteretic Modeling

Following the modeling and placement of structural elements, including their respective distributed loads and point loads assignments, the structural elements are provided with two-joint multilinear plastic links at their nodal ends to define the moment-curvature relationships, and consequently the response, of the elements under cyclic loading.

Within the introduction of the multilinear plastic links, a Hysteresis Type is necessary to define the Hysteretic Model a dynamic analysis requires to describe the force-deformation characteristics of a structural member. For the purpose of analyzing the structure under dynamic loading, the Takeda Hysteresis Type is selected as it efficiently models the strength degradation of reinforced concrete under cyclic loading behavior and offers less computational requirements opposed to other hysteresis models. The general descriptions of Hysteresis Types are provided in Section 2.4.1 of this thesis.

4.3.1 Unconfined Concrete Properties

The Mander Unconfined Concrete Model is used to define stress-strain behaviors, and subsequently moment-curvature relationships, attributed to those structural members detailing unconfined concrete definitions by the structural drawings. The stress-strain curve according to the Mander Unconfined Concrete Model is defined to characterize the behavior of concrete. In determining the peak compressive strain value used in the stress-strain curve definition, the ACI 318M (2002) Code details an assumption for the maximum usable strain at extreme concrete compression fiber to be equal to 0.3%. For a more conservative estimation of the peak compressive strain value with respect to higher strength concretes, the modulus of elasticity of concrete and the unconfined concrete compressive strain are adopted from Bai et al. (2007).

In determining the unconfined concrete strains for higher strength concretes, the modulus of elasticity (E_c) is given from Bai et al. (2007):

$$\text{Grade 85 Concrete:} \quad E_c = 4370\ (f_{co})^{0.52} = 4370\ (85)^{0.52} \approx 44\,033\ MPa$$

Grade 40 Concrete: $E_c = 4370\ (f_{co})^{0.52} = 4370\ (40)^{0.52} \approx 29\ 755\ MPa$

And the unconfined concrete strain (ε_{co}) is given from Bai et al. (2007):

Grade 85 Concrete: $\varepsilon_{co} = \frac{4.11\ (f_{co})^{0.75}}{E_c} = \frac{4.11\ (85)^{0.75}}{44\ 033} \approx 2.613\ x\ 10^{-3}\ {}^{m}/_{m}$

Grade 40 Concrete: $\varepsilon_{co} = \frac{4.11\ (f_{co})^{0.75}}{E_c} = \frac{4.11\ (40)^{0.75}}{29\ 755} \approx 2.197\ x\ 10^{-3}\ {}^{m}/_{m}$

Where:

f_{co} = the in-situ uniaxial compressive strength of concrete

For the purpose of introducing the unconfined concrete stress-strain curve within the defined concrete properties, the ACI 318M (2002) Code considers the strain at which ultimate moments are developed to be in the range of 0.3% to 0.4% for members of normal proportions and materials. As the sections introduced into SAP2000 are modeled as compression-controlled, an assumed value for the ultimate concrete strain capacity is taken as 0.5% (ATC-40, 1996), which details the concrete post-peak failure strain. Table 4.5 summarizes the unconfined concrete properties attributed to reinforced concrete members detailing unconfined sections according to the structural drawings of the building.

Table 4.5: Material Properties for Unconfined Concretes

	E_c (MPa)	f'_{co} (MPa)	ε_{co} ($^{m}/_{m}$)	ε_{sp} ($^{m}/_{m}$)
Grade 85	43 332	85	2.613 e $^{-3}$	5.000 e $^{-3}$
Grade 40	29 725	40	2.197 e $^{-3}$	5.000 e $^{-3}$

Where:

E_c = Young's modulus of elasticity of concrete

f'_{co} = unconfined concrete strength

ε_{co} = unconfined concrete strain

ε_{sp} = spalling strain

After defining the parameters describing the concrete properties and introducing the peak compressive stresses, corresponding peak compressive strains, and ultimate concrete strain capacity values, SAP2000 automatically determines the intermediate stress and strain values, as well as the ultimate concrete stress capacities, according to the Mander Unconfined Concrete Model. The resulting stress-strain curves used in defining the unconfined concrete materials of modeled elements are shown in Figure 4.2.

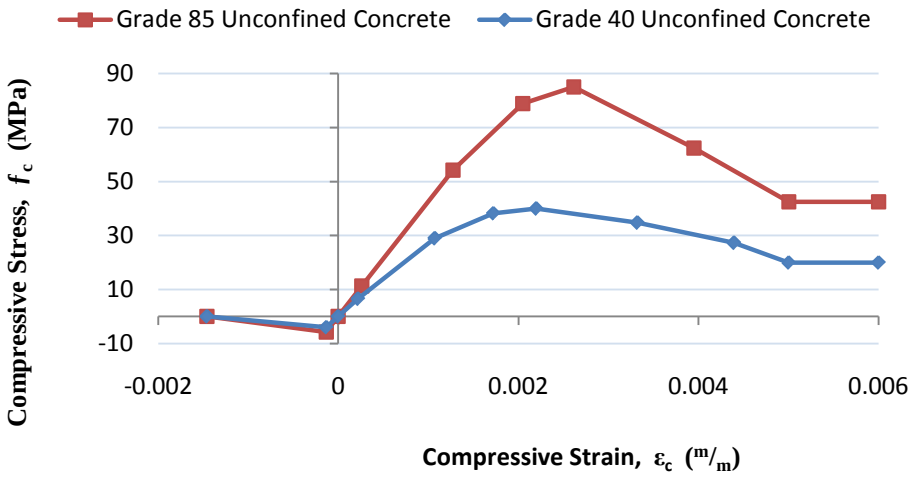

Figure 4.2: Unconfined Concretes Stress-Strain Relationships

The range of $-0.002 \leq \varepsilon_c < 0$ is the post-cracking resistance in tension, which is neglected by Section Designer when developing the stress-strain curves for the Mander Unconfined Concrete Models.

4.3.2 Confined Concrete Properties

The Mander Confined Concrete Model is used to define stress-strain behaviors, and subsequently moment-curvature relationships, attributed to those structural members detailing confined concrete definitions by the structural drawings. Table 4.6 summarizes the confined concrete properties attributed to reinforced concrete members detailing confined sections.

Table 4.6: Material Properties for Confined Concretes

	E_c (MPa)	f'_{cc} (MPa)	ε_{cc} ($^{m}/_{m}$)	f'_{cu} (MPa)	ε_{cu} ($^{m}/_{m}$)
Grade 85	43 332	85	2.613 e $^{-3}$	42.5	5.000 e $^{-3}$
Grade 40	29 725	40	2.197 e $^{-3}$	20	5.000 e $^{-3}$

Where:

E_c = Young's modulus of elasticity of concrete

f'_{cc} = confined concrete strength

ε_{cc} = confined concrete strain

f'_{cu} = confined concrete ultimate strength

ε_{cu} = confined concrete ultimate strain

After defining the parameters describing the concrete properties and introducing the peak compressive stresses, corresponding peak compressive strains, and ultimate concrete strain capacity values, SAP2000 automatically determines the intermediate stress and strain values, as well as the ultimate concrete stress capacities, according to the Mander Confined Concrete Model. The resulting stress-strain curves used in defining the confined concrete materials of modeled elements are provided for two column-wall members in Appendix B of this thesis.

4.3.3 Reinforcing Steel Properties

The steel used for reinforcing concrete members in the structure is applied based on the properties detailed by the BS 4449: 1997 carbon steel bars, as specified by the design specifications of the building.

The BS 4449: 1997 reinforcing steel assumes an elastic behavior until reaching the yield stress of f_{ys} = 460 MPa with a corresponding yield strain of ε_{ys} = 0.0023 $^{m}/_{m}$. The post-yield region remains flat until the onset of strain hardening at ε_{sh} = 0.015 $^{m}/_{m}$. Thereafter, the steel is assumed to reach its ultimate stress at f_{su} = 500 MPa with a corresponding ultimate strain capacity of ε_{su} = 0.14 $^{m}/_{m}$. Young's modulus of elasticity for the steel is specified as E_s = 200 000 MPa. Table 4.7 summarizes the reinforcing steel properties.

Table 4.7: Material Properties for Reinforcing Steel

	E_s (MPa)	f_{ys} (MPa)	ε_{ys} ($^{m}/_{m}$)	f_{su} (MPa)	ε_{su} ($^{m}/_{m}$)	ε_{sh} ($^{m}/_{m}$)
Steel	200 000	460	2.300 e $^{-3}$	500	0.14	0.015

Where:

E_s = Young's modulus of elasticity of steel

f_{ys} = yield stress of steel

ε_{ys} = yield strain of steel

f_{su} = ultimate stress of steel

ε_{su} = ultimate strain of steel

ε_{sh} = strain hardening of steel

Considering the above properties defined in SAP2000 for reinforcing steel, Figure 4.3 presents the reinforcing steel stress-strain relationship provided to the modeled reinforced concrete members in the building.

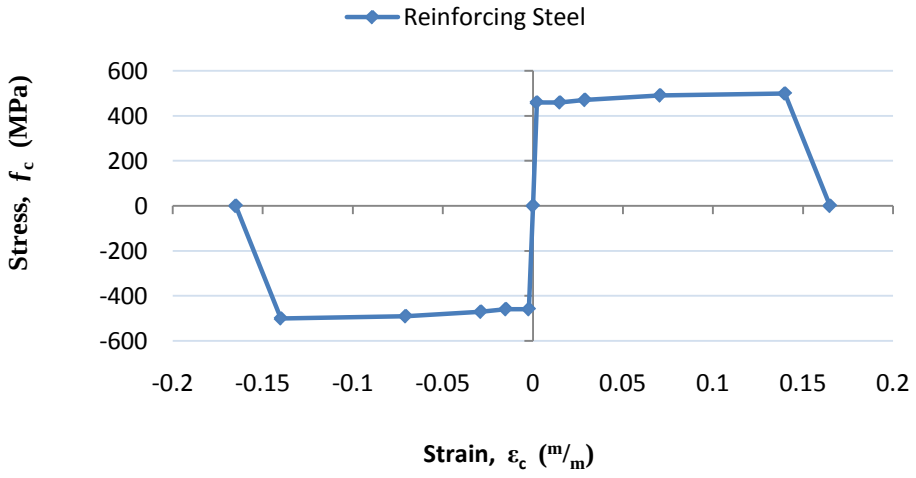

Figure 4.3: Reinforcing Steel Stress-Strain Relationship

4.4 Moment-Curvature Relationships

With the necessary material properties defined, moment-curvature relationships are developed for each structural member in the building using Section Designer. Since the program uses the strain compatibility approach to analyze reinforced concrete sections under constant axial loads, the development of moment-curvature relationships in Section Designer requires input of the axial loads exerted on the structural member.

The required axial loads exerted on structural members at different storeys in the structure are obtained from the building's initial ETABS analysis, as described in Section 4.1 of this thesis. Table 4.8 presents the storey levels of the structure for which the structural members' axial loads are obtained.

Table 4.8: Storey levels with structural members ETABS analysis axial loads

Storey Levels (with obtained ETABS axial loads)
P2
L3
L14
L25
L36
L47
L58
L69

The axial loads are required for use in Section Designer to generate each member's moment-curvature relationship. Upon drawing the section, defining dimensions, defining material properties, detailing reinforcement, defining the concrete model and its confinement definitions, and defining reinforcing steel model definitions, Section Designer provides an option for automatically calculating the section's moment-curvature relationship described by a constant axial load. The axial load value obtained from the initial ETABS analysis for the particular section being modeled is assigned to the program as a constant axial load exerted on the section, and Section Designer subsequently provides the moment-curvature relationship of the modeled section. For analysis purposes, the moment-curvature relationships for all the structural members modeled are obtained in both the x- and y-directions, which represent the uncoupled and coupled directions respectively. The moment-curvature relationship is presented by the program through a moment-curvature graph and its corresponding data points. As described in Section 4.3, each line element in SAP2000 representing a modeled section includes the introduction of two-joint multilinear plastic links that define the response of the section when subjected to dynamic loading. Within the link element definitions, each modeled element's moment-curvature relationship is assigned to its respective link for its appropriate direction. The resulting moment-curvature relationships attributed to the coupled and uncoupled directions for all six boxed core sections, two modeled column-wall members and one modeled coupling beam member are provided in Appendix B of this thesis.

CHAPTER 5 - RESULTS AND DISCUSSION

5.1 Equivalent Static Analysis

This type of analysis assumes the response of the building predominantly controlled by the fundamental mode of the structure. The equivalent static analysis assumes the behavior of the building as a single-degree-of-freedom (SDOF) system responding elastically to an applied lateral force simulating an earthquake. The applied lateral force acting on the structure is defined by the design base shear of the building. This approach applies the design base shear force of the structure at the top of the SDOF system as a single lateral force in a slow and gradual manner until the full magnitude of the design base shear force is achieved. The structural properties of the building are assumed constant and the analysis begins from an unstressed state of the structure. The induced system response is directly proportional to the applied loads and behaves in the linear range where the building retains its original shape and is free of permanent deformations upon load removal. For the static analysis of the building in consideration, the load cases YQUAKE and XQUAKE represent the coupled and uncoupled static equivalent seismic load, respectively.

As pre-programmed into ETABS for a moderate seismic zone and governed by the UBC (1997), the total design base shear, V, in a given direction is determined from the UBC (1997) formula as follows:

$$V = \frac{C_v\, I}{R\, T}\; W$$

Where:

V = total design lateral force or shear at the base

C_v = seismic coefficient given in UBC (1997) Table 16-R = 0.25

I = importance factor given in UBC (1997) Table 16-K = 1.0

R = force modification factor given in UBC (1997) Table 16-N = 5.5

T = structural period of vibration (s) of the building in the considered direction

W = total building weight including 25% live load = 1,653,580 kN

The total design base shear should not exceed the following UBC (1997) formula:

$$V = \frac{2.5\ C_a\ I}{R}\ W$$

Where C_a is the seismic coefficient given in UBC (1997) Table 16-Q, which is 0.18 for this building. The total design base shear shall not be less than the following UBC (1997) formula:

$$V = 0.11\ C_a\ I\ W$$

The structural period, T, is determined according to the UBC (1997) as follows:

$$T = C_t\ (h_n)^{3/4}$$

Where C_t is 0.0488 as program calculated by ETABS according to the UBC (1997) for this reinforced concrete shear wall building system, and h_n is the height above the base to Level n, which is 300.4 m for this building. Given in Table 3.8, the building specifications detail a seismic zone factor, z, of 0.15. As adopted by the ETABS program in accordance with the UBC (1997), when the seismic zone factor does not exceed the value of 0.35, the structural period, T, considered for the calculation of the static equivalent seismic force is taken as $1.4 \cdot T$ for a moderate seismic zone and determined to be 4.93 s for the coupled and uncoupled directions.

Additionally, the vertical distribution of the total force over the height of the structure conforms to the following formula according to the UBC (1997):

$$V = F_t + \sum_{i=1}^{n} F_i$$

Where:

F_t = that portion of the base shear, V, considered concentrated at the top of the structure in addition to F_n

F_i, F_n = Design Seismic Force applied to Level i or n respectively

In addition to F_n, the concentrated force F_t at the top of the structure is determined from the following UBC (1997) formula:

$$F_t = 0.07\,T\,V \leq 0.25\,V$$

In addition to the Design Seismic Force, the portion of the base shear considered concentrated at the top of the structure, F_t, is calculated to be 8,185 kN for this building. The remaining portion of the base shear is distributed according to the UBC (1997) over the height of the structure, inclusive of the nth level, according to the following formula:

$$F_x = \frac{(V - F_t)\,w_x\,h_x}{\sum_{i=1}^{n} w_i\,h_i}$$

Where:

F_x = Design Seismic Force applied to Level x

w_i, w_x = that portion of W located at or assigned to Level i or x respectively

h_i, h_x = height (m) above the base to Level i or x respectively

5.1.1 Equivalent Static Analysis Results

As the building is analyzed in ETABS and subjected to the YQUAKE and XQUAKE equivalent static seismic loads in the coupled and uncoupled directions respectively, the design base shear of the building is calculated to be 1.98% of the total building weight (W), which corresponds to a design base shear, V, of 32,740 kN. The remaining portion of the base shear distributed over the height of the structure, F_x, for each storey level is given in Appendix A of this thesis. The distributed forces at each storey level over the height of the building are readily seen in Appendix C of this thesis.

Under the equivalent static seismic loads YQUAKE and XQUAKE in the coupled and uncoupled directions respectively, the equivalent static analysis results are provided in Appendix C of this thesis.

It is noted that the force response of column-wall members and coupling beams are only developed for the coupled direction. As these members are considered part of the shear wall system in the coupled direction, they are deemed ineffective in providing resistance to seismic loads in the uncoupled direction.

5.2 Dynamic Modal Spectrum Analysis

The dynamic modal spectrum analysis permits for an elastic building response using the peak dynamic response of all modes. Using the ordinates of the UBC (1997) response spectrum curve that correspond to the modal periods, the peak modal responses of the building are calculated from the response spectrum curve, which is based on the modal frequency and modal mass of the structure. The maximum modal contributions are then combined using the Complete Quadratic Combination (CQC) method, as recognized by the UBC (1997), to yield more accurate analysis results where the frequencies of major contributing modes are spaced very closely together. The CQC method used for combining the maximum modal responses is adopted to provide an accurate determination of the maximum seismic response of the building.

As detailed by the ETABS analysis program, the response of a structure to a seismic ground motion is associated with the dynamic equilibrium equations as follows:

$$K\,u(t) + C\,\dot{u}(t) + M\,\ddot{u}(t) = m_x\,\ddot{u}_{gx}(t) + m_y\,\ddot{u}_{gy}(t) + m_z\,\ddot{u}_{gz}(t)$$

Where:

K = stiffness matrix

C = proportional damping matrix

M = diagonal mass matrix

$u, \dot{u}, \ddot{u}$ = relative displacements, velocities and accelerations measured relative to the ground, respectively

m_x, m_y, m_z = unit acceleration loads

$\ddot{u}_{gx}, \ddot{u}_{gy}, \ddot{u}_{gz}$ = components of uniform ground acceleration

Throughout the response spectrum analysis, the likelihood of maximum response to these equations is targeted where a singular positive result is provided for each response quantity. The response is quantified by the formulation of maximum displacements, forces, and stresses for which each response quantity result is calculated by ETABS to represent a statistical measure of the probable maximum magnitude for that quantity. The resulting maximum positive and negative responses provide a range for which the actual structural response of the building is expected to fall within. For the purpose of the work presented within this research, only the maximum positive structural response values are targeted in each direction of loading.

5.2.1 UBC (1997) Response Spectrum Curve

The earthquake ground acceleration in each direction is defined according to the UBC (1997) response spectrum curve, specified as a pseudo-spectral acceleration response versus the period of the structure. The response spectrum is developed for a damping ratio of 5% as required by the UBC (1997). The input parameters defining the UBC (1997) response spectrum curve are provided in Table 3.8 of this thesis.

The UBC (1997) response spectrum curve described by the input parameters, as detailed by the design specifications of the building, is shown in Figure 5.1.

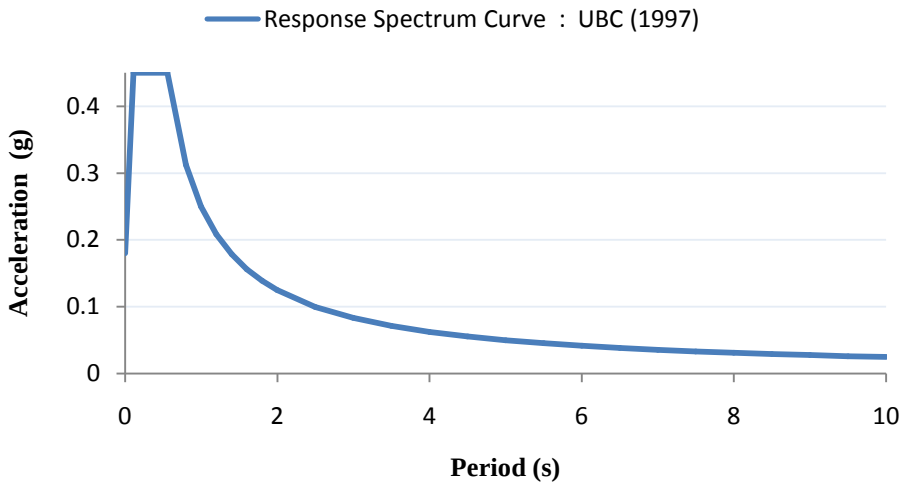

Figure 5.1: UBC (1997) Response Spectrum Curve

For the dynamic modal spectrum analysis of the building in consideration, the load cases SPECY and SPECYC represent the dynamic modal spectrum seismic loads in the coupled direction, and the load cases SPECX and SPECXC represent the dynamic modal spectrum seismic loads in the uncoupled direction. In accordance with UBC (1997), the design acceleration ordinates of SPECYC and SPECXC are multiplied by the acceleration of gravity (g = 9.815 $^{m}/_{s^2}$) and scaled in accordance with UBC (1997) to 90% of the equivalent static loads for each respective direction. Furthermore, the design acceleration ordinates of SPECY and SPECX are also multiplied by the acceleration of gravity.

5.2.2 Force Modification Factor

Through the use of the force modification factor, the value of the static base shear of the seismic load is reduced, thereby ensuring the structure can enter the inelastic range when subjected to the dynamic modal spectrum analysis, consequently achieving a more economical design by relying on the inelastic capacity of the structure. The applicability of using a force modification factor of R = 5.5 stems from the UBC (1997) for concrete shear walls building frame systems, as detailed by the design specifications of the building. The force modification factor is defined as the ratio of the elastic strength demand to the inelastic strength demand of the structure. In general, reinforced concrete shear wall structures designed to respond nonlinearly when subjected to seismic ground motions possess an increase in inelastic deformations as the lateral yielding strength of the structure decreases.

5.2.3 Dynamic Modal Spectrum Analysis Results

Under the dynamic modal spectrum seismic loads SPECY and SPECX in the coupled and uncoupled directions respectively, the dynamic modal spectrum analysis results are provided in Appendix D of this thesis.

It is noted that the maximum force response of column-wall members and coupling beams are only developed for the coupled direction. As these members are considered part of the shear wall

system in the coupled direction, they are deemed ineffective in providing resistance to seismic loads in the uncoupled direction.

5.3 Time-History Analysis

The elastic dynamic time-history analysis provides the dynamic response of a structure when subjected to a specified seismic ground motion time history. The analysis is executed at each increment of time thereby maintaining all phase information throughout the building's excitation to a seismic load.

5.3.1 Overview

In appropriately analyzing the building, ETABS and SAP2000 assume the structure as a multi-degree-of-freedom (MDOF) system responding elastically to actual ground accelerations specified by the time-history ground motion. The response of the structure provides corresponding internal forces and displacements determined using linear elastic analysis.

As pre-programmed into ETABS and SAP2000, the dynamic equilibrium equations to be solved throughout this type of analysis are provided by:

$$K\,u(t) + C\,\dot{u}(t) + M\,\ddot{u}(t) = r(t)$$

Where:

K = stiffness matrix

C = proportional damping matrix

M = diagonal mass matrix

$u, \dot{u}, \ddot{u}$ = displacements, velocities and accelerations of the structure measured relative to the ground under the specified ground motion, respectively

r = vector of applied load

For a time-history case, the load $r(t)$ is applied as a function of space and time. The programs provide the following formula as a finite sum of spatial load vectors multiplied by time functions:

$$r(t) = \sum_i f_i\,(t)\,p_i$$

Where:

$f_i(t)$ = time functions

p_i = spatial load vectors

5.3.2 Linear Time-History Analysis

Throughout the linear time-history analysis, ETABS uses a mode superposition approach to provide for a highly efficient and accurate procedure in performing a time-history analysis. This approach assumes linear variation of the time functions, $f_i(t)$, between input data time points when computing structural response through closed-form integration of the modal equations. Such an approach restricts numerical instability problems associated with the convergence of specified time steps during analysis computation.

Prior to performing the linear time-history analysis, the modal vectors of the structure are required. ETABS provides two types of modal analyses: Ritz-vector analysis or Eigenvector analysis. For the purpose of conducting a reliable time-history analysis, twenty modes deemed sufficient to capture maximum analysis response are defined to follow a Ritz-vector analysis in which all of the spatial load vectors, p_i, are used as starting load vectors. By using the spatial vectors as starting load vectors, the Ritz-vectors provide more accurate results in comparison with using the same number of Eigenvectors. As the Ritz-vector algorithm performs faster than the Eigenvector algorithm, a Ritz-vector analysis type is recommended by ETABS for time-history analyses. Moreover, Eigenvectors provide undamped free-vibration modes; whereas, for the purpose of this research, the structure is subjected to cyclic loads and the Ritz-vector modes are load-dependent.

5.3.2.1 Ground Motion Record

The CHICHI earthquake, also known as the 921 Earthquake, devastated the northwest region of Taiwan on September 21st, 1999. Measuring 7.6 on the Richter scale by the U.S. Geological Survey (USGS) organization, the epicenter of the large and damaging earthquake was near the small country town of Chichi, Nantou County, Taiwan. Assuming casualties, collapsed buildings and other reported damages in the tens of thousands, the CHICHI earthquake is the second deadliest earthquake recorded in the history of Taiwan.

The use of an actual recorded ground motion provides a realistic simulation of the earthquake event throughout a time-history analysis. In performing the time-history analyses, a representative ground motion record is selected from the USGS organization using the actual CHICHI earthquake record. As the acceleration values provided by the USGS earthquake record are given as a function of gravity, the CHICHI record is scaled against the value of gravity and adopted in the analyses using characteristics matching those of a moderate seismic zone, as required by the design specifications of the building. The ground motion record is manipulated to represent the target linear response spectrum using spectrum matching, whereby the linear response spectrum of the motion matches the target design response spectrum. According to the UBC (1997), a scale factor is applied to the record such that the response spectrum from the scaled ground motion does not fall below the target design response spectrum over the period range 0.2 – 1.5 times the fundamental period of vibration, T, of the building. As the building is excited using horizontal ground motions in the coupled and uncoupled directions, the motion in each individual direction is scaled to its corresponding vector of the response spectrum. Calculated as the square root of the sum of the squares (SRSS) of the response spectra for the two directions, the vector of the response spectrum does not fall below $\sqrt{2}$ times the target spectrum over the specified period range, as required by the SRSS combination.

Following the spectrum matching, the horizontal ground motion in the coupled direction is provided in Figure 5.2.

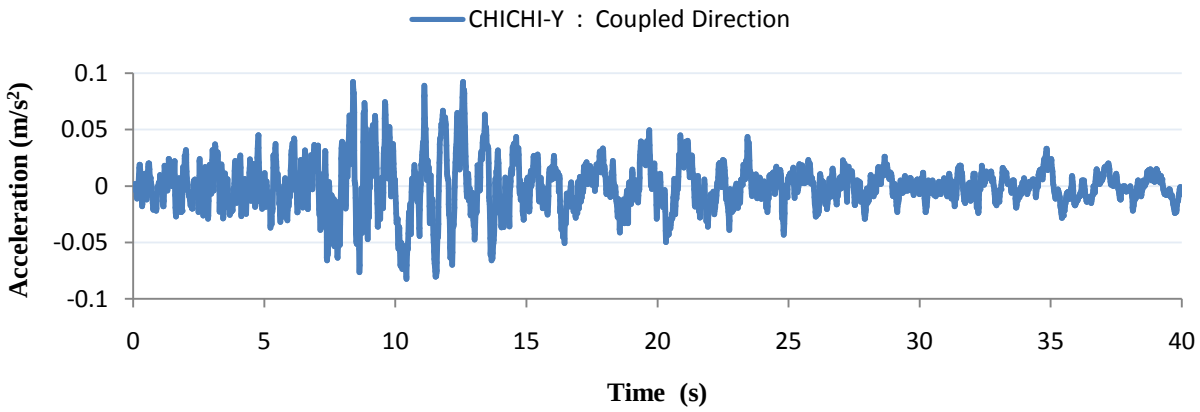

Figure 5.2: CHICHI earthquake ground motion acceleration in the coupled direction

The horizontal ground motion in the uncoupled direction is provided in Figure 5.3.

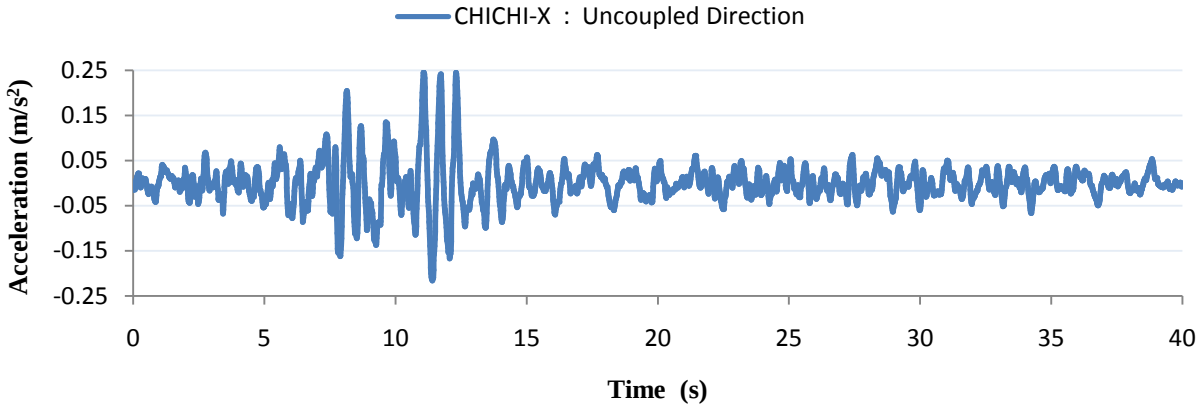

Figure 5.3: CHICHI earthquake ground motion acceleration in the uncoupled direction

Among the UBC (1997) Earthquake Design requirements, dynamic analyses are based on an appropriate ground motion representation bearing a minimum of having a ten-percent probability of being exceeded in fifty years, where a time history-analysis is performed using pairs of appropriately selected and scaled horizontal ground-motion time-history components from three or more events (UBC 1997). Due to time constraints associated with the completion of the

project, and the demanding detail and intricacies required by the extensive modeling of the high-rise building in ETABS and SAP2000, one time-history ground motion record is used for the purpose of performing linear and nonlinear time-history analyses within this work.

For the time-history analyses of the building in consideration, the load cases CHICHI-Y and CHICHI-X represent the coupled and uncoupled time-history seismic loads, respectively.

5.3.2.2 Application of Load

The application of the load during the ETABS analysis considers the time-history ground motion accelerations as spatial load vectors. The analysis is carried out at discrete time steps specified by a number of output time steps and time step size, and the response is calculated at the end of each time step size increment. The total duration of the analysis is given by the multiplication of the number of output time steps with the time step size. For the linear time-history analysis in ETABS, the number of output time steps is specified at 4000 with an output time step size of 0.01. Such definitions incorporated into the analysis offer results reported at finely spaced output time steps which provide increased accuracy in capturing the maximum structural response of the building. The input parameters attributed to the ETABS analysis define a total analysis duration of forty seconds, which matches the duration of ground motion given by the time-history record used to excite the structure.

5.3.2.3 Analysis Restraints

The complete ETABS model is restrained for analysis in all directions thereby creating a fixed base condition. The restraints set forth in the analysis options prevent the base of the model from translating along the x, y and z directions, inclusive of rotation in the z-axis.

5.3.2.4 Geometric Nonlinearity

The P-Delta effect is nonlinear structural behavior causing additional overturning moments in a structure when subjected to lateral movement. In building analysis, a storey mass laterally displaced to a deformed position generates nonlinear overturning moments, equal in magnitude to the sum of the storey weights, P, multiplied by the lateral displacements, Delta. These additional overturning moments on a structure are referred to as the P-Delta effect.

As required for analysis by the UBC (1997), the P-Delta effect is particularly useful for considering the effect of gravity loads on the lateral stiffness of a building. For use throughout the analysis of the modeled building, non-iterative P-Delta parameters are described based on the mass of the structure.

5.3.2.5 Linear Time-History Analysis Results

Under the dynamic time-history seismic load CHICHI in the coupled and uncoupled directions, the linear time-history analysis results are provided in Appendix E of this thesis.

It is noted that the maximum force response of column-wall members and coupling beams are only developed for the coupled direction. As these members are considered part of the shear wall system in the coupled direction, they are deemed ineffective in providing resistance to seismic loads in the uncoupled direction.

5.3.3 Nonlinear Time-History Analysis

The building model in SAP2000 is defined using the same modal superposition approach, Ritz-vector analysis, ground motion record, loading, analysis restraints and geometric nonlinearity as described in the previous sections for the ETABS building model. In performing a nonlinear time-history analysis, the application of load in SAP2000 follows the same programming principles as those for a linear time-history analysis in ETABS.

The nonlinear time-history analysis assumes the structure as a multi-degree-of-freedom (MDOF) system responding primarily linear elastic with a limited number of predefined nonlinear elements, where all nonlinear behavior is restricted to the link elements in the model. When the structure is subjected to an arbitrary load, the dynamic equilibrium equations assumed by SAP2000 are given as:

$$K_L\, u(t) + C\, \dot{u}(t) + M\, \ddot{u}(t) + r_N(t) = r(t)$$

Where:

K_L = stiffness matrix for linear elastic elements

C = proportional damping matrix

M = diagonal mass matrix

r_N = vector of forces from the nonlinear degrees of freedom in the link elements

$u, \dot{u}, \ddot{u}$ = displacements, velocities and accelerations of the structure measured relative to the ground under the specified ground motion, respectively

r = vector of applied load

5.3.3.1 Multilinear Plastic Links

As described in Section 4.3 of this thesis, the structural elements in the SAP2000 model are provided with two-joint multilinear plastic links to define the moment-curvature relationships, and consequently the nonlinear response, of the elements under cyclic loading.

Throughout the SAP2000 model, all the modeled structural elements are afforded two-joint links placed at the top and bottom of each individual member. The links are restricted from translating along all axes, inclusive of rotation in the z-axis, but are permitted to rotate in the coupled and uncoupled directions. Within each link element, a moment-curvature relationship, as discussed in Section 4.4 of this thesis, is defined in the coupled and uncoupled directions to allow the member to respond nonlinearly in a time-history analysis. Moreover, an effective damping of 5% according to the UBC (1997), as well as a linear effective stiffness, is defined for each selected degree of freedom in the individual link. The linear effective stiffness definition for a specific

degree of freedom represents the total elastic stiffness afforded to the link element for that degree of freedom. In the absence of specifying nonlinear properties for a particular degree of freedom, SAP2000 uses the user-defined linear effective stiffness for that particular degree of freedom for the nonlinear time-history analysis. In defining the linear effective stiffness for each link in a selected degree of freedom, the linear slope of its respective moment-curvature relationship is used.

The resulting moment-curvature relationships attributed to the coupled and uncoupled directions for all six boxed core sections, two modeled column-wall members and one modeled coupling beam member are provided in Appendix B of this thesis.

5.3.3.2 Nonlinear Time-History Analysis Results

Under the dynamic time-history seismic load CHICHI in the coupled and uncoupled directions, the nonlinear time-history analysis results are provided in Appendix F of this thesis.

Appendix G presents the link elements hysteresis response results in floor thirty-six for a core wall member, column-wall member T2C10 and coupling beam member T2B-C1 located in the bottom-left portion of the SAP2000 model floor plan, respectively.

It is noted that the maximum force response of column-wall members and coupling beams are only developed for the coupled direction. As these members are considered part of the shear wall system in the coupled direction, they are deemed ineffective in providing resistance to seismic loads in the uncoupled direction.

5.4 Comparison of Results

Under all the seismic loads in the coupled and uncoupled directions, the resulting maximum inter-storey drifts and maximum storey shears for the overall building response in each direction is provided. The superimposed analysis results are provided in Appendix H of this thesis.

It is noted that the maximum force response of column-wall members and coupling beams are only developed for the coupled direction. As these members are considered part of the shear wall system in the coupled direction, they are deemed ineffective in providing resistance to seismic loads in the uncoupled direction.

Figure 5.4 presents the modeled floors from the base of the structure up to the 3rd storey level. This figure shows larger members in the bottom floors, as required by the structural drawings of the building.

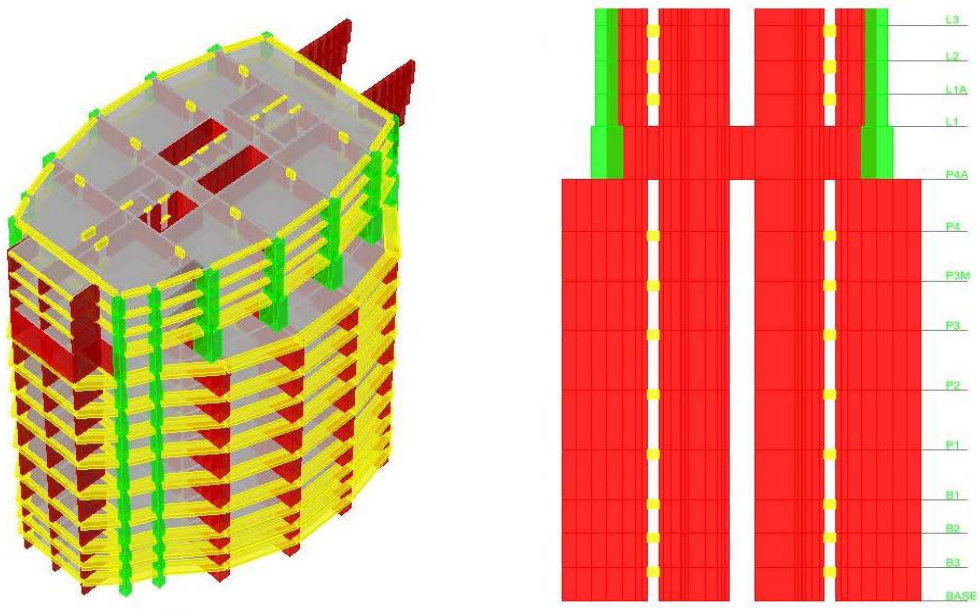

(a) (b)

Figure 5.4: Modeled storey levels spanning L3 to BASE: (a) 3-D view; (b) Coupled direction elevation view

5.4.1 Inter-Storey Drift in the Coupled Direction

Through the comparison of drift in the coupled direction, the following can be concluded:

Equivalent Static Analysis (ESA)

The result of the Equivalent Static Analysis (ESA) in the coupled direction shows the drift up to the ground floor significantly less than the remainder of the structure, as seen in Figure 5.5. This is attributed to the higher storey stiffness of lower floors, as a result of larger members required according to the structural drawings of the building.

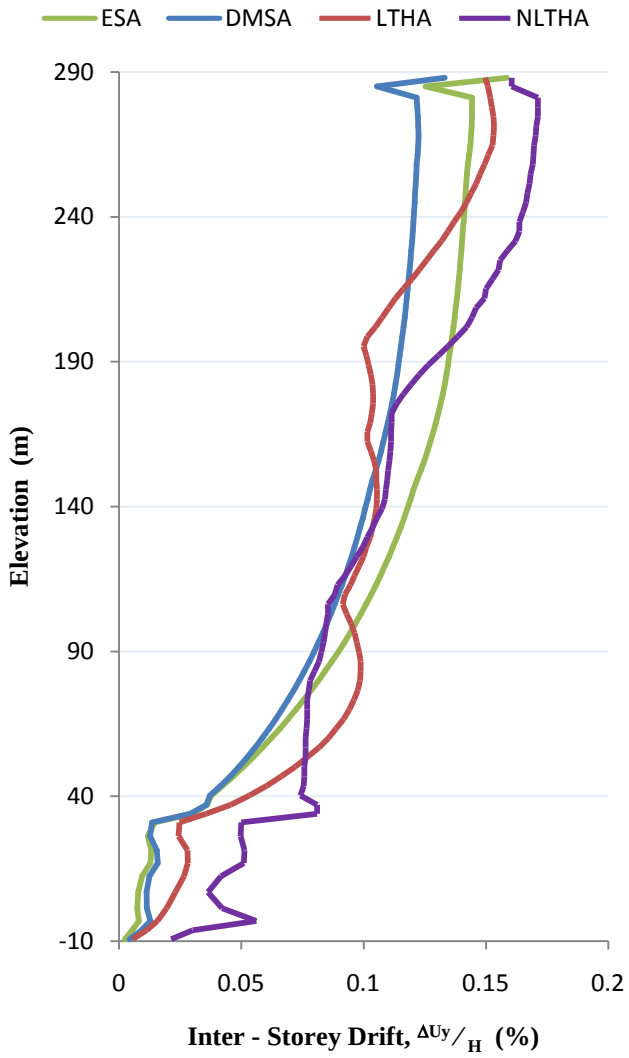

Figure 5.5: Maximum Inter-Storey Drift in the Coupled Direction

Dynamic Modal Spectrum Analysis (DMSA)

The result of the Dynamic Modal Spectrum Analysis (DMSA) shows its drift overlapping the ESA drift up to the ground floor, as seen in Figure 5.5, but tends to provide less drift with respect to the ESA over the remainder of the building. As the equivalent static analysis assumes the building responding in its fundamental mode when subjected to earthquake excitation, higher drifts at upper storeys are expected. This is attributed to higher floors engaging longer periods of vibration, and in the dynamic modal spectrum analysis, less acceleration is applied to those floors.

Linear Time-History Analysis (LTHA)

The result of the Linear Time-History Analysis (LTHA) shows its drift deviated from the result of the ESA and the DMSA near the bottom or top one-third of the structure, as seen in Figure 5.5. As this analysis is conducted using the same ETABS model as the ESA and the DMSA, the source of difference could either be due to the method of analysis or the source of excitation, which is the CHICHI earthquake in this case.

Figure 5.6 presents the floor accelerations due to the DMSA and the LTHA, which are different for the same floors when compared to their respective drifts. An important point to consider is that the results of the time-history analysis are shown as extreme values within the duration of the earthquake. This means in Figure 5.6, the acceleration of floors may not occur simultaneously, therefore concluding that the drift should be less because the acceleration is less would be incorrect.

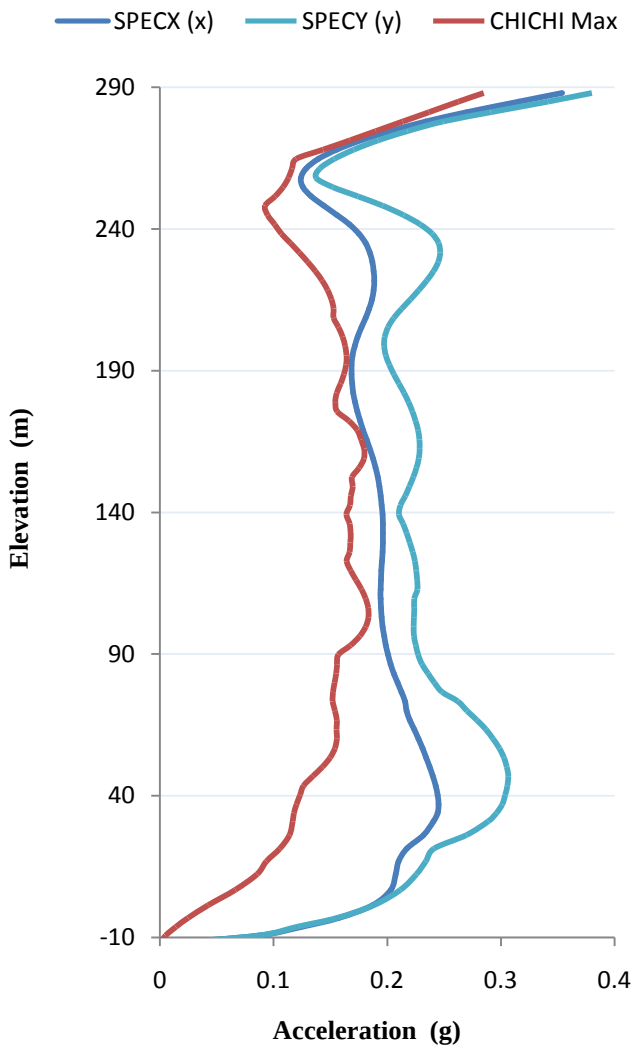

Figure 5.6: DMSA and LTHA floor accelerations

The drift at each floor is a function of the storey shear and storey stiffness. As the LTHA and the DMSA are performed using the same ETABS model, there are no discrepancies in stiffness and the only reason for the difference would be attributed to the difference between storey shears due to the DMSA and the LTHA.

Figure 5.7 presents the storey shear for the coupled direction. This figure shows the LTHA providing higher storey shears near the bottom or top one-third of the building. This is due to the peak amplitude in frequency content of the CHICHI earthquake in which the lower and upper floors of the building experience larger excitations.

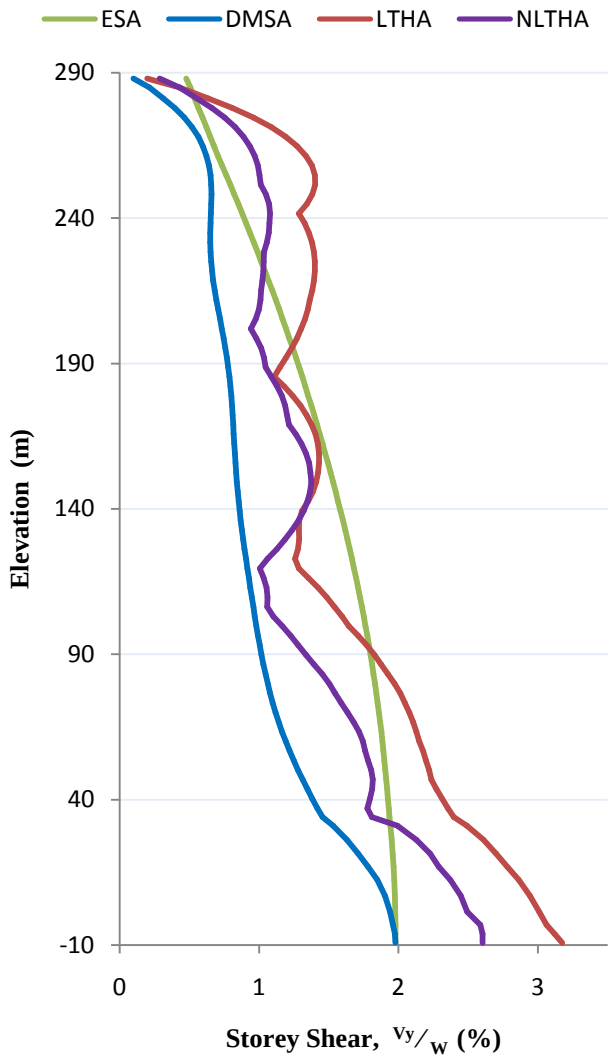

Figure 5.7: Maximum Storey Shear in the Coupled Direction

Figure 5.8 presents the Fourier spectrum of the CHICHI earthquake applied in the coupled direction. This figure shows the most governing frequency of the CHICHI earthquake lies between 0.5 and 1.5 Hz, which is equivalent to periods of 0.67 and 2 seconds.

Figure 5.9 presents modes six and nine of the structure, which lie in the range of 0.67 and 2 seconds. These mode shapes explain the larger drifts in the lower and upper one-thirds of the structure for the coupled direction.

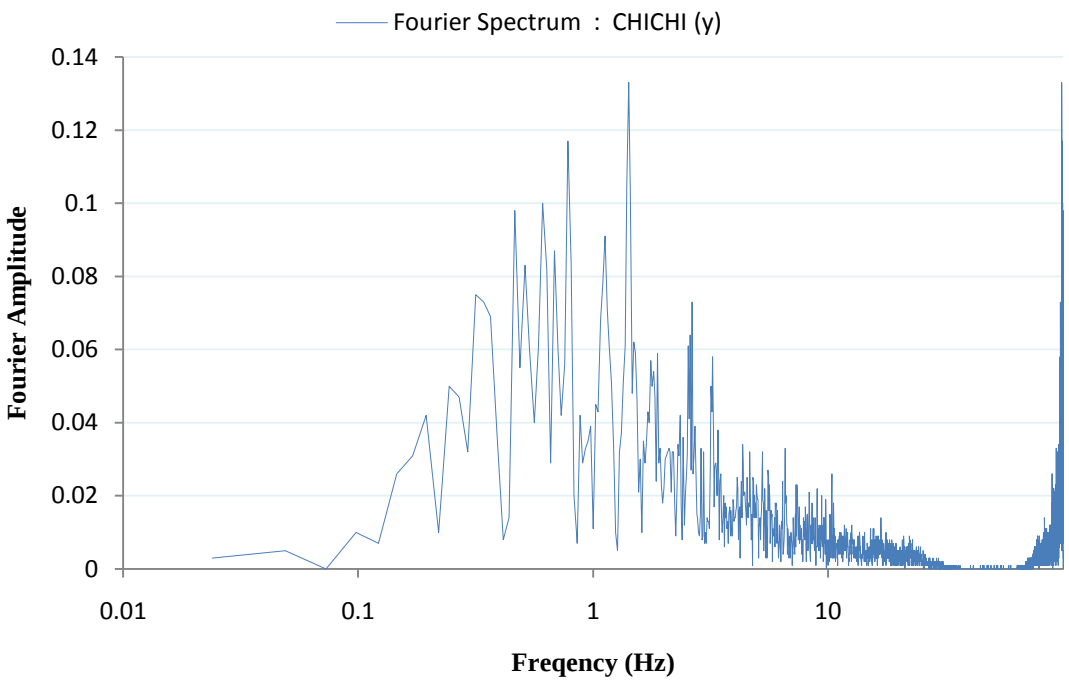

Figure 5.8: Fourier Spectrum for CHICHI earthquake in the coupled direction

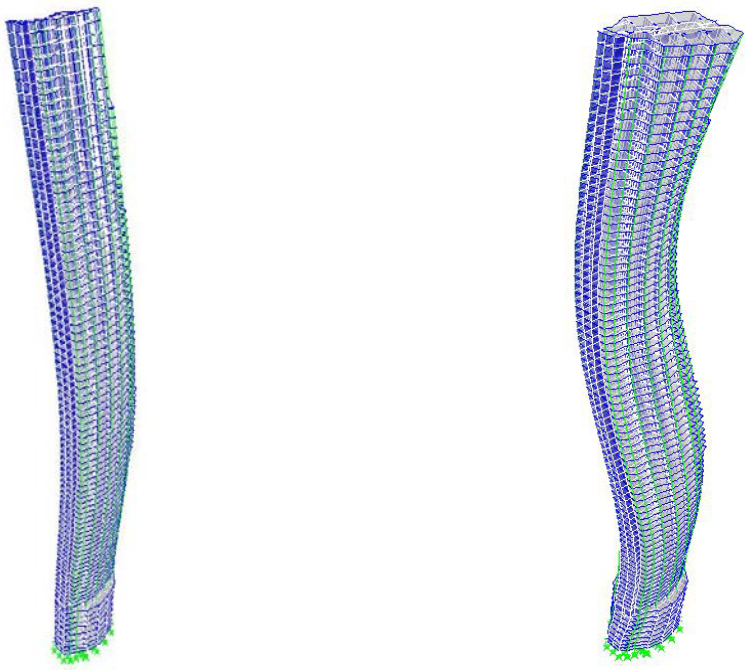

(a) (b)

Figure 5.9: Mode Shapes: (a) Mode 6 (t = 1.73 s); (b) Mode 9 (t = 0.78 s)

Nonlinear Time-History Analysis (NLTHA)

The Nonlinear Time-History Analysis (NLTHA) follows the same behavior as the LTHA, except that it provides more drift in the bottom and top one-thirds of the structure, as seen in Figure 5.5. This is attributed to the concentration of cracked stiffness in the link elements afforded to the column and wall members. In the ETABS model, cracked stiffness is used for each element; whereas in the SAP2000 model, cracked stiffness is concentrated in the link elements, thereby creating a softer model.

When subjected to the CHICHI earthquake ground motion in the coupled direction throughout the nonlinear time-history analysis, the response of this building did not enter the nonlinear range.

Appendix G of this thesis presents the link elements hysteresis response for typical members in the 36^{th} storey level. As seen in these figures, the hysteresis response of all the members remain in the linear range which is shown by the response curves overlapping one another. In the event of the building responding in the nonlinear range, the hysteresis response curves would be similar to the hysteresis type given by the Multilinear Takeda Model shown in Figure 2.3 of this thesis.

5.4.2 Inter-Storey Drift in the Uncoupled Direction

Through the comparison of drift in the uncoupled direction, the following can be concluded:

Equivalent Static Analysis (ESA)

The result of the Equivalent Static Analysis (ESA) in the uncoupled direction shows the drift increasing linearly throughout the height of the building, as seen in Figure 5.10.

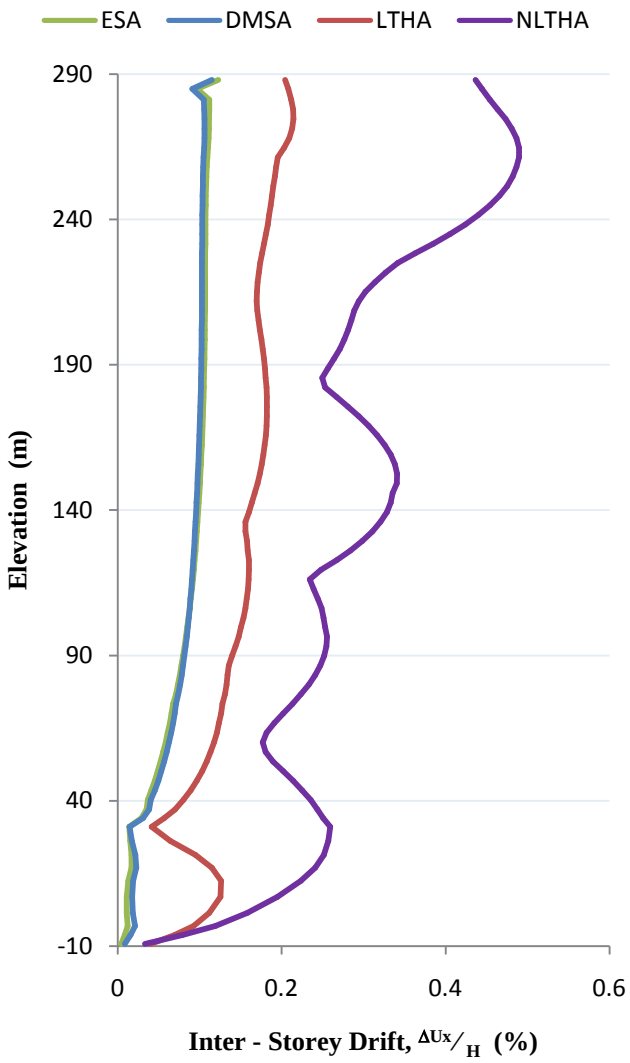

Figure 5.10: Maximum Inter-Storey Drift in the Uncoupled Direction

Dynamic Modal Spectrum Analysis (DMSA)

The result of the Dynamic Modal Spectrum Analysis (DMSA) shows the drift overlapping the ESA drift throughout the elevation of the structure, as seen in Figure 5.10. This is attributed to the dominance of structural response behaving in the fundamental mode of the building, which is due to the stiffness of the structure in the uncoupled direction.

Linear Time-History Analysis (LTHA)

The result of the Linear Time-History Analysis (LTHA) provides higher drifts when compared to the ESA and the DMSA, as seen in Figure 5.10. As this analysis is conducted using the same ETABS model as the ESA and the DMSA, the source of difference could either be due to the method of analysis or the source of excitation, which is the CHICHI earthquake in this case.

The drift at each floor is a function of the storey shear and storey stiffness. As the LTHA and the DMSA are performed using the same ETABS model, there are no discrepancies in stiffness and the only reason for the difference would be attributed to the difference between storey shears due to the DMSA and the LTHA.

Figure 5.11 presents the storey shear for the uncoupled direction. This figure shows the LTHA providing higher storey shears throughout the height of the building, although it does not follow a smoothly increasing trend. This is due to the frequency content of the CHICHI earthquake in which the lower and upper one-thirds of the building experience greater excitation.

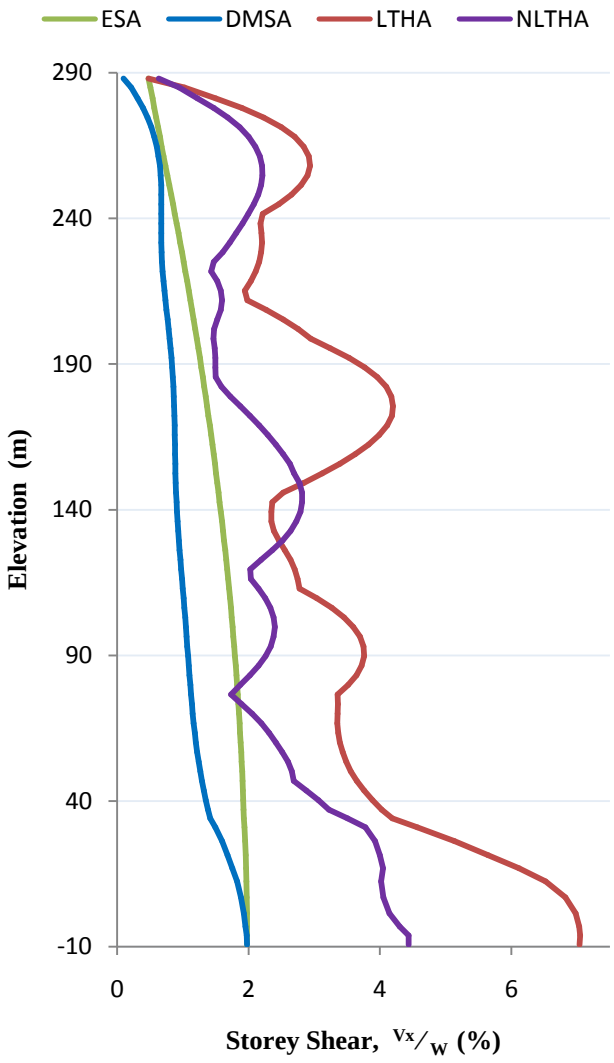

Figure 5.11: Maximum Storey Shear in the Uncoupled Direction

Figure 5.12 presents the Fourier spectrum of the CHICHI earthquake applied in the uncoupled direction. This figure shows the most governing frequency of the CHICHI earthquake lies between 0.67 and 1.34 Hz, which is equivalent to periods of 0.75 and 1.5 seconds.

Figure 5.13 presents modes eight of the structure, which lies in the range of 0.75 and 1.5 seconds. These mode shapes, along with Figure 5.14, explain the larger drifts in the LTHA load case in comparison to the ESA and the DMSA.

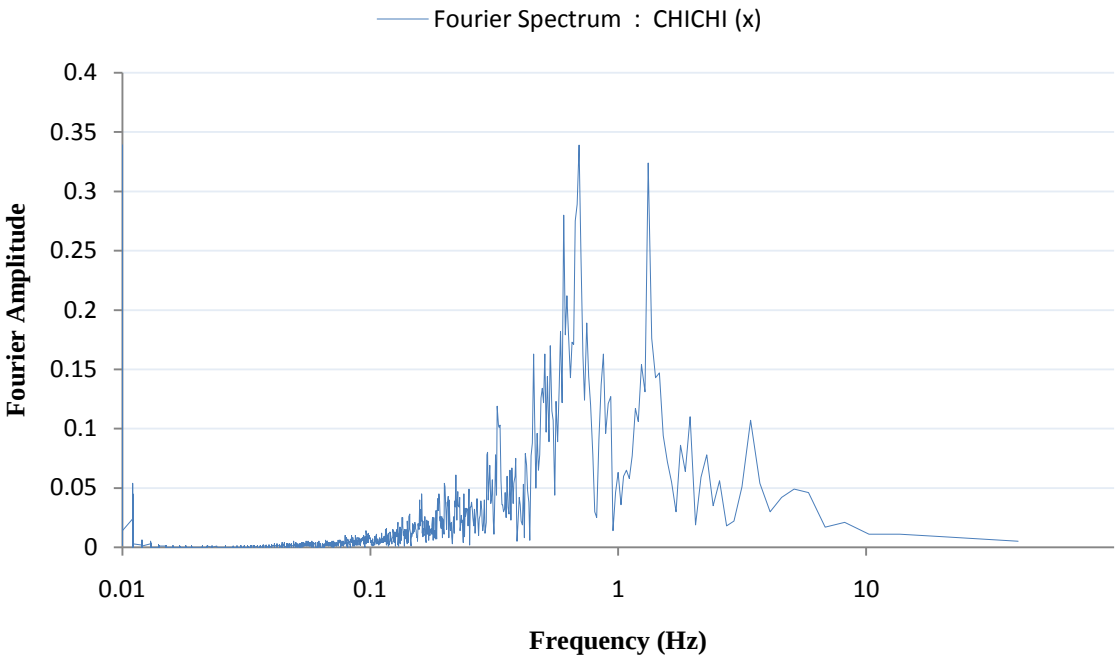

Figure 5.12: Fourier Spectrum for CHICHI earthquake in the uncoupled direction

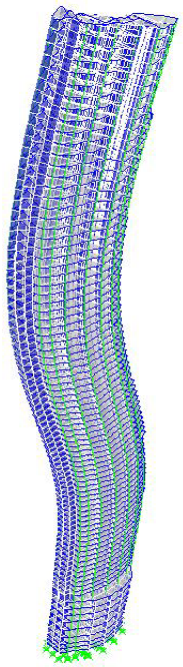

Figure 5.13: Mode Shape for Mode 8 (t = 0.91 s)

As the acceleration peaks in Figure 5.14 for the 0.5 – 1.0 seconds range of the CHICHI (x) earthquake, and the results of the time-history analysis are shown as extreme values, the larger drifts in the LTHA are caused.

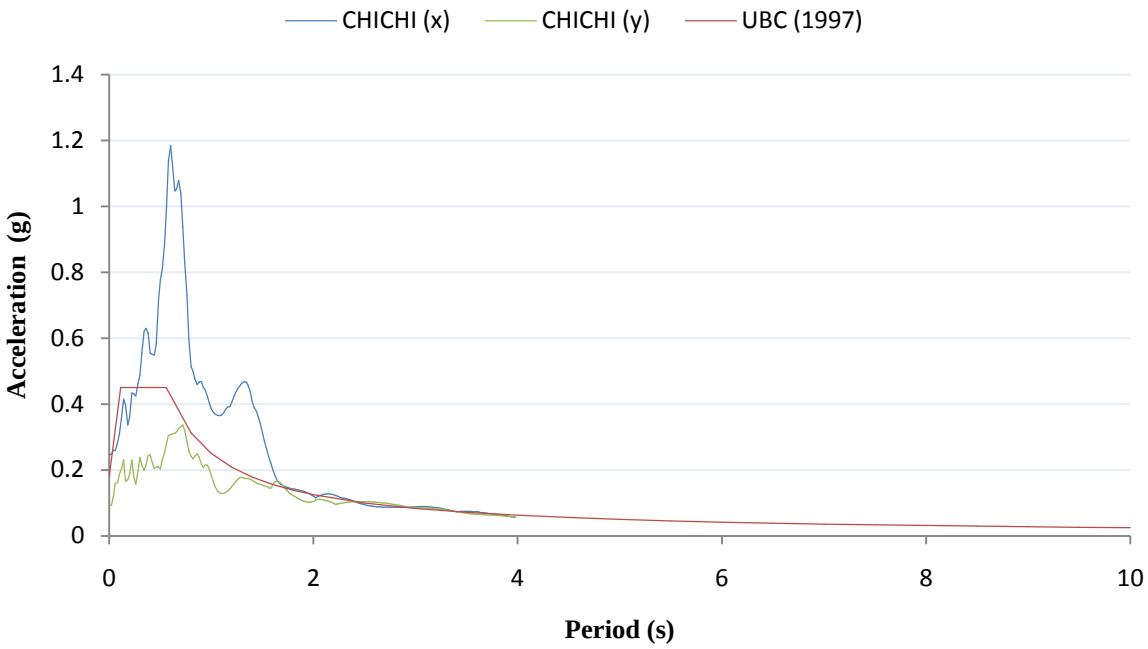

Figure 5.14: Response Spectrum Curves

Nonlinear Time-History Analysis (NLTHA)

The Nonlinear Time-History Analysis (NLTHA) follows the same behavior as the LTHA, except that it provides more drift throughout the height of the structure, as seen in Figure 5.10. This is attributed to the concentration of cracked stiffness in the link elements afforded to the column and wall members. In the ETABS model, cracked stiffness is used for each element; whereas in the SAP2000 model, cracked stiffness is concentrated in the link elements, thereby creating a softer model.

Similar to the coupled direction, when the structure is subjected to the CHICHI earthquake ground motion in the uncoupled direction throughout the nonlinear time-history analysis, the response of this building did not enter the nonlinear range. This is shown by the response curves of link elements hysteresis overlapping one another, as presented in Appendix G of this thesis.

CHAPTER 6 - SUMMARY, CONCLUSIONS AND RECOMMENDATIONS

6.1 Summary

The work presented throughout this thesis investigates a high-rise reinforced concrete tower incorporating tall reinforced concrete shear wall systems as it is subjected to a strong earthquake ground motion. The preliminary structure consists of an 88-storey high-rise building standing 300.4 m in height, pre-designed according to the seismic provisions of the UBC (1997) for a moderate seismic zone and detailed according to the ACI 318M (2002) Code, as it is provided by structural drawings for use within the purpose of this research. In order to successfully analyze the building for lateral loading effects, the structure is appropriately modeled according to the structural drawings of the building. The structure is modeled to resist static and dynamic motion through six boxed core wall assemblies acting as simple cantilever walls in the uncoupled direction, and linked with coupling beams at storey levels in the coupled direction.

The modeling of the structure for elastic analyses is performed on ETABS which involves a process of using horizontal and vertical basic line elements to model structural members. Each typical floor level details a total of six boxed core walls functioning as shear walls, which serve as the lateral force resisting systems of the structure under loading. By creating a replica of the building using the structural drawings, the ETABS model features matching material properties, member dimensions and floor plan configurations to the original building at all storey levels of the structure. Following the modeling process in ETABS, elastic analyses are performed using equivalent static, dynamic modal spectrum and linear time-history analyses.

The accurate modeling of structural elements and their essential characteristics relating to the inelastic response of the shear wall system is necessary to achieve meaningful results from the nonlinear analysis of the building undergoing seismically induced ground motions. For effectively modeling the building in its entirety for inelastic analysis in SAP2000, the second podium, third and thirty-sixth storey levels are chosen according to structural drawings as typical floor levels found consistent in reinforcement details to their respective similar storeys over the height of the structure.

The building is modeled on SAP2000 using vertical frame elements linked by weightless rigid members in the horizontal direction, which create a unified floor model per building storey. The gravity loads acting directly on and tributary to the individual elements in the ETABS model are incorporated into the completed SAP2000 model to replicate the distribution of static gravity loads and members weights from the ETABS building model. In the modeling of structural members in SAP2000, the same basic elements as those in the ETABS model are used to model the wall, column and beam members. Each structural member is individually modeled using Section Designer and detailed according to the structural drawings of the pre-designed building. Placement of the members is performed using SAP2000, where the members are placed into the floor model at their respective center of masses in accordance to the framing plan of the building. The wall members comprising the shear wall systems are modeled as assembled units of walls forming boxed cores, where the individual walls forming these boxed cores craft the shear wall systems in the coupled and uncoupled directions that extend over the height of the building. In order to greatly reduce analysis time, the slab member from the ETABS model is removed from the floor model of SAP2000. The base reactions and forces acting tributary to individual elements from the ETABS model are applied to the SAP2000 model. Following the equivalent distribution of loads, the SAP2000 and ETABS models are individually analyzed and the targeted floors are compared for matching floor weights and load distribution of structural elements. The resulting model in SAP2000 features similar floor weights and load distributions of structural elements to the ETABS model.

For the modeling of structural elements in SAP2000, material properties, stress-strain relationships and moment-curvature relationships are necessary to model the response of the elements under cyclic loading. The Mander Unconfined and Confined Concrete models are used to describe the stress-strain behavior of the material and the Takeda Hysteresis Type is used to describe the force-deformation characteristics of the structural members. Moment-curvature relationships are developed for every individual structural component using Section Designer and the structural elements are provided with two-joint multilinear plastic links at their nodal ends to define the moment-curvature relationships, and consequently the response, of the structural members. The structural members throughout the height of the building remain unchanged in terms of material properties, member dimensions and floor plan locations. Most

importantly, the structural members forming the shear wall system remain unaltered in material properties or floor plan location over the height of the building. Following the complete modeling of the representative storey levels, each of the three aforementioned storey levels are entirely replicated to build their corresponding similar floor levels, and consequently form the floors in the overall building. Following the modeling process in SAP2000, inelastic analysis is performed using a nonlinear time-history analysis.

The ground motion record used to excite the structure under dynamic analyses is selected from the USGS organization using the actual CHICHI earthquake record, which provides a realistic simulation of the earthquake event throughout time-history analyses. The ground motion record is manipulated to represent the target linear response spectrum using spectrum matching, whereby the linear response spectrum of the motion matches the target design response spectrum. As the building is excited using horizontal ground motions in the coupled and uncoupled directions, the motion in each individual direction is scaled to its corresponding vector of the response spectrum. The CHICHI record is adopted in the analyses using characteristics matching those of a moderate seismic zone, as required by the design specifications of the building.

As the structure undergoes static and dynamic loading, the analyses are compared using the resulting maximum inter-storey drift and maximum storey shear response for the overall building in the coupled and uncoupled directions.

6.2 Concluding Remarks

Based on the results of this research, the following conclusions are made:

- Following the execution of analyses for this particular building, the linear time-history analysis performed on ETABS proves the most proficient in capturing the response of the building under dynamic loading in the coupled and uncoupled directions.

- Under all the seismic loads in the coupled and uncoupled directions, the resulting maximum force response of column-wall members and coupling beam members are only developed for the coupled direction. As these members are considered part of the shear wall system in the coupled direction, they are deemed ineffective in providing resistance to seismic loads in the uncoupled direction.

- Through the comparison of drift in the coupled direction, the following can be concluded:

    - The result of the Equivalent Static Analysis (ESA) shows the drift up to the ground floor significantly less than the above floors. This is attributed to the storey stiffness of lower floors being higher than the remainder of the building.

    - The result of the Dynamic Modal Spectrum Analysis (DMSA) shows its drift overlapping the ESA drift up to the ground floor, but tends to provide less drift with respect to the ESA over the remainder of the building. This is attributed to higher floors engaging longer periods of vibration and less acceleration is applied to those floors in the DMSA; alternatively, the ESA assumes building response in its fundamental mode and provides higher drifts at upper storey levels.

    - The result of the Linear Time-History Analysis (LTHA) shows its drift deviated from the result of the ESA and the DMSA in the bottom and top one-thirds of the structure. This is attributed to the LTHA providing higher storey shears in the bottom and top one-thirds of the building in which the frequency content of the CHICHI earthquake experiences greater excitation.

    - The result of the Nonlinear Time-History Analysis (NLTHA) follows the same behavior as the LTHA, except that it provides more drift in the bottom and top one-thirds of the structure. This is attributed to the concentration of cracked stiffness in the link elements creating a softer model. Furthermore, when the structure is subjected to the CHICHI earthquake ground motion, the response of this building in the coupled direction did not enter the nonlinear range.

- Through the comparison of drift in the uncoupled direction, the following can be concluded:

    - The result of the Equivalent Static Analysis (ESA) shows the drift increasing linearly throughout the height of the building.

    - The result of the Dynamic Modal Spectrum Analysis (DMSA) shows its drift overlapping the ESA drift throughout the elevation of the structure. This is attributed to the stiffness of the structure in the uncoupled direction causing the response of the building in its fundamental mode.

    - The result of the Linear Time-History Analysis (LTHA) presents higher drifts when compared to the ESA and the DMSA. This is attributed to the acceleration peaks of the CHICHI (x) earthquake, and the results of the time-history analysis shown as extreme values, causing the larger drifts.

    - The result of the Nonlinear Time-History Analysis (NLTHA) follows the same behavior as the LTHA, except that it provides more drift throughout the height of the structure. This is attributed to the concentration of cracked stiffness in the link elements creating a softer model. Furthermore, when the structure is subjected to the CHICHI earthquake ground motion, the response of this building in the uncoupled direction did not enter the nonlinear range.

- In terms of practical application, the dynamic modal spectrum analysis is best suited for design offices as it captures higher mode effects in high-rise buildings with respect to the equivalent static analysis and does not demand a high level of modeling and analysis procedures in comparison to the linear and nonlinear time-history analyses.

6.3 Recommendations for Future Work

Based on the work presented throughout this thesis, the following recommendations for future work are made:

- The modeling of a building this size for the nonlinear time-history analysis performed in SAP2000 requires extensively intricate work and is remarkably time consuming, especially when several trial and error methods are required in the development of the model leading to the desired results. The SAP2000 model used in the nonlinear time-history analysis did not provide the most accurate results in this case and may require further modifications to better replicate the actual building.

- As the extent of work presented by the modeling of this tower in ETABS and SAP2000 constrained time, only one earthquake ground motion is used in this research. The requirements of three or more events from the UBC (1997) would provide more accurate results when performing linear and nonlinear time-history analyses.

- In furthering work afforded to this particular modeled building, stronger earthquake ground motions are required to force the response of the structure into the nonlinear range.

- As this study is part of a two phase project where the work presented by this thesis focuses on the extensive modeling of the structure, the second phase of the project adopts the modeled structure for work performed by future research.

REFERENCES

ACI Committee 318. 2002. Building code requirements for structural concrete (ACI 318M–02) and Commentary (ACI 318RM–02). American Concrete Institute, Farmington Hills, Mich.

ATC-40. 1996. Seismic evaluation and retrofit of concrete building. Applied Technology Council, Redwood City, Calif.

Bai, Z.Z., Au, F.T.K., and Kwan, A.K.H. 2007. Complete nonlinear response of reinforced concrete beams under cyclic loading. Department of Civil Engineering, University of Hong Kong, PRC.

Computers and Structures, Inc. 2005. CSI analysis reference manual. Computers and Structures, Inc., Berkeley, Calif.

Computers and Structures, Inc. 2005. SAP2000 advanced [computer program]. Version 10.0.1. Computers and Structures, Inc., Berkeley, Calif.

Computers and Structures, Inc. 2005. Section Designer [computer program]. Version 10.0.0. Computers and Structures, Inc., Berkeley, Calif.

Computers and Structures, Inc. 2008. ETABS nonlinear [computer program]. Version 9.2.0. Computers and Structures, Inc., Berkeley, Calif.

Dowell, R.K., Seible, F.S., and Wilson, E.L. 1998. Pivot hysteretic model for reinforced concrete members. ACI Structural Journal, 95: 607–617.

Fintel, M. 1995. Performance of buildings with shear walls in earthquakes of the last thirty years. Prestressed Concrete Institute Journal, 40: 62–80.

Heidebrecht, A.C. 1997. Seismic level of protection for building structures. Canadian Journal of Civil Engineering, 24: 20–33.

Mander J.B., Priestly, M.J.N., and Park, R. 1988. Theoretical stress-strain model for confined concrete. ASCE Journal of Structural Engineering, 114(8): 1804–1826.

Munshi, J.A., and Ghosh, S.K. 1998. Analysis of seismic performance of a code designed reinforced concrete building. Engineering Structures, 20: 608–616.

Paulay, T., and Priestley, M.J.N. 1992. Seismic design of reinforced concrete and masonry buildings. John Wiley and Sons, Inc., New York, NY.

Penelis, G.G., and Andreas, J.K. 1997. Earthquake-resistant concrete structures. E & FN SPON, Inc., Chapman & Hall, London, UK.

SEAOC. 1995. Performance based seismic engineering of buildings. Vision 2000 Committee, Structural Engineers Association of California, Sacramento, Calif.

Sheikh, S.A., and Yeh, C.C. 1992. Analytical moment-curvature relations for tied concrete columns. ASCE Journal of Structural Engineering, 118(2): 529–544.

Stonehouse, B., Heidebrecht, A.C., and Kianoush, M.R. 1999. Evaluation of the level of seismic protection afforded to reinforced concrete shear wall systems. Canadian Journal of Civil Engineering, 26: 572–589.

Takeda, T., Sozen, M.A., and Nielson, N.N. 1970. Reinforced concrete response to simulated earthquakes. ASCE Journal of Structural Engineering, 96(12): 2257–2273.

UBC. 1997. Uniform Building Code, International Conference of Building Officials, Whittier, Calif.

APPENDIX A - EQUIVALENT STATIC SHEAR FORCES

Modeled Section | *Right-Bottom*

Storey Level	Elevation (m)	Storey Force, F_x (MN)
L76	288.0	8.185
L75	285.0	8.679
L74	281.2	9.174
L73	277.9	9.650
L72	274.6	10.12
L71A	271.3	10.59
L71	268.0	11.05
L70	264.7	11.50
L69	261.4	11.95
L68	258.1	12.44
L67	254.8	12.93
L66	251.5	13.41
L65	248.2	13.89
L64	244.9	14.36
L63	241.6	14.83
L62	238.3	15.28
L61	235.0	15.74
L60	231.7	16.18
L59	228.4	16.62
L58	225.1	17.06
L57	221.8	17.49
L56	218.5	17.92
L55	215.2	18.34
L54	211.9	18.76
L53	208.6	19.17
L52	205.3	19.57
L51	202.0	19.97
L50	198.7	20.36
L49	195.4	20.75
L48	192.1	21.13
L47	188.8	21.50
L46	185.5	21.86
L45	182.2	22.22
L44	178.9	22.57
L43	175.6	22.91
L42	172.3	23.25
L41	169.0	23.58
L40A	165.7	23.91
L40	162.4	24.23
L39	159.1	24.54
L38	155.8	24.85
L37	152.5	25.15
L36	149.2	25.45
L35	145.9	25.74

L34	142.6	26.03
L33	139.3	26.31
L32	136.0	26.59
L31	132.7	26.86
L30	129.4	27.12
L29	126.1	27.38
L28	122.8	27.63
L27	119.5	27.88
L26	116.2	28.12
L25	112.9	28.35
L24	109.6	28.57
L23	106.3	28.79
L22	103.0	29.00
L21	99.70	29.21
L20	96.40	29.41
L19	93.10	29.60
L18	89.80	29.79
L17	86.50	29.97
L16	83.20	30.14
L15	79.90	30.31
L14	76.60	30.47
L13	73.30	30.63
L12	70.00	30.77
L11	66.70	30.92
L10	63.40	31.05
L9	60.10	31.18
L8	56.80	31.31
L7	53.50	31.42
L6	50.20	31.54
L5	46.90	31.64
L4	43.60	31.74
L3	40.30	31.84
L2	37.00	31.92
L1A	34.00	32.00
L1	31.00	32.15
P4A	26.20	32.29
P4	21.40	32.40
P3M	16.90	32.49
P3	12.40	32.58
P2	6.900	32.64
P1	1.400	32.69
B1	-3.100	32.72
B2	-6.200	32.73
B3	-9.300	32.74

Table A-1: Remaining portion of Equivalent Static Shear distributed over the height of the building

APPENDIX B - CONCRETE SECTIONS DETAILS AND MOMENT-CURVATURE RELATIONSHIPS

Modeled Section | *Right-Bottom*

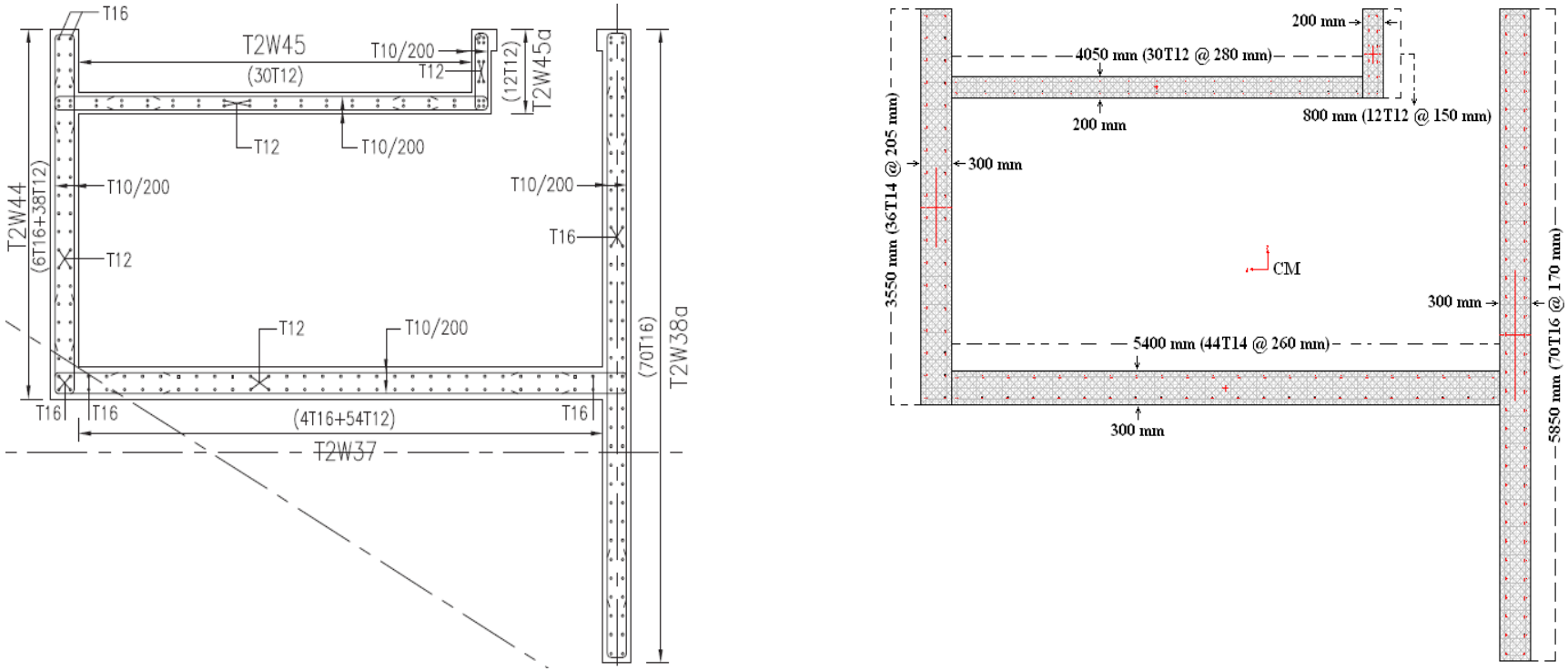

(a) (b)

Figure B-1: Unconfined boxed-core assembled section located right-bottom of floor plan: (a) structural drawings; (b) Section Designer model

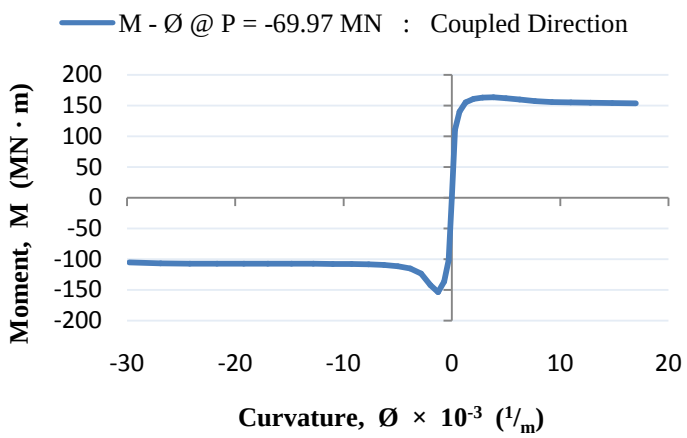

(a)

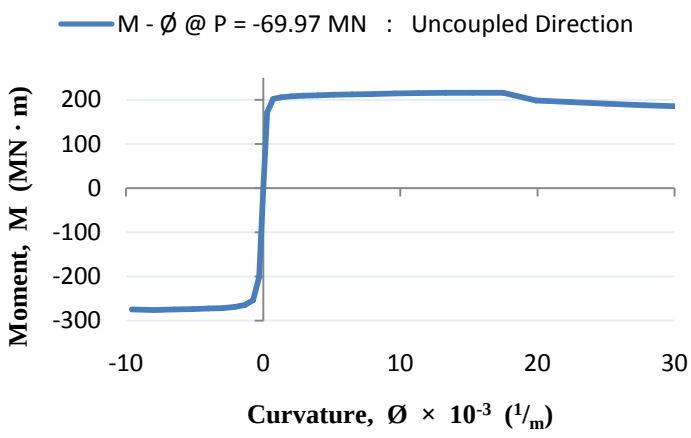

(b)

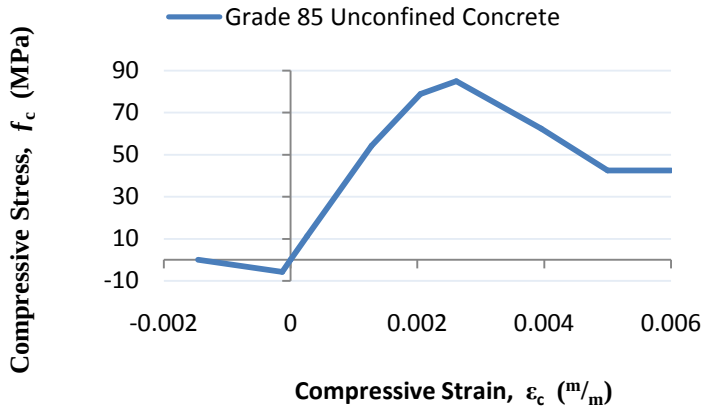

(c)

Figure B-2: Right-Bottom Modeled Section: (a) Coupled Direction Moment-Curvature Graph; (b) Uncoupled Direction Moment-Curvature Graph; (c) Grade 85 Unconfined Concrete Stress-Strain Graph

Modeled Section | *Right-Top*

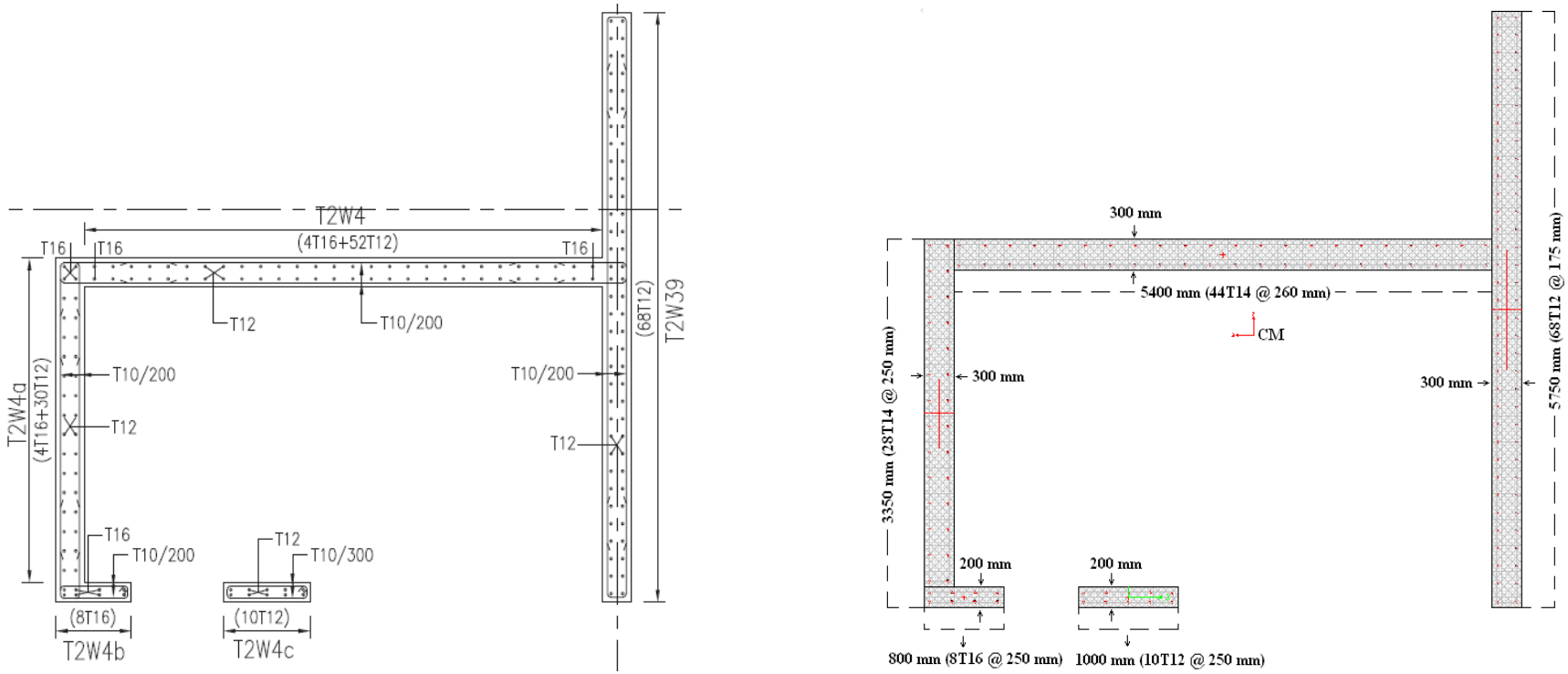

(a) (b)

Figure B-3: Unconfined boxed-core assembled section located right-top of floor plan: (a) structural drawings; (b) Section Designer model

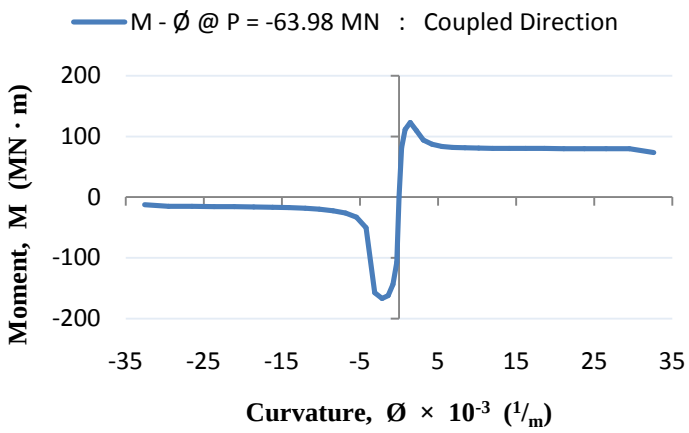

(a)

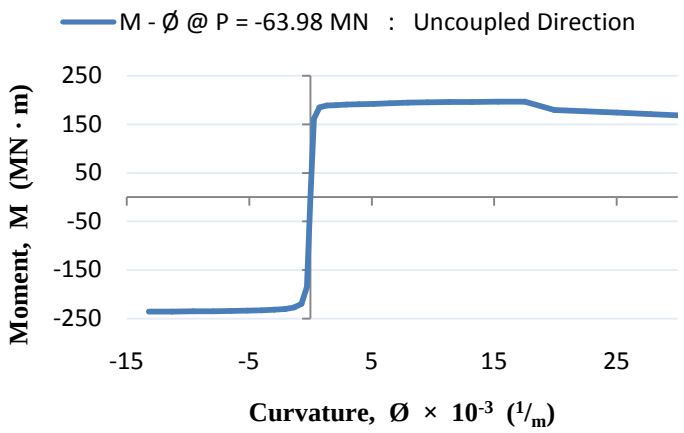

(b)

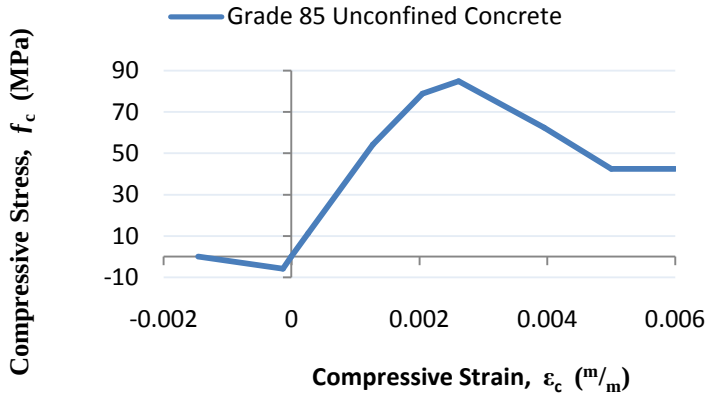

(c)

Figure B-4: Right-Top Modeled Section: (a) Coupled Direction Moment-Curvature Graph; (b) Uncoupled Direction Moment-Curvature Graph; (c) Grade 85 Unconfined Concrete Stress-Strain Graph

Modeled Section | *Center-Bottom*

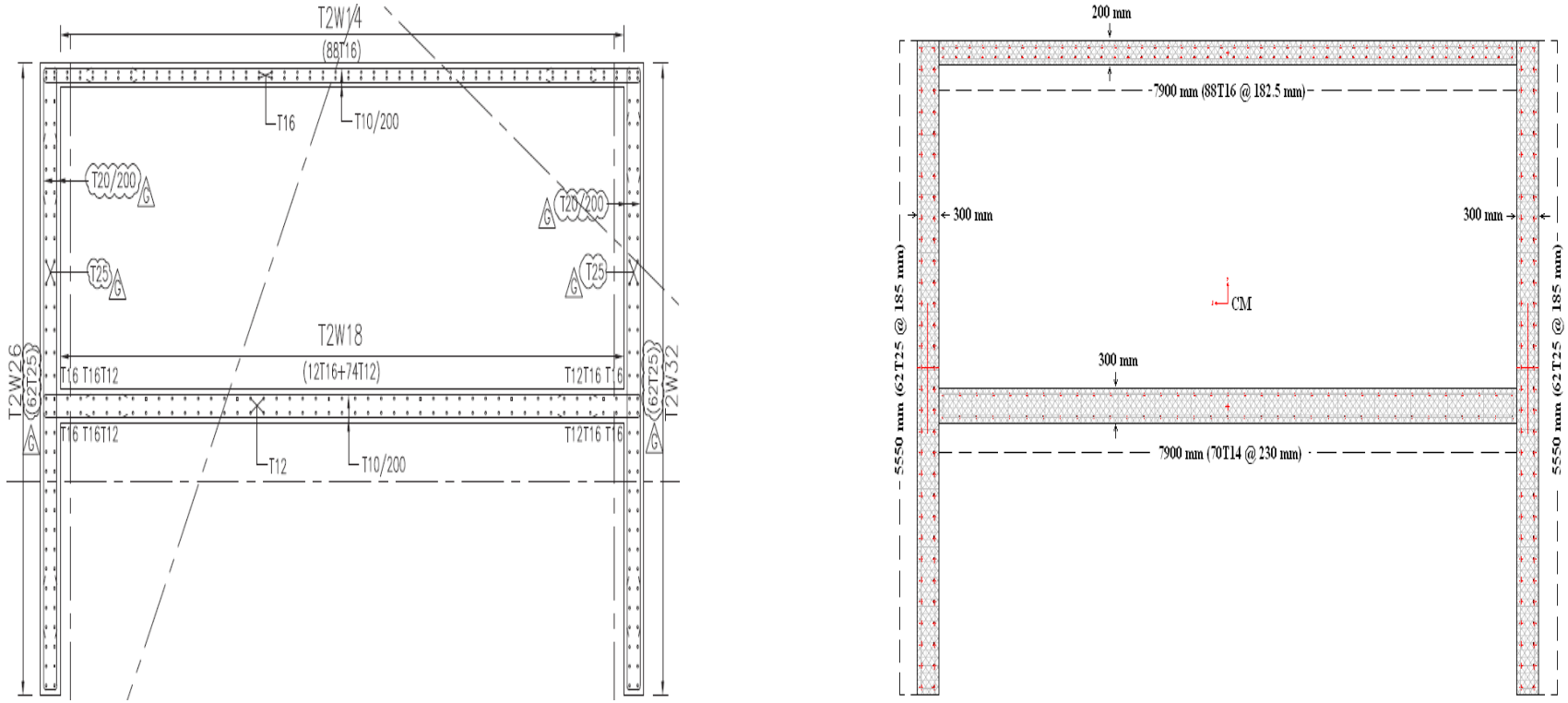

(a) (b)

Figure B-5: Unconfined boxed-core assembled section located center-bottom of floor plan: (a) structural drawings; (b) Section Designer model

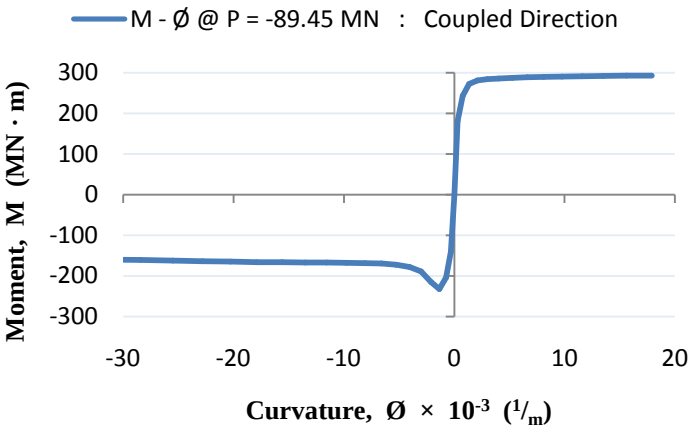

(a)

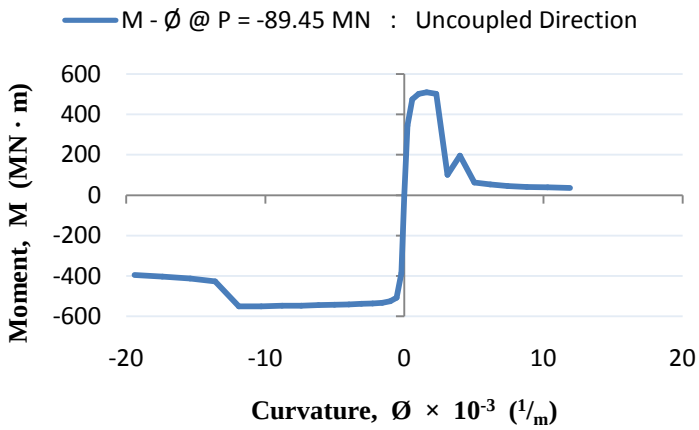

(b)

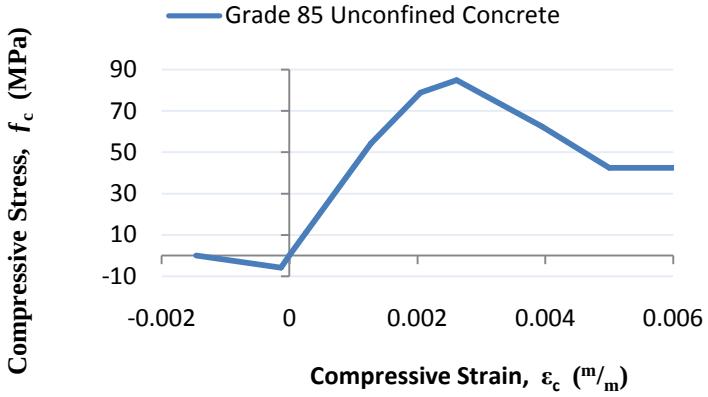

(c)

Figure B-6: Center-Bottom Modeled Section: (a) Coupled Direction Moment-Curvature Graph; (b) Uncoupled Direction Moment-Curvature Graph; (c) Grade 85 Unconfined Concrete Stress-Strain Graph

Modeled Section | *Center-Top*

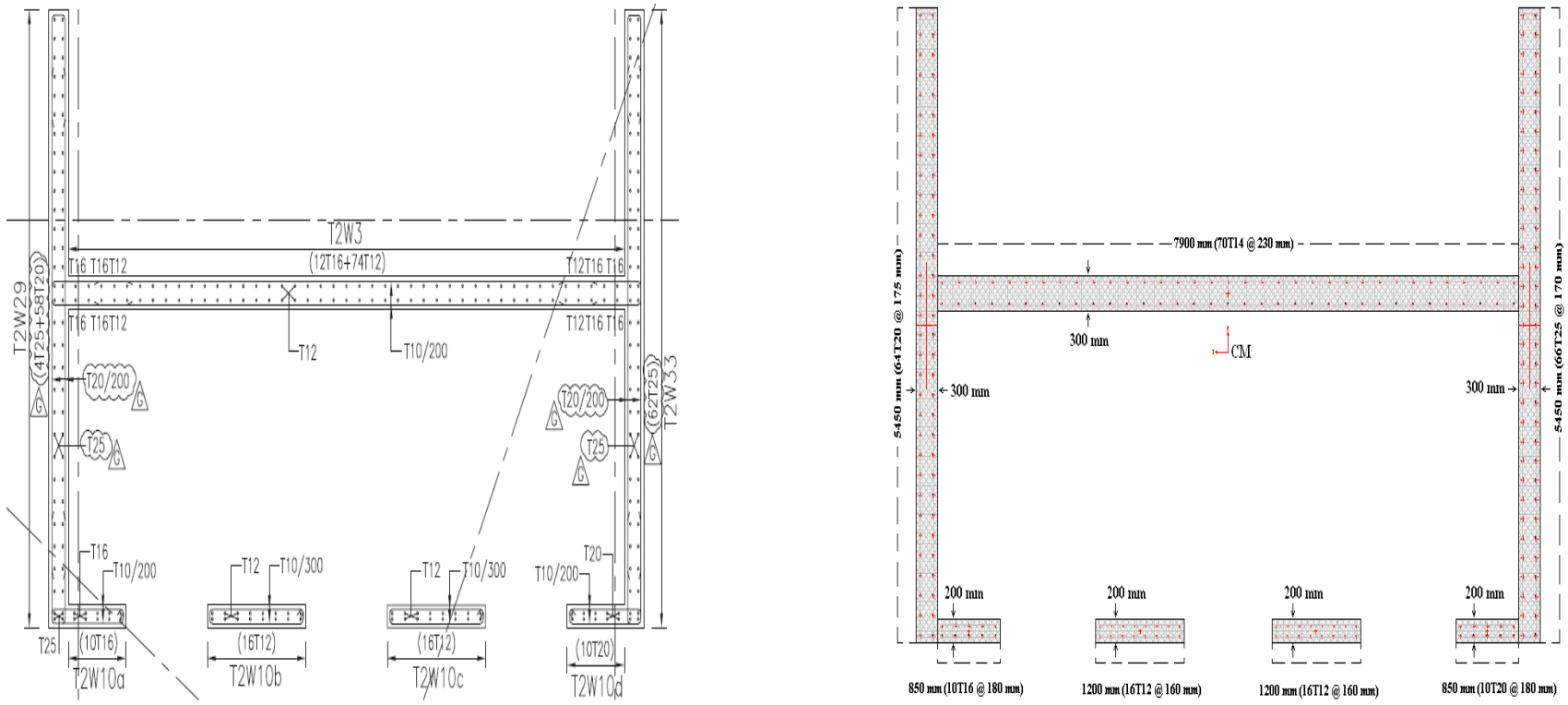

(a) (b)

Figure B-7: Unconfined boxed-core assembled section located center-top of floor plan: (a) structural drawings; (b) Section Designer model

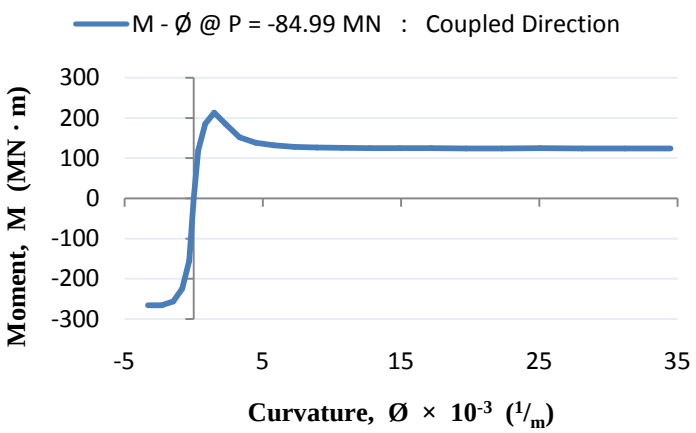

(a)

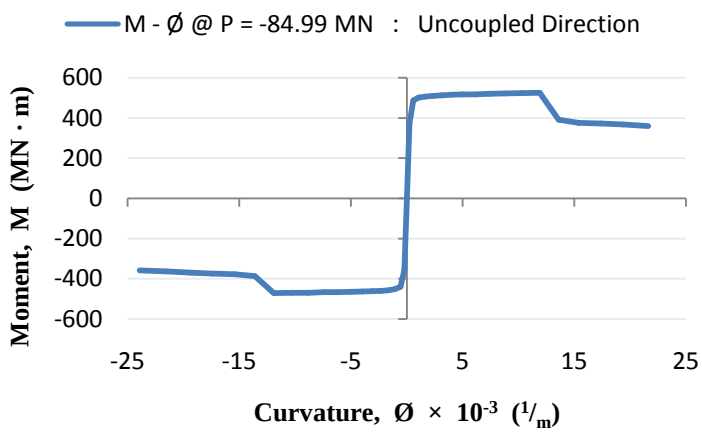

(b)

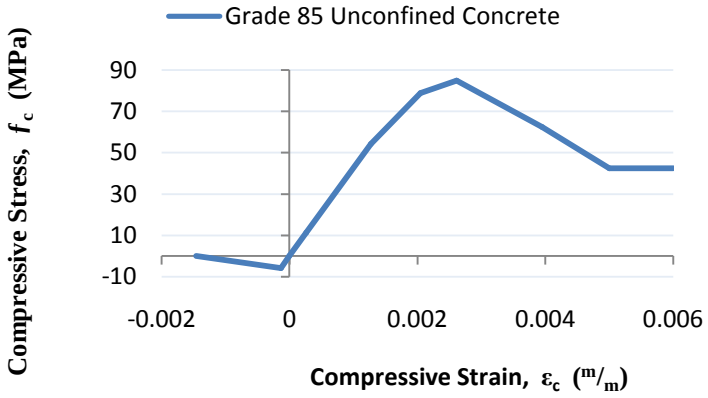

(c)

Figure B-8: Center-Top Modeled Section: (a) Coupled Direction Moment-Curvature Graph; (b) Uncoupled Direction Moment-Curvature Graph; (c) Grade 85 Unconfined Concrete Stress-Strain Graph

Modeled Section | *Left-Bottom*

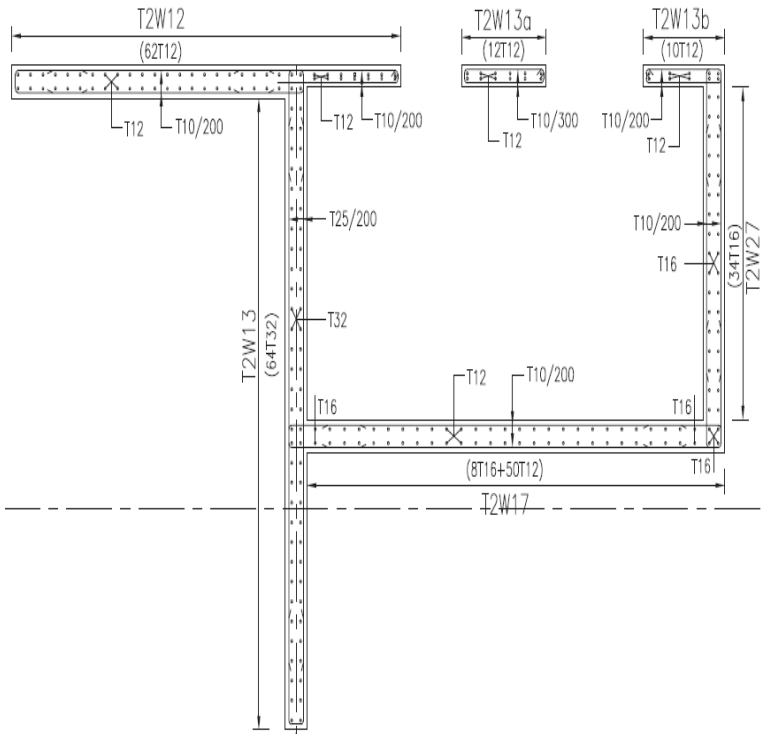

(a)

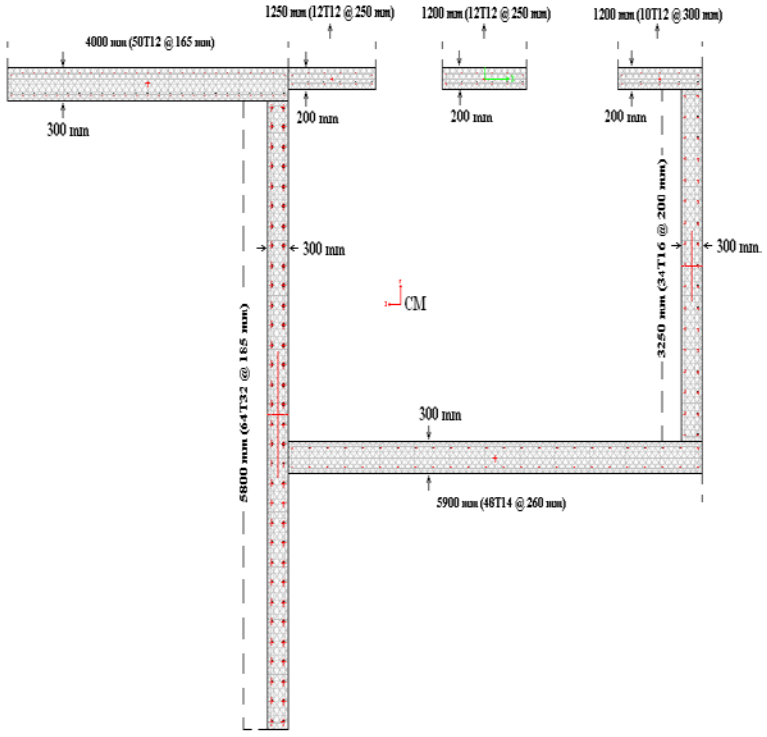

(b)

Figure B-9: Unconfined boxed-core assembled section located left-bottom of floor plan: (a) structural drawings; (b) Section Designer model

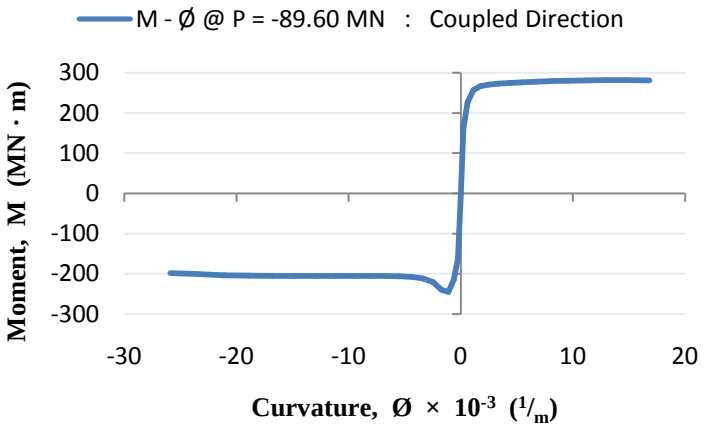

(a)

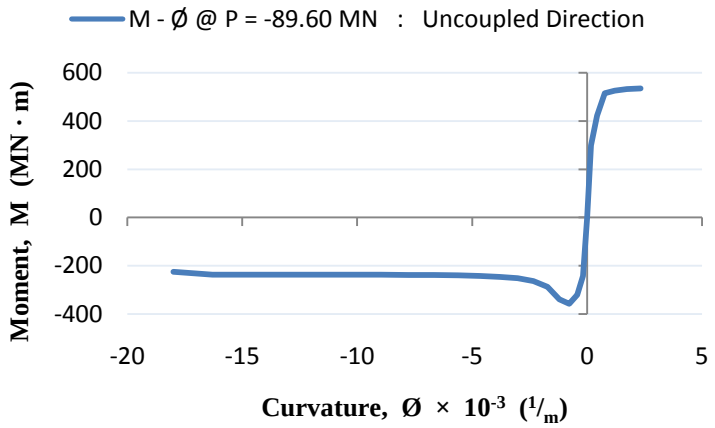

(b)

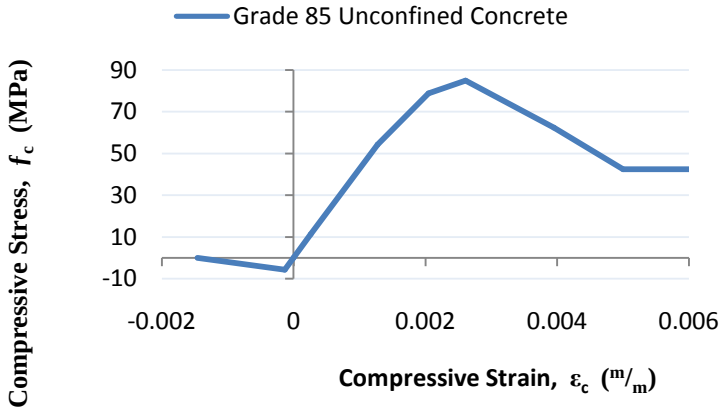

(c)

Figure B-10: Left-Bottom Modeled Section: (a) Coupled Direction Moment-Curvature Graph; (b) Uncoupled Direction Moment-Curvature Graph; (c) Grade 85 Unconfined Concrete Stress-Strain Graph

Modeled Section | *Left-Top*

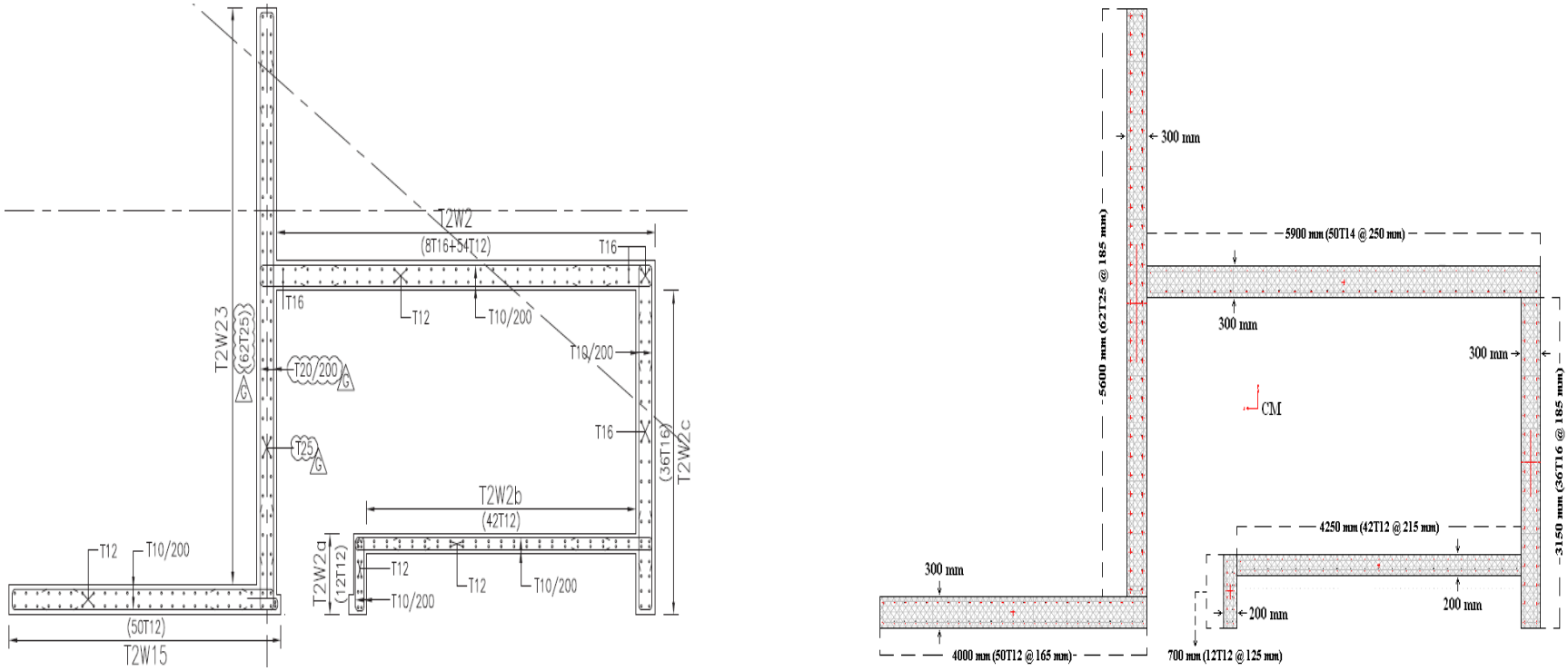

(a) (b)

Figure B-11: Unconfined boxed-core assembled section located left-top of floor plan: (a) structural drawings; (b) Section Designer model

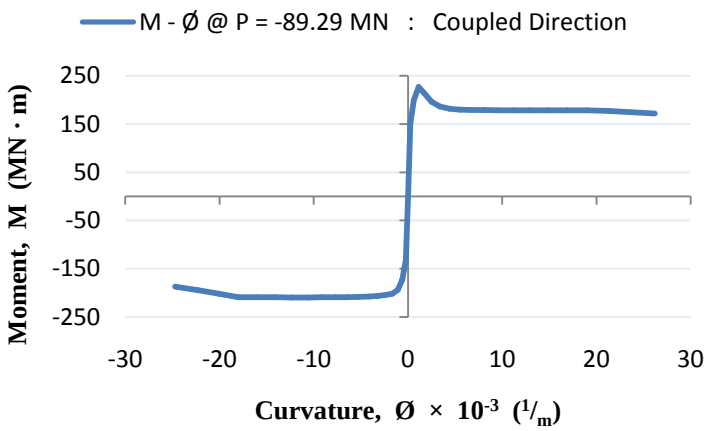

(a)

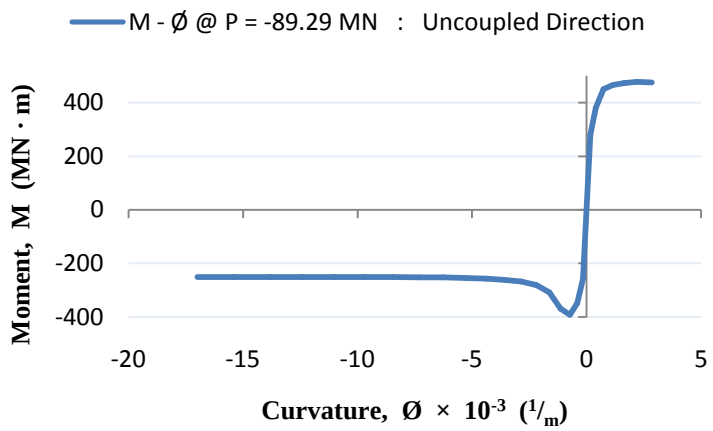

(b)

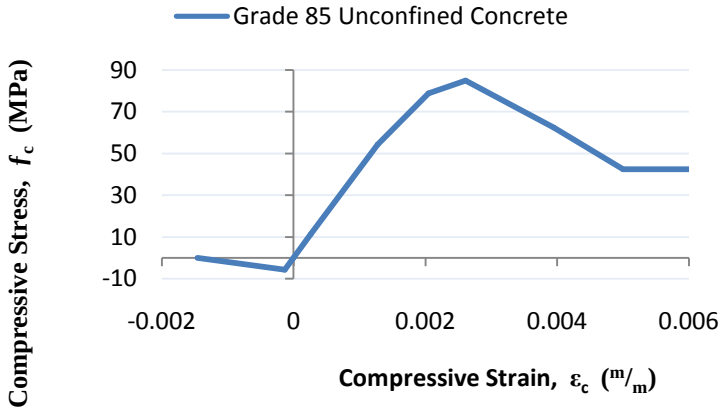

(c)

Figure B-12: Left-Top Modeled Section: (a) Coupled Direction Moment-Curvature Graph; (b) Uncoupled Direction Moment-Curvature Graph; (c) Grade 85 Unconfined Concrete Stress-Strain Graph

Modeled Section | *Column-Wall Member* | *T2C3*

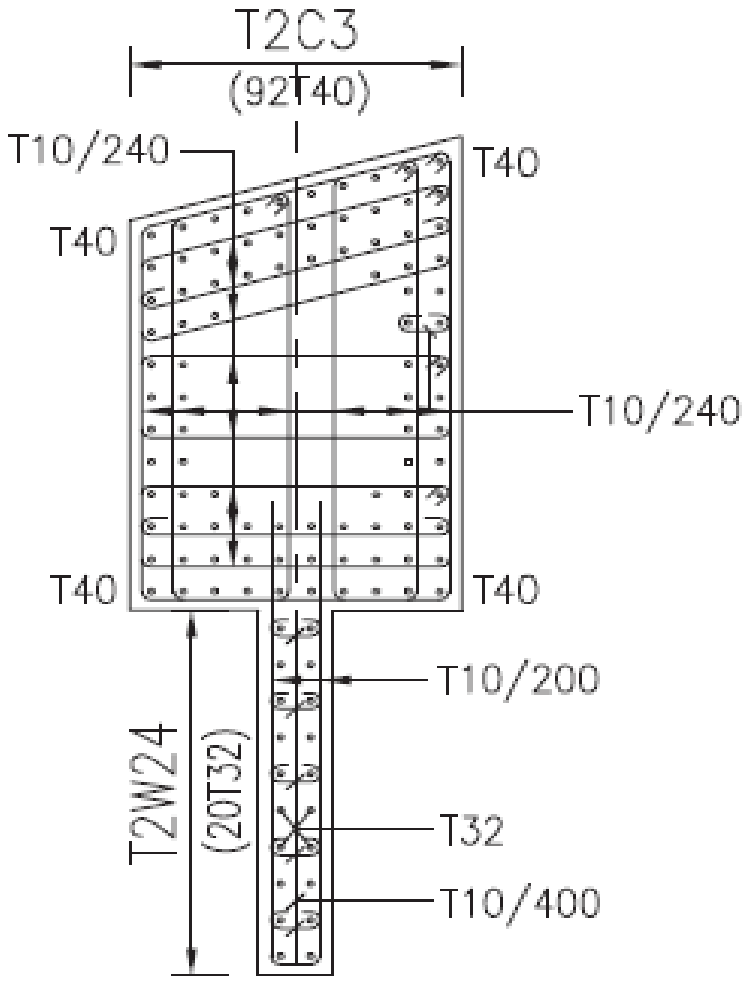

(a)

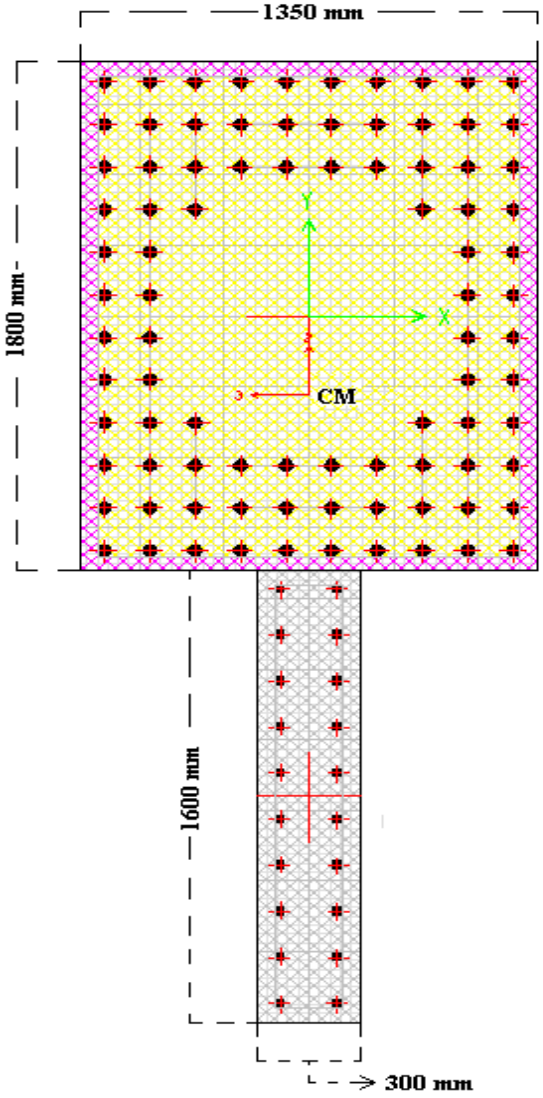

Column Member

Concrete Cover = 50 mm (x & y directions)

Transverse Reinforcement
88T40 @ 150 mm

Transverse Confining Reinforcement
ρ_w = 0.6%
Tie spacing in 1350 mm width @ S_X = 125 mm
Tie spacing in 1800 mm height @ S_Y = 120 mm

Wall Membe

Concrete Cover = 50 mm (x & y directions)

Transverse Reinforcement
20T32 @ 180 mm

Transverse Confining Reinforcement
ρ_w = 0.6%
Tie spacing in 300 mm width @ S_X = 190 mm
Tie spacing in 1600 mm height @ S_Y = 70 mm

(b)

Figure B-13: Column-Wall Member T2C3: (a) structural drawings; (b) Section Designer model

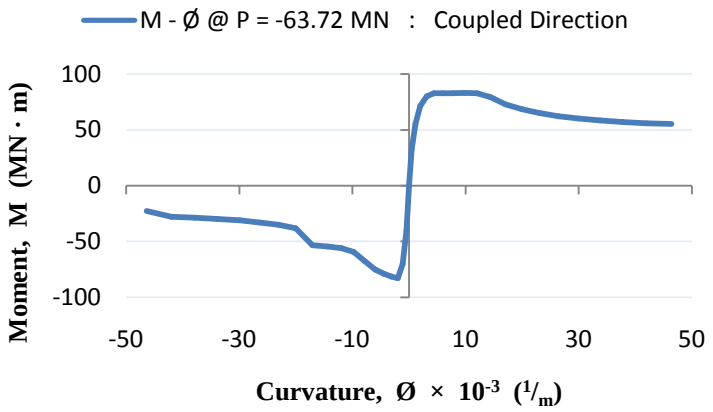

(a)

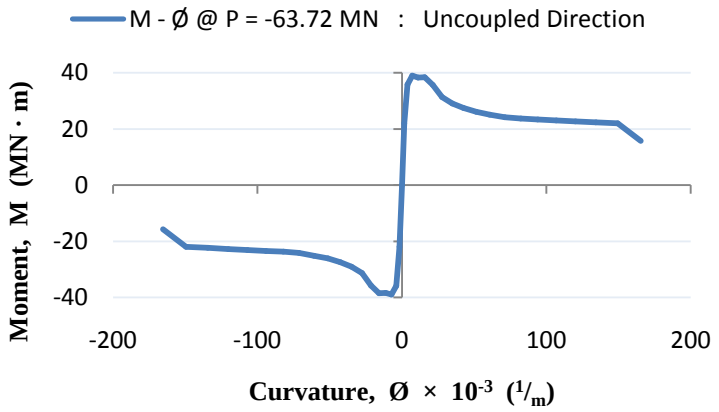

(b)

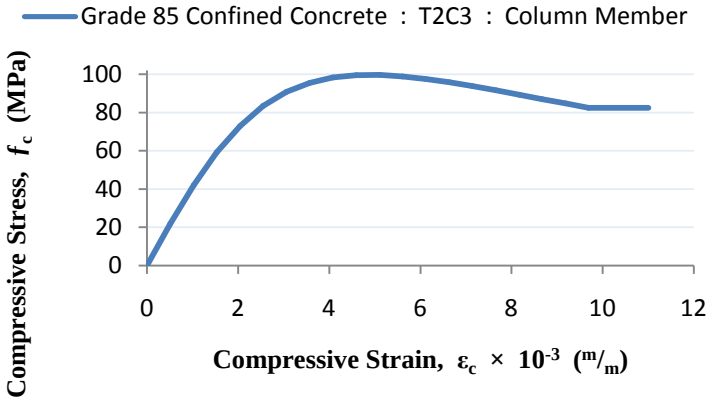

(c)

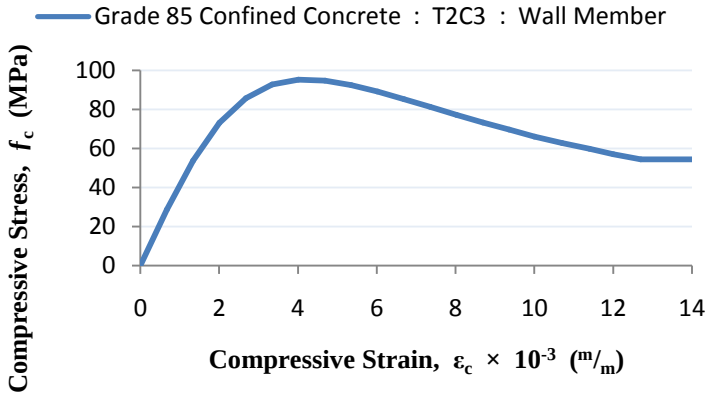

(d)

Figure B-14: Column-Wall Member T2C3: (a) Coupled Direction Moment-Curvature Graph; (b) Uncoupled Direction Moment-Curvature Graph; (c) Column Member Grade 85 Confined Concrete Stress-Strain Graph; (d) Wall Member Grade 85 Confined Concrete Stress-Strain Graph

Modeled Section | *Column-Wall Member* | *T2C4*

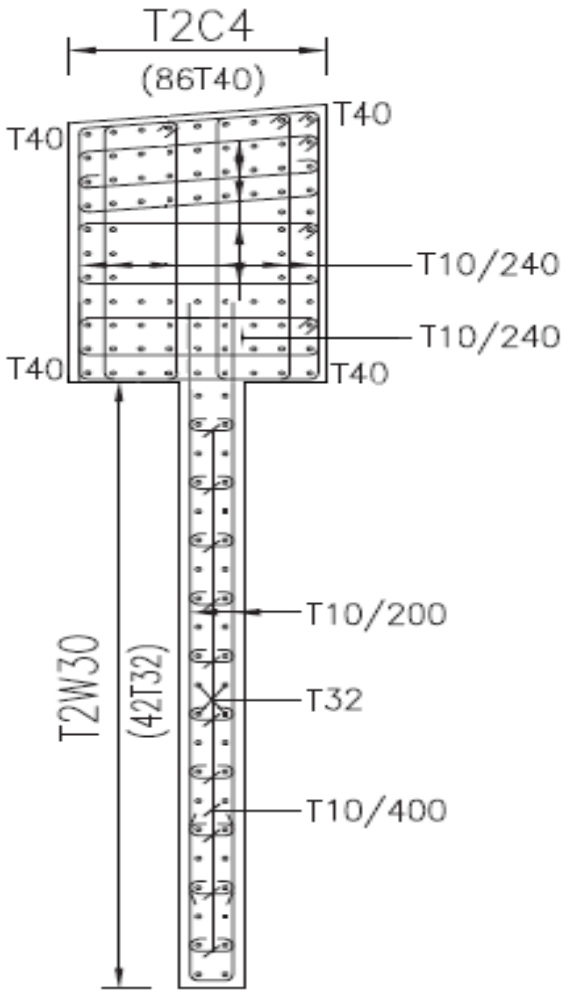

(a)

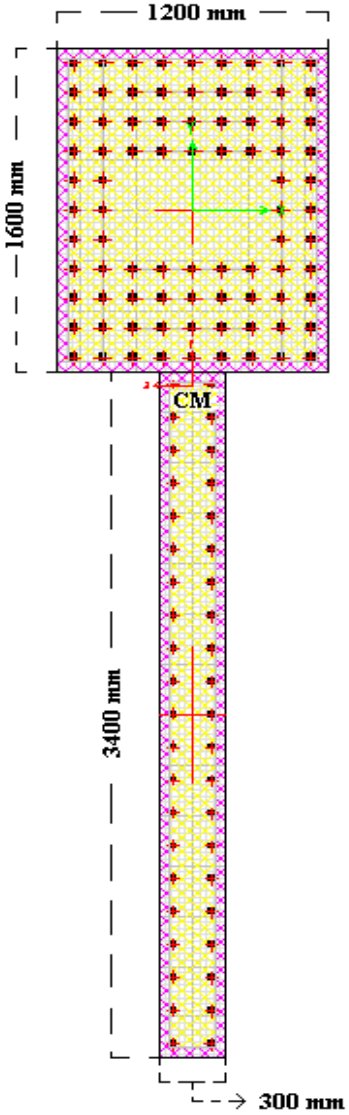

Column Member

Concrete Cover = 50 mm (x & y directions)

Transverse Reinforcement
84T40 @ 150 mm

Transverse Confining Reinforcement
ρ_w = 0.6%
Tie spacing in 1350 mm width @ S_X = 120 mm
Tie spacing in 1800 mm height @ S_Y = 125 mm

Wall Member

Concrete Cover = 50 mm (x & y directions)

Transverse Reinforcement
42T32 @ 165 mm

Transverse Confining Reinforcement
ρ_w = 0.6%
Tie spacing in 300 mm width @ S_X = 190 mm
Tie spacing in 1600 mm height @ S_Y = 70 mm

(b)

Figure B-15: Column-Wall Member T2C4: (a) structural drawings; (b) Section Designer model

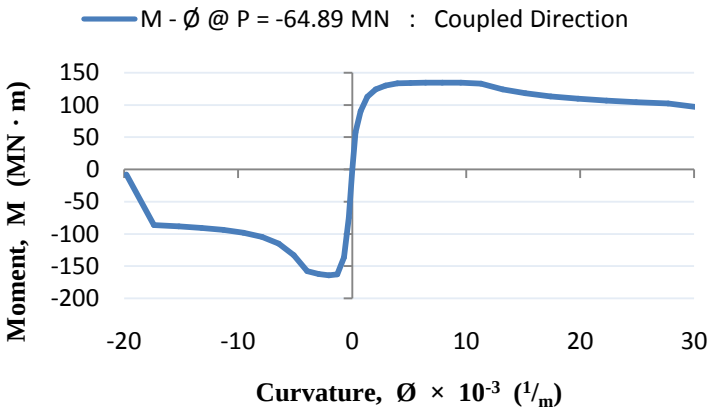

(a)

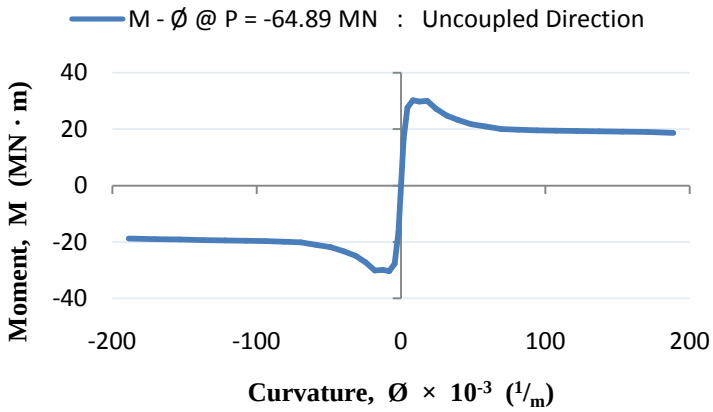

(b)

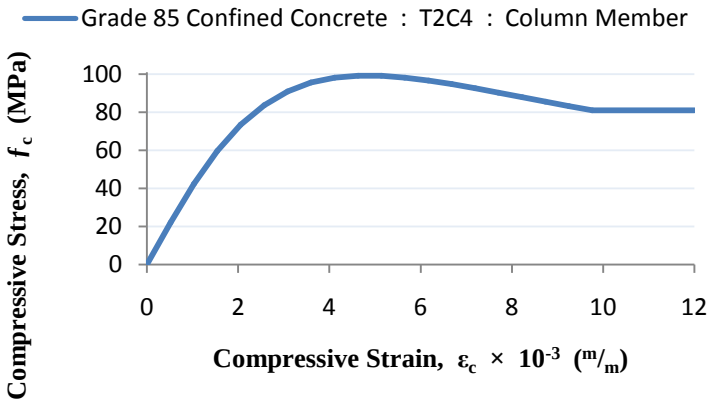

(c)

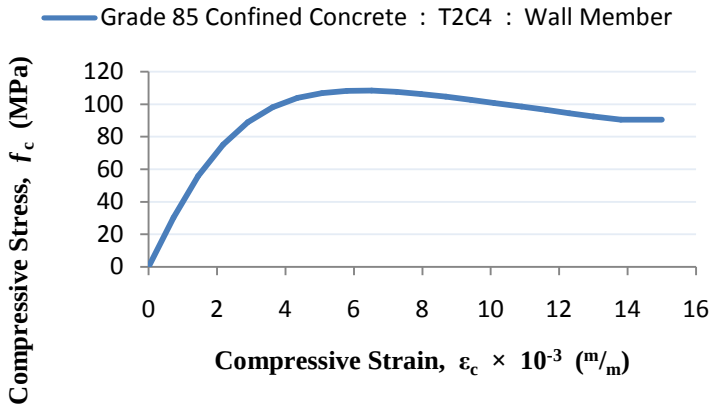

(d)

Figure B-16: Column-Wall Member T2C4: (a) Coupled Direction Moment-Curvature Graph; (b) Uncoupled Direction Moment-Curvature Graph; (c) Column Member Grade 85 Confined Concrete Stress-Strain Graph; (d) Wall Member Grade 85 Confined Concrete Stress-Strain Graph

Modeled Section | *Coupling Beam Member* | *T2B-C1*

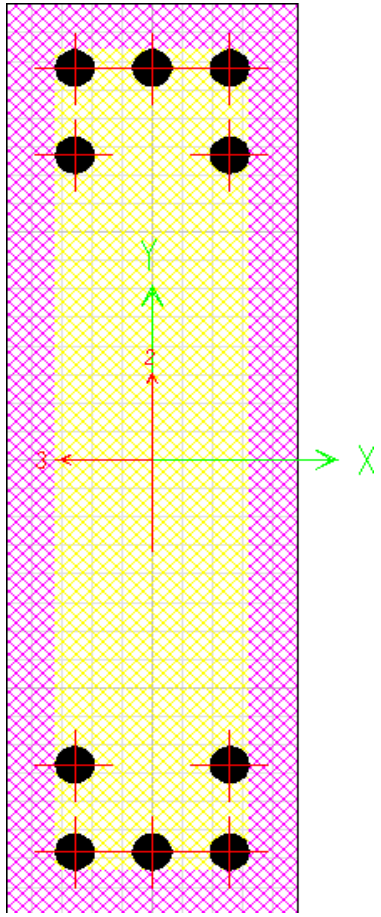

Coupling Beam Member

Concrete Cover = 50 mm (x & y directions)

Transverse Reinforcement
10T40

Transverse Confining Reinforcement
ρ_w = 0.6%
Tie spacing in 300 mm width @ S_X = 190 mm
Tie spacing in 1000 mm height @ S_Y = 200 mm

Figure B-17: Coupling Beam Member T2B-C1 Section Designer model

Beam Mark	Level	Beam Size (mm)	Concrete (MPa)	a1	a2	b1	b2
T2B-C1	3	1000 x 300	85	3T40	2T40	3T40	2T40

Table B-1: Coupling Beam Member T2B-C1 Structural Drawings Reinforcement Details

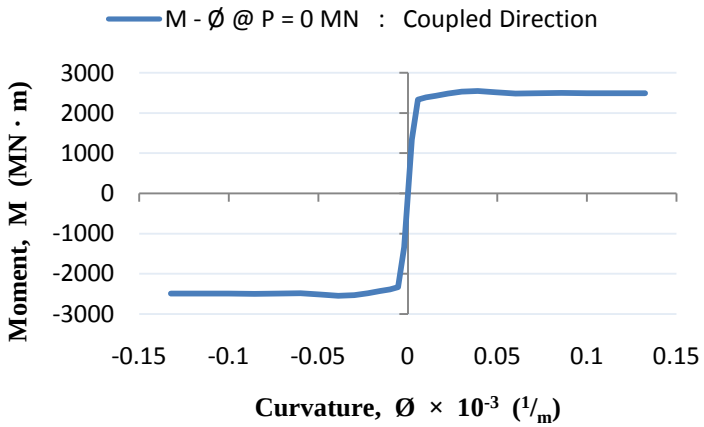

(a)

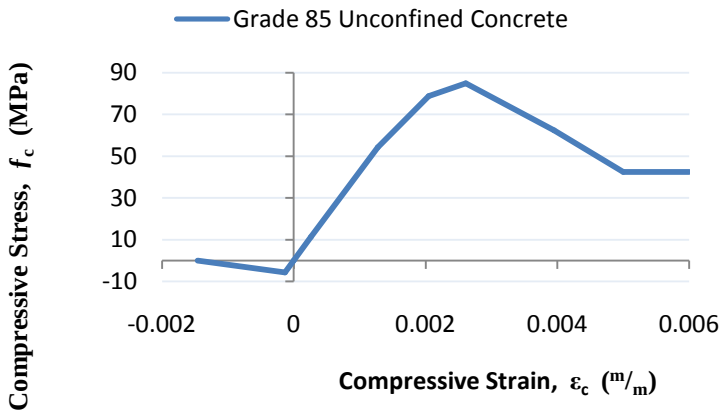

(b)

Figure B-18: Coupling Beam Member T2B-C1: (a) Coupled Direction Moment-Curvature Graph; (b) Grade 85 Unconfined Concrete Stress-Strain Graph

APPENDIX C - EQUIVALENT STATIC ANALYSIS RESULTS

Coupled and Uncoupled Directions Response | *Overall Building*

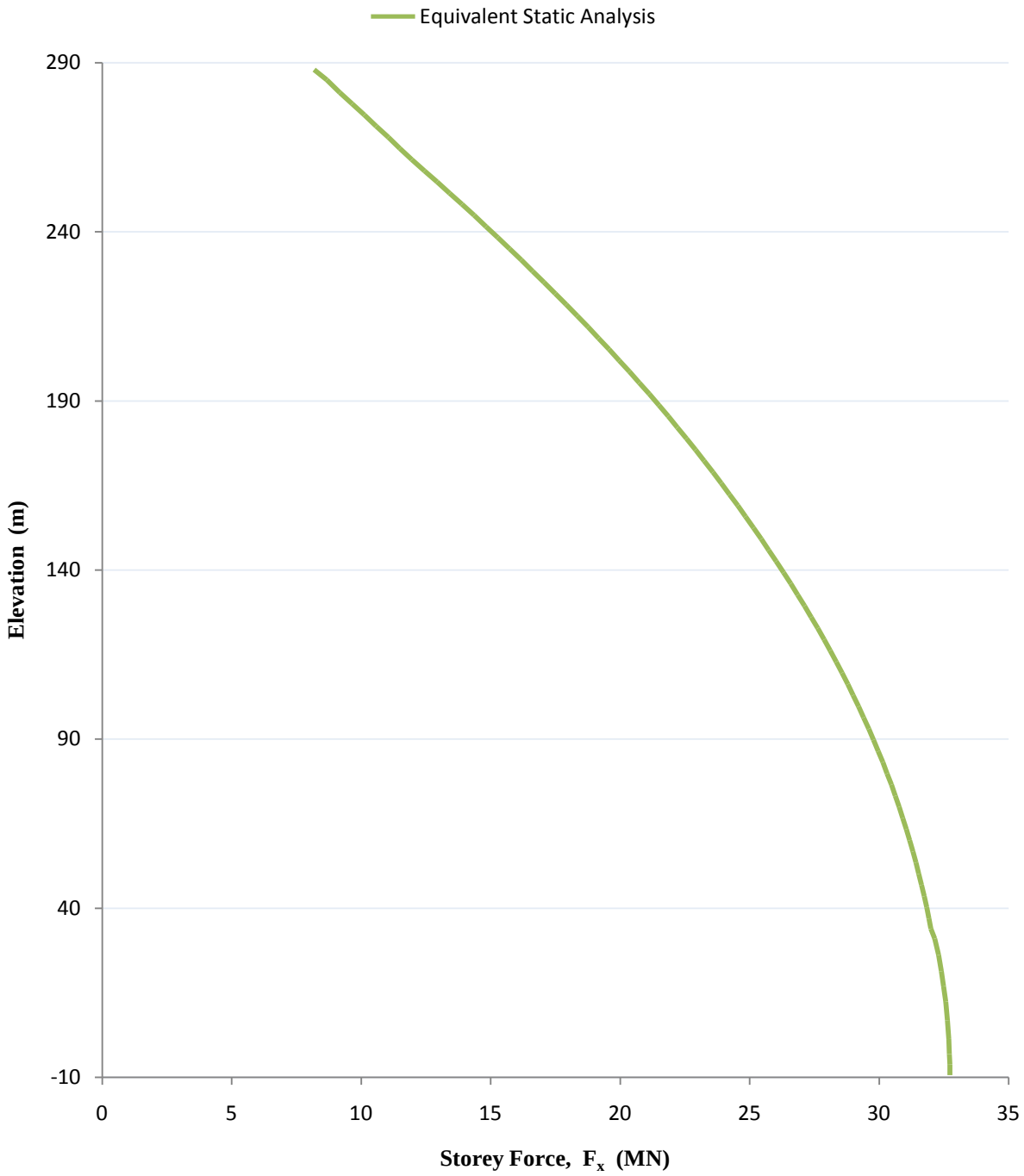

Figure C-1: Equivalent Static Shear Force distributed over the height of the building

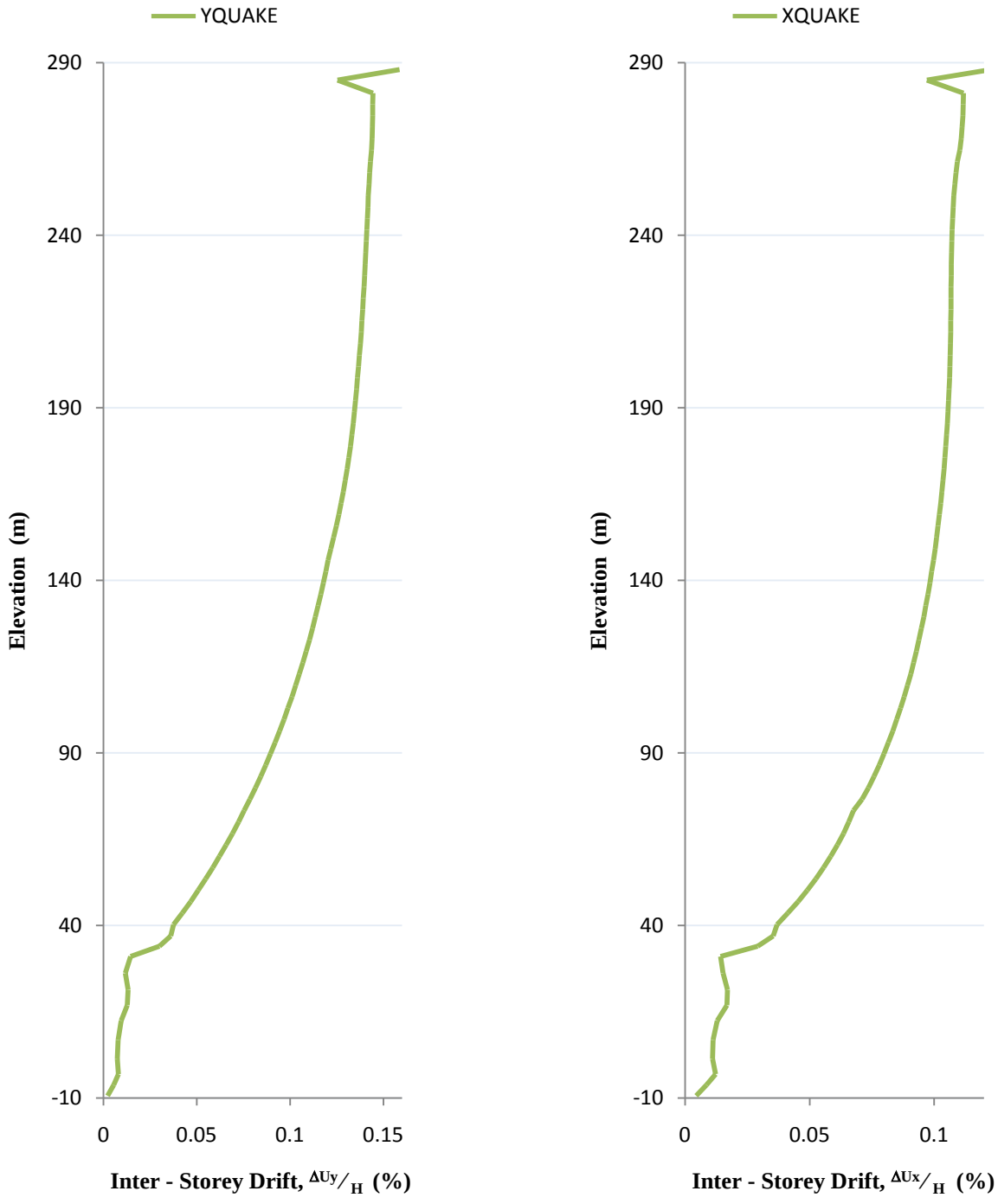

(a) (b)

Figure C-2: Equivalent Static Analysis Overall Building Response-Maximum Inter-Storey Drift: (a) Coupled Direction; (b) Uncoupled Direction

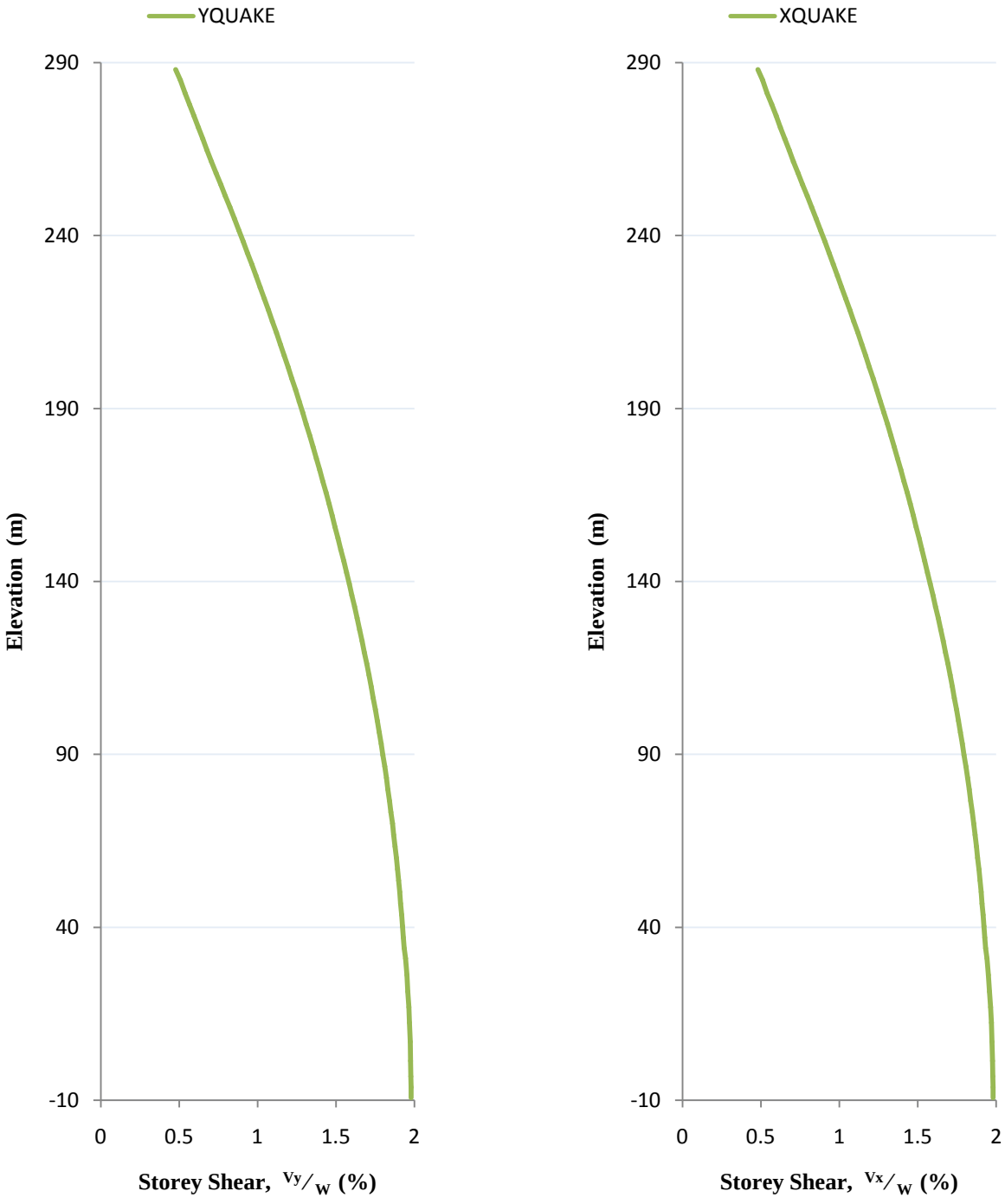

(a) (b)

Figure C-3: Equivalent Static Analysis Overall Building Response-Maximum Storey Shear: (a) Coupled Direction; (b) Uncoupled Direction

Coupled Direction Response | *Core Member* | *Left-Bottom*

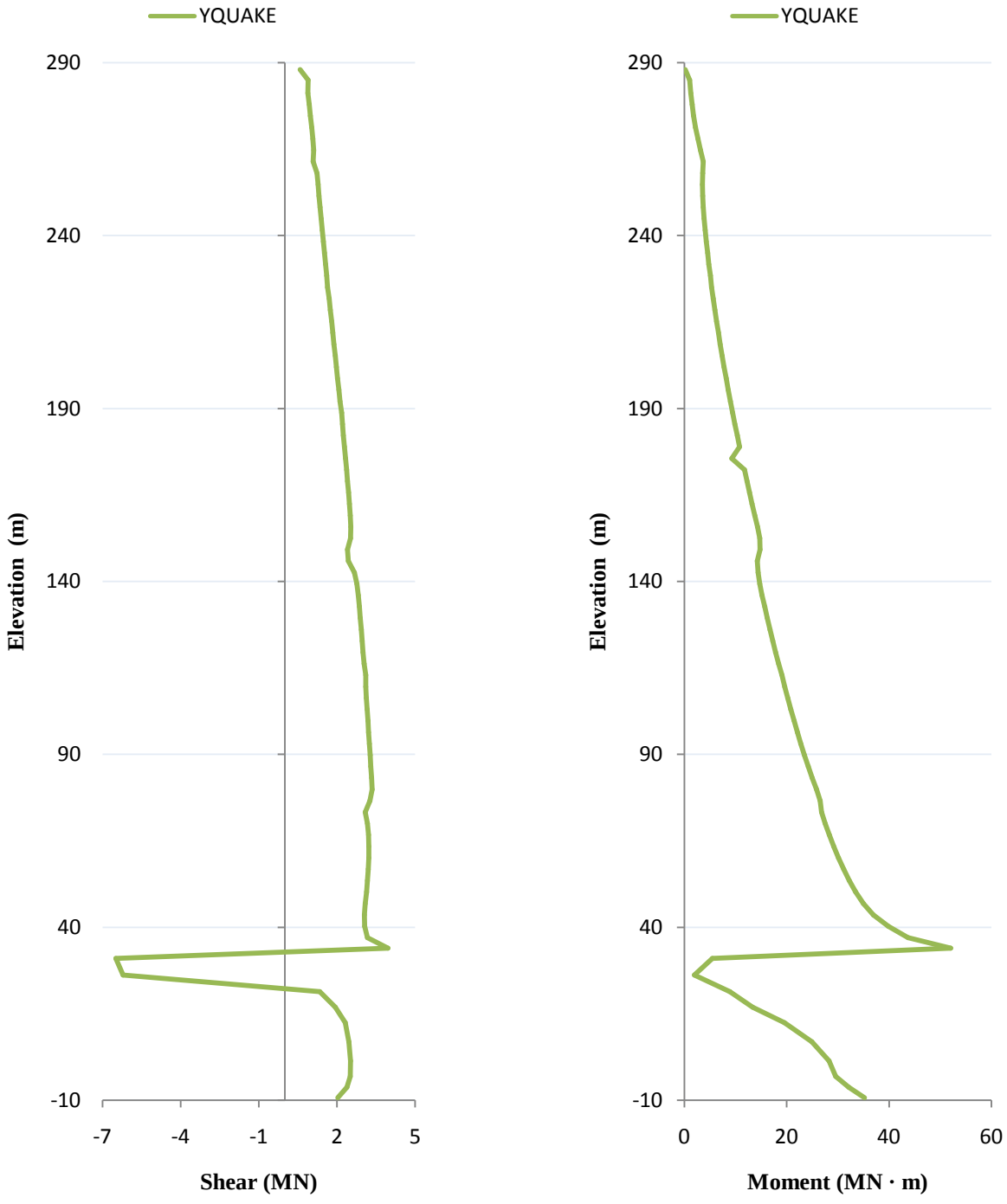

(a) (b)

Figure C-4: Equivalent Static Analysis Left-Bottom Core Member Coupled Direction Response: (a) Shear; (b) Moment

Coupled Direction Response | *Core Member* | *Center-Bottom*

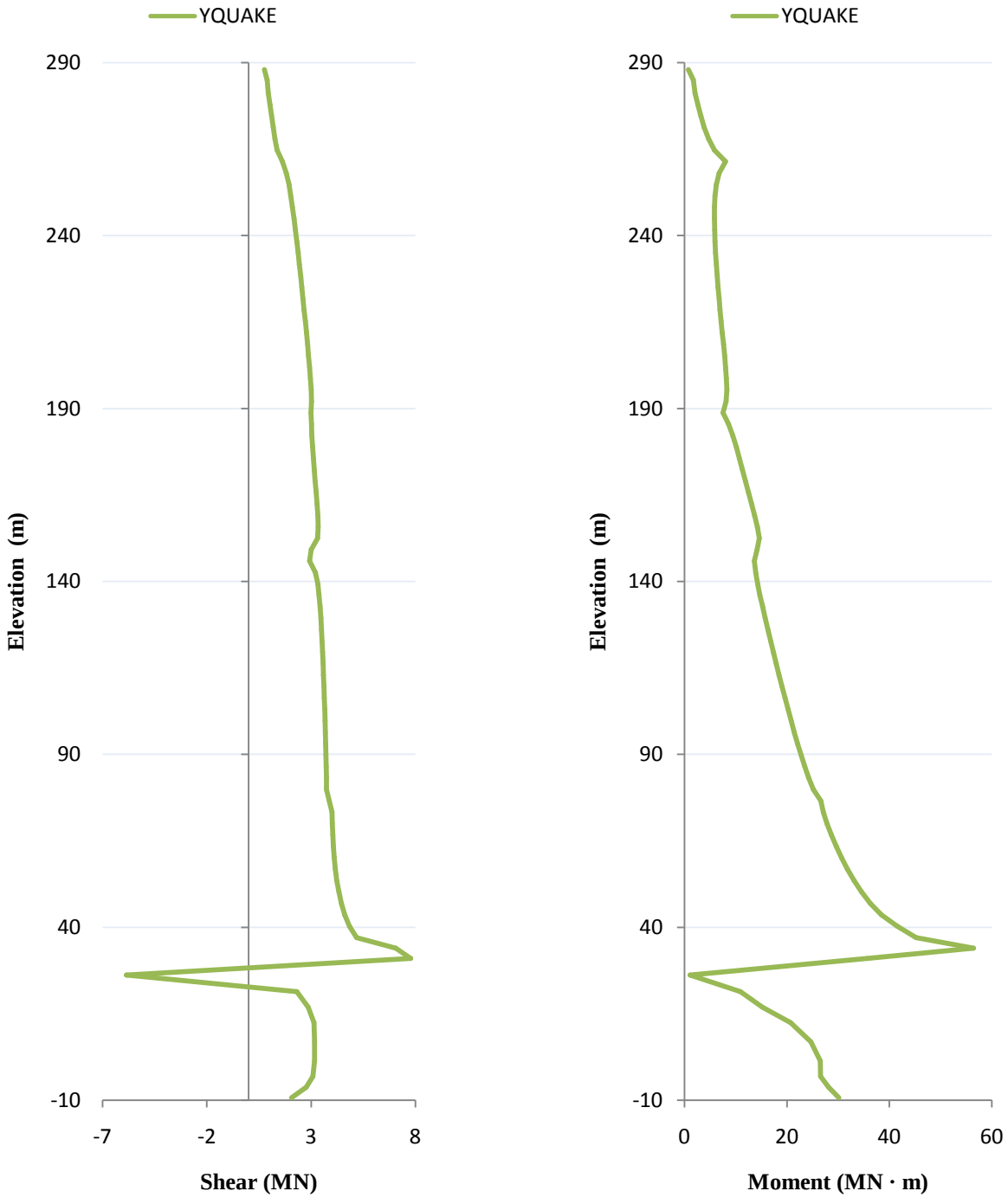

(a) (b)

Figure C-5: Equivalent Static Analysis Center-Bottom Core Member Coupled Direction Response: (a) Shear; (b) Moment

Uncoupled Direction Response | *Core Member* | *Left-Bottom*

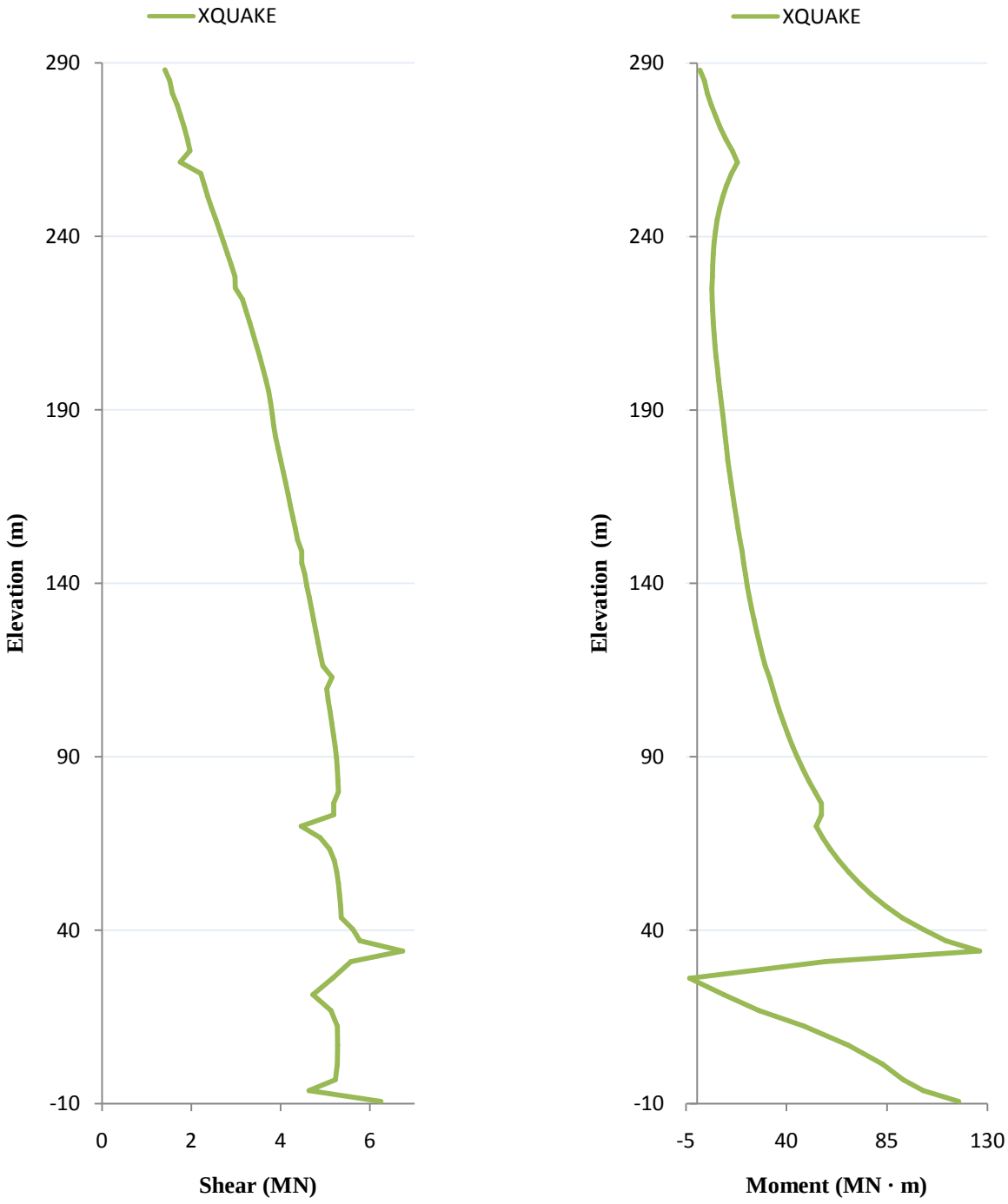

(a) (b)

Figure C-6: Equivalent Static Analysis Left-Bottom Core Member Uncoupled Direction Response: (a) Shear; (b) Moment

Uncoupled Direction Response | *Core Member* | *Center-Bottom*

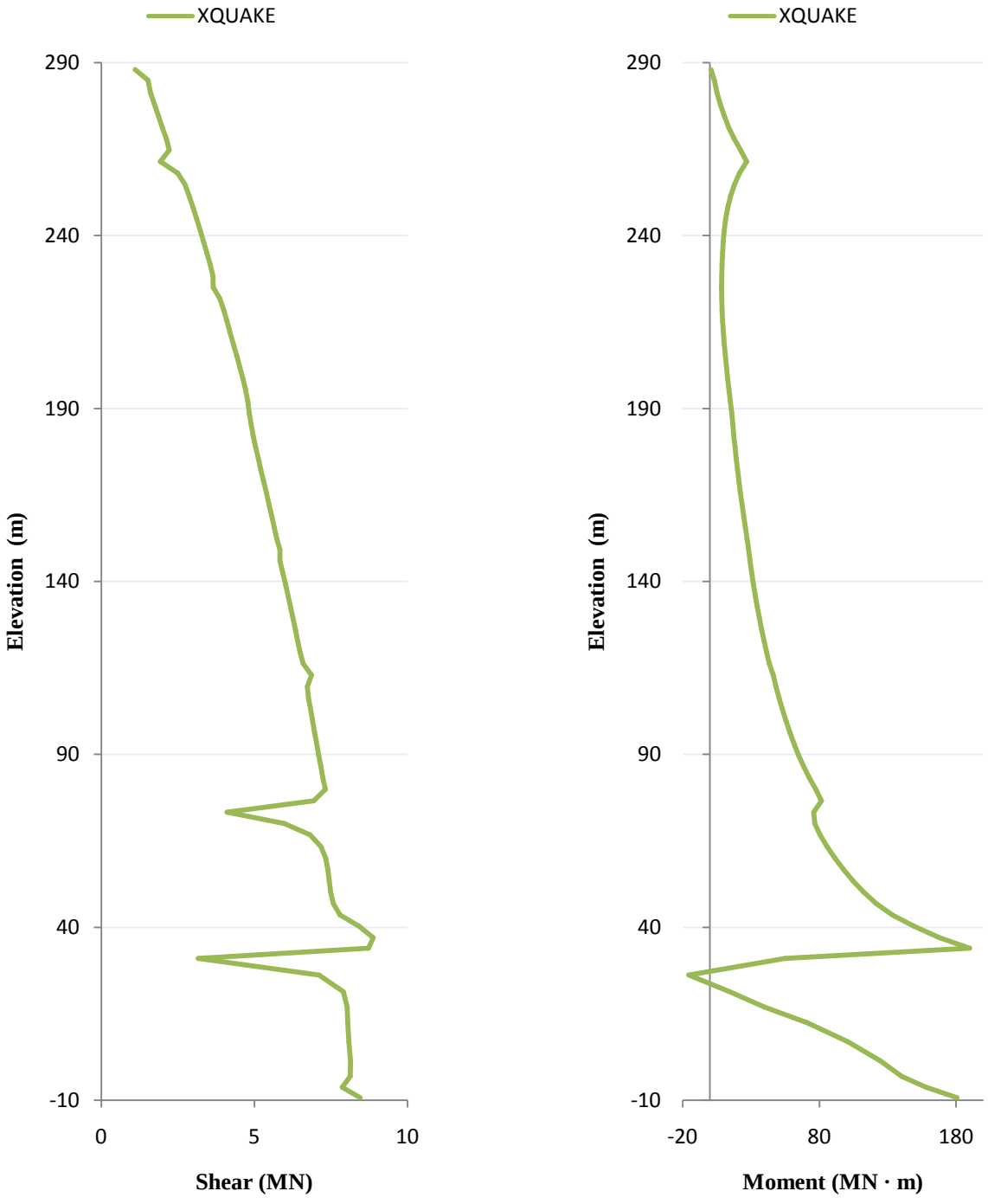

(a) (b)

Figure C-7: Equivalent Static Analysis Center-Bottom Core Member Uncoupled Direction Response: (a) Shear; (b) Moment

Coupled Direction Response | *Column-Wall Member* | *T2C10*

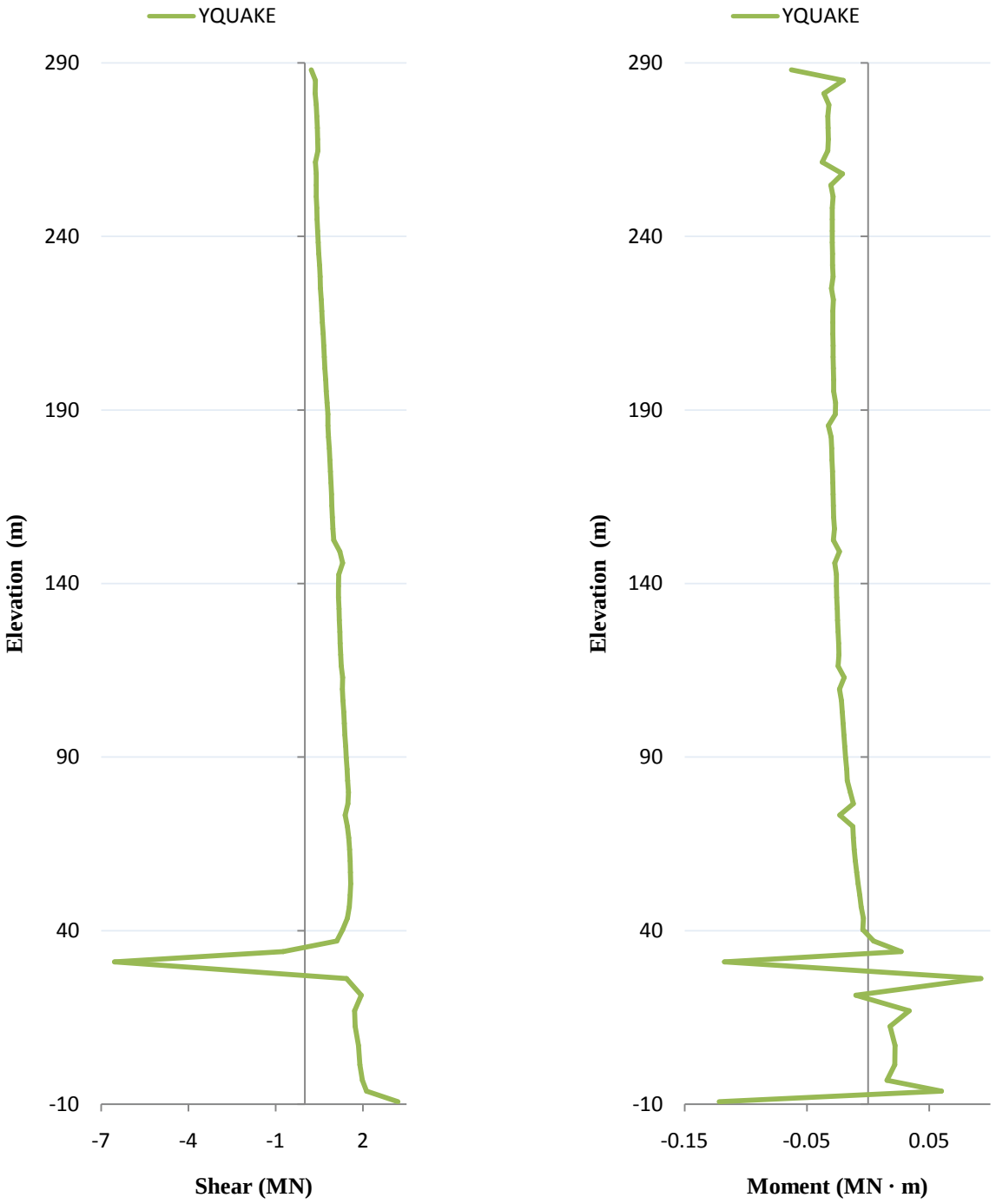

(a) (b)

Figure C-8: Equivalent Static Analysis Column-Wall Member Response (T2C10 located bottom-left of floor plan): (a) Shear; (b) Moment

Coupled Direction Response | *Column-Wall Member* | *T2C11*

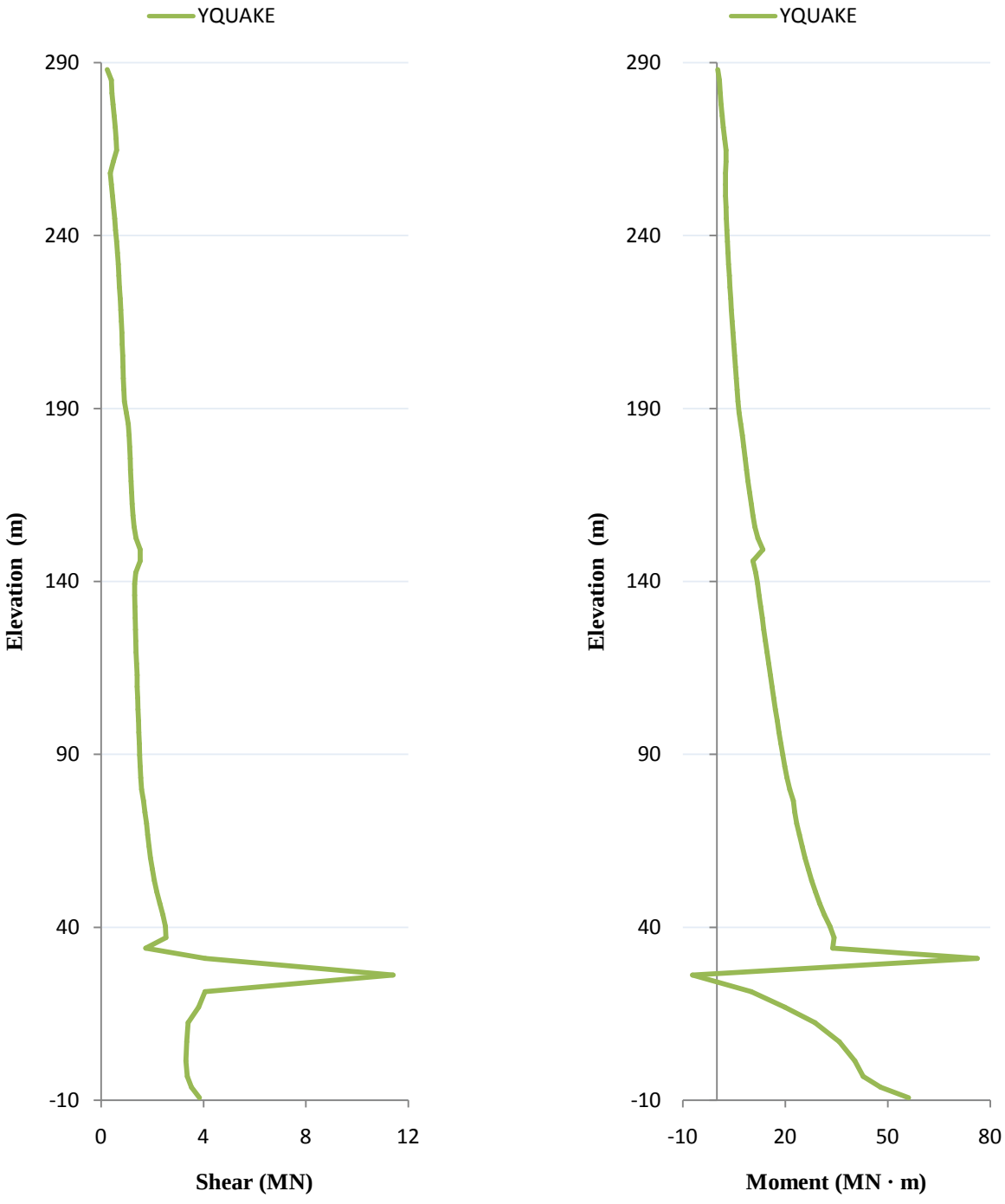

(a) (b)

Figure C-9: Equivalent Static Analysis Column-Wall Member Response (T2C11 located central bottom-left of floor plan): (a) Shear; (b) Moment

Coupled Direction Response | *Coupling Beam Member* | *T2B-C1* | *Left End*

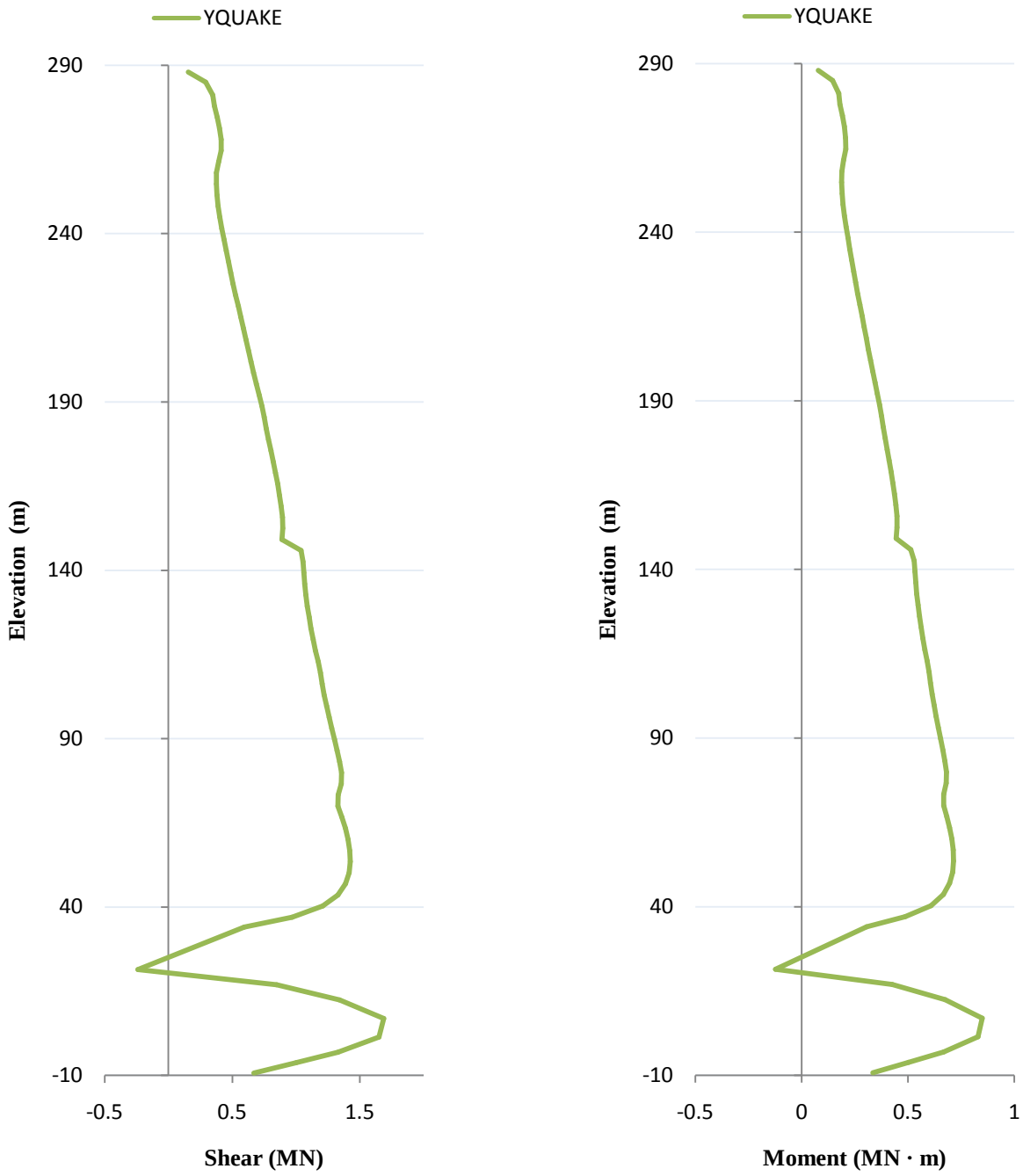

(a) (b)

Figure C-10: Equivalent Static Analysis Coupling Beam Member Response at Left End (T2B-C1 located bottom-left of floor plan): (a) Shear; (b) Moment

Coupled Direction Response | *Coupling Beam Member* | *T2B-C1* | *Right End*

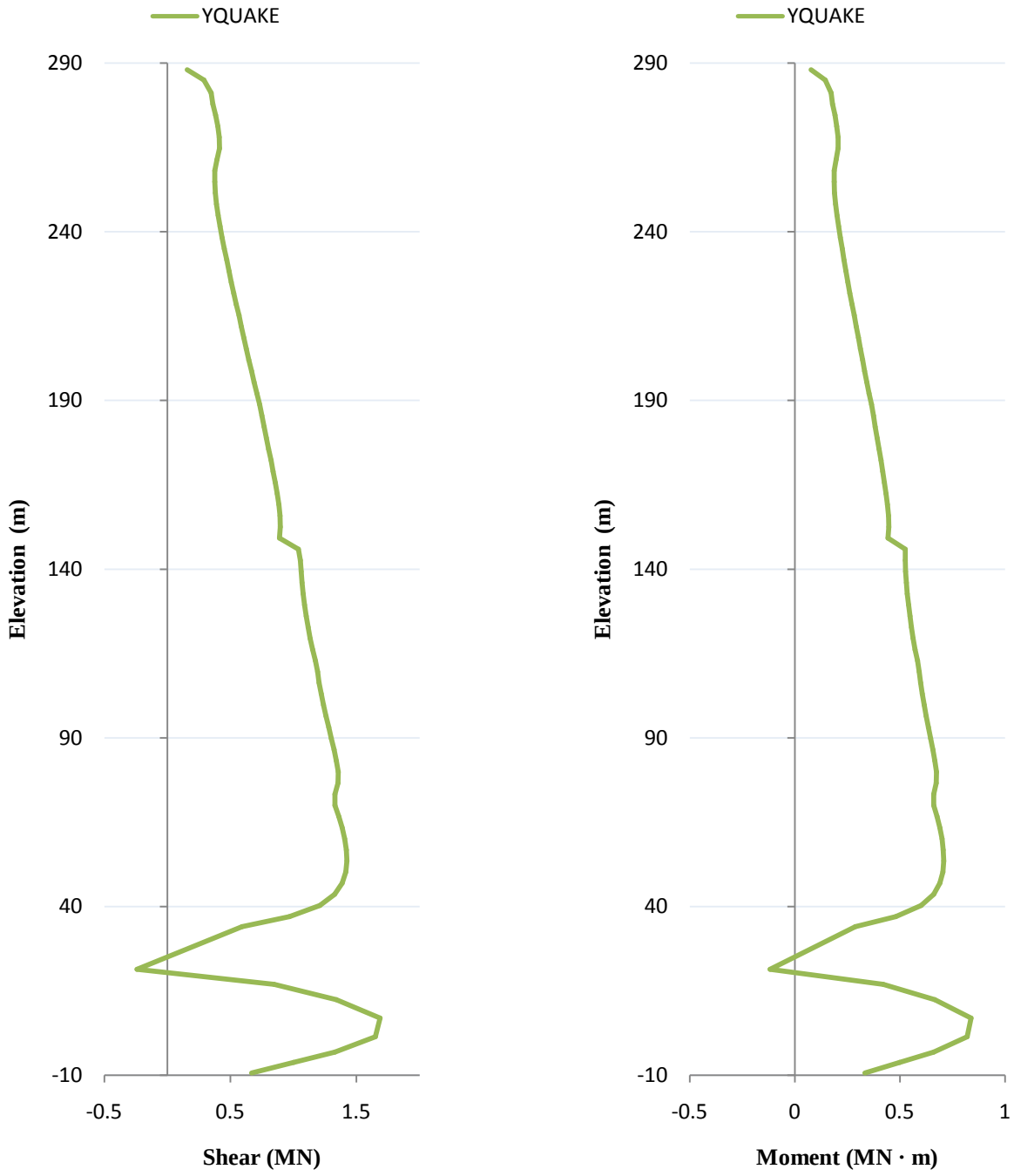

(a) (b)

Figure C-11: Equivalent Static Analysis Coupling Beam Member Response at Right End (T2B-C1 located bottom-left of floor plan): (a) Shear; (b) Moment

Coupled Direction Response | *Coupling Beam Member* | *T2B-D1* | *Left End*

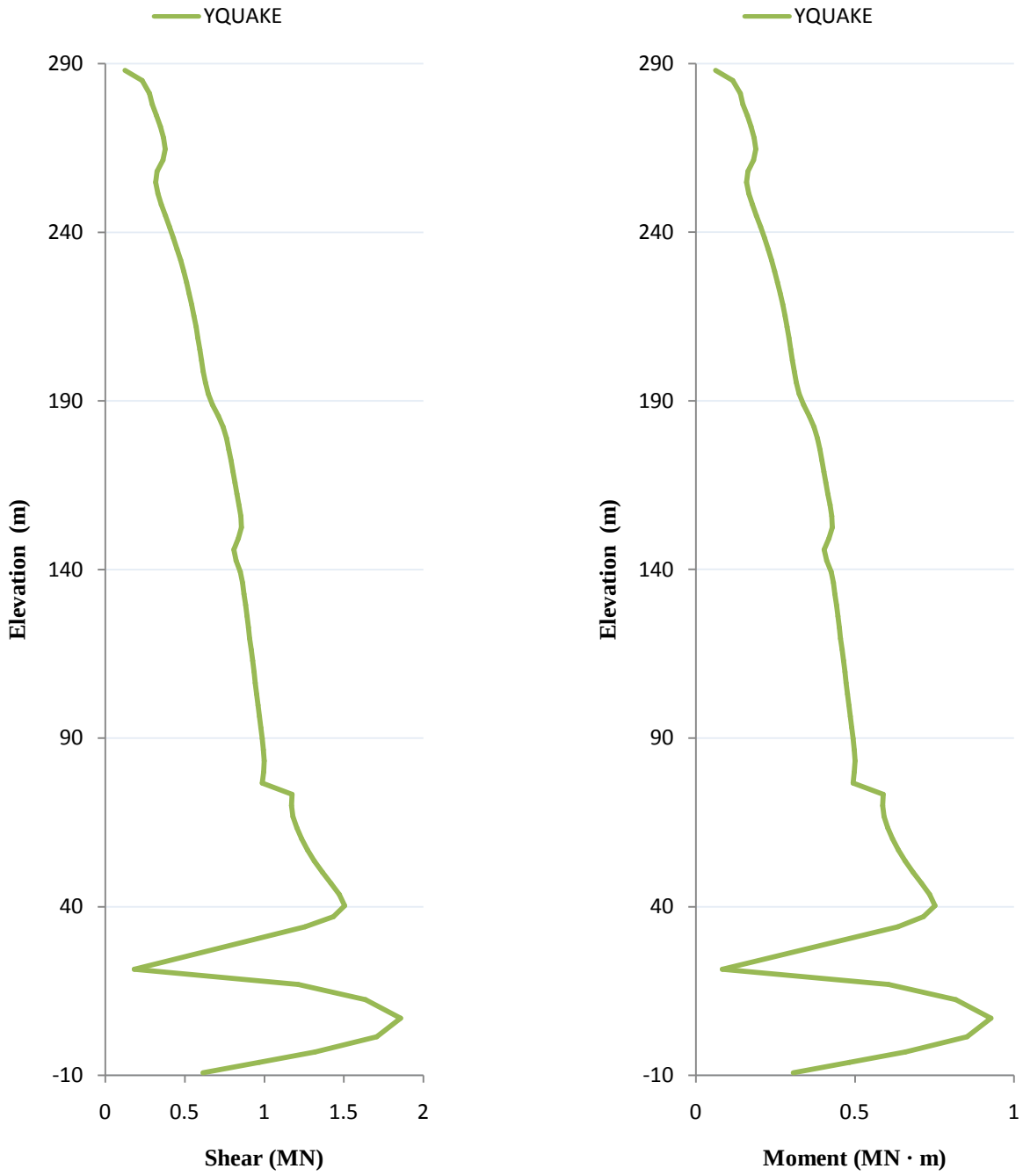

(a) (b)

Figure C-12: Equivalent Static Analysis Coupling Beam Member Response at Left End (T2B-D1 located central bottom-left of floor plan): (a) Shear; (b) Moment

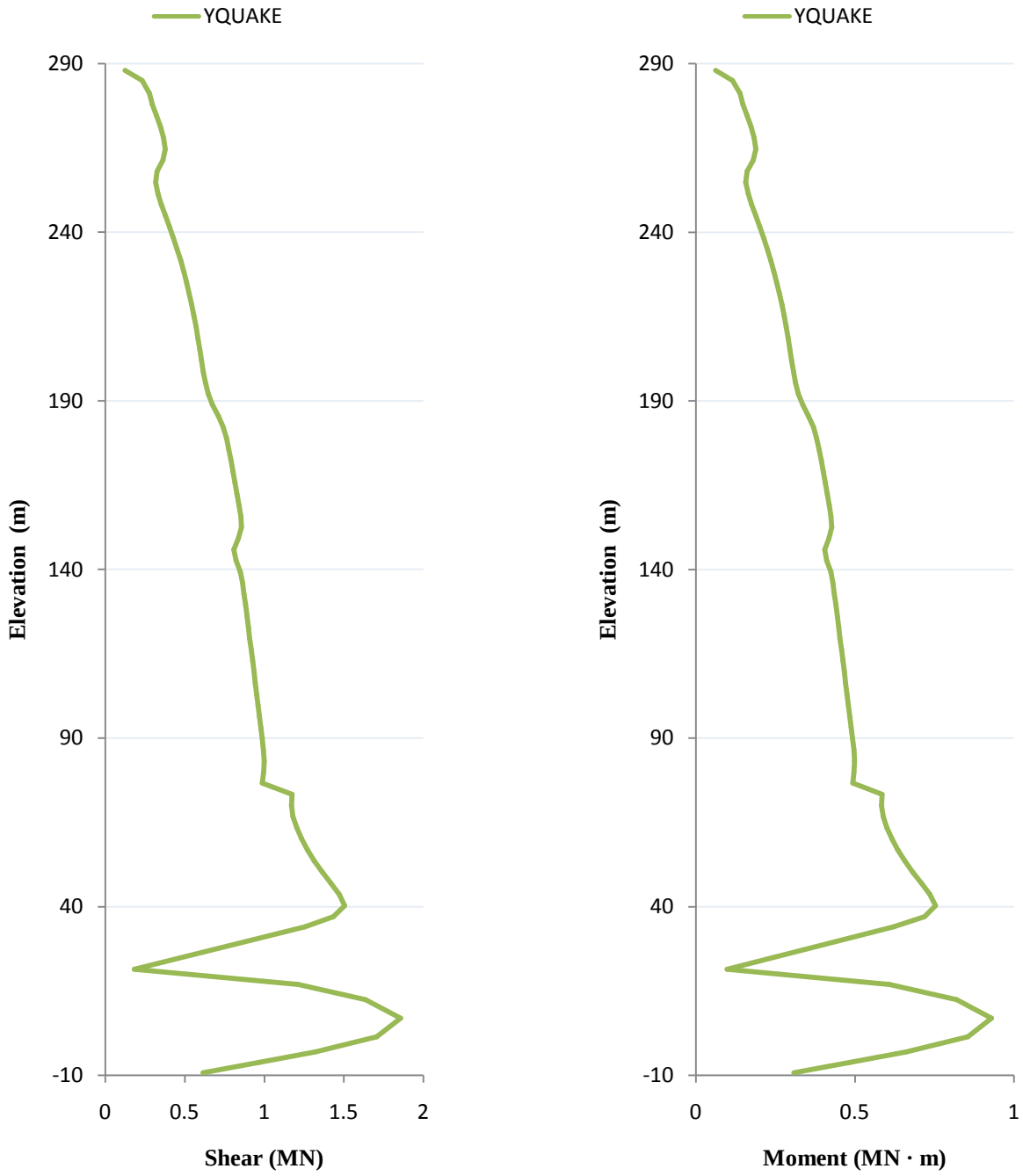

(a) (b)

Figure C-13: Equivalent Static Analysis Coupling Beam Member Response at Right End (T2B-D1 located central bottom-left of floor plan): (a) Shear; (b) Moment

APPENDIX D - DYNAMIC MODAL SPECTRUM ANALYSIS RESULTS

Coupled and Uncoupled Directions Response | *Overall Building*

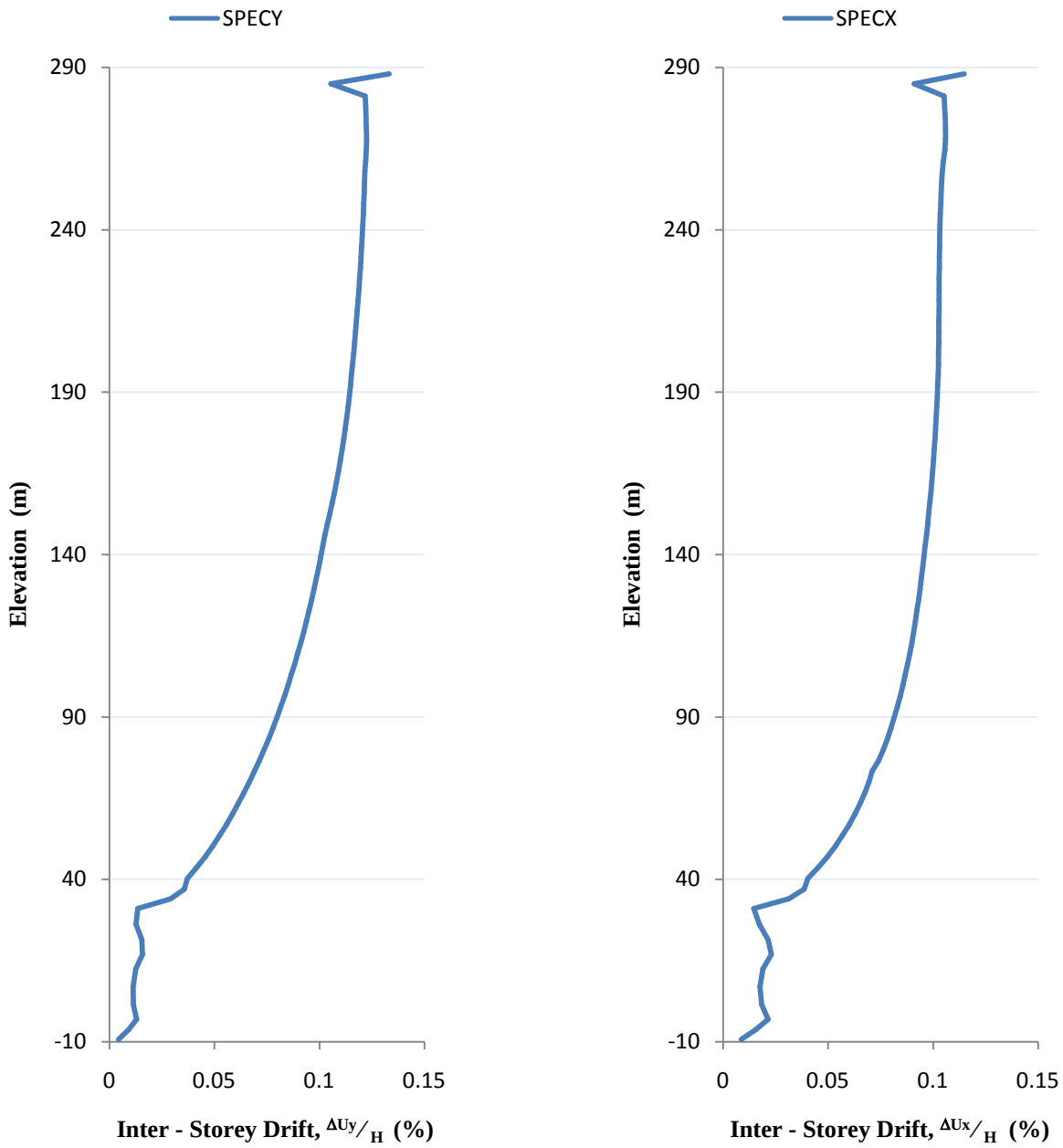

(a) (b)

Figure D-1: Dynamic Modal Spectrum Analysis Overall Building Maximum Inter-Storey Drift: (a) Coupled Direction; (b) Uncoupled Direction

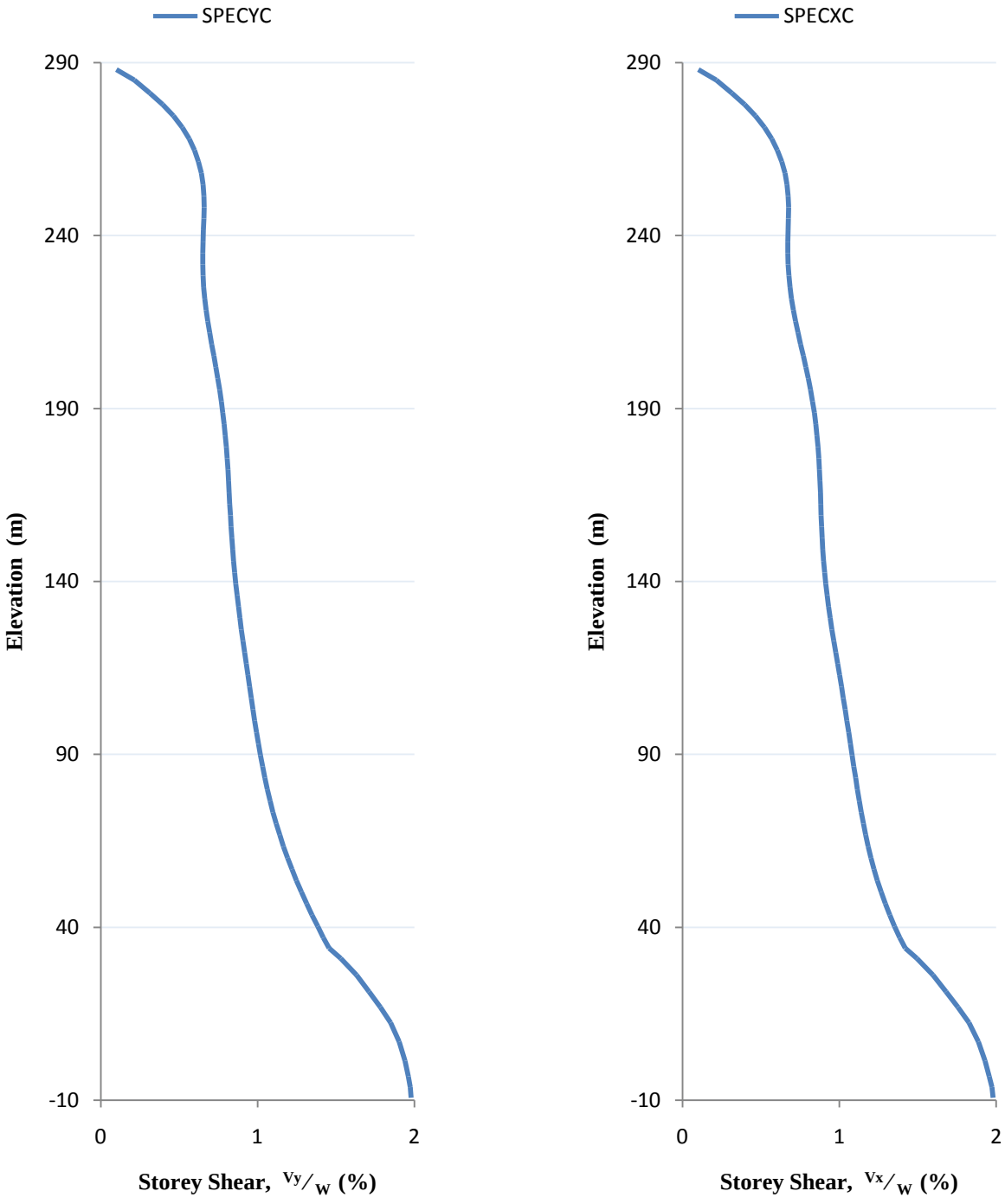

(a) (b)

Figure D-2: Dynamic Modal Spectrum Analysis Overall Building Maximum Storey Shear: (a) Coupled Direction; (b) Uncoupled Direction

Coupled Direction Response | *Core Member* | *Left-Bottom*

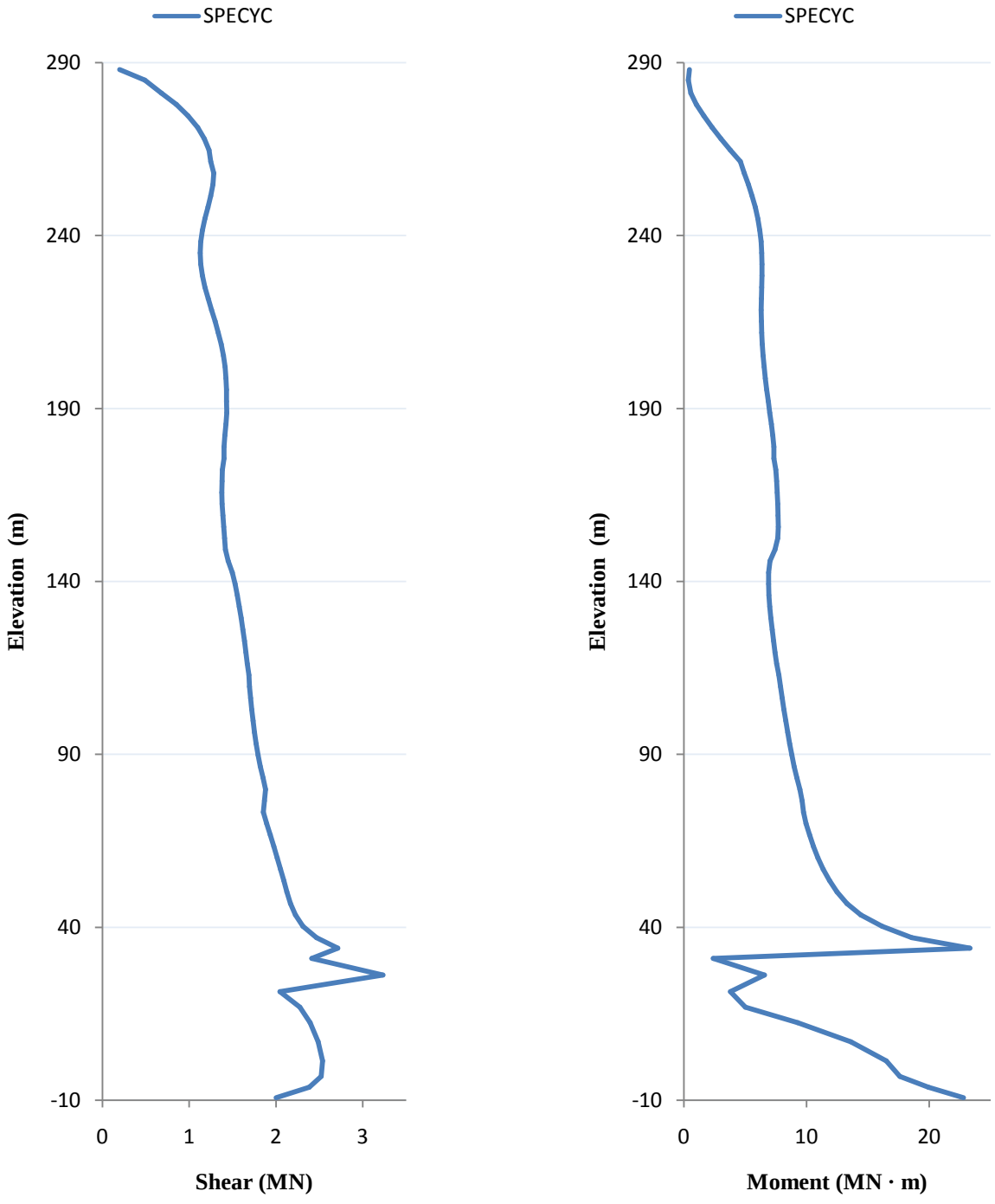

(a) (b)

Figure D-3: Dynamic Modal Spectrum Analysis Left-Bottom Core Member Coupled Direction Response: (a) Maximum Shear; (b) Maximum Moment

Coupled Direction Response | *Core Member* | *Center-Bottom*

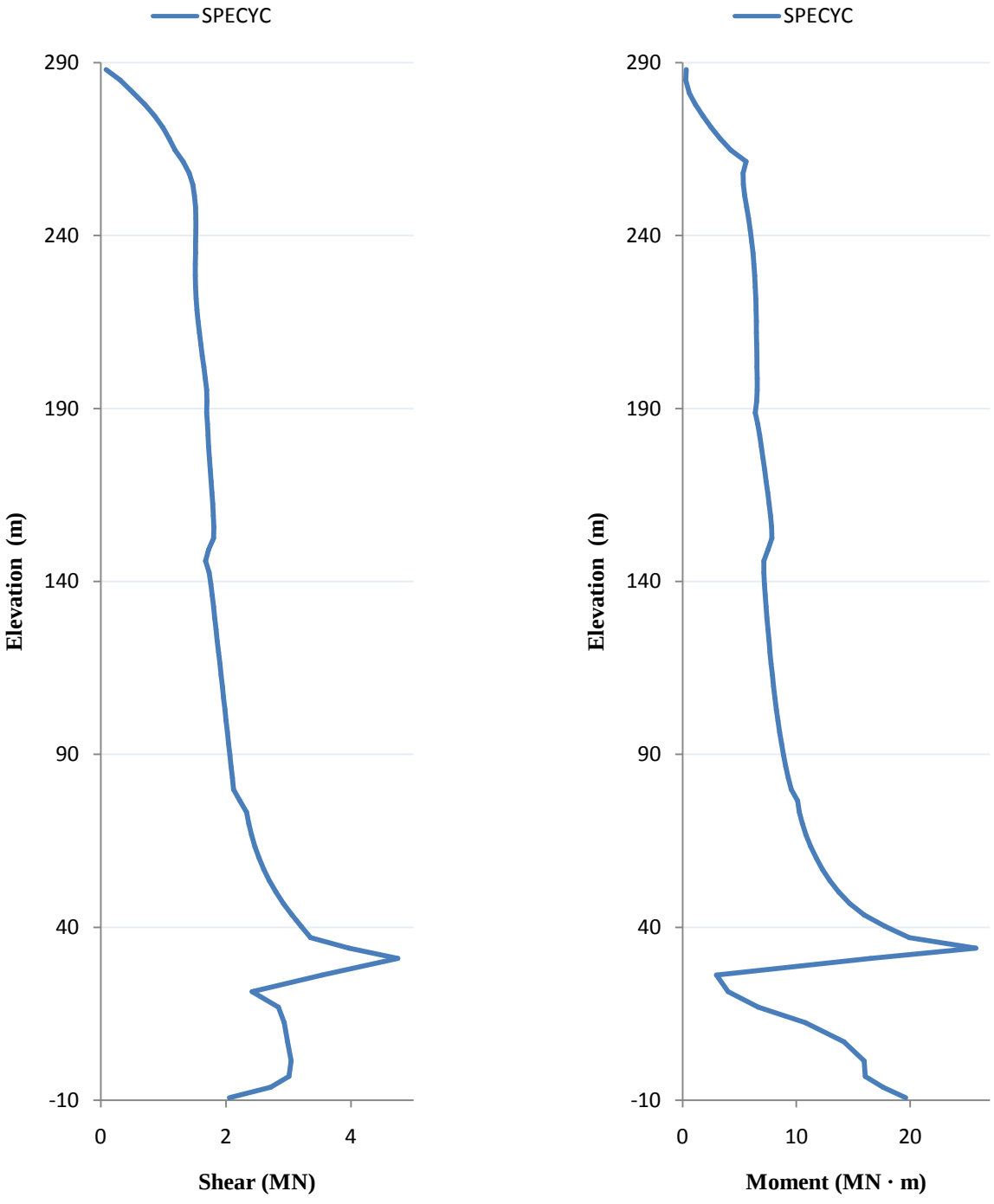

(a) (b)

Figure D-4: Dynamic Modal Spectrum Analysis Center-Bottom Core Member Coupled Direction Response: (a) Maximum Shear; (b) Maximum Moment

Uncoupled Direction Response | *Core Member* | *Left-Bottom*

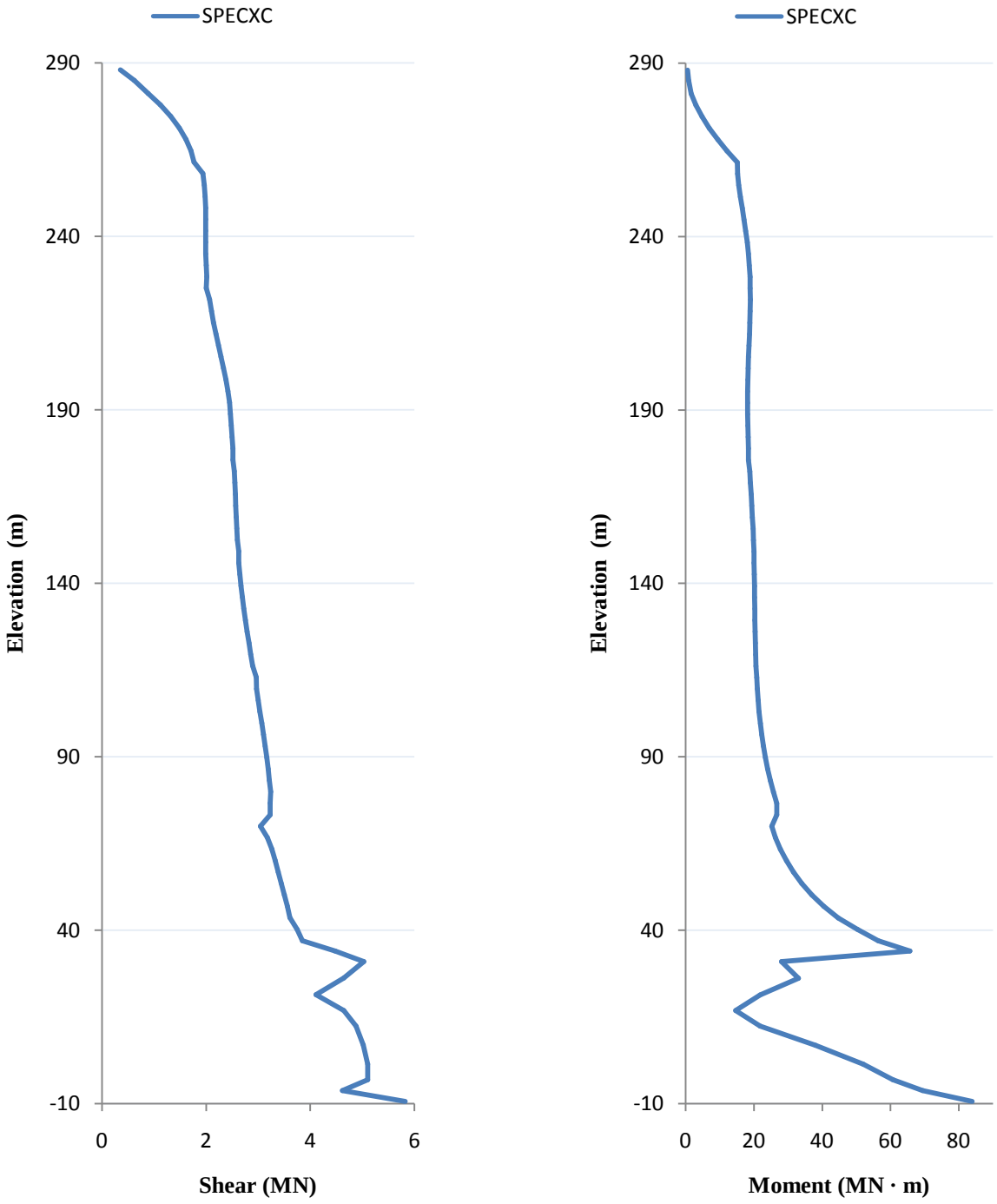

(a) (b)

Figure D-5: Dynamic Modal Spectrum Analysis Left-Bottom Core Member Uncoupled Direction Response: (a) Maximum Shear; (b) Maximum Moment

Uncoupled Direction Response | *Core Member* | *Center-Bottom*

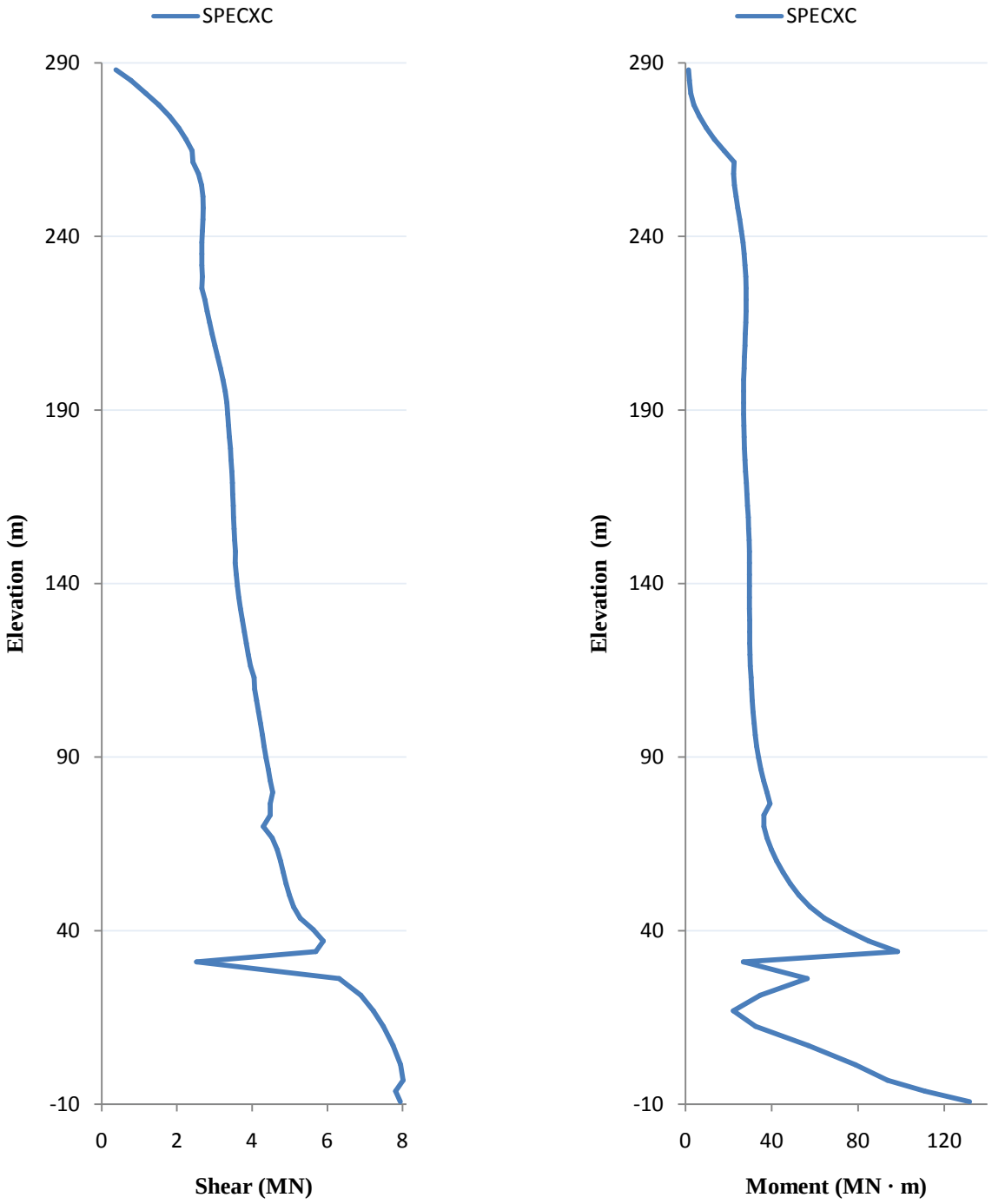

(a) (b)

Figure D-6: Dynamic Modal Spectrum Analysis Center-Bottom Core Member Uncoupled Direction Response: (a) Maximum Shear; (b) Maximum Moment

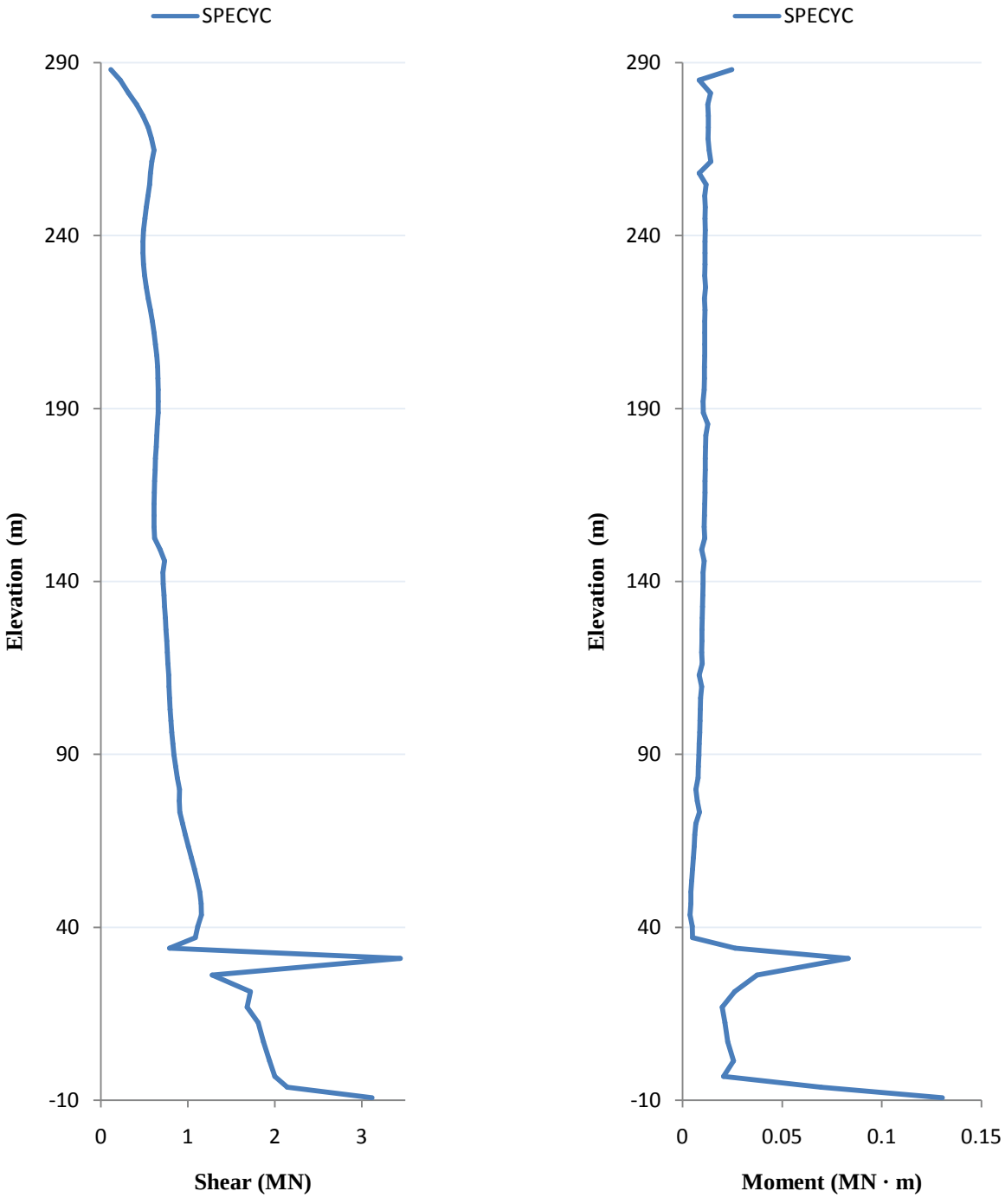

(a) (b)

Figure D-7: Dynamic Modal Spectrum Analysis Column-Wall Member Response (T2C10 located bottom-left of floor plan): (a) Maximum Shear; (b) Maximum Moment

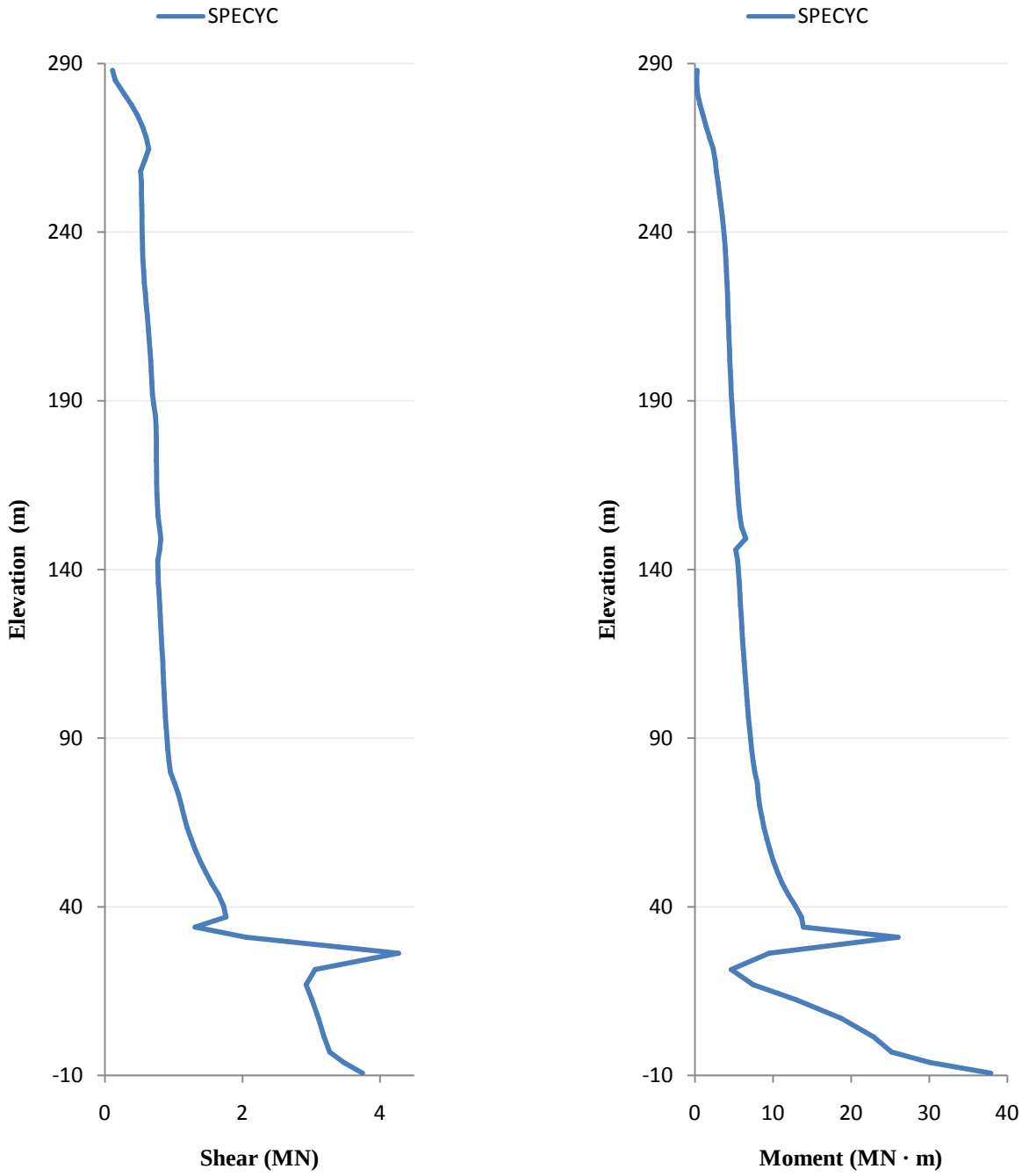

(a) (b)

Figure D-8: Dynamic Modal Spectrum Analysis Column-Wall Member Response (T2C11 located central bottom-left of floor plan): (a) Maximum Shear; (b) Maximum Moment

Coupled Direction Response | *Coupling Beam Member* | *T2B-C1* | *Left End*

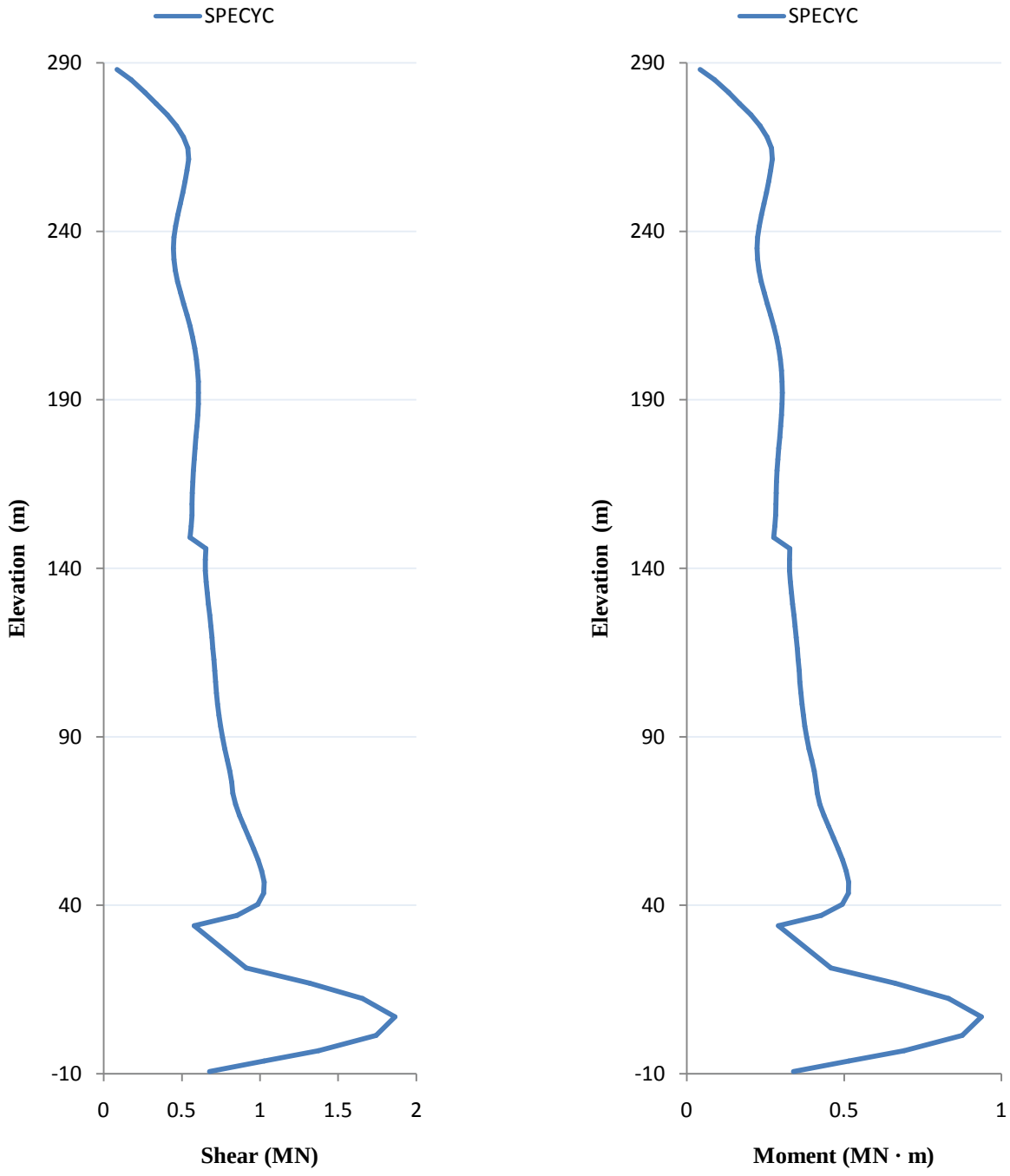

(a) (b)

Figure D-9: Dynamic Modal Spectrum Analysis Coupling Beam Member Response at Left End (T2B-C1 located bottom-left of floor plan): (a) Maximum Shear; (b) Maximum Moment

Coupled Direction Response | *Coupling Beam Member* | *T2B-C1* | *Right End*

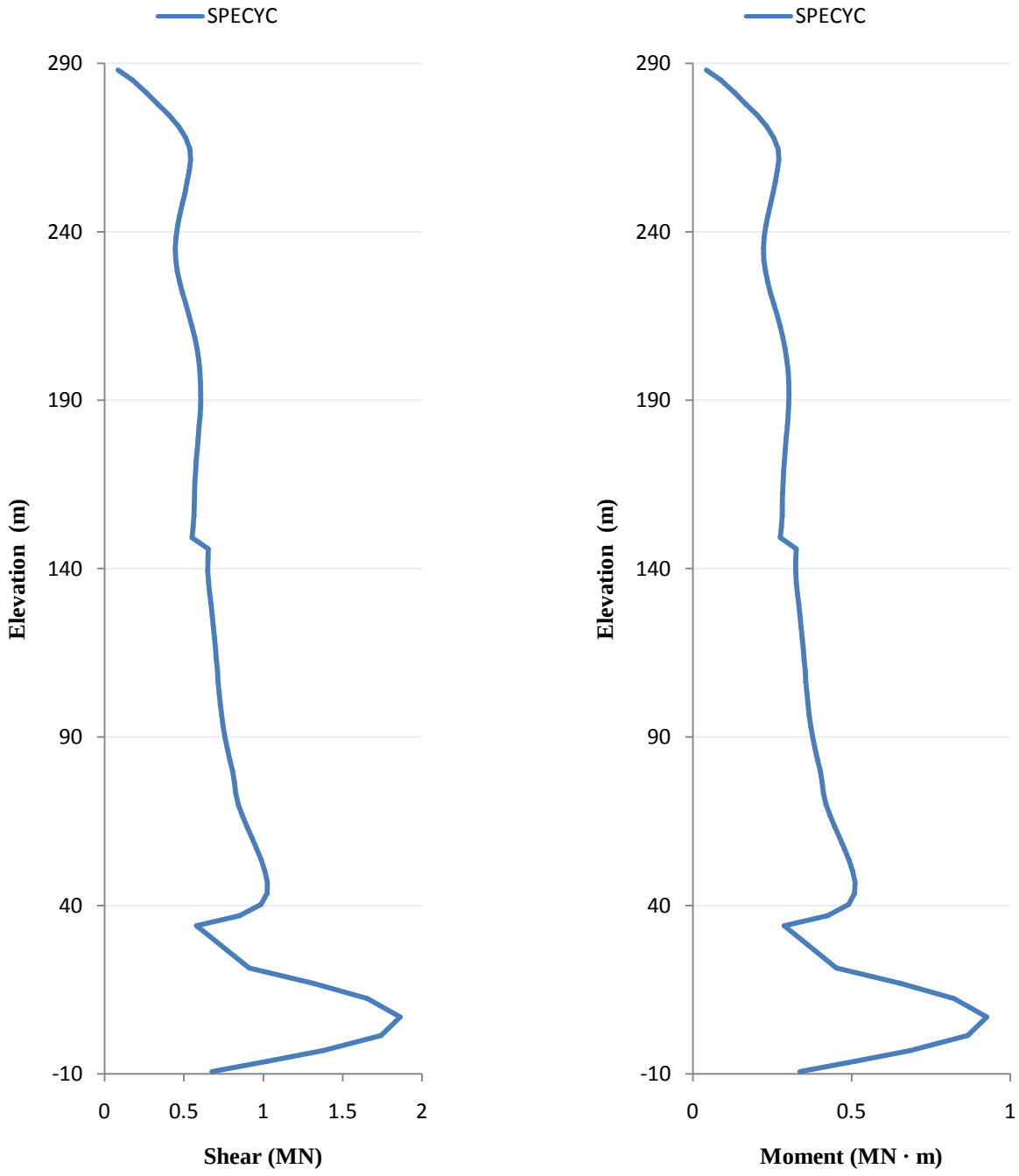

(a) (b)

Figure D-10: Dynamic Modal Spectrum Analysis Coupling Beam Member Response at Right End (T2B-C1 located bottom-left of floor plan): (a) Maximum Shear; (b) Maximum Moment

Coupled Direction Response | *Coupling Beam Member* | *T2B-D1* | *Left End*

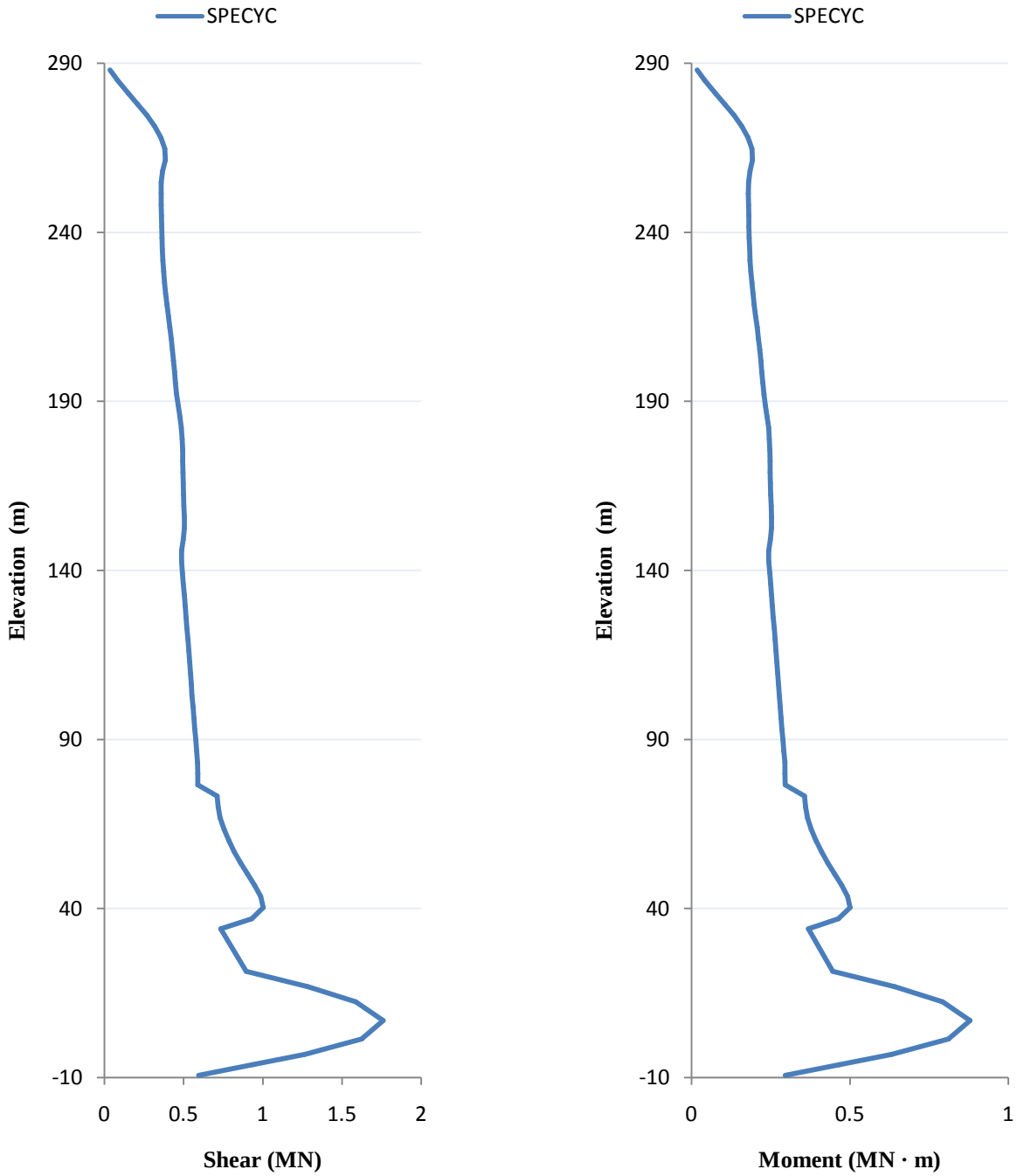

(a) (b)

Figure D-11: Dynamic Modal Spectrum Analysis Coupling Beam Member Response at Left End (T2B-D1 located central bottom-left of floor plan): (a) Maximum Shear; (b) Maximum Moment

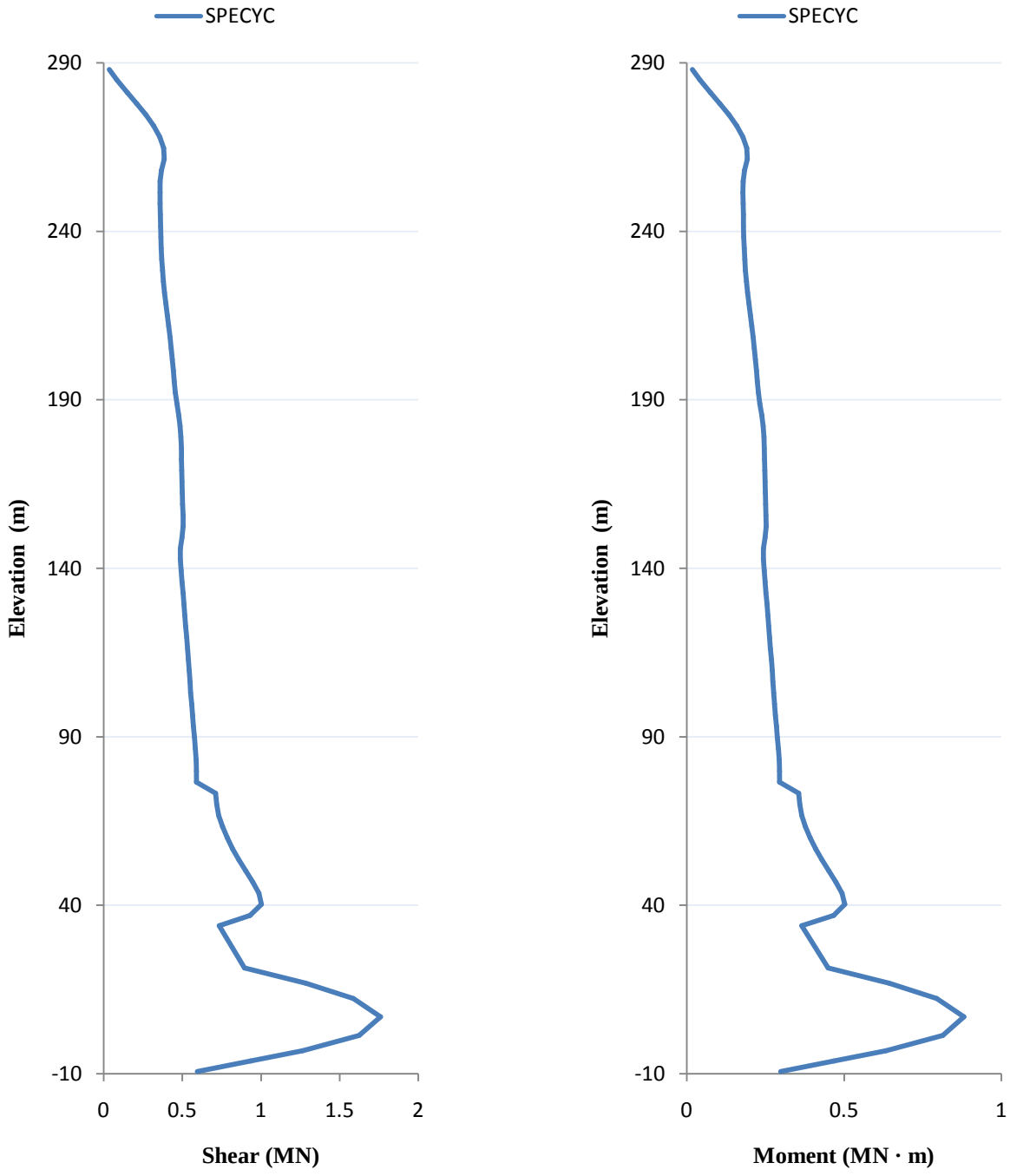

(a) (b)

Figure D-12: Dynamic Modal Spectrum Analysis Coupling Beam Member Response at Right End (T2B-D1 located central bottom-left of floor plan): (a) Maximum Shear; (b) Maximum Moment

APPENDIX E - LINEAR TIME-HISTORY ANALYSIS RESULTS

Coupled and Uncoupled Directions Response | *Overall Building*

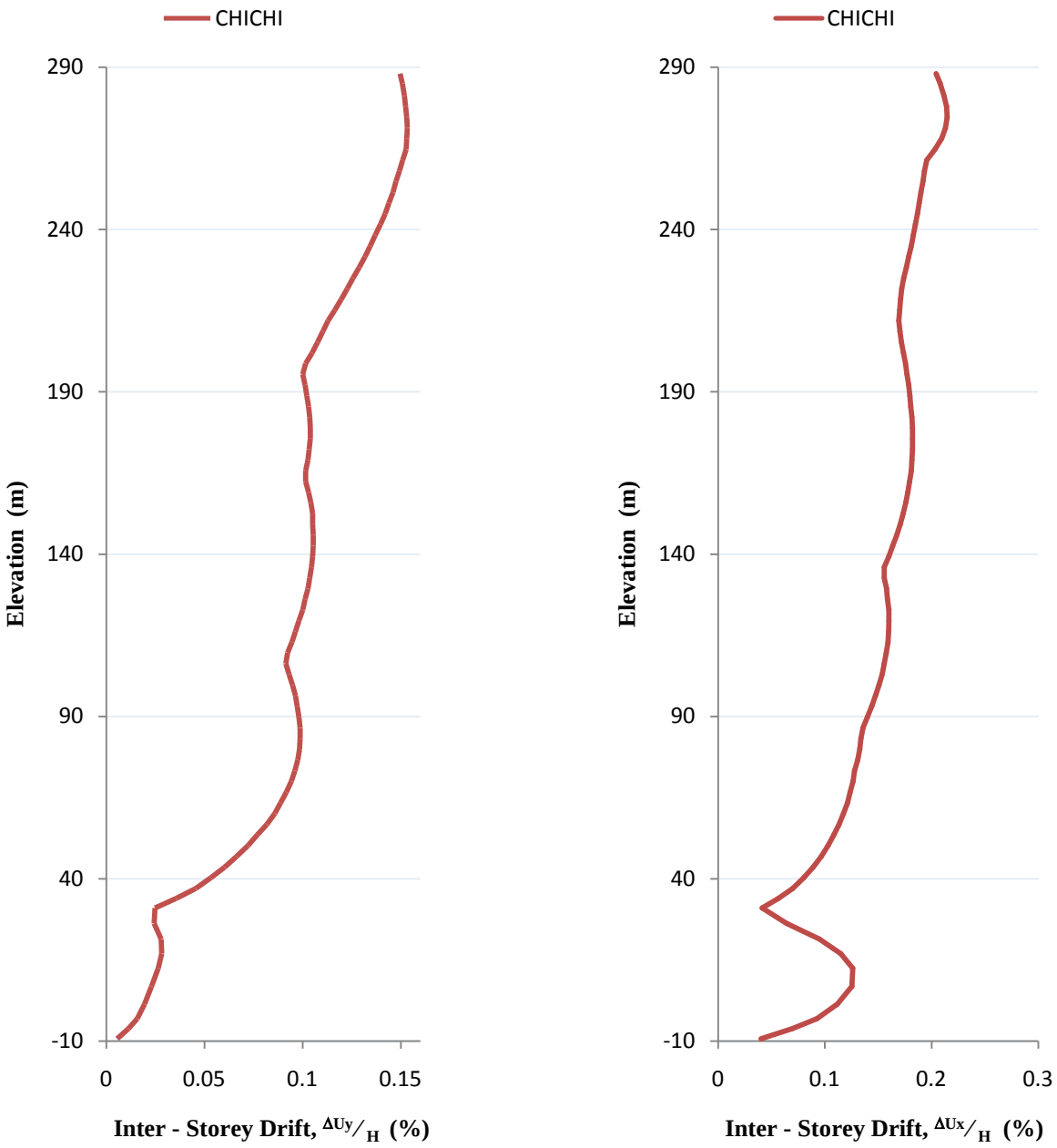

(a) (b)

Figure E-1: Linear Time-History Analysis Overall Building Maximum Inter-Storey Drift: (a) Coupled Direction; (b) Uncoupled Direction

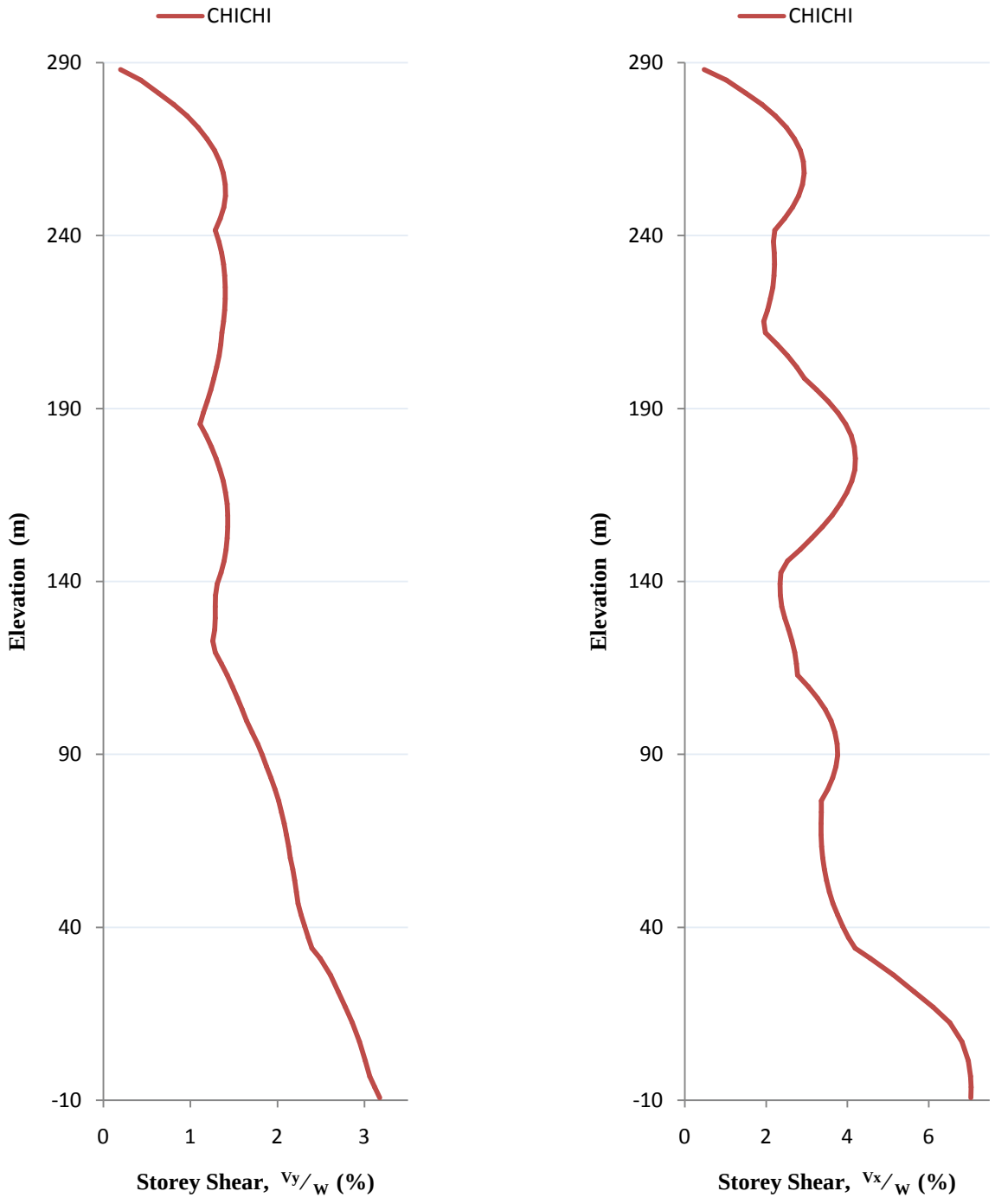

(a) (b)

Figure E-2: Linear Time-History Analysis Overall Building Maximum Storey Shear: (a) Coupled Direction; (b) Uncoupled Direction

Coupled Direction Response | *Core Member* | *Left-Bottom*

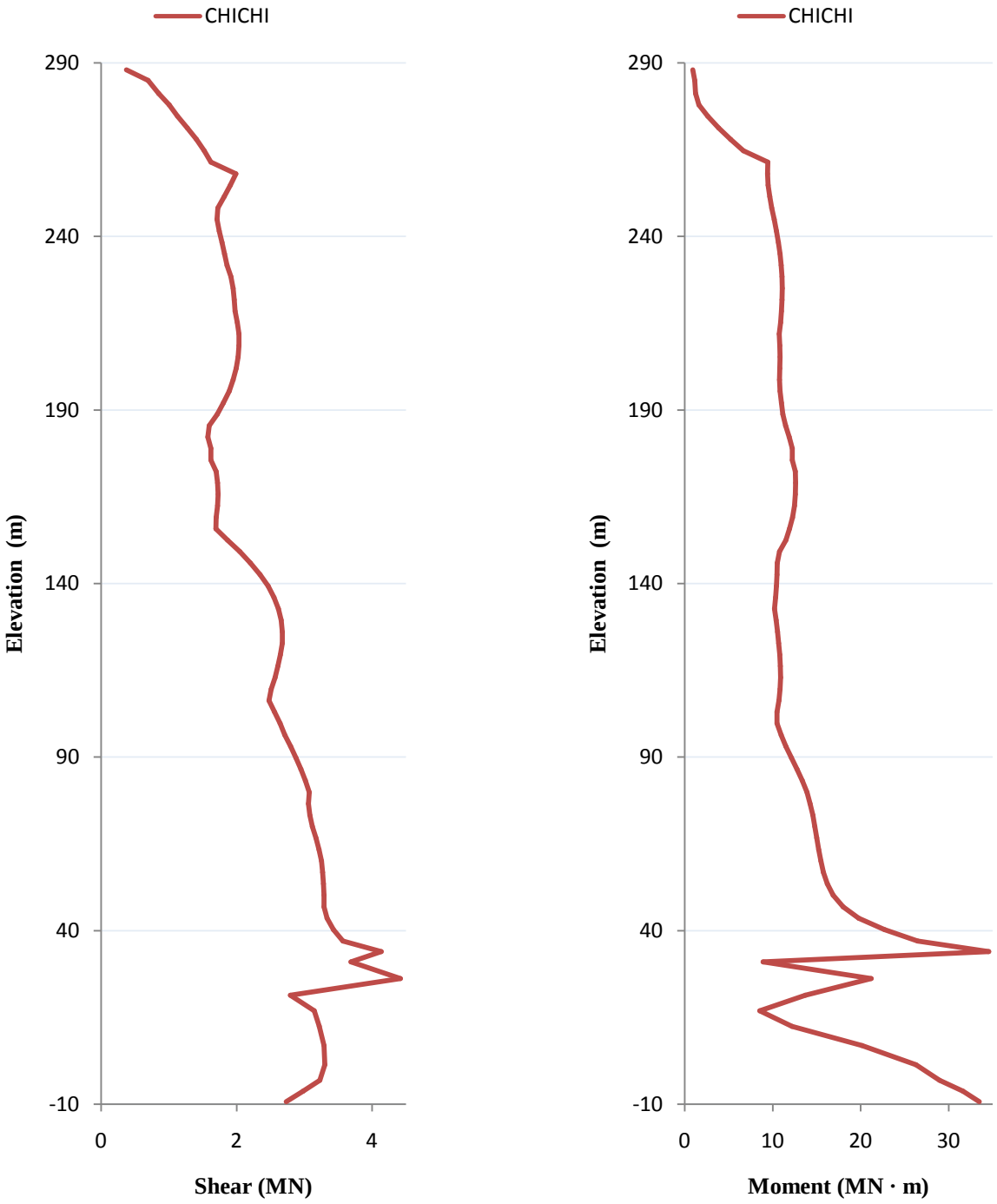

(a) (b)

Figure E-3: Linear Time-History Analysis Left-Bottom Core Member Coupled Direction Response: (a) Maximum Shear; (b) Maximum Moment

Coupled Direction Response | *Core Member* | *Center-Bottom*

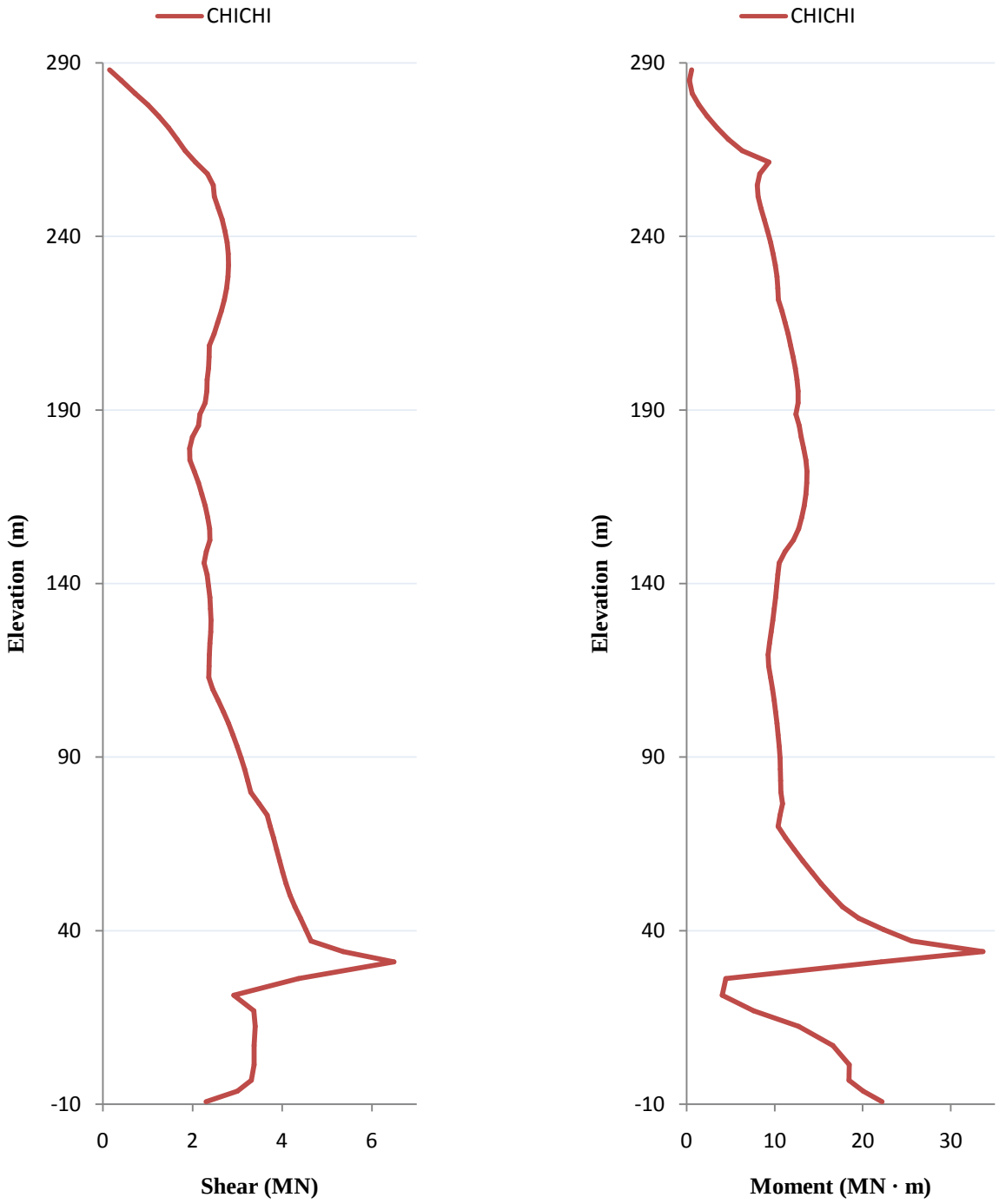

(a) (b)

Figure E-4: Linear Time-History Analysis Center-Bottom Core Member Coupled Direction Response: (a) Maximum Shear; (b) Maximum Moment

Uncoupled Direction Response | *Core Member* | *Left-Bottom*

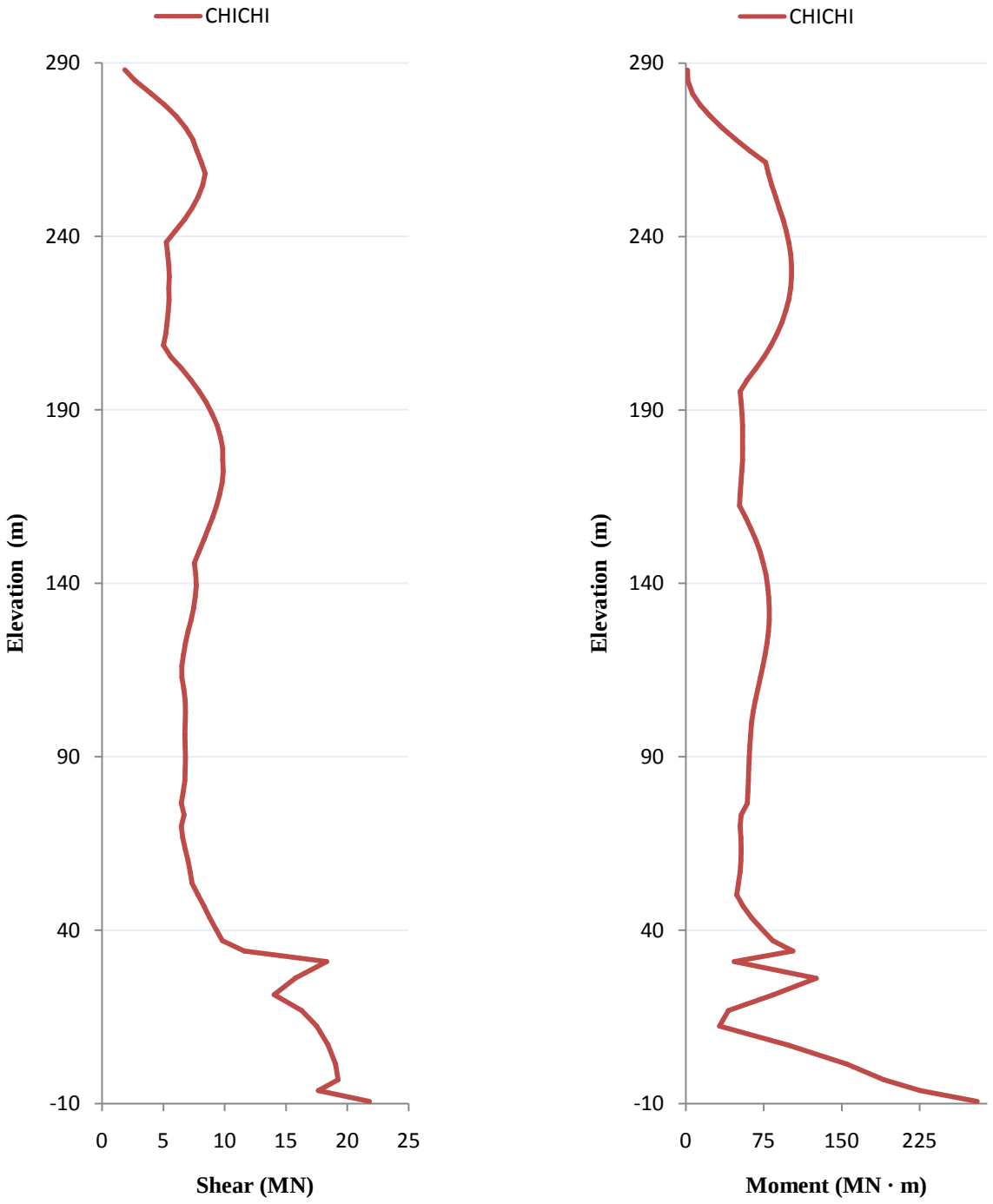

(a) (b)

Figure E-5: Linear Time-History Analysis Left-Bottom Core Member Uncoupled Direction Response: (a) Maximum Shear; (b) Maximum Moment

Uncoupled Direction Response | *Core Member* | *Center-Bottom*

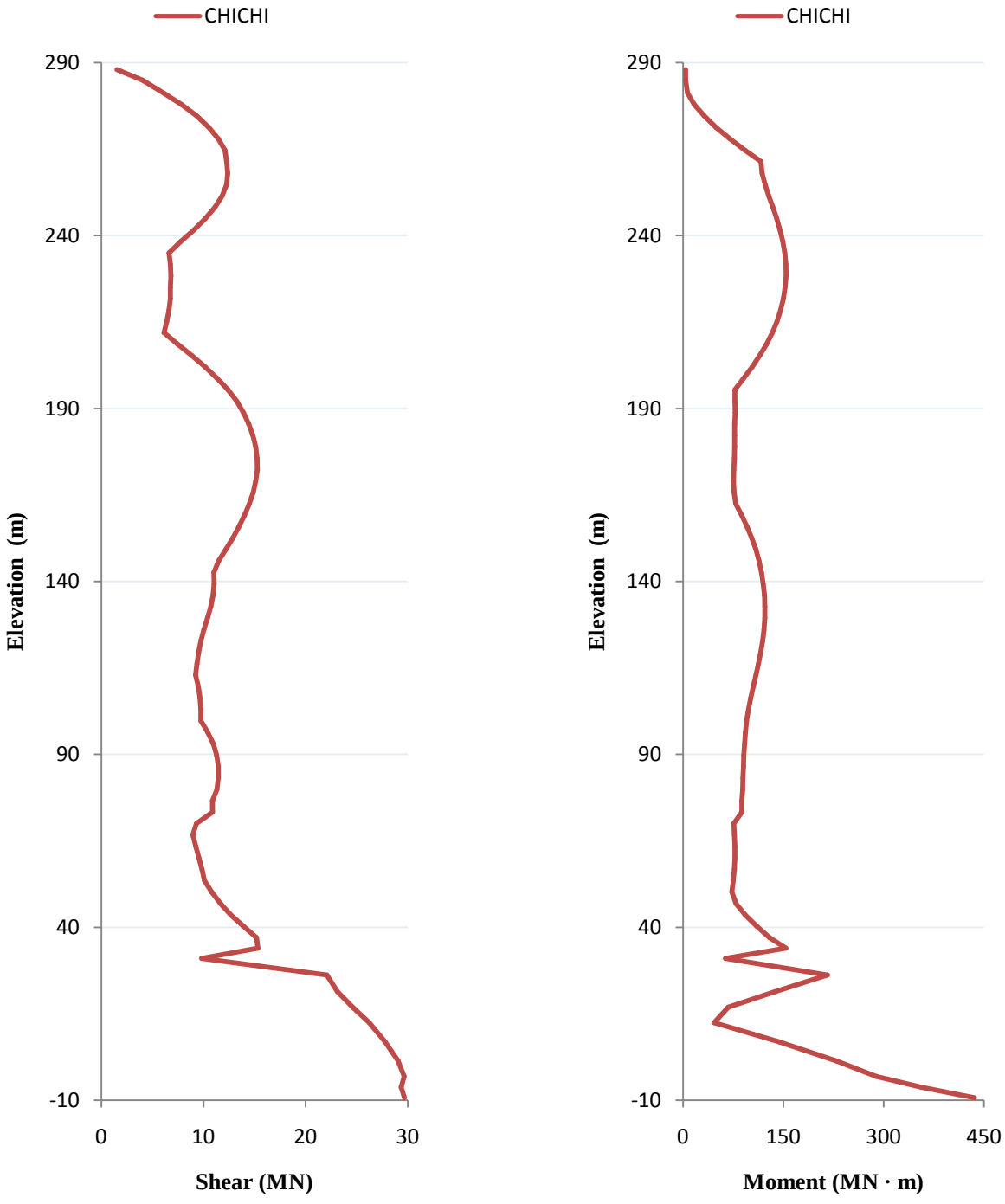

(a) (b)

Figure E-6: Linear Time-History Analysis Center-Bottom Core Member Uncoupled Direction Response: (a) Maximum Shear; (b) Maximum Moment

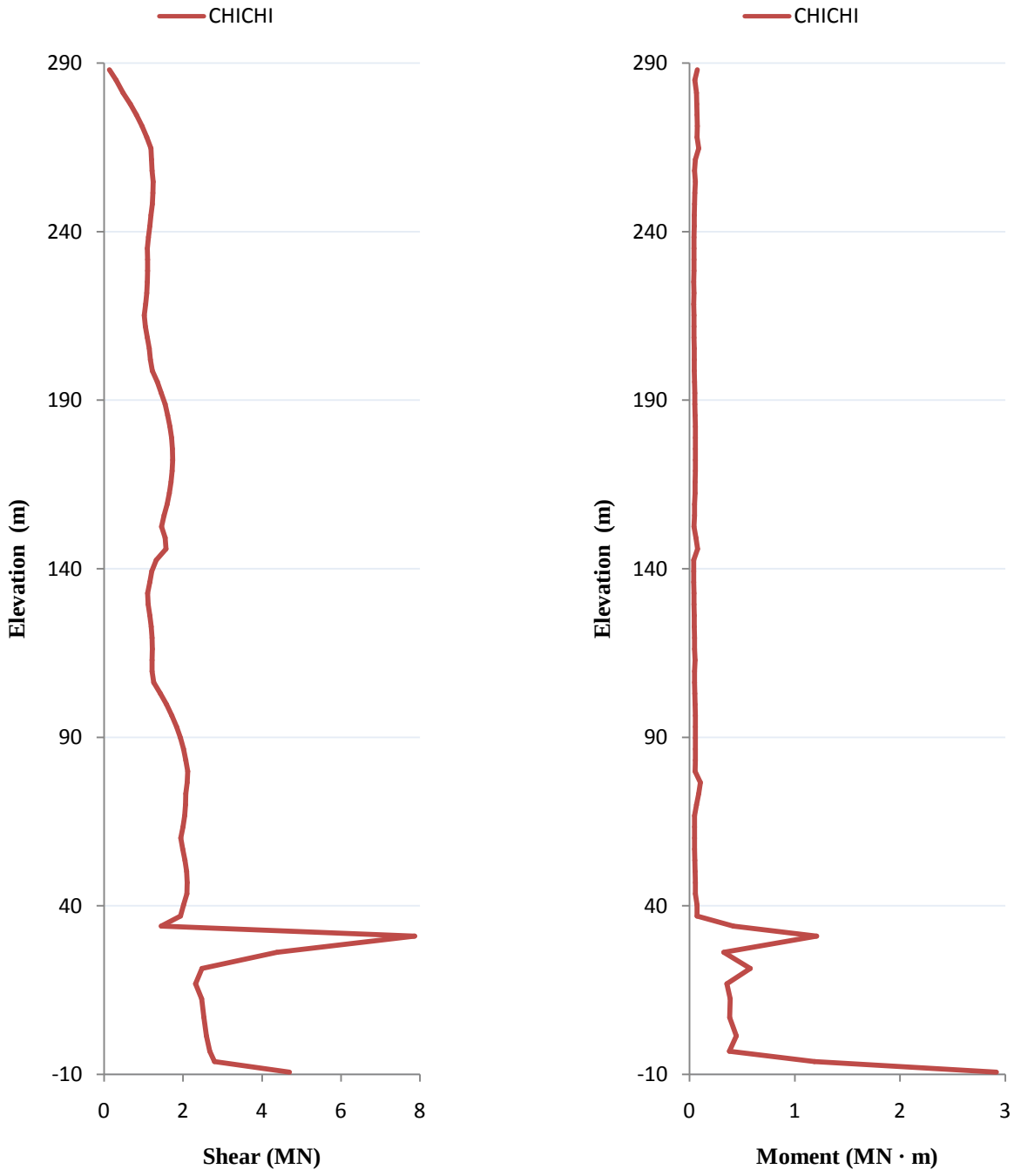

(a) (b)

Figure E-7: Linear Time-History Analysis Column-Wall Member Response (T2C10 located bottom-left of floor plan): (a) Maximum Shear; (b) Maximum Moment

Coupled Direction Response | *Column-Wall Member* | *T2C11*

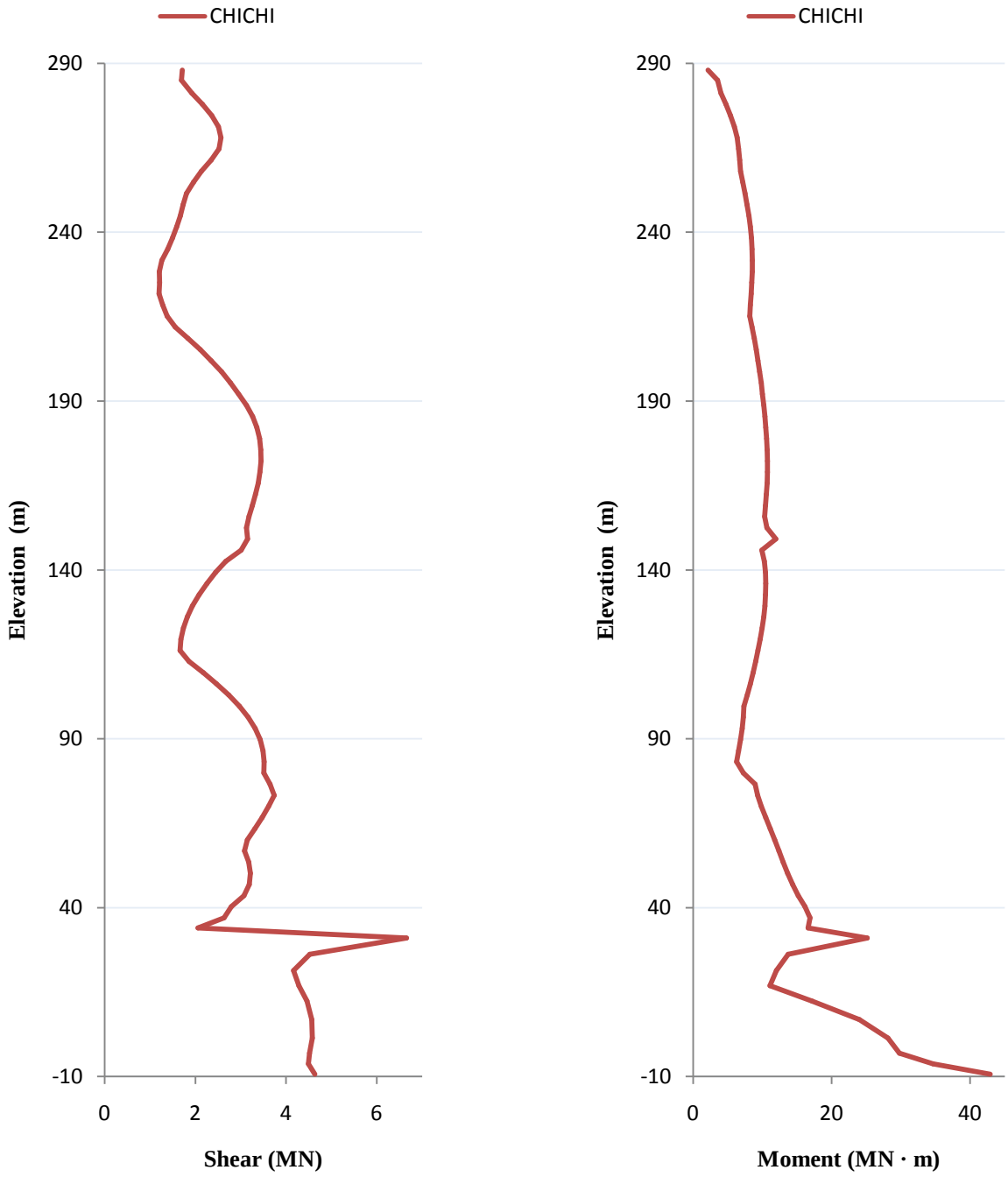

(a) (b)

Figure E-8: Linear Time-History Analysis Column-Wall Member Response (T2C11 located central bottom-left of floor plan): (a) Maximum Shear; (b) Maximum Moment

Coupled Direction Response | *Coupling Beam Member* | *T2B-C1* | *Left End*

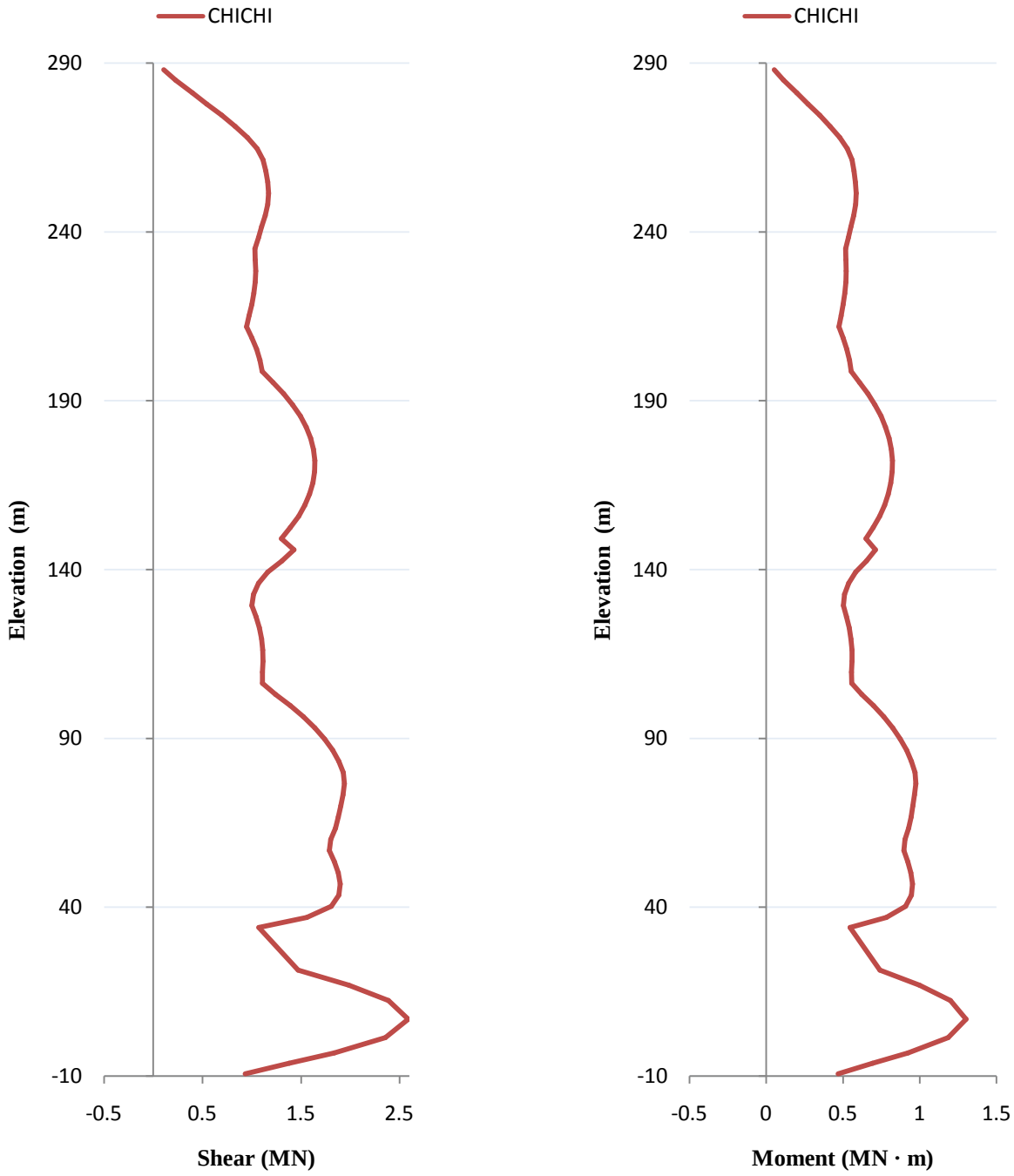

(a) (b)

Figure E-9: Linear Time-History Analysis Coupling Beam Member Response at Left End (T2B-C1 located bottom-left of floor plan): (a) Maximum Shear; (b) Maximum Moment

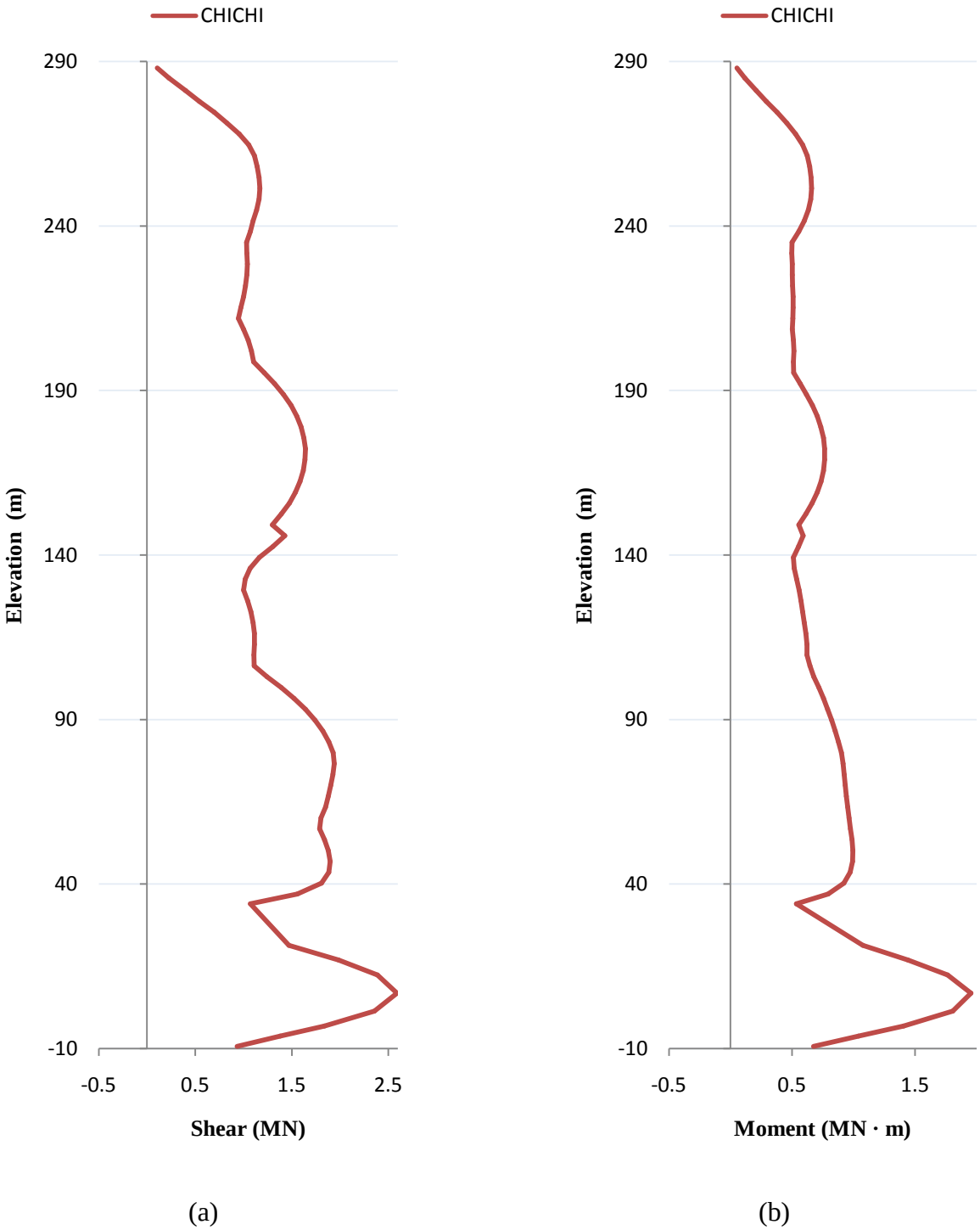

(a) (b)

Figure E-10: Linear Time-History Analysis Coupling Beam Member Response at Right End (T2B-C1 located bottom-left of floor plan): (a) Maximum Shear; (b) Maximum Moment

Coupled Direction Response | *Coupling Beam Member* | *T2B-D1* | *Left End*

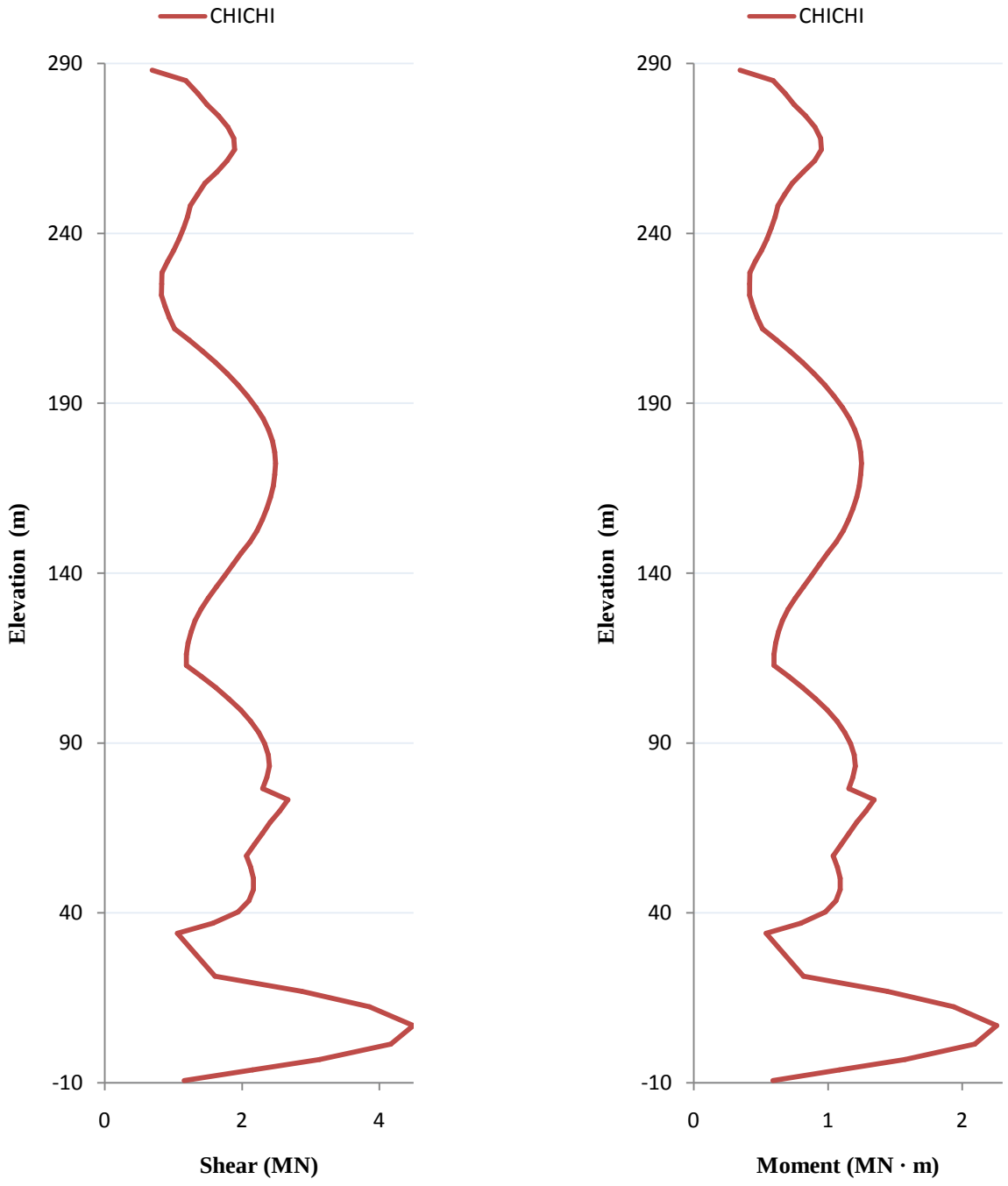

(a) (b)

Figure E-11: Linear Time-History Analysis Coupling Beam Member Response at Left End (T2B-D1 located central bottom-left of floor plan): (a) Maximum Shear; (b) Maximum Moment

Coupled Direction Response | *Coupling Beam Member* | *T2B-D1* | *Right End*

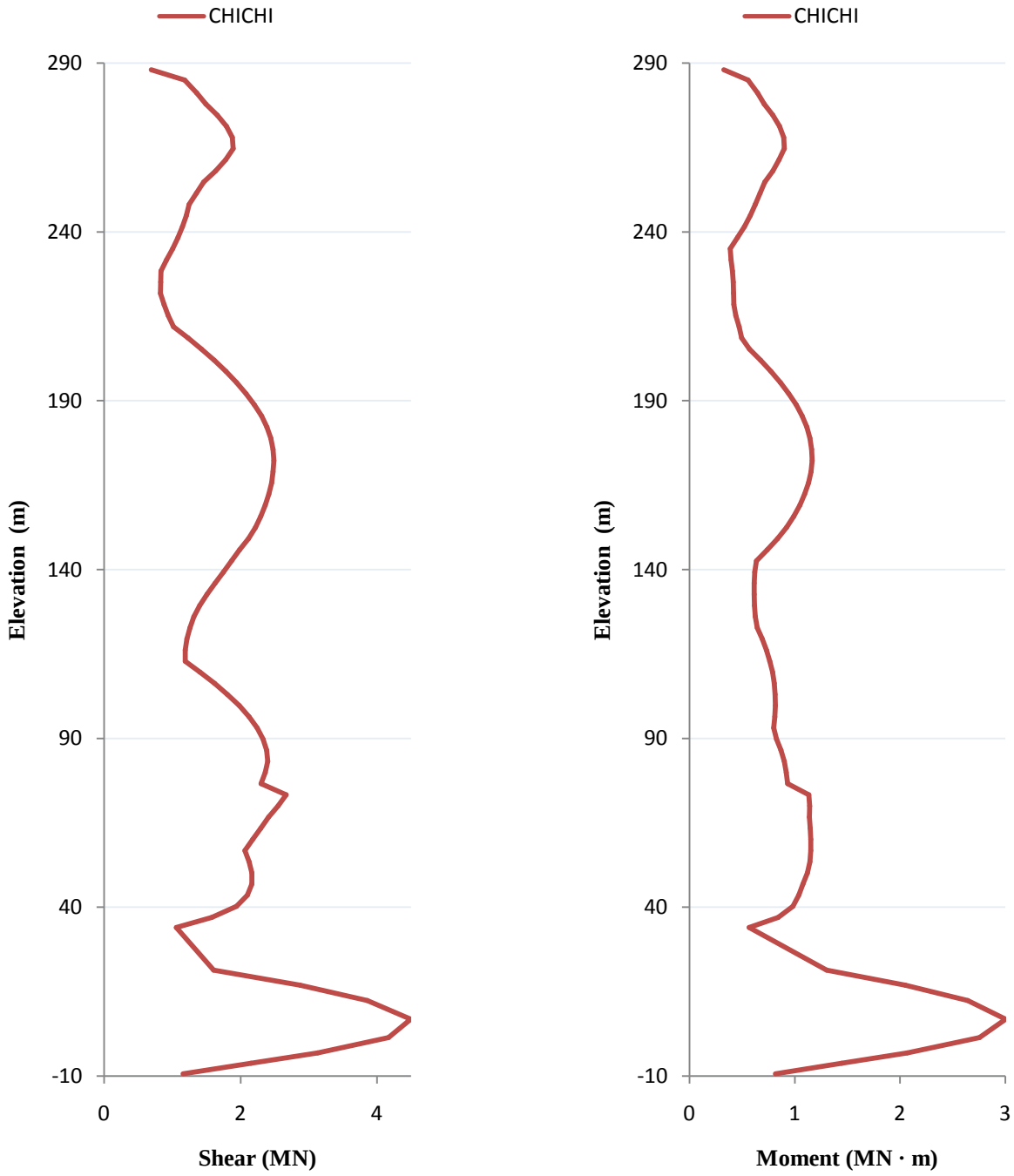

(a) (b)

Figure E-12: Linear Time-History Analysis Coupling Beam Member Response at Right End (T2B-D1 located central bottom-left of floor plan): (a) Maximum Shear; (b) Maximum Moment

APPENDIX F - NONLINEAR TIME-HISTORY ANALYSIS RESULTS

Coupled and Uncoupled Directions Response | *Overall Building*

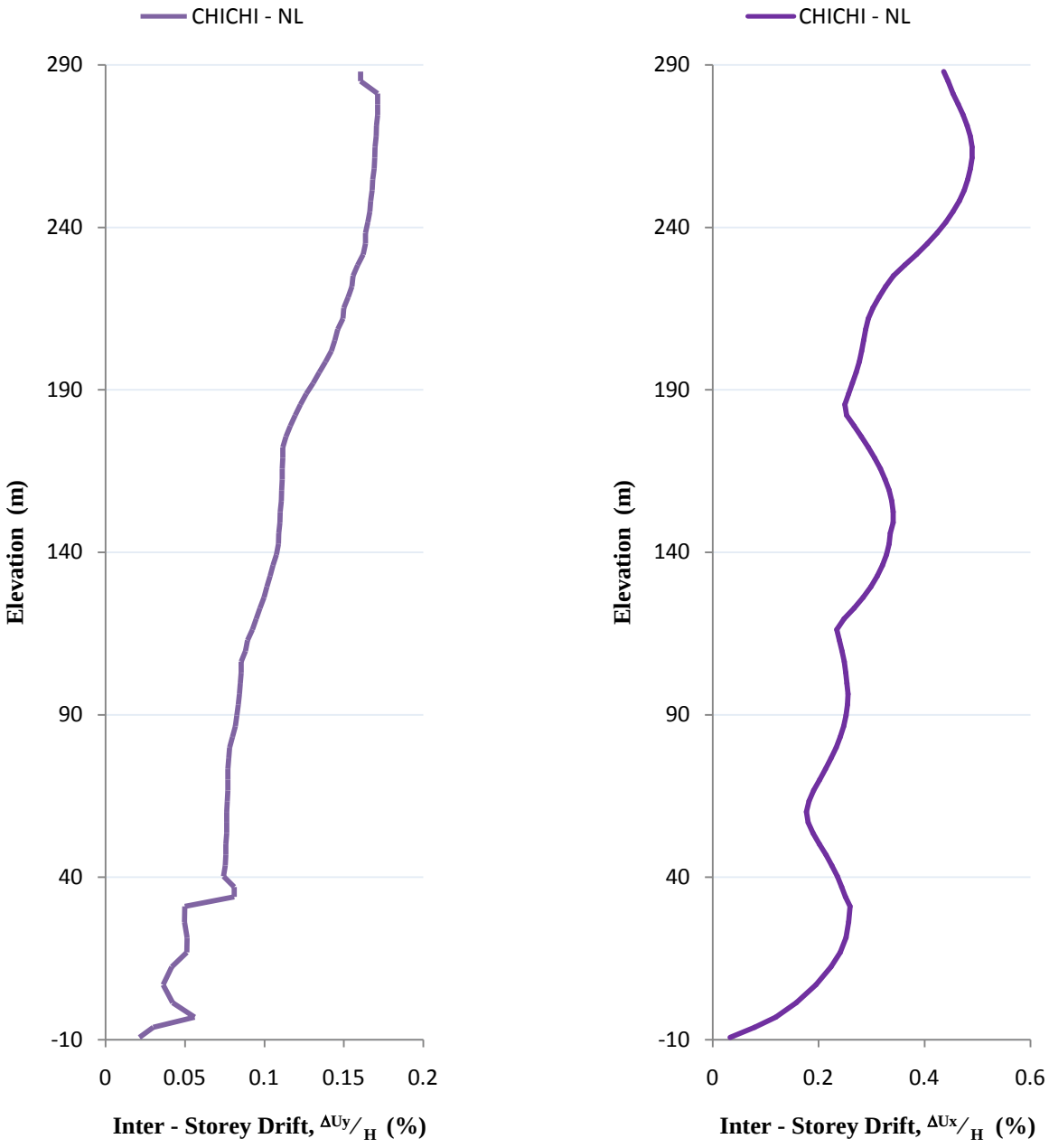

(a) (b)

Figure F-1: Nonlinear Time-History Analysis Overall Building Maximum Inter-Storey Drift: (a) Coupled Direction; (b) Uncoupled Direction

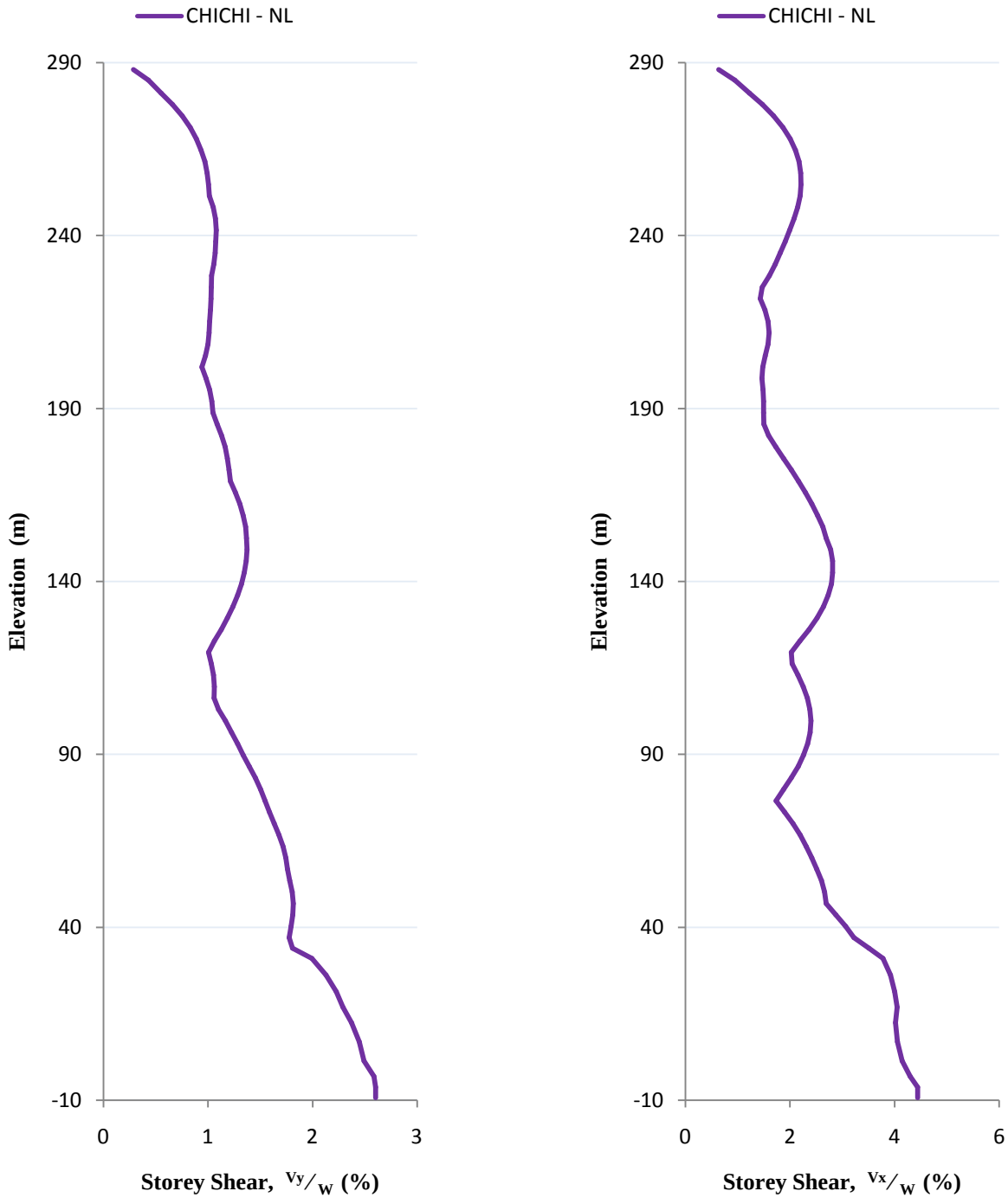

(a) (b)

Figure F-2: Nonlinear Time-History Analysis Overall Building Maximum Storey Shear: (a) Coupled Direction; (b) Uncoupled Direction

Coupled Direction Response | *Core Member* | *Left-Bottom*

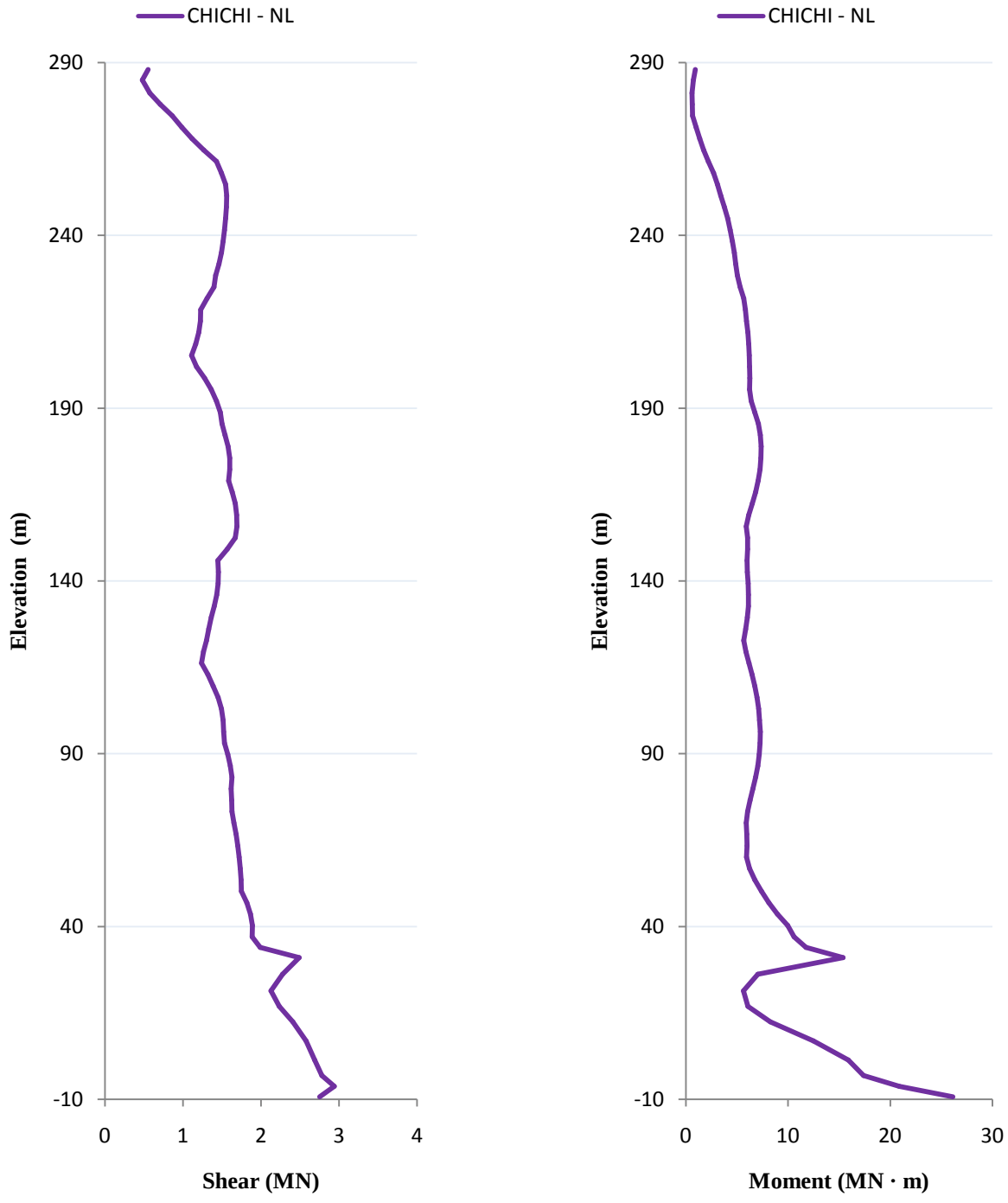

(a) (b)

Figure F-3: Nonlinear Time-History Analysis Left-Bottom Core Member Coupled Direction Response: (a) Maximum Shear; (b) Maximum Moment

Coupled Direction Response | *Core Member* | *Center-Bottom*

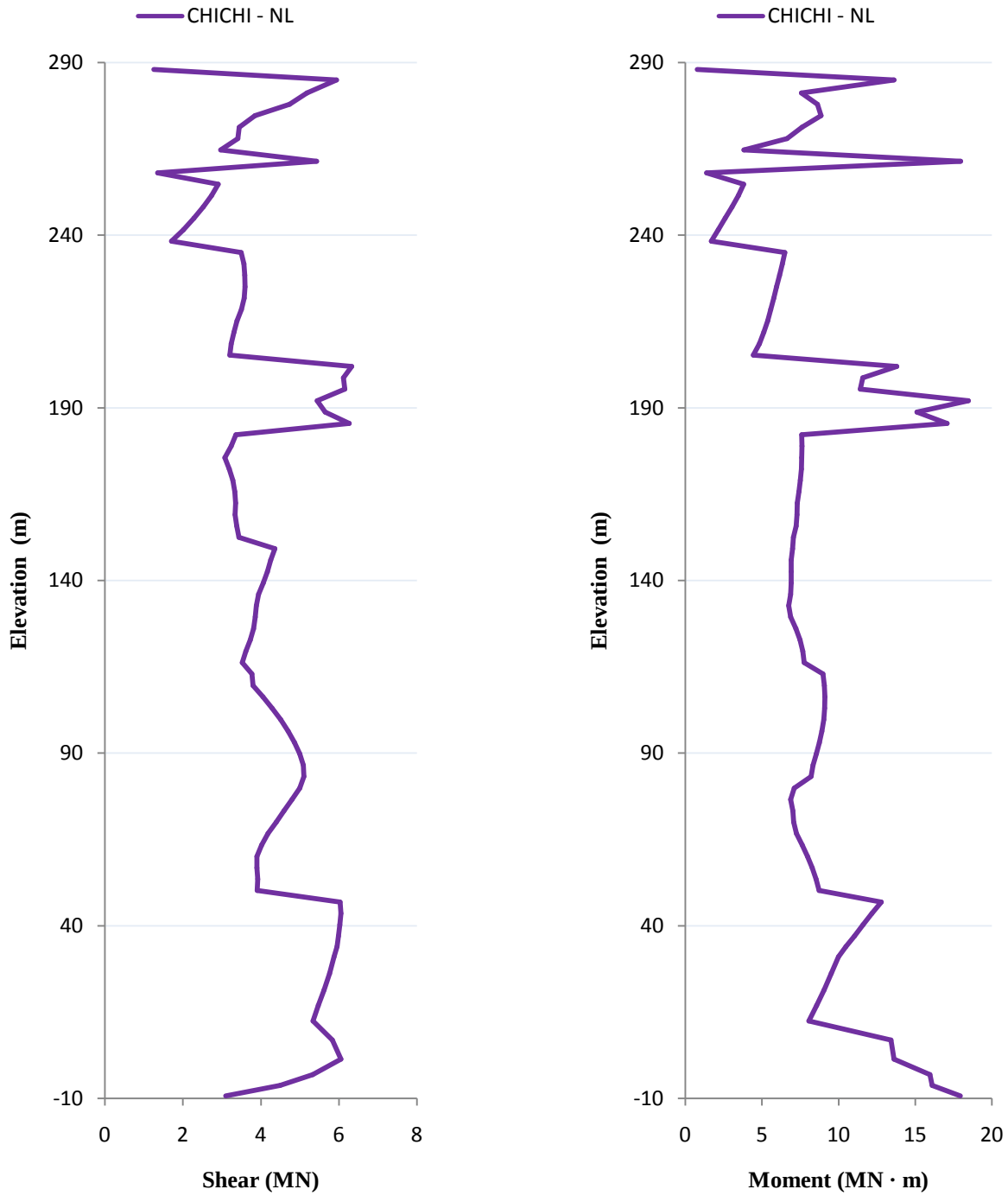

(a) (b)

Figure F-4: Nonlinear Time-History Analysis Center-Bottom Core Member Coupled Direction Response: (a) Maximum Shear; (b) Maximum Moment

Uncoupled Direction Response | *Core Member* | *Left-Bottom*

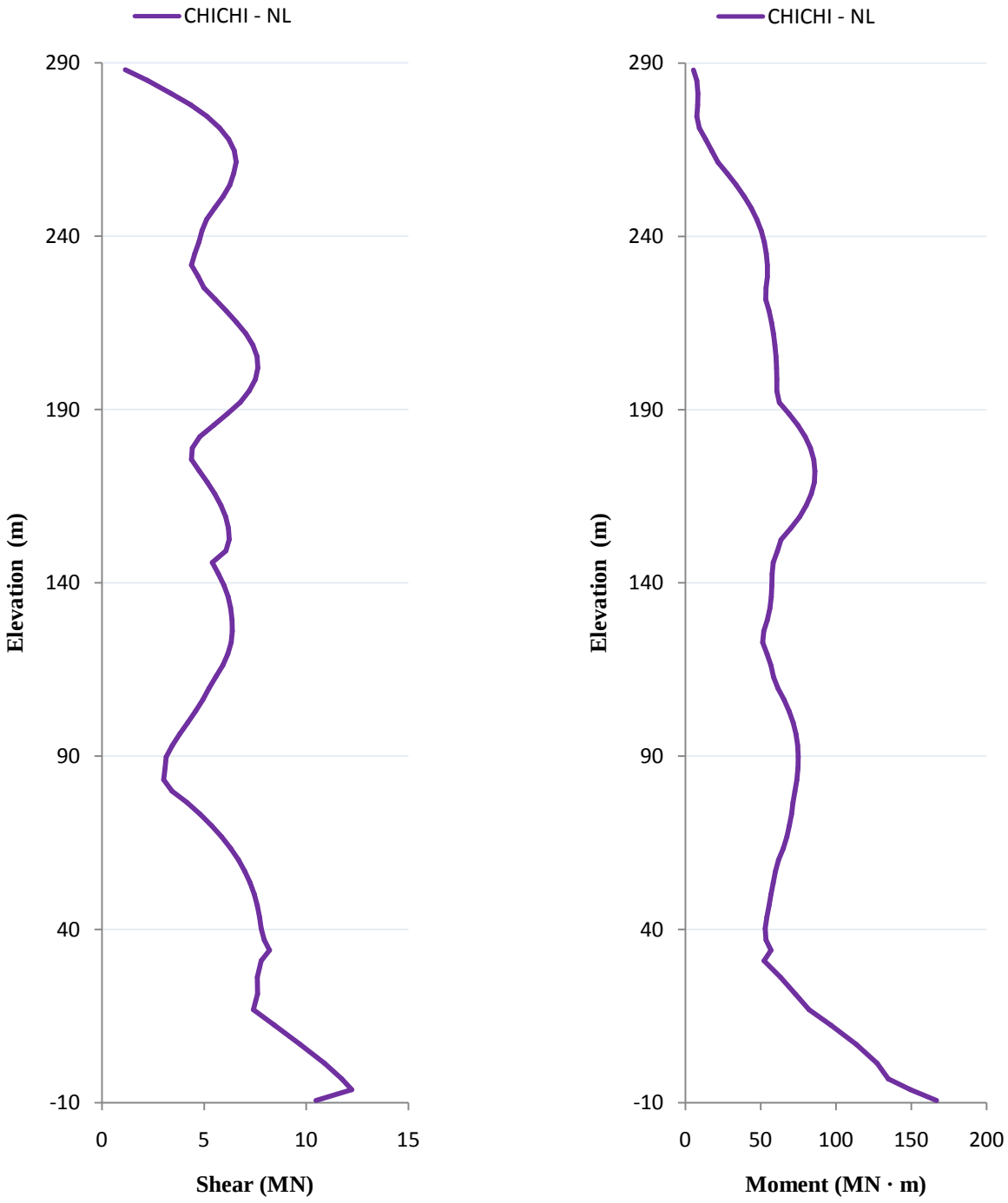

(a) (b)

Figure F-5: Nonlinear Time-History Analysis Left-Bottom Core Member Uncoupled Direction Response: (a) Maximum Shear; (b) Maximum Moment

Uncoupled Direction Response | *Core Member* | *Center-Bottom*

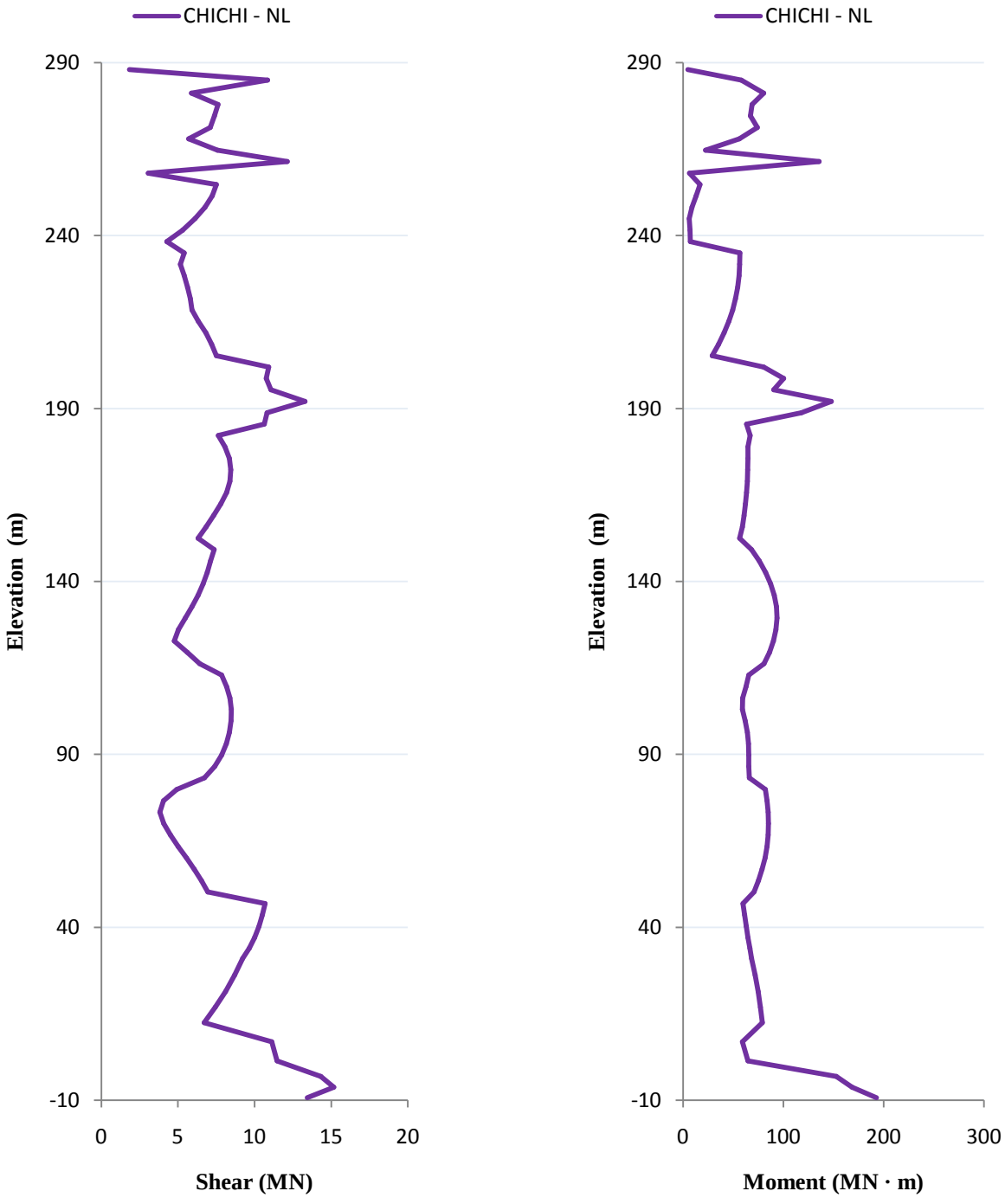

(a) (b)

Figure F-6: Nonlinear Time-History Analysis Center-Bottom Core Member Uncoupled Direction Response: (a) Maximum Shear; (b) Maximum Moment

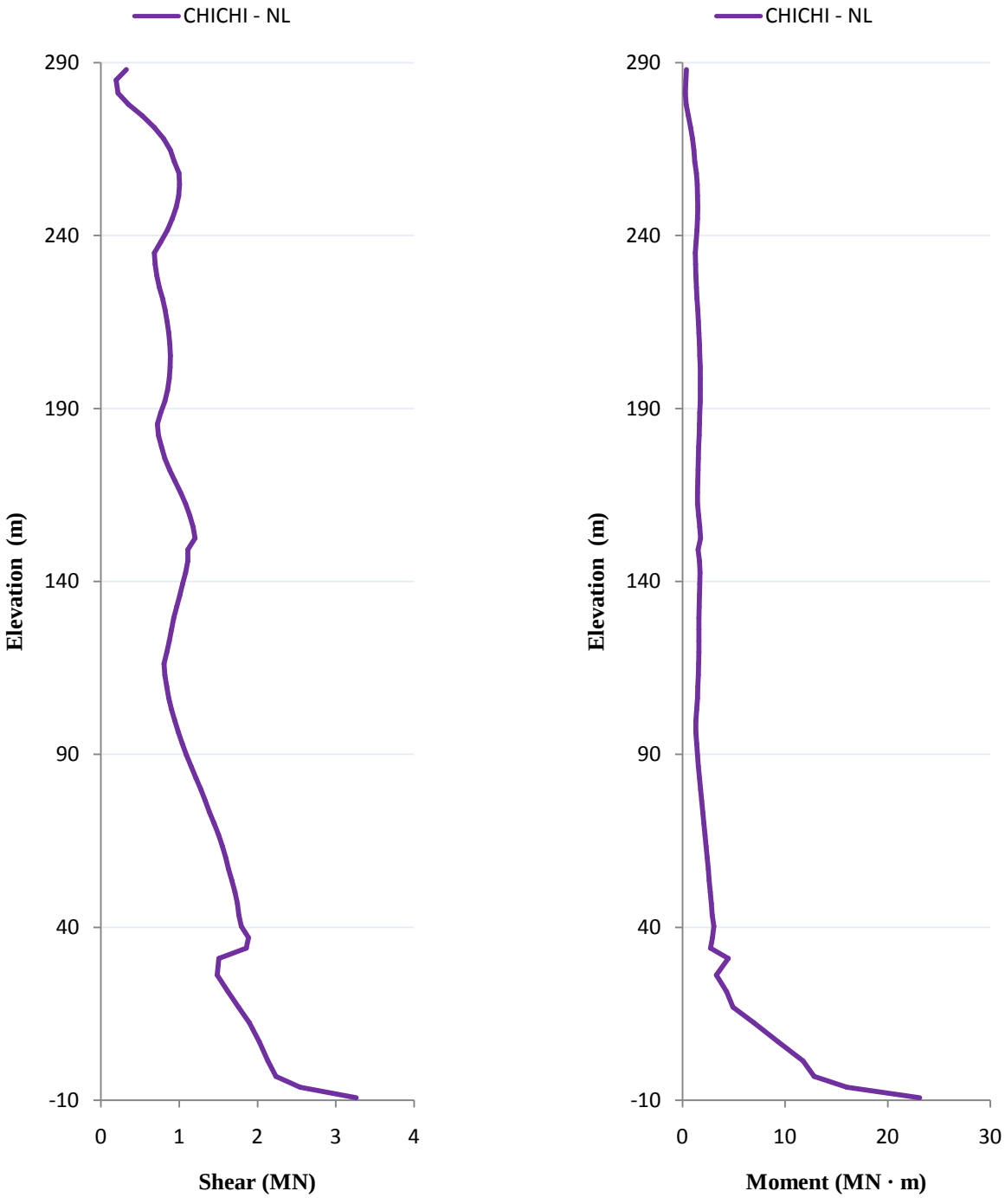

(a) (b)

Figure F-7: Nonlinear Time-History Analysis Column-Wall Member Response (T2C10 located bottom-left of floor plan): (a) Maximum Shear; (b) Maximum Moment

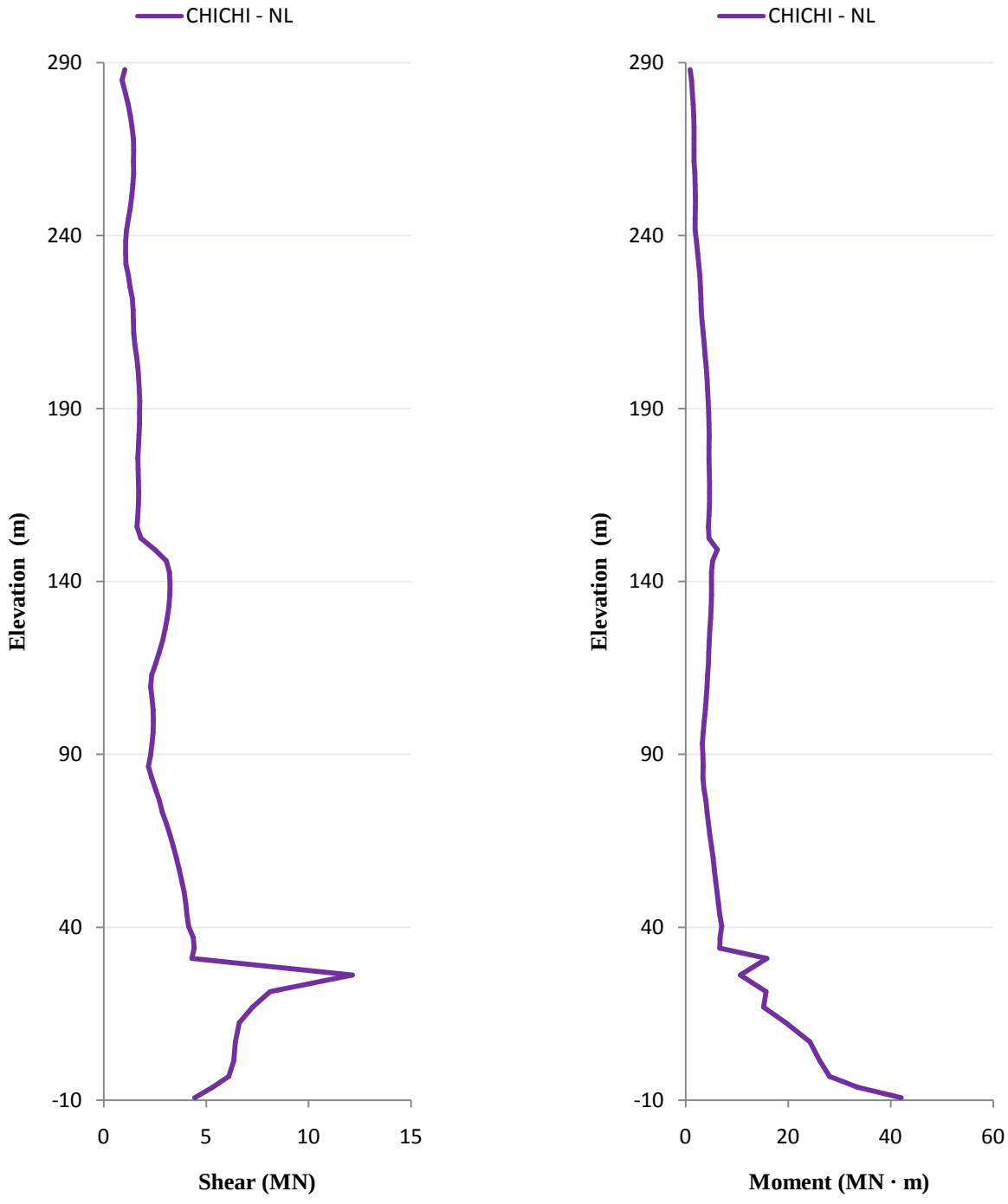

(a) (b)

Figure F-8: Nonlinear Time-History Analysis Column-Wall Member Response (T2C11 located central bottom-left of floor plan): (a) Maximum Shear; (b) Maximum Moment

Coupled Direction Response | *Coupling Beam Member* | *T2B-C1* | *Left End*

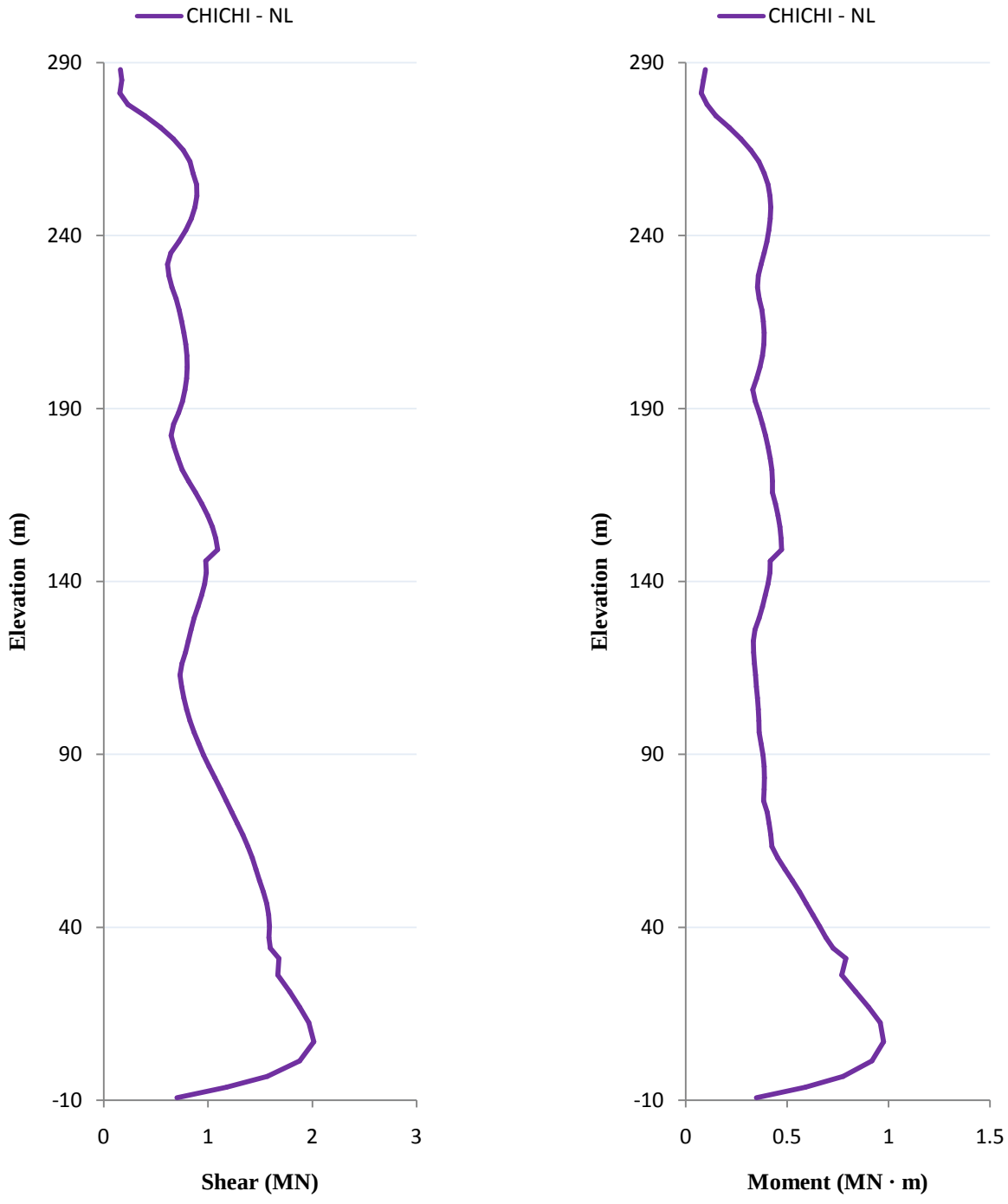

(a) (b)

Figure F-9: Nonlinear Time-History Analysis Coupling Beam Member Response at Left End (T2B-C1 located bottom-left of floor plan): (a) Maximum Shear; (b) Maximum Moment

Coupled Direction Response | *Coupling Beam Member* | *T2B-C1* | *Right End*

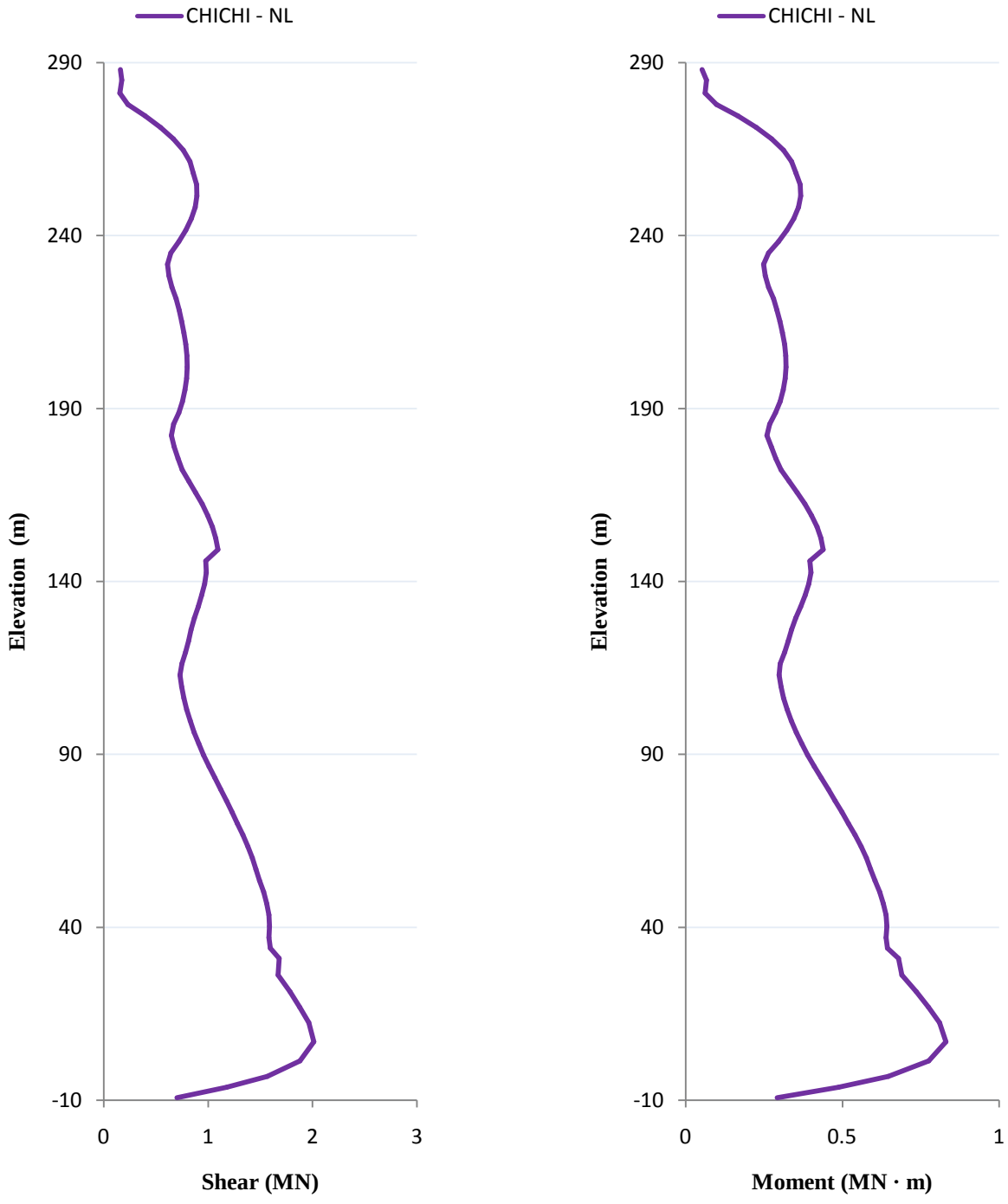

(a) (b)

Figure F-10: Nonlinear Time-History Analysis Coupling Beam Member Response at Right End (T2B-C1 located bottom-left of floor plan): (a) Maximum Shear; (b) Maximum Moment

Coupled Direction Response | *Coupling Beam Member* | *T2B-D1* | *Left End*

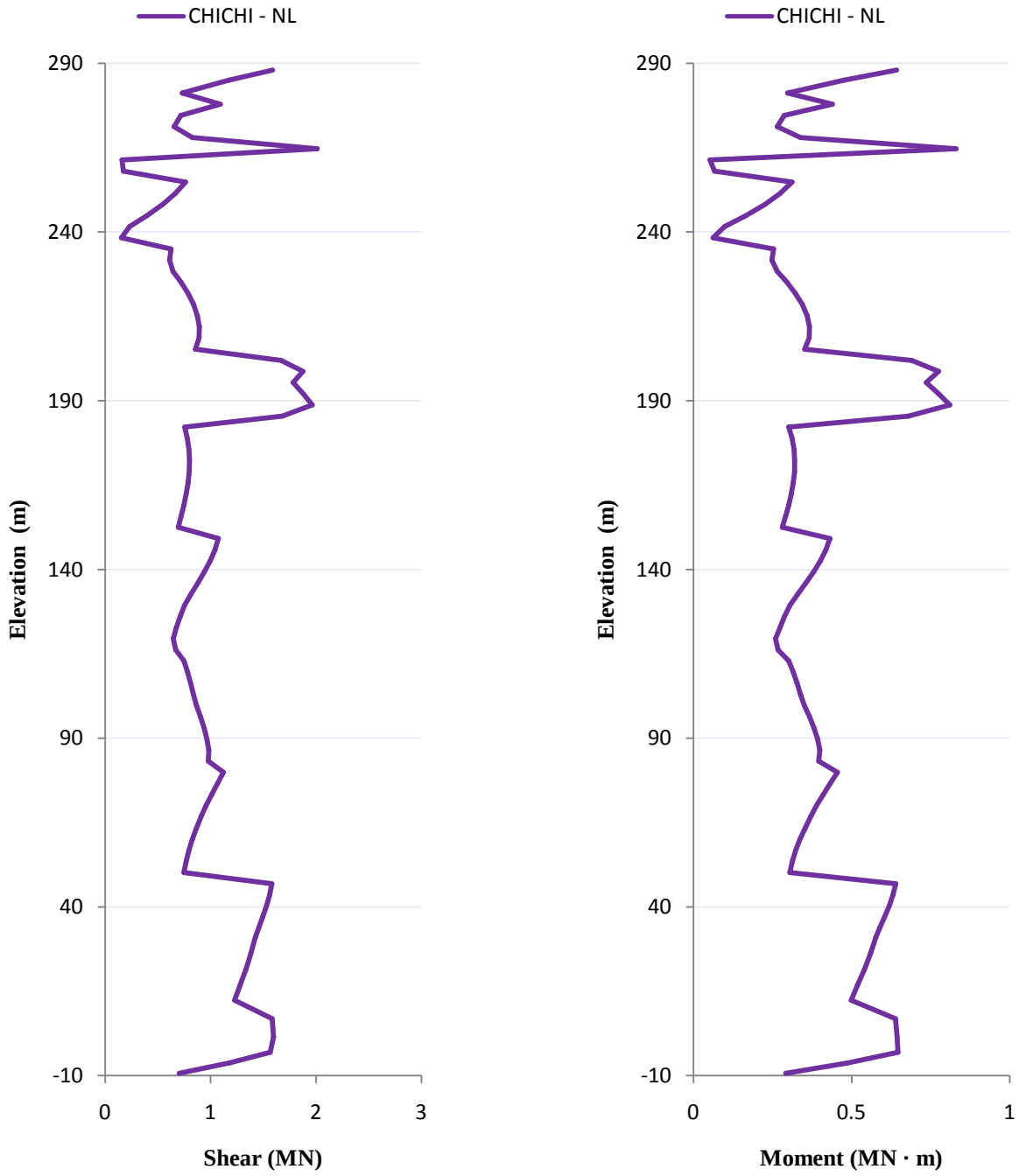

(a) (b)

Figure F-11: Nonlinear Time-History Analysis Coupling Beam Member Response at Left End (T2B-D1 located central bottom-left of floor plan): (a) Maximum Shear; (b) Maximum Moment

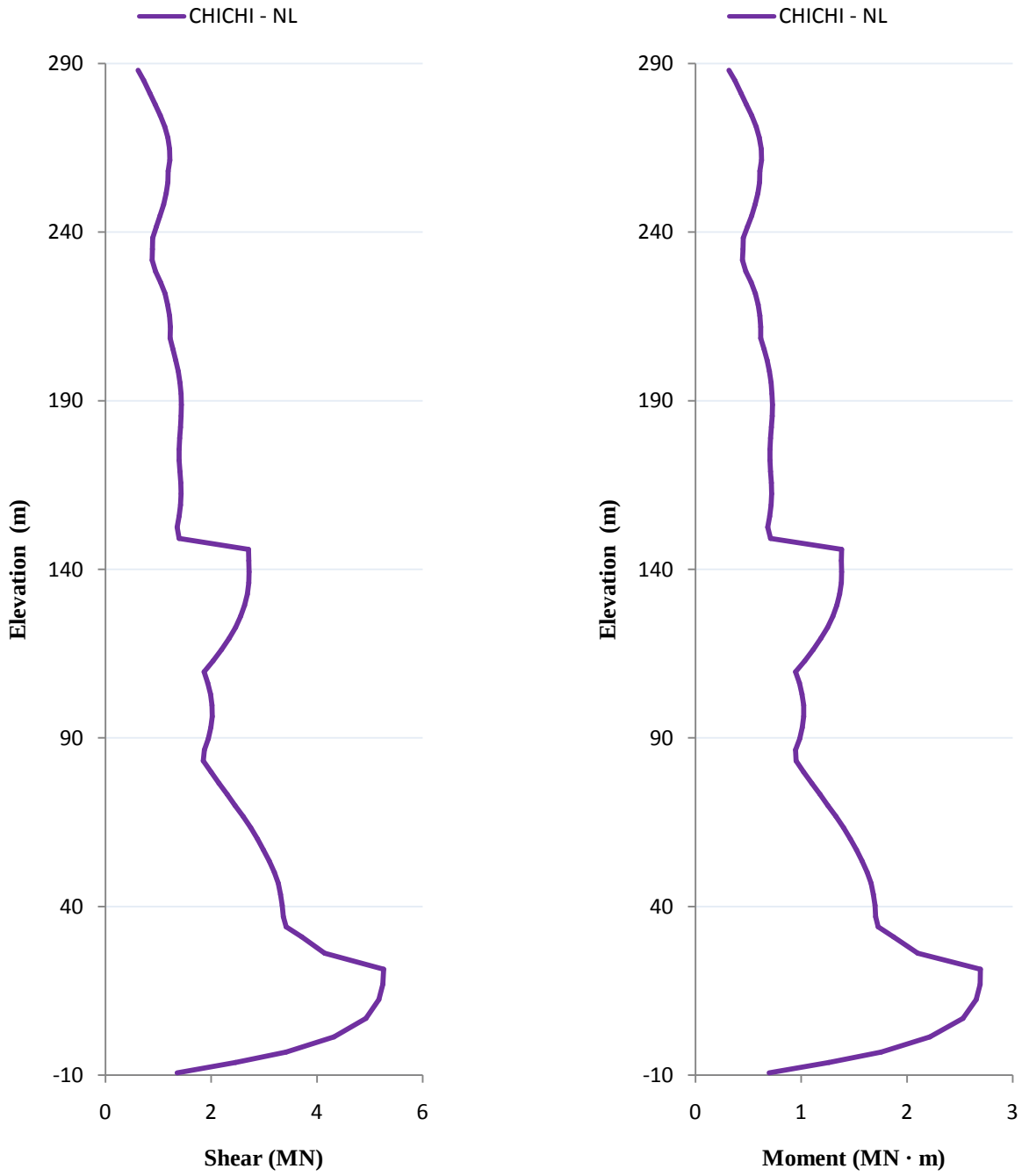

(a) (b)

Figure F-12: Nonlinear Time-History Analysis Coupling Beam Member Response at Right End (T2B-D1 located central bottom-left of floor plan): (a) Maximum Shear; (b) Maximum Moment

APPENDIX G - LINK ELEMENTS HYSTERESIS RESPONSES

Link Hysteresis Response | *Core Member* | *Left-Bottom*

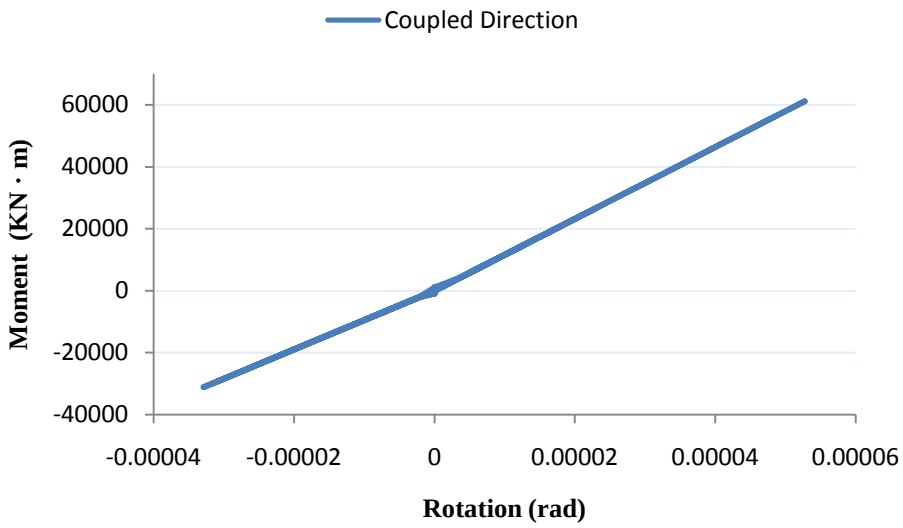

(a)

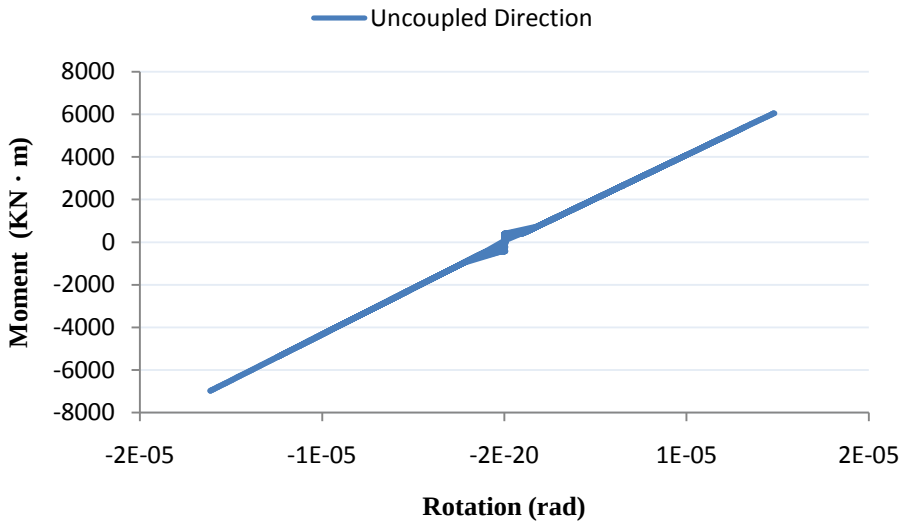

(b)

Figure G-1: FL 36 - Link Hysteresis Response for Left-Bottom Core Member: (a) Coupled Direction; (b) Uncoupled Direction

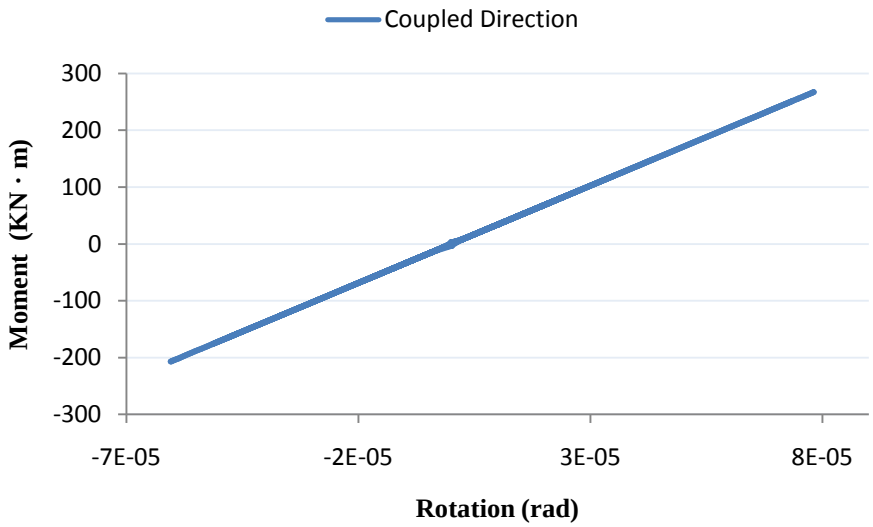

(a)

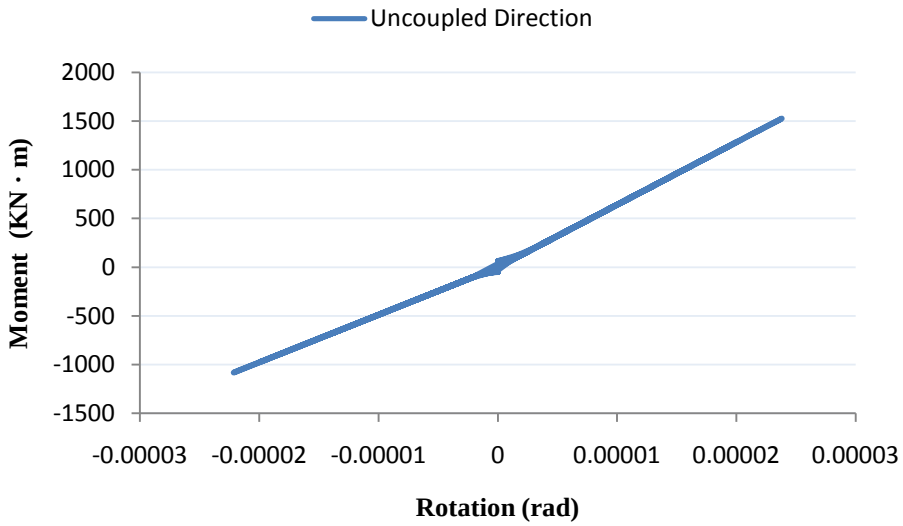

(b)

Figure G-2: FL 36 - Link Hysteresis Response for Column-Wall Member T2C10 located bottom-left of floor plan: (a) Coupled Direction; (b) Uncoupled Direction

Link Hysteresis Response | *Coupling Beam Member* | *T2B-C1*

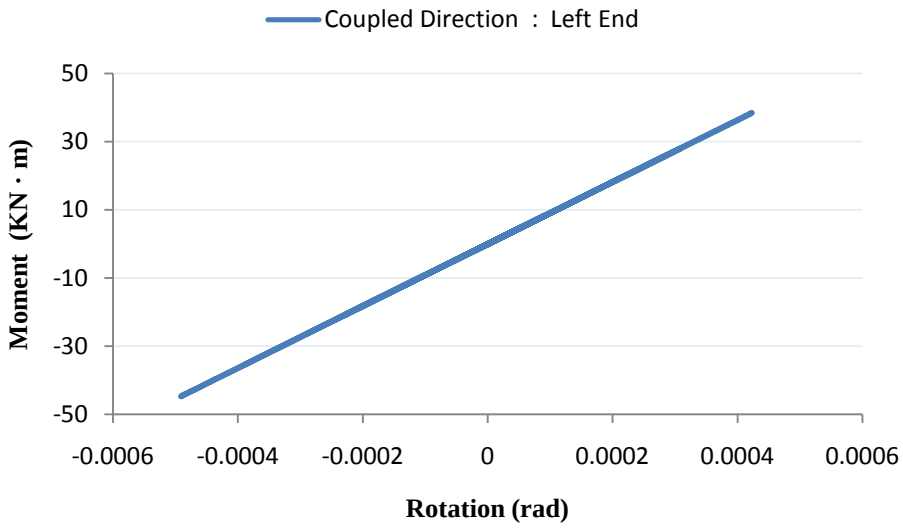

(a)

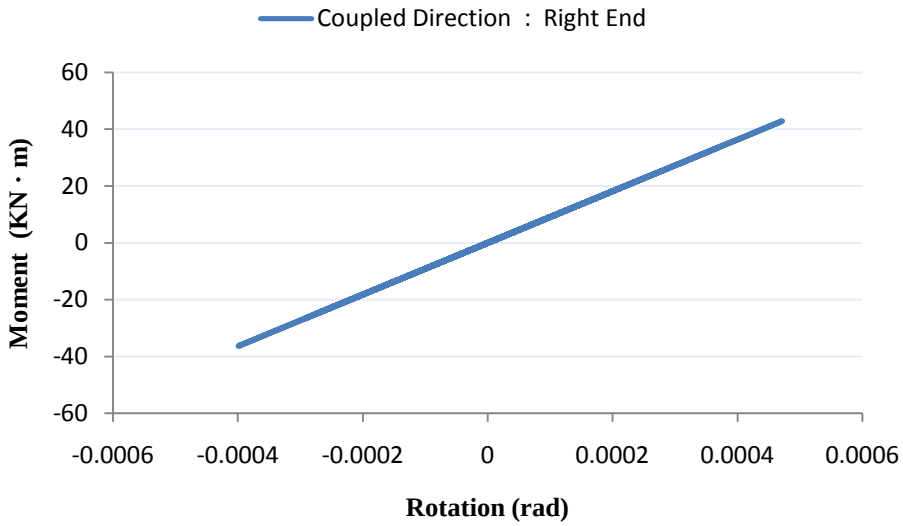

(b)

Figure G-3: FL 36 - Link Hysteresis Response for Coupling Beam Member T2B-C1 located bottom-left of floor plan: (a) Left End; (b) Right End

APPENDIX H - SUPERIMPOSED ANALYSES RESULTS

Coupled Direction Response | *Core Member* | *Left-Bottom*

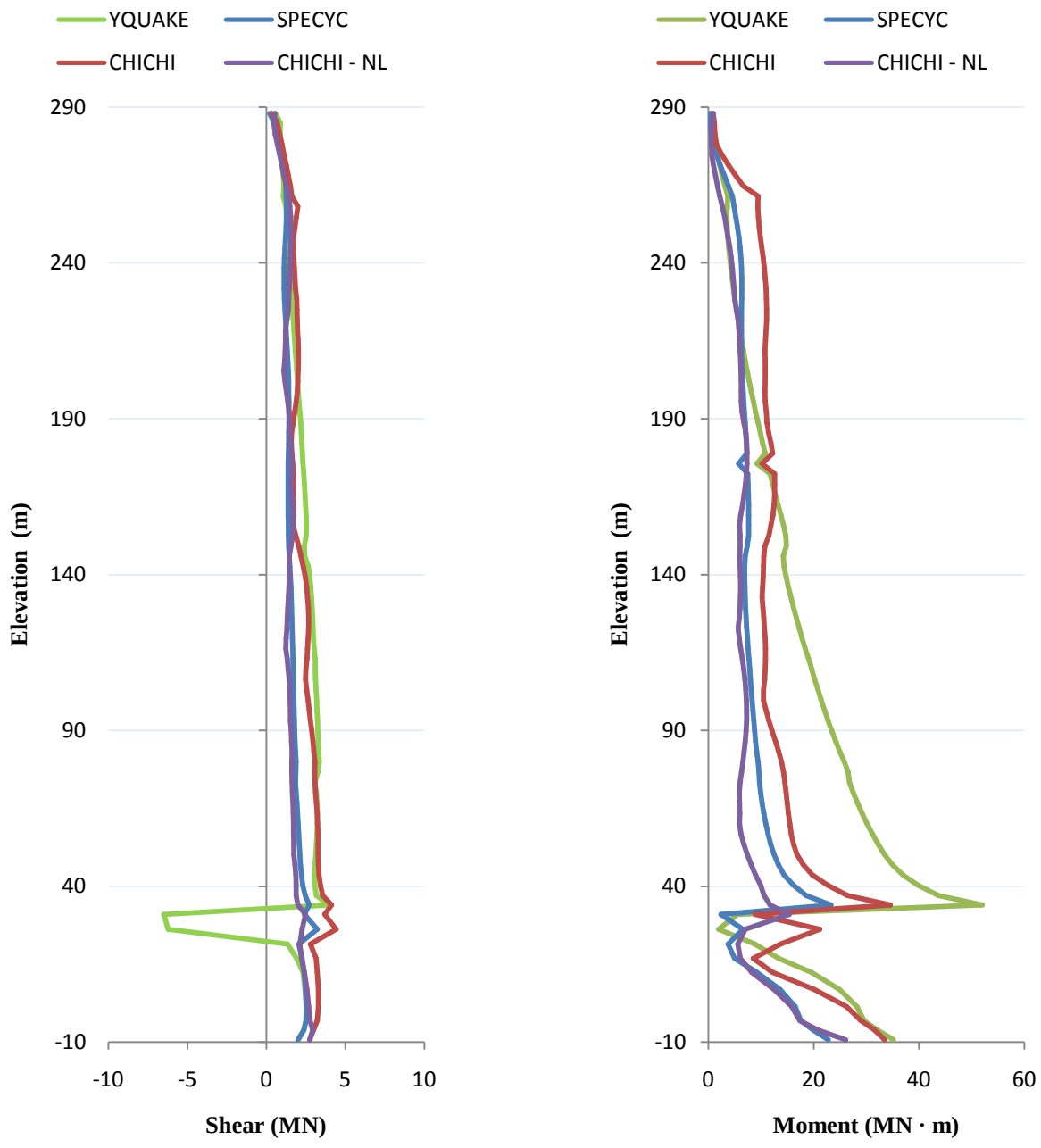

(a) (b)

Figure H-1: Left-Bottom Core Member Coupled Direction Response: (a) Maximum Shear; (b) Maximum Moment

Coupled Direction Response | *Core Member* | *Center-Bottom*

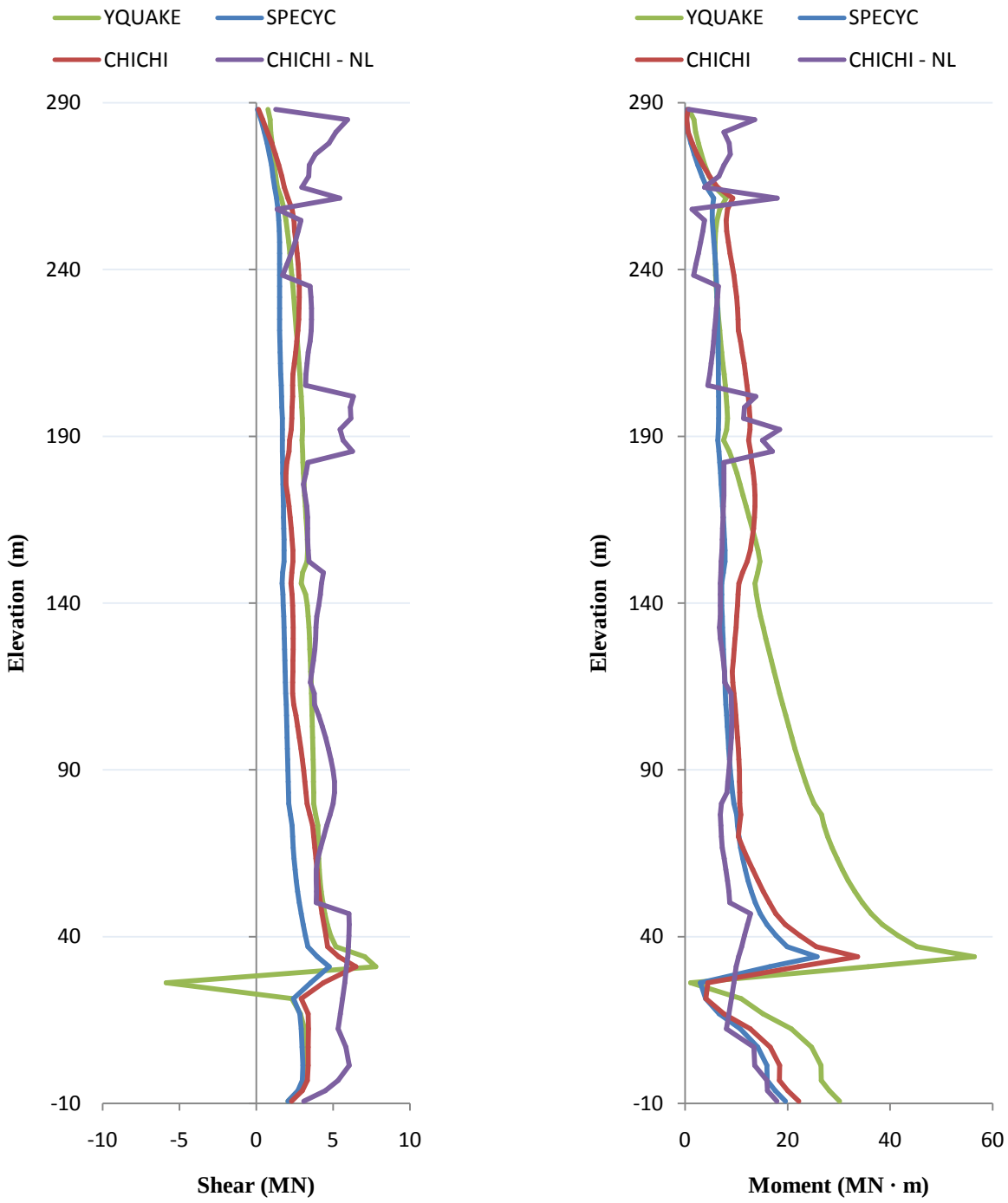

(a) (b)

Figure H-2: Center-Bottom Core Member Coupled Direction Response: (a) Maximum Shear; (b) Maximum Moment

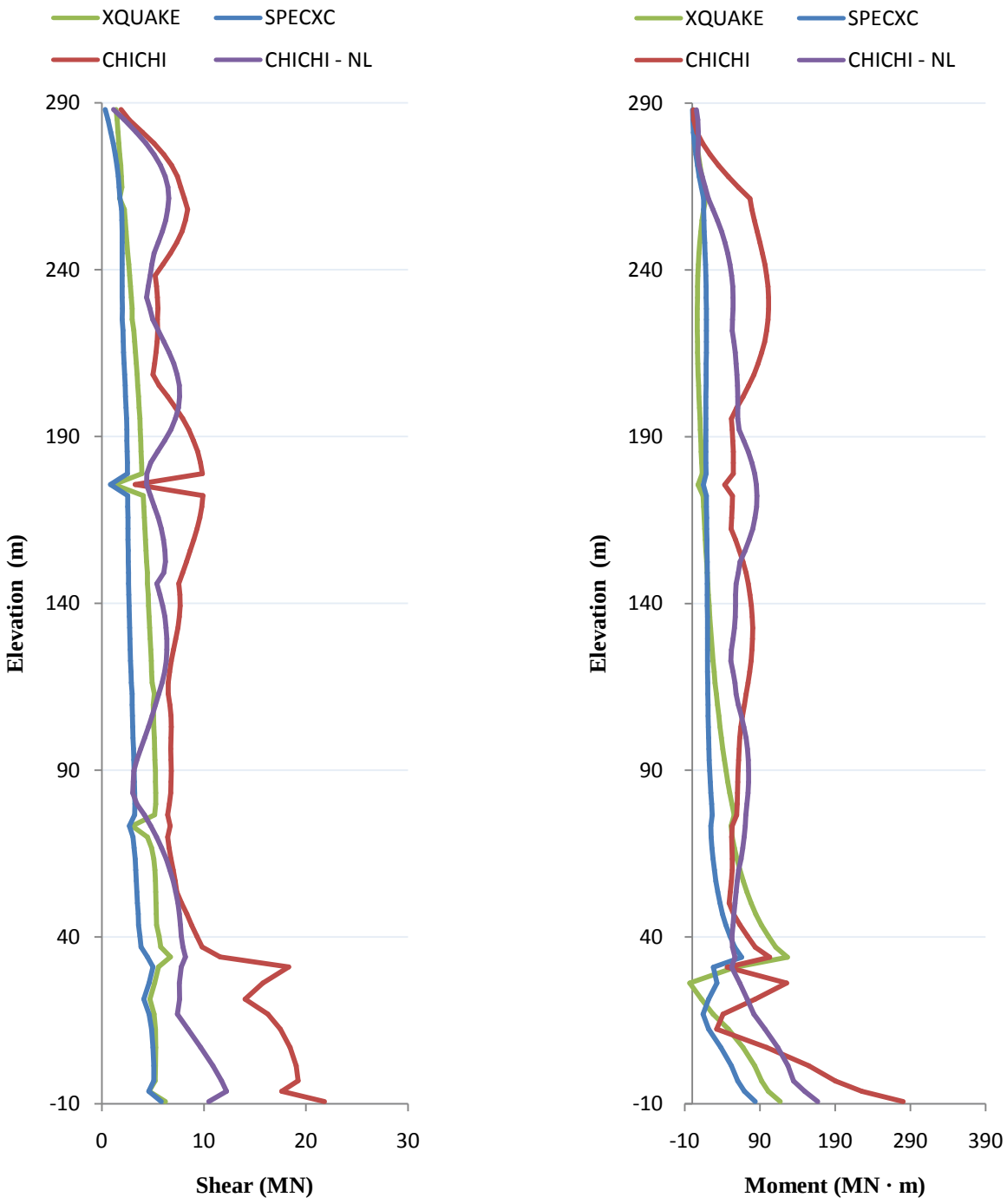

(a) (b)

Figure H-3: Left-Bottom Core Member Uncoupled Direction Response: (a) Maximum Shear; (b) Maximum Moment

Uncoupled Direction Response | *Core Member* | *Center-Bottom*

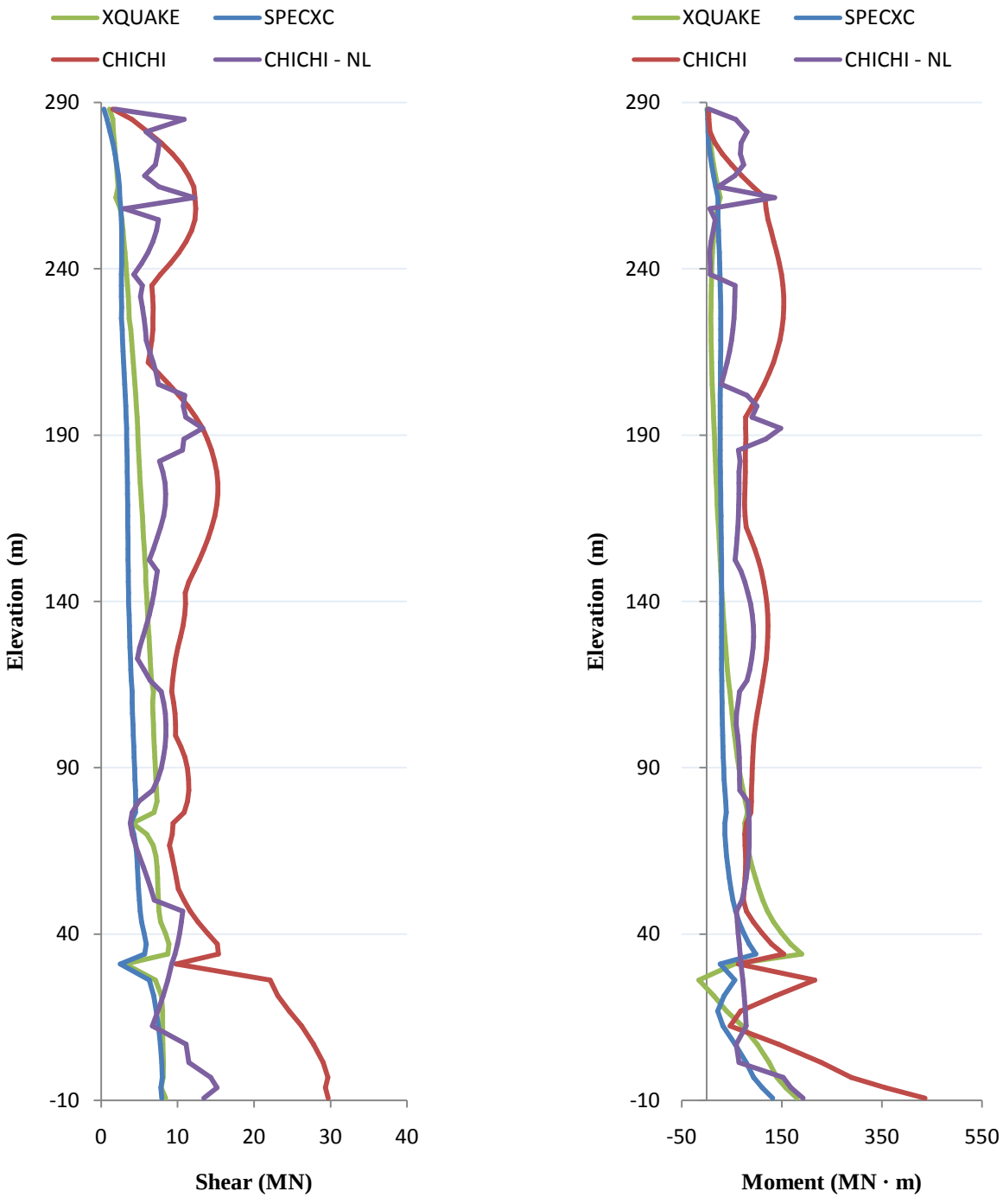

(a) (b)

Figure H-4: Center-Bottom Core Member Uncoupled Direction Response: (a) Maximum Shear; (b) Maximum Moment

Coupled Direction Response | *Column-Wall Member* | *T2C10*

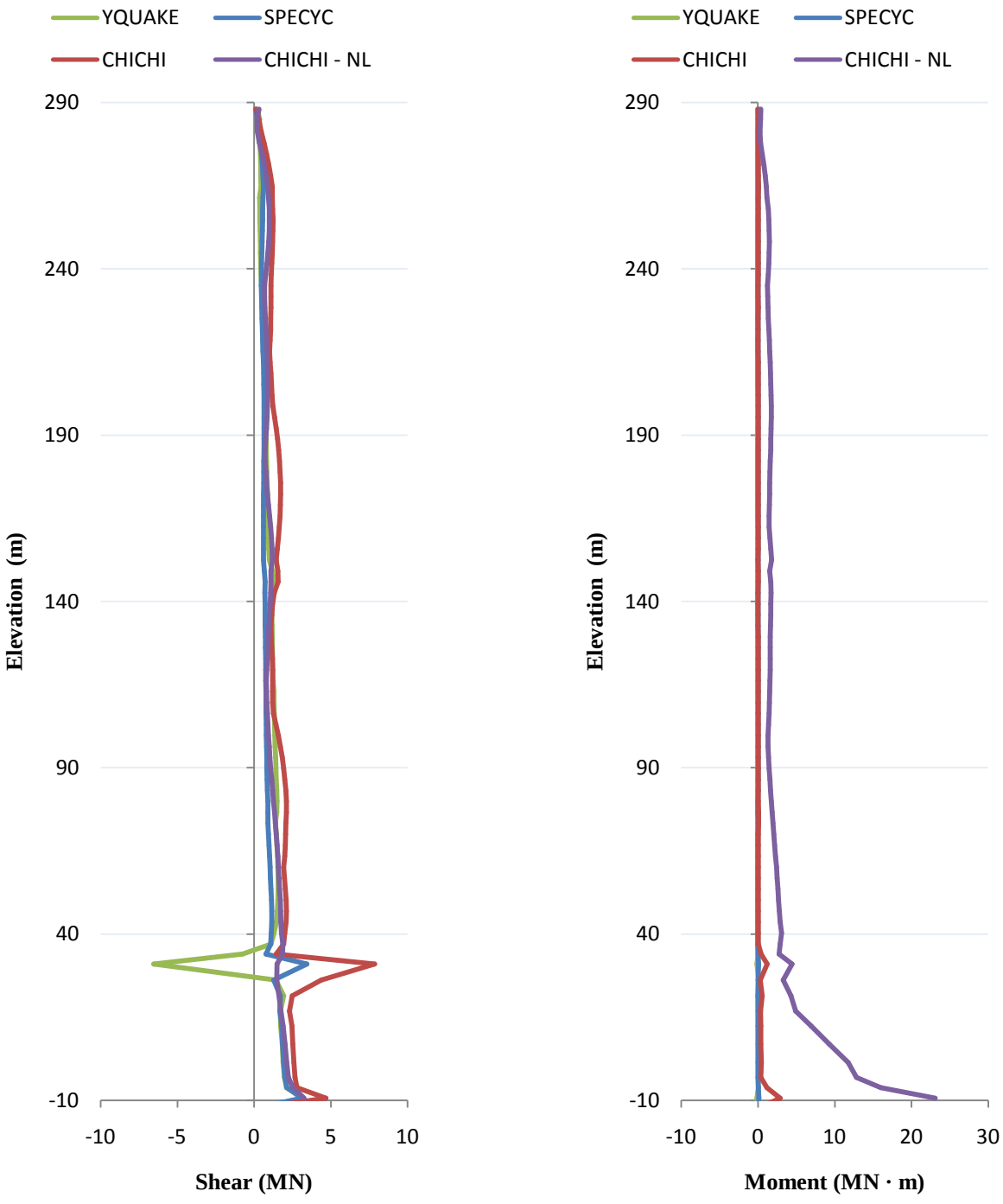

(a) (b)

Figure H-5: Column-Wall Member Response (T2C10 located bottom-left of floor plan): (a) Maximum Shear; (b) Maximum Moment

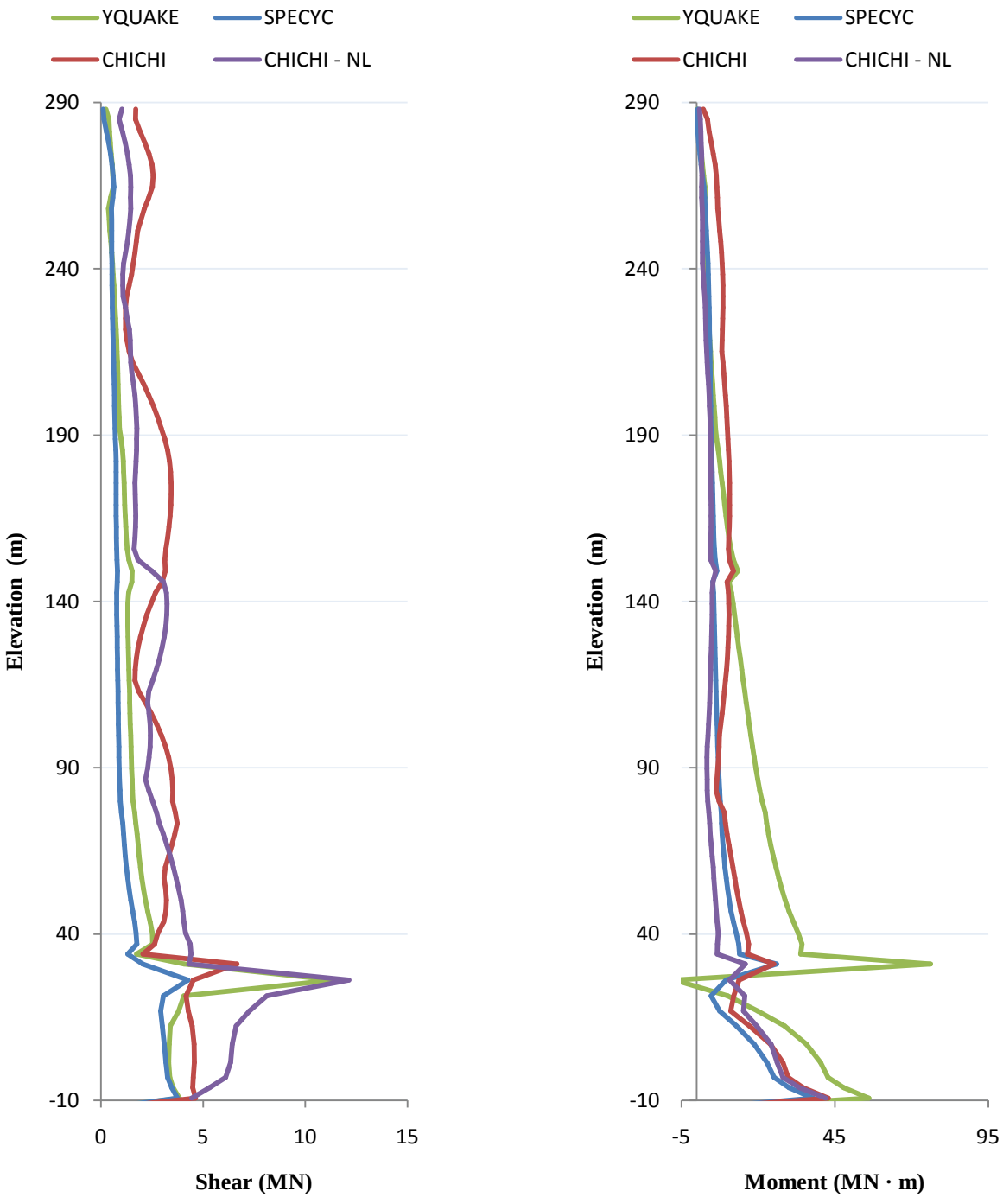

(a) (b)

Figure H-6: Column-Wall Member Response (T2C11 located central bottom-left of floor plan): (a) Maximum Shear; (b) Maximum Moment

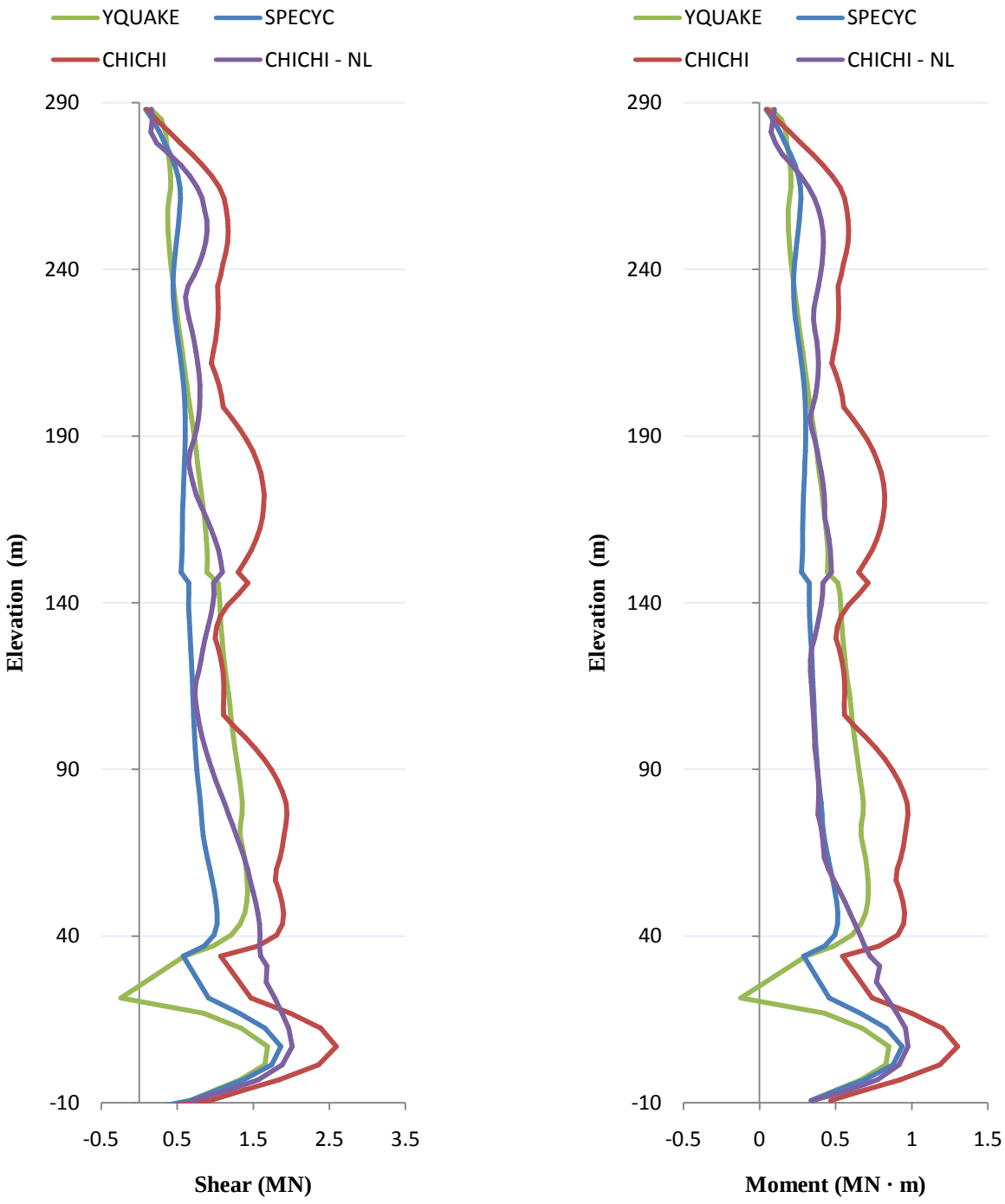

(a) (b)

Figure H-7: Coupling Beam Member Response at Left End (T2B-C1 located bottom-left of floor plan): (a) Maximum Shear; (b) Maximum Moment

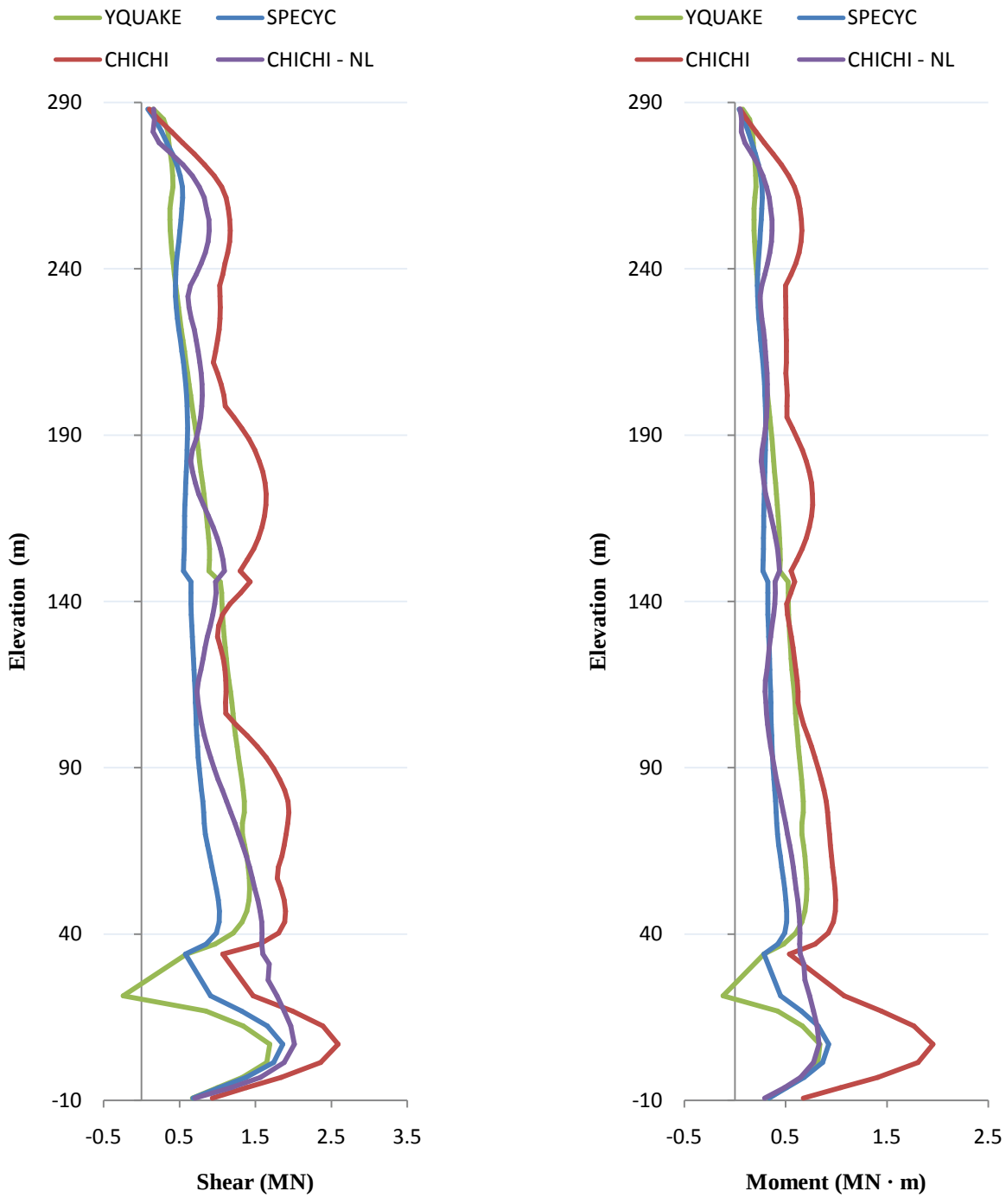

Figure H-8: Coupling Beam Member Response at Right End (T2B-C1 located bottom-left of floor plan): (a) Maximum Shear; (b) Maximum Moment

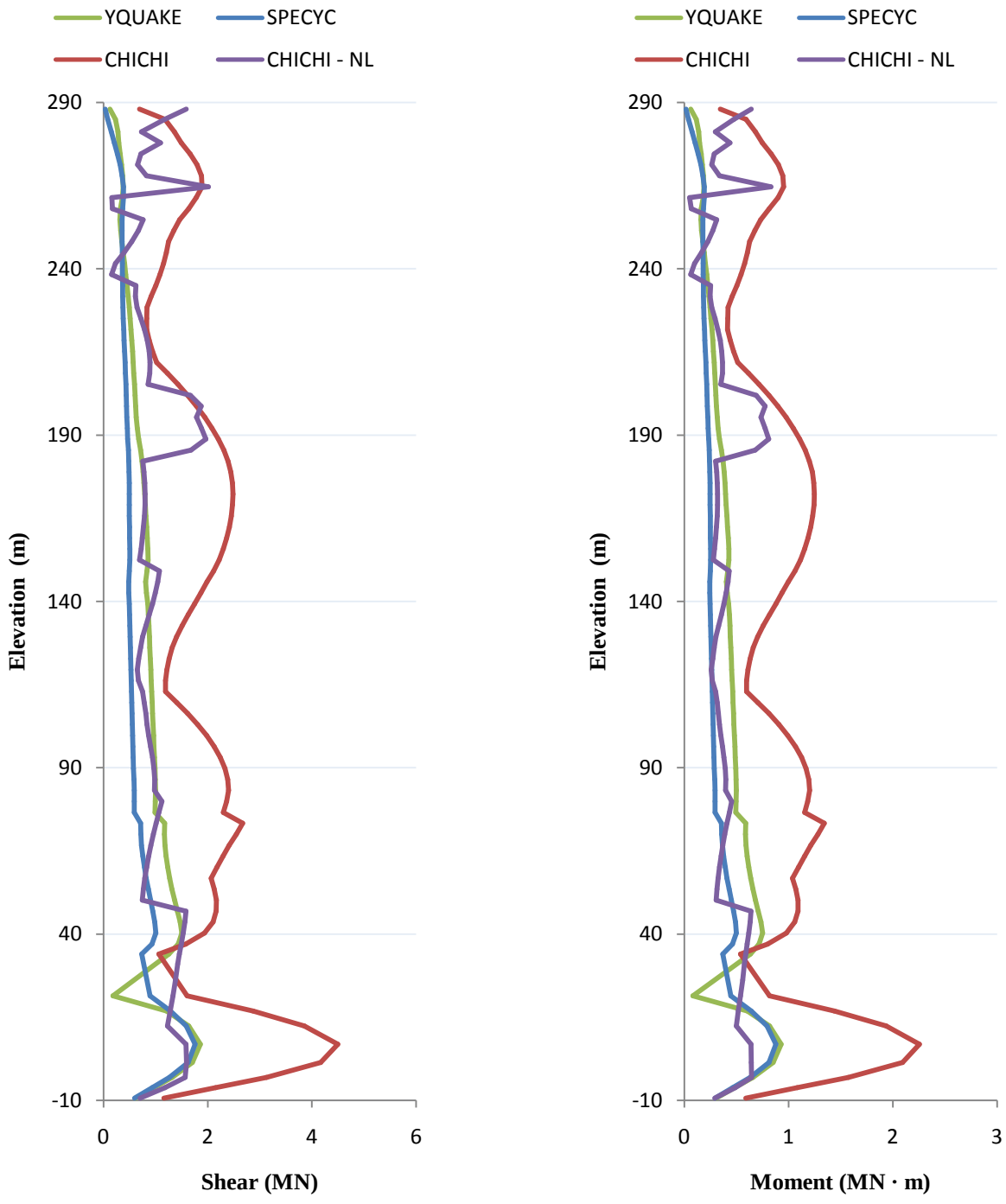

Figure H-9: Coupling Beam Member Response at Left End (T2B-D1 located central bottom-left of floor plan): (a) Maximum Shear; (b) Maximum Moment

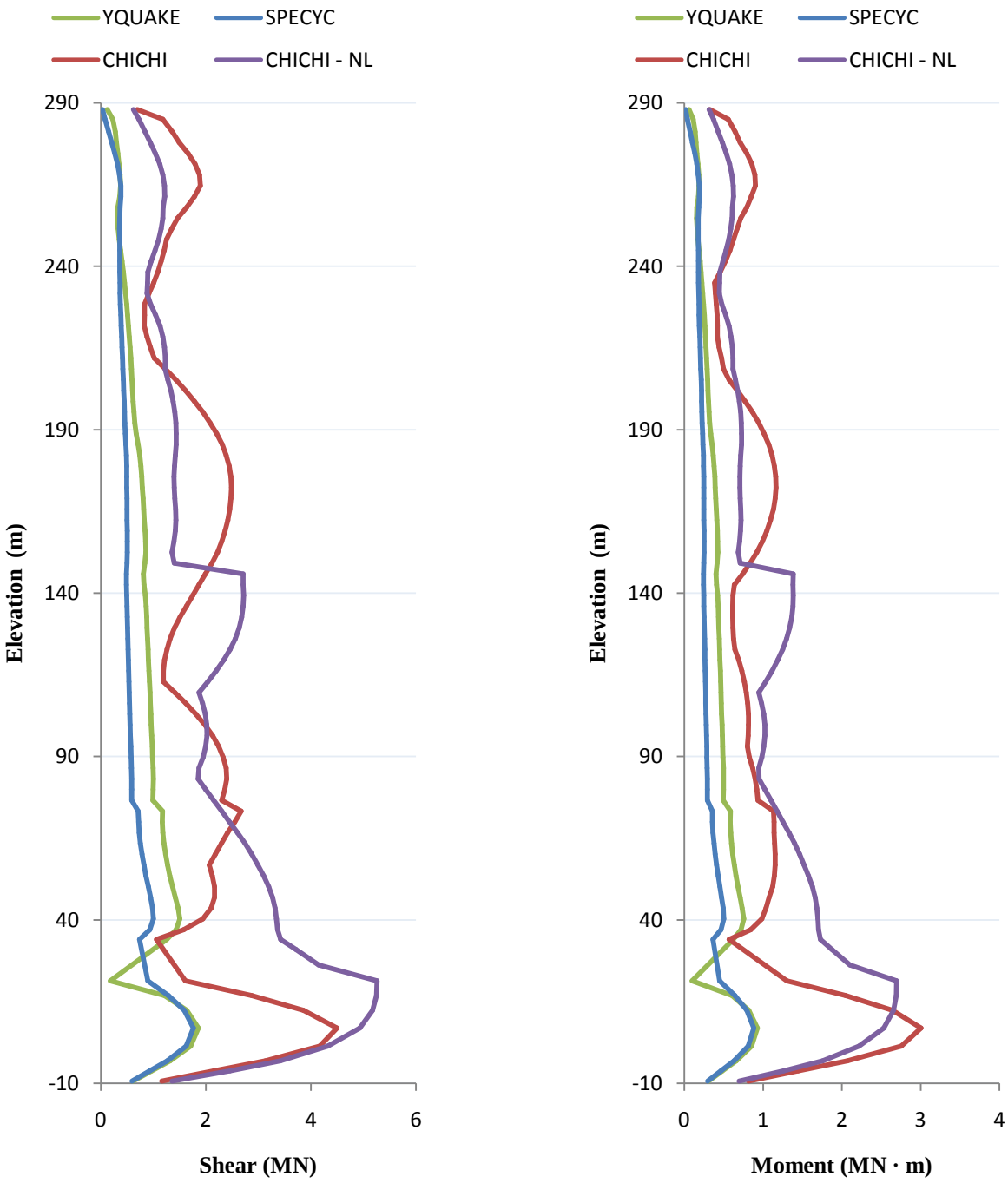

(a) (b)

Figure H-10: Coupling Beam Member Response at Right End (T2B-D1 located central bottom-left of floor plan): (a) Maximum Shear; (b) Maximum Moment